LEABHARLANN CHOLÁISTE NA TRÍONÓIDE, BAILE ÁTHA CLIATH | TRINITY COLLEGE LIBRARY DUBLIN
Ollscoil Átha Cliath | The University of Dublin

Terms and Conditions of Use of Digitised Theses from Trinity College Library Dublin

Copyright statement

All material supplied by Trinity College Library is protected by copyright (under the Copyright and Related Rights Act, 2000 as amended) and other relevant Intellectual Property Rights. By accessing and using a Digitised Thesis from Trinity College Library you acknowledge that all Intellectual Property Rights in any Works supplied are the sole and exclusive property of the copyright and/or other IPR holder. Specific copyright holders may not be explicitly identified. Use of materials from other sources within a thesis should not be construed as a claim over them.

A non-exclusive, non-transferable licence is hereby granted to those using or reproducing, in whole or in part, the material for valid purposes, providing the copyright owners are acknowledged using the normal conventions. Where specific permission to use material is required, this is identified and such permission must be sought from the copyright holder or agency cited.

Liability statement

By using a Digitised Thesis, I accept that Trinity College Dublin bears no legal responsibility for the accuracy, legality or comprehensiveness of materials contained within the thesis, and that Trinity College Dublin accepts no liability for indirect, consequential, or incidental, damages or losses arising from use of the thesis for whatever reason. Information located in a thesis may be subject to specific use constraints, details of which may not be explicitly described. It is the responsibility of potential and actual users to be aware of such constraints and to abide by them. By making use of material from a digitised thesis, you accept these copyright and disclaimer provisions. Where it is brought to the attention of Trinity College Library that there may be a breach of copyright or other restraint, it is the policy to withdraw or take down access to a thesis while the issue is being resolved.

Access Agreement

By using a Digitised Thesis from Trinity College Library you are bound by the following Terms & Conditions. Please read them carefully.

I have read and I understand the following statement: All material supplied via a Digitised Thesis from Trinity College Library is protected by copyright and other intellectual property rights, and duplication or sale of all or part of any of a thesis is not permitted, except that material may be duplicated by you for your research use or for educational purposes in electronic or print form providing the copyright owners are acknowledged using the normal conventions. You must obtain permission for any other use. Electronic or print copies may not be offered, whether for sale or otherwise to anyone. This copy has been supplied on the understanding that it is copyright material and that no quotation from the thesis may be published without proper acknowledgement.

Evaluation of the anti-cancer effects of novel pyrrolo-1,5-benzoxazepines in neuroblastoma

Thesis submitted to the

University of Dublin, Trinity College

for the Degree of

Doctor of Philosophy

By

Jennifer Lennon, BA (Mod), MSc

School of Biochemistry and Immunology

Trinity College Dublin

March 2015

TRINITY COLLEGE
1 4 MAY 2015
LIBRARY DUBLIN

Thesis 10551

Declaration

I declare that this thesis has not been submitted as an exercise for a degree at this or any other university and it is entirely my own work. I agree to deposit this thesis in the University's open access institutional repository or allow the library to do so on my behalf, subject to Irish Copyright Legislation and Trinity College Library conditions of use and acknowledgement.

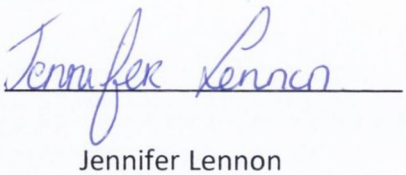

Jennifer Lennon

Acknowledgements

First and foremost I would like to thank Danny; without her continuous help, guidance and support, I wouldn't have made it to this point. Thank you for giving me the opportunity to carry out this project. I am so grateful for your patience and encouragement (and for finding every single typo in this thesis!). To the post docs in the Zisterer lab, firstly to Lisa and Seema, thanks for welcoming me into the lab, for all the help and advice over the years. Particular thanks to Paula for all the help with the *in vivo* experiments, and to Sandra for taking the time to train me, help with the planning and most importantly answering so many questions.

To everyone in the lab; Jade, I couldn't have asked for a nicer, more thoughtful, fun person to work with. Thanks for always being around for a chat and for being a great friend. I'll really miss working together. Mary, it's been brilliant working with you, I'm so happy I can leave knowing the sinks are safe in your capable hands! Fintan, you're the only other person I know who'll always understand the agony of an AMPK blot! Kasia, Siobhan, Claire, Brian and Kim, it's been great sharing a lab and working with you all. To all the past and present members of the reading room, thanks for being the loveliest, friendliest group of people you hope to work alongside every day.

Thank you to everyone in the department of Biochemistry and Immunology, Mary Pat, Miriam, Liam, Noel, Dave, Des, Brian, Audrey, Glynis and everyone in the prep room. In particular, thank you to Barry for his help in planning so many flow cytometry experiments. I'm indebted to him for his expertise over the last four years.

Thank you to Dr. Anne O'Meara, Dr. Cormac Owens and all the other members of the Oncology Department in Our Lady's Children's Hospital, Crumlin.

To my family; firstly my parents, for their love, support and encouragement (and not to forget all the lifts home on rainy nights after long days in the lab). Thanks to my brothers (yes this is it, time for the real world); to my amazing sister Kate, who couldn't have been more supportive and encouraging over the last four years. Thanks to Clare and Katie for all the nights in, walks, films and just for being brilliant friends.

Finally to Paul, you've been here from the start (mitochondriacs in St Stephens Green!). Thank you for your love, strength and support, especially over the last few months. You've made me laugh on the days I wanted to cry, kept me calm and made me realise an end was in sight when I didn't really believe it. I couldn't have done this without you.

This work was funded by the National Children's Research Centre.

Table of Contents *Pg*

Declaration i
Acknowledgments ii
Table of contents iii
List of figures and tables vi
Abbreviations xiii
Abstract xvi
Presentations, publications and awards xviii

Chapter 1. Introduction

1.1 Neuroblastoma 1
1.1.1 Classification and staging 1
1.1.2 Presentation 3
1.1.3 Diagnosis 4
1.1.4 Genetic abnormalities associated with neuroblastoma 5
1.1.4.1 Ploidy 5
1.1.4.2 MYCN amplification 6
1.1.4.3 p53 7
1.1.4.4 1p Loss of Heterozygosity 9
1.1.4.5 11q deletion 10
1.1.5 Familial Neuroblastoma 10
1.2 Current treatments 11
1.3 Novel treatment strategies 14
1.4 Analysis of drug interactions 17
1.5 Multidrug resistance 18
1.6 Apoptosis 19
1.6.1 Caspases 20
1.6.2 Intrinsic pathway 24
1.6.3 Extrinsic pathway 24
1.6.4 Bcl-2 family 27
1.6.4.1 Bcl-2 29
1.6.4.2 Mcl-1 31
1.6.4.3 Bcl-xL 33
1.6.4.4 Pro-apoptotic Bcl-2 proteins 34
1.7 ROS-mediated apoptosis 35
1.8 5'AMP-activated protein kinase 37
1.9 Mammalian target of rapamycin 40
1.10 Autophagy 44
1.11 The cell cycle 46
1.12 Microtubules 48
1.13 Microtubule targeting agents 51
1.14 The PBOX compounds 53
1.15 Objectives of the project 57

Chapter 2. Materials and methods

2.1 Materials and suppliers 58
2.2 Postal addresses of suppliers 60
2.3 Cell Maintenance 62
2.3.1 Cell counting 62
2.3.2 Cryopreservation of cells 63
2.4 Reagents 63
2.5 Preparation of stock solutions 64
2.6 AlamarBlue viability assay 64
2.7 Flow cytometry 65
2.8 Determination of ROS production
2.8.2 ROS-Glo Assay 66
2.8.3 DCFH-DA staining 67
2.9 Clonogenic Assays
2.9.1 Optimisation of seeding density 68
2.9.2 Treatment of colonies 68
2.10 Western Blot
2.10.1 Preparation of cell lysates 70
2.10.2 Preparation of cytosolic fractions 70
2.10.3 Determination of protein concentration 70
2.10.4 Sodium Dodecylsulphate-Polyacrylamide Gel Electrophoresis 71
2.10.5 Western Blotting 72
2.10.6 Densitometric analysis 75
2.11 siRNA knockdown of Mcl-1 75
2.12 Immunomagnetic separation of neuroblastoma cells from bone marrow aspirates 76
2.13 *in vivo* tumour model of neuroblastoma
2.13.1 Mice 77
2.13.2 *In vivo* tumour study 77
2.14 Analysis of drug interactions 78
2.15 Statistics 79

Chapter 3. Investigation into the anti-cancer effects of novel pyrrolo-1,5-benzoxazepines in drug sensitive and multidrug resistant neuroblastoma cells

3.1 Introduction 80
3.2 Results
3.2.1 Validity of the AlamarBlue viability assay in determining the effects of cytotoxic drugs on SHSY5Y cell viability 82
3.2.3 Effect of vehicles, DMSO and ethanol, on viability of SHSY5Y cells 84
3.2.4 PBOX-6 and -15, doxorubicin, etoposide, carboplatin and vincristine reduce the viability of neuroblastoma cell lines 86
3.2.5 Determination of fold resistance of PBOX-6 and 15, etoposide, carboplatin, doxorubicin and vincristine in drug resistant neuroblastoma cell lines 94
3.2.6 Optimisation of cell seeding density for clonogenic assay 99
3.2.7 PBOX-6 and 15 inhibits the clonogenicity of SHSY5Y cells in a dose-dependent manner 101
3.2.8 PBOX-6 decreases the viability of neuroblastoma cells isolated from 103

primary bone marrow samples
3.2.9 The effect of PBOX-6 and 15 on SHSY5Y cell cycle progression and induction of apoptosis 107
3.2.10 PBOX-6 induces PARP cleavage in SHSY5Y cells 111
3.2.11 The effect of PBOX-6 on the Bcl-2 family of proteins 114
3.3 Discussion 120

Chapter 4. PBOX-6 and -15 synergistically enhance the anti-cancer effects of carboplatin, etoposide and doxorubicin in neuroblastoma cells

4.1 Introduction 129
4.2 Results
4.2.1 PBOX-15 works in combination with other chemotherapeutics to reduce the viability of SHSY5Y cells 132
4.2.2 The effect of PBOX-6 and -15 in combination with a number of current chemotherapeutics used to treat neuroblastoma 134
4.2.3 PBOX-6 synergistically increases the apoptotic effect of carboplatin 72hrs hours post treatment in drug sensitive and multidrug resistant neuroblastoma cell lines 145
4.2.4 A combination of PBOX-6 and carboplatin enhances PARP cleavage in SHSY5Y cells 153
4.2.5 The effect of PBOX-6/carboplatin combination of Bcl-2 family members. 156
4.2.6 The PBOX-6/carboplatin combination induces depolarisation of the mitochondrial membrane and release of cytochrome-c 160
4.2.7 Involvement of caspase-3, 8 and -9 in the apoptotic pathway induced by the PBOX-6/carboplatin combination 162
4.2.8 Knockdown of Mcl-1 sensitises SHSY5Y and CHLA-90 cells to carboplatin 167
4.2.9 PBOX-6 significantly decreases tumour volume in a mouse model of neuroblastoma 170
4.3 Discussion 173

Chapter 5. Investigation into the role of the AMPK/mTOR signalling pathways in PBOX-induced apoptosis in neuroblastoma cells

5.1 Introduction 182
5.2 Results
5.2.1 PBOX-6 activates AMPK in SHSY5Y cells 186
5.2.2 PBOX-6 induces production of reactive oxygen species 188
5.2.3 Pretreatment with the antioxidant N-acetylcysteine inhibits the PBOX-6 mediated activation of AMPK 191
5.2.4 The antioxidant N-acetylcysteine protects against the anti-proliferative effects of PBOX-6 and -15 193
5.2.5 Pretreatment with N-acetylcysteine reduces PBOX induced apoptosis 197
5.2.6 PBOX-6 inhibits the mTOR signalling pathway in SHSY5Y cells 200
5.2.7 Pretreatment with the antioxidant N-acetylcysteine inhibits the 205

PBOX-6 mediated decrease in Mcl-1 expression
5.2.8 PBOX-6 induces autophagy in SHSY5Y cells 207
5.2.9 Inhibition of autophagy enhances PBOX-6 induced apoptosis in SHSY5Y cells 210
5.3 Discussion 219

Chapter 6. Concluding Remarks 231

Chapter 7. Future works 237

References 245

Appendix 276

Publications

Lennon *et al.*, 2014. Biochem Pharmacol. 76(4) 611-24.

List of figures

Figures

Chapter 1

Fig. 1.1	Clinical Presentation of neuroblastoma	4
Fig. 1.2	Structure of p-glycoprotein	19
Fig. 1.3	Structure of multidrug resistance protein-1	20
Fig. 1.4	Morphological changes during apoptotic cell death	22
Fig. 1.5	Activation of caspases	24
Fig. 1.6	The extrinsic and intrinsic pathway of apoptosis	26
Fig. 1.7	Structure of Bcl-2 proteins	28
Fig. 1.8	Proposed models to explain the control of MOMP by Bcl-2 proteins	29
Fig. 1.9	Structure of anti-apoptotic Mcl-1	31
Fig. 1.10	The Warburg Effect	36
Fig. 1.11	Regulation of AMPK	37
Fig. 1.12	The AMPK signalling pathway	38
Fig. 1.13	Structure of mTORC1 and mTROC2	40
Fig. 1.14	The mTOR signalling pathway	41
Fig. 1.15	Schematic diagram of the steps of autophagy	45
Fig. 1.16	The stages of the cell cycle	47
Fig. 1.17	The structure of microtubules	49
Fig. 1.18	Polymerisation dynamics of microtubules	50
Fig. 1.19	The binding sites of vinblastine, colchicine and paclitaxel on the tubulin polymer	53
Fig. 1.20	Structure of two representative pro-apoptotic members of the PBOX family, PBOX-6 and PBOX-15	53

Chapter 2

Fig. 2.1	Representative flow cytometric histograms of propidium iodide stained SHSY5Y cells.	65
Fig. 2.2	BSA standard curve used to determine protein concentration of cellular lysates	71
Fig. 2.3	Calculation of tumour volume	76

Chapter 3

Fig. 3.1	The linear relationship between SHSY5Y cell density and fluorescence	83
Fig. 3.2	Effect of ethanol and DMSO on viability of SHSY5Y cells.	85
Fig. 3.3	PBOX-6 reduces the viability of neuroblastoma cell lines	87
Fig. 3.4	PBOX-15 reduces the viability of neuroblastoma cell lines	88
Fig. 3.5	Vincristine reduces the viability of neuroblastoma cell lines	89
Fig. 3.6	Doxorubicin reduces the viability of neuroblastoma cell lines	90
Fig. 3.7	Etoposide reduces the viability of neuroblastoma cell lines	91
Fig. 3.8	Carboplatin reduces the viability of neuroblastoma cell lines	92

Fig. 3.9	Optimisation of seeding density of SHSY5Y cells for clonogenic assay	100
Fig. 3.10	PBOX-6 and 15 inhibit the clonogenicity of SHSY5Y cells	102
Fig. 3.11	PBOX-6 decreases the viability of primary neuroblastoma cells	106
Fig. 3.12	PBOX-6 and -15 induces apoptosis in SHSY5Y cells in a time-dependent manner	109
Fig. 3.13	PBOX-6 and -15 induces apoptosis in SHSY5Y cells in a dose-dependent manner	110
Fig. 3.14	PBOX-6 and -15 induces G2/M arrest in SHSY5Y cells	111
Fig. 3.15	PBOX-6 induces PARP cleavage in SHSY5Y cells	113
Fig. 3.16	PBOX-6 decreases the expression of anti-apoptotic Mcl-1 in a time and dose- dependent manner	116
Fig. 3.17	PBOX-6 induces phosphorylation and cleavage of anti-apoptotic Bcl-2 in SHSY5Y cells	117
Fig. 3.18	PBOX-6 increases the expression of pro-apoptotic Bak in SHSY5Y cells	118
Fig. 3.19	Bax expression is unaltered upon treatment with PBOX-6 in SHSY5Y cells	119

Chapter 4

Fig. 4.1	Combination of PBOX-15 and carboplatin enhanced the observed decrease in cell viability in SH5Y5Y cells	133
Fig. 4.2	PBOX-15 enhances the apoptotic effects of carboplatin in SHSY5Y cells.	137
Fig. 4.3	PBOX-6 enhances the apoptotic effects of carboplatin in SHSY5Y cells.	139
Fig. 4.4	PBOX-6 enhances the apoptotic effects of etoposide in SHSY5Y cells	141
Fig. 4.5	PBOX-6 enhances the apoptotic effects of doxorubicin in SHSY5Y cells	143
Fig. 4.6	PBOX-6 enhances the apoptotic effects of carboplatin in SHSY5Y cells 72hrs post treatment	147
Fig. 4.7	PBOX-6 enhances the apoptotic effects of carboplatin in CHLA-90 cells 48hrs post treatment	149
Fig. 4.8	PBOX-6 enhances the apoptotic effects of carboplatin in CHLA-90 cells 72hrs post treatment	151
Fig. 4.9	PBOX-6 and carboplatin alone and in combination induce cleavage of PARP	154
Fig. 4.10	A combination of PBOX-6 and carboplatin enhances PARP cleavage in SHSY5Y cells	155
Fig. 4.11	The PBOX-6/carboplatin combination reduces the expression of anti-apoptotic Mcl-1 and induces cleavage of Bcl-2 in drug sensitive and MDR neuroblastoma cell lines	157
Fig. 4.12	The PBOX-6/carboplatin combination induces activation of Bak in drug sensitive and MDR neuroblastoma cell lines	158
Fig. 4.13	Densitometric analysis of Mcl-1, Bcl-2 and Bak expression following treatment with PBOX.-6, carboplatin or a combination of PBOX-6 and carboplatin in SHSY5Y and CHLA-90 cells	159

Fig. 4.14	The PBOX-6/carboplatin combination evokes depolarisation of the mitochondrial membrane and the release of cytochrome c	161
Fig. 4.15	Apoptosis induced by the PBOX-6/carboplatin combination is caspase dependent in SHSY5Y and CHLA-90 neuroblastoma cell lines	164
Fig. 4.16	PBOX-6/carboplatin induces activation of caspase-3, -8 and -9	165
Fig. 4.17	Densitometric analysis of caspase-3. -8 and -9 activation following treatment with PBOX-6, carboplatin or a combination of PBOX-6 and carboplatin in SHSY5Y and CHLA-90 cells	166
Fig. 4.18	Optimisation of conditions for transfection efficiency in SHSY5Y and CHLA-90 cells	168
Fig. 4.19	Knockdown of Mcl-1 sensitises SHSY5Y and CHLA-90 cells to carboplatin	169
Fig. 4.20	Administration of PBOX-6 significantly inhibits tumour growth in an in vivo mouse model of neuroblastoma	172

Chapter 5

Fig. 5.1	PBOX-6 activates AMPK and inactivates ACC in SHSY5Y cells in a time dependent manner	187
Fig. 5.2	PBOX-6 induces production of reactive oxygen species.	190
Fig. 5.3	Pretreatment with NAC inhibits PBOX-6 mediated phosphorylation of AMPK and ACC in SHSY5Y cells	192
Fig. 5.4	PBOX-6 and -15 reduce the viability of SHSY5Y neuroblastoma cell lines.	194
Fig. 5.5	Pretreatment with the antioxidant NAC significantly inhibits the anti-proliferative effects of PBOX-6 in SHSY5Y cells	195
Fig. 5.6	Pretreatment with the antioxidant NAC significantly inhibits the anti-proliferative effects of PBOX-15 in SHSY5Y cells.	196
Fig. 5.7	Pretreatment with the antioxidant NAC significantly inhibits induction of apoptosis by PBOX-6 in SHSY5Y cells	198
Fig. 5.8	Pretreatment with the antioxidant NAC significantly inhibits induction of apoptosis by PBOX-15 in SHSY5Y cells	199
Fig. 5.9	PBOX-6 inhibits the mTOR signalling pathway in SHSY5Y cells in a time dependent manner	202
Fig. 5.10	PBOX-6 inhibits the mTOR signalling pathway in SHSY5Y cells in a time dependent manner	203
Fig. 5.11	Densitometric analysis of phospho-mTOR, mTOR, phospho-p70 S6 kinase, phospho-S6kinase and phospho-eEF2K expression in SHSY5Y cells	204
Fig. 5.12	Pretreatment with the antioxidant NAC inhibits PBOX-6 mediated decrease in Mcl-1 expression	206
Fig. 5.13	PBOX-6 induces autophagy in SHSY5Y cells as monitored by acridine orange staining of AVO and by the appearance of the LC3-II band by western blotting	209
Fig. 5.14	Chloroquine inhibits autophagy in SHSY5Y cells.	213
Fig. 5.15	Bafilomycin-A1 inhibits autophagy in SHSY5Y cells.	214
Fig. 5.16	Inhibition of autophagy enhances PBOX-6 mediated	215

	apoptosis in SHSY5Y cells.	
Fig. 5.17	Inhibition of autophagy enhances PBOX-6 mediated apoptosis in SHSY5Y cells.	216
Fig. 5.18	Autophagy inhibition enhances PBOX-6 mediated apoptosis though a decrease in anti-apoptotic Mcl-1, cleavage and inactivation of anti-apoptotic Bcl-2 and activation of executioner caspase-3	217
Fig. 5.19	Densitometric analysis of PARP, Mcl-1, Bcl-2 and pro-caspase-3 expression in SHSY5Y cells	218

List of tables

Tables

Chapter 1

Table 1.1	International Neuroblastoma Staging System	2
Table 1.2	International Neuroblastoma Risk Group	2
Table 1.3	Treatment strategies for neuroblastoma	12

Chapter 2

Table 2.1	Preparation of the H_2O_2 Substrate solution	67
Table 2.2	Preparation of ROS-Glo™ Detection Solution	67
Table 2.3	Optimisation of seeding density for clonogenic assay	68
Table 2.4	Preparation of BSA standards	71
Table 2.5	Composition of resolving and stacking gels used in SDS-PAGE	72
Table 2.6	Western blotting details for specific proteins	74
Table 2.7	Conditions for Neon transfection optimisation	75
Table 2.7	Recommended symbols for describing synergism or antagonism in drug combination studies analysed with the CI method	78

Chapter 3

Table 3.1	IC_{50} values of PBOX compounds and standard chemotherapeutic drugs in a range of neuroblastoma cell lines	93
Table 3.2	Fold resistance of PBOX-6, PBOX-15 vincristine, doxorubicin, etoposide and carboplatin in SK-N-BE(2)c cells in comparison to drug sensitive neuroblastoma cell lines	96
Table 3.3	Fold resistance of PBOX-6, PBOX-15 vincristine, doxorubicin, etoposide and carboplatin in CHLA-90 cells in comparison to drug sensitive neuroblastoma cell lines	97
Table 3.4	Fold resistance of PBOX-6, PBOX-15 vincristine, doxorubicin, etoposide and carboplatin in SK-N-FI cells in comparison to drug sensitive neuroblastoma cell lines	98
Table 3.5	Characteristics of neuroblastoma patient samples in *ex vivo* study	105

Chapter 4

Table 4.1	CI values of PBOX-15 in combination with carboplatin in SHSY5Y cells	138
Table 4.2	CI values of PBOX-6 in combination with carboplatin in SHSY5Y cells	140
Table 4.3	CI values of PBOX-6 in combination with etoposide in SHSY5Y cells	142
Table 4.4	CI values of PBOX-6 in combination with doxorubicin in SHSY5Y cells.	144

Table 4.5	CI values of PBOX-6 in combination with carboplatin in SHSY5Y cells	148
Table 4.6	CI values of PBOX-6 in combination with carboplatin in CHLA-90 cells	150
Table 4.7	CI values of PBOX-6 in combination with carboplatin in MDR CHLA-90 cells	152
Table 4.8	Conditions for Neon transfection optimisation	168

Abbreviations

4E-BP1	eukaryotic initiation factor 4E-binding protein
ABC	ATP-binding cassette
ACC	Acetyl-CoA carboxylase
ADCC	antibody-dependent cell-mediated cytotoxicity
AIF	apoptosis initiating factor
ALK	Anaplastic lymphoma kinase
ALL	Acute lymphocytic leukaemia
ATRA	all trans-retinoic acid
AML	Acute myeloid leukaemia
AMPK	5' AMP binding protein kinase
APAF-1	Apoptotic-protease activating factor-1
APC	anaphase promoting complex
APS	Ammonium persulphate
ATP	Adenosine triphosphate
Bak	Bcl-2 homologous antagonist/killer
Bax	Bcl-2 associated protein
Bcl-2	B-cell leukaemia/lymphoma-2
BCRP	Breast cancer resistant protein
BH domains	Bcl-2 homology domains
BMT	Bone marrow transplant
BSA	Bovine serum albumin
CADM1	Cell adhesion molecule 1
CARD	Caspase recruitment domain
CDK	Cyclin dependent kinase
CHD5	Chromodomain helicase DNA binding domain 5
CI	Combination index
CLL	Chronic lymphocytic leukaemia
CML	Chronic myeloid leukaemia
DD	Death domain
DED	Death effector domain
DMEM	Dulbecco's Modified Eagle Medium
DMEM/F12	Dulbecco's Modified Eagle Medium: Nutrient Mixture F-12
dH_20	Deionised water
DISC	Death inducing signalling complex
DMSO	Dimethyl sulphoxide
DNA	Deoxyribonucleic acid
DTT	Dithiothreitol
ECL	Enhanced chemoiluminescence
EFS	event-free survival
eEF2K	eukaryotic elongation factor 2
FACS	Fluorescent activated cell sorting analysis
FADD	Fas associated death domain
FasL	Fas ligand
GAP	GTPase activating protein
GM-CSF	granulocyte–macrophage colony-stimulating factor
HVA	homovanillic acid
IAP	Inhibitor of apoptosis protein
IC50	50% inhibitory concentration

Il-2	Interleukin-2
INSS	International Neuroblastoma Staging System
INRG	International Neuroblastoma Risk Group
JNK	c-Jun-N-terminal kinase
kDa	Kilodalton
LOH	loss of heterozygosity
mAB	Monoclonal antibody
MAP	microtubule associated proteins
Mcl-1	Myeloid leukaemia cell differentiation protein-1
Mdm2	mouse double minute homolog 2
MDR	Multidrug resistance
MTA	Microtubule targeting agent
MTOC	microtubule organising centre
mTOR	mammalian target of rapamycin
N.D	Not determined
NK	Natural killer
NT	No (drug) treatment
OS	Overall survival
p70 S6K	p70 ribosomal S6 kinase
PAGE	Polyacrylamide gel electrophoresis
PARP	Poly (ADP-ribose) polymerase
PBMC	Peripheral blood mononuclear cell
PBOX	Pyrrolo-1,5-benzoxazepine
PBR	Peripheral benzodiazepine receptor
PBS	Phosphate buffered saline
Pen-strep	Penicillin-streptomycin
PHOX2B	Paired-like homeobox 2b
PI3K	Phosphatidylinositol-4,5-bisphosphate 3-kinase
PIP2	Phosphatidylinositol-4,5-bisphosphate
PIP3	Phosphatidylinositol-3,4,5-trisphosphate
P-gp	P-glycoprotein
PI	Propidium iodide
PVDF	Polyvinylidene difluoride
RBC	Red blood cell
RNA	Ribonucleic acid
ROS	Reactive oxygen species
Rsk	ribosomal S6 kinase
SDS	Sodium dodecyl sulphate
SAC	spindle assembly checkpoint
S.E.M	Standard error of the mean
siRNA	Small interfering RNA
SMAC/DIABLO	second mitochondria-derived activator of caspases/direct IAP binding protein with low pI
ST1-571	Signal transduction inhibitor-571
TCA	tricarboxylic acId
TEMED	N,N,N′,N′-Tetramethylethylenediamine
TNF	Tumour necrosis factor
TRAIL	TNF receptor associated death domain
Tris	Tris(hydroxymethyl)aminomethane
w/v	Weight/volume
VMA	vanillylmandelic acid

xg	Times gravity

Abstract

Neuroblastoma, a malignancy of neuroectodermal origin, accounts for 15% of childhood cancer deaths. Despite both advances in understanding the biology of the cancer and aggressive treatment strategies, it continues to be one of the most difficult paediatric cancers to successfully treat. More than 60% of patients present at diagnosis with adverse features, and less than 40% of these achieve disease free long term survival. A major obstacle in the effective treatment of neuroblastoma is the development of multidrug resistance (MDR) to a broad range of cytotoxic drugs. This MDR phenotype often includes amplification of the proto oncogene MYCN, mutation/deletion of p53, deletion of loci at 1p or 11q and over expression of MDR proteins leading to altered drug transport and an increase in drug efflux. There is thus a compelling demand for new treatment strategies for this cancer that can bypass such resistance mechanisms.

The pyrrolo-1,5-benzoxazepine (PBOX) compounds are a series of novel microtubule-targeting agents that potently induce apoptosis in various cancer cell lines, *ex vivo* patient samples and *in vivo* cancer models. In the first part of this study, the ability of two members, PBOX-6 and -15, to reduce the viability of a panel of neuroblastoma cell lines was examined and found to exhibit a lower fold resistance in MDR cells when compared to standard chemotherapeutics. The effect of PBOX-6 and -15 on clonogenic survival of SHSY5Y cells, primary neuroblastoma cells isolated from bone marrow aspirates and an *in vivo* murine model of neuroblastoma, was also investigated while part of the molecular mechanism through which the PBOX-6 induces apoptosis in neuroblastoma cells was delineated.

PBOX-6 synergistically enhanced apoptosis induced by etoposide, carboplatin and doxorubicin. Exposure of drug sensitive and resistant cell lines to a combination of PBOX-6/carboplatin induced cleavage and inactivation of Bcl-2, a downregulation of Mcl-1 and a concomitant increase in pro-apoptotic Bak. Furthermore activation of caspase-3, -8 and -9 was demonstrated. Gene silencing of Mcl-1 by siRNA was shown to sensitise both drug sensitive and multidrug resistant cells to carboplatin-induced apoptosis demonstrating the importance of Mcl-1 downregulation in the apoptotic pathway mediated by the PBOX compounds in neuroblastoma.

In the final part of this study, the molecular events associated with Mcl-1 downregulation were investigated. PBOX-6 was shown to induce production of reactive oxygen species (ROS) leading to activation of 5'AMP-activated protein kinase (AMPK), the master regulator of cellular homeostasis. Pretreatment with the antioxidant N-acetylcysteine (NAC) inhibited both the production of ROS and activation of AMPK. The anti-proliferative and pro-apoptotic effects of the PBOXs were impaired by pretreatment with NAC, while the PBOX-6 mediated decrease in Mcl-1 expression was prevented. Investigation of the downstream targets of AMPK revealed PBOX- induced AMPK activation lead to inhibition of the mammalian target of rapamycin (mTOR) signalling pathway. This study proposes that the PBOX mediated decrease in Mcl-1 may be attributable to inhibition of the mTOR pathway, resulting in a block in Mcl-1 translation. Finally PBOX-6 was shown to induce autophagy in neuroblastoma cell which may function as a survival mechanism as pretreatment with autophagy inhibitors, chloroquine and bafilomycin-A1, significantly enhanced PBOX-induced apoptosis. This provides a rationale for the use of autophagy inhibitors to further promote PBOX-6-induced apoptosis in neuroblastoma.

In conclusion, this study has demonstrated the ability of novel PBOXs to induce apoptosis in drug sensitive and resistant cell lines, to reduce the viability of *ex vivo* patient samples, to synergise with current treatments for neuroblastoma and to reduce tumour burden in an *in vivo* murine model of neuroblastoma, indicating the potential of the novel PBOX compounds, either alone or in combination, for the treatment of drug sensitive and multidrug resistant neuroblastoma. This study provides new insights into understanding the molecular and cellular mechanisms involved in PBOX-6-induced cell death.

Presentations, publications and awards

Presentations

February 2012 I.A.C.R, Belfast
Poster presentation

December 2012 National Children's Research Centre Research Symposium
Oral presentation

February 2013 I.A.C.R, Dublin
Poster presentation

December 2013 National Children's Research Centre Research Symposium
Oral presentation

January 2014 E.A.C.R Cell Death in Cancer meeting, Amsterdam
Poster presentation

Publications

Lennon JC, Bright SA, Carroll E, Butini S, Campiani G, O'Meara A, Williams DC, Zisterer DM. The novel pyrrolo-1,5-benzoxazepine, PBOX-6, synergistically enhances the apoptotic effects of carboplatin in drug sensitive and multidrug resistant neuroblastoma cells. Biochem Pharmacol. 2014 Feb 15;87(4):611-24.

Awards

Recipient of prize for best poster presentation at the 'Discover Research Night' Dublin 2013.

Chapter 1

Introduction

1.1 Neuroblastoma

The paediatric malignancy neuroblastoma is a neoplasm of the sympathetic nervous system, which arises in cells of the neural crest (Cheung *et al.*, 2013). Cells of the neural crest migrate from the neural tube to give rise to a number of differentiated cell types which control the function of multiple organs including the liver, lungs and stomach (Nelson., 2011). Since the 1970s the incidence of cancer in children has been steadily increasing (Nuchtern *et al.*, 2012) and although neuroblastoma is relatively rare, it is the most commonly diagnosed tumour in the first year of life and is the most common extra cranial solid tumour in early childhood, accounting for 15% of cancer deaths in young children (Maris *et al.*, 2010). Approximately 37% of patients diagnosed are under twelve months while 90% are less than five years (Maris *et al.*, 2010) with the median age of diagnosis being 19 months.

In spite of both advances in understanding the biology of the cancer and aggressive treatment strategies, including surgery, chemotherapy, radiation therapy, immunotherapy and differentiation therapy, it continues to be one of the most difficult paediatric cancers to successfully treat with more than 60% of patients classified as high risk, with less than 40% of these patients being long term survivors (Cheung *et al.*, 2013). Many of these patients develop a progressive disease with failure to respond to chemotherapy.

1.1.1 Classification and Staging

Newly diagnosed patients are classified into one of a number of possible risk groups/stages based on a number of different staging strategies. The first is the International Neuroblastoma Staging System (INSS), first developed in 1988; this is a post-operative staging system which uses the extent of surgical resection to classify patients (Brodeur *et al.*, 1988). Due to variability between different surgeons in different countries and advance in our knowledge of the biology and genetics of this cancer, this system has been updated to incorporate newer biological factors into the INSS (Brodeur *et al.*, 1993). In this system patients are classified into one of six stages (1, 2A, 2B, 3, 4, 4S) ranging from stage 1 in which the tumour is confined to the area of origin and can be completely

excised by surgery to stage 4 in which the primary tumour has metastasised to distant lymph nodes, bone marrow and other organs including the liver and skin (Table 1.1).

Stage 1	The tumour can be removed completely during surgery. Lymph nodes removed during surgery may or may not contain cancer, but other lymph nodes near the tumour do not.
Stage 2A	The tumour is located only in the area it started and cannot be completely removed during surgery. Nearby lymph nodes do not contain cancer.
Stage 2B	The tumour is located only in the area where it started and may or may not be completely removed during surgery. Nearby lymph nodes contain cancer.
Stage 3	The tumour cannot be removed with surgery. It has spread to regional lymph nodes (lymph nodes near the tumour) or other areas near the tumour, but not to other parts of the body.
Stage 4	The original tumour has spread to distant lymph nodes (lymph nodes in other parts of the body), bones, bone marrow, liver, skin, and/or other organs (except for those listed in stage 4S, below).
Stage 4S	The original tumour is located only where it started (as in stage 1, 2A, or 2B), and it has spread only to the skin, liver, and/or bone marrow (in infants younger than one). The spread to the bone marrow is minimal (usually less than 10% of cells examined show cancer).

Table 1.1 International Neuroblastoma Staging System. Taken from Brodeur *et al.*, (1993).

A second staging system, the International Neuroblastoma Risk Group (INRG) Staging System is a pre-operative, pre-treatment classification system which uses imaging tests taken before surgery and in contrast to the INSS, does not include surgical results or spread to lymph nodes to determine the stages as described in Table 1.2.

Stage L1	The tumour is located only in the area where it started; no risk factors found on imaging scans, such as CT or MRI.
Stage L2	The tumour has not spread beyond the area where it started and the nearby tissue; risk factors are found on imaging scans, such as CT or MRI.
Stage M	The tumour has spread to other parts of the body (except stage MS, see below).
Stage MS	The tumour only has spread to the skin, liver, and/or bone marrow.

Table 1.2 International Neuroblastoma Risk Group. Taken from Cohen *et al.*, (2009).

Patients may also be classified based on the Children's Oncology Group Neuroblastoma Risk Stratification System which divides patients into three groups (low, intermediate or high risk) based on the stage of the disease according to the INSS system, age at diagnosis, *MYCN* gene status, tumour ploidy and tumour histopathology (Cohen *et al.*, 2009). In addition to these three groups a subset of patients (approximately 5% of all cases), classified as 4S, are diagnosed with an advanced disease but have a favourable outcome (van Noesel *et al*, 2012). These children, less than one year, present with a small tumour localised to the adrenal gland and metastases present in the liver and skin but limited to less than 10% in the bone marrow (Cohen *et al*, 2009). These patients can be classified as low risk as the disease is often coupled with a high rate of spontaneous regression with a 75-90% survival rate (Bénard *et al.*, 2008). Spontaneous regression is as yet an unexplained phenomenon which is most commonly observed in infants less than 6 months with stage 1, 2, or 3 tumours without MYCN amplification. Other common features include tumours with a near triploid number of chromosomes, no MYCN amplification, and no loss of chromosome 1p. One hypothesis has been proposed to account for this response is the expression of telomerase. High expression is associated with poor response rate in neuroblastoma. Inhibition of telomerase may result in genomic crisis leading to tumour regression as in neuroblastoma where telomere shortening has been shown to correlate with tumour regression (Hiyama *et al.*, 2003).

1.1.2 Presentation

The presentation of neuroblastoma is extremely variable, ranging from an asymptomatic mass to a tumour which has widely metastasised causing a life threatening illness. Initial symptoms can be ambiguous but the most common presentation is the presence of a growth in the abdomen (65% of cases) but also the neck or chest (Cheung *et al.*, 2013). The majority of symptoms are due to the presence of a tumour or metastasis from the primary site. These include abdominal distension, bone pain, fever, anaemia, hypertension and paralysis (Fig. 1.1). Other symptoms include dark circles around the eyes, lumps under the skin and weakness (Mueller *et al.*, 2009).

Stage 1 tumours are frequently present in one location and can be successfully removed by surgery. During the later stages of the disease, tumour cells spread through the

haematopoietic system to regional lymph nodes and the bone marrow (Maris *et al.*, 2010). Surgery is often ineffective in this more advanced condition as tumours surround critical nerves and blood supply. Tumours can arise anywhere along the sympathetic nervous system with the majority occurring in the adrenal medulla. Primary tumours can occur in the neck, upper chest and along the spinal cord causing paralysis. Tumour cells can metastasise and invade the bone marrow and liver.

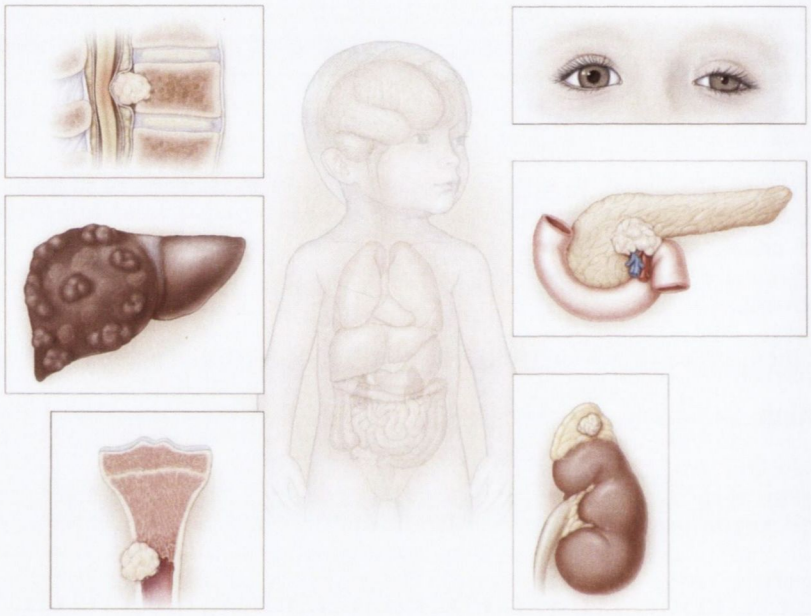

Figure 1.1 Clinical presentation of neuroblastoma.

Tumours can arise anywhere along the sympathetic nervous system, with the majority occurring in the adrenal medulla. They can spread along the spinal column causing cord compression with resulting paralysis. Late stage tumours can infiltrate the organs surrounding critical nerves and blood vessels rendering them unresectable. Tumours can metastasise through the hematopoietic system to distant sites, most notably the bone marrow. Taken from Maris *et al.*, (2010).

1.1.3 Diagnosis

Diagnosis of neuroblastoma requires thorough clinical investigation to distinguish it from other paediatric cancers. Under a light microscope neuroblastoma cells cannot be discriminated from other childhood tumours such as lymphoma, therefore various diagnostic methods are utilised such as immunohistochemistry and imaging. A urine vanillylmandelic acid (VMA)/homovanillic acid (HVA) test is given to monitor levels of

catecholamines such as adrenaline and noradrenalin as neuroblastoma cells have been shown to produce these hormones resulting in elevated levels (Strenger *et al.*, 2007). Patients may undergo a CT or MRI scan to determine the size, location and possible metastasis of the tumour. A biopsy will be taken to collect a sample of the primary tumour. An extensive panel of diagnostic tests will be undertaken on this sample such as MYNC amplification status, chromosomal abnormalities and DNA index. A biopsy may also be taken to determine the presence or absence of tumour cells in the bone marrow.

1.1.4 Genetic abnormalities associated with neuroblastoma

Numerous genetic abnormalities have been identified to be associated with neuroblastoma, the majority of which occur at the somatic level. There are multiple reports in the literature detailing associations of genomic alterations with tumour phenotype, with regional deletions often reported as being a marker for disease progression and failure to respond to treatment (Brodeur *et al.*, 2003; Caren *et al.*, 2010; Schleiermacher *et al.*, 2012). The incidence of chromosomal aberrations increases with age at diagnosis and is strongly indicative of patient outcome (Cheung *et al.*, 2013). These genetic alterations include activation of oncogenes such as *MYCN*, changes in DNA content, whole chromosome gain or losses or structural chromosomal rearrangements. In general, low-risk, intermediate-risk and stage 4S neuroblastomas exhibit chromosomal gains such as chromosome 1q, 11p and 17q, whereas high-risk neuroblastomas have intrachromosomal rearrangements such as loss of heterozygosity at 1p36 or 11q (Maris *et al.*, 2010).

1.1.4.1 Ploidy

Non-malignant cells are diploid in contrast to neuroblastoma cells which become aneuploid meaning 'without normal ploidy' or hyperploid. Levels of DNA ploidy can differ in patients depending on the stage of the disease allowing for DNA content to be used as a prognostic indicator (Janoueix-Lerosey *et al.*, 2009). Low risk neuroblastoma is usually hyperdiploid or triploid and is associated with earlier stages of disease, which responds better to chemotherapy, and usually predicts a more favourable prognosis. Ploidy is only a useful prognostic indicator up until the age of two. A link between ploidy and other

chromosomal aberrations has been noted; near triploid tumours exhibit a whole chromosomal gain of 17q associated with a favourable prognosis in contrast to near diploid tumours exhibiting an unbalanced 17q gain (Vermeulen *et al.*, 2010).

1.1.4.2 MYCN amplification

MYC proteins are a family of proto-oncogenes which orchestrate expression of 10-15% of all cellular genes including those involved in cell cycle, survival, adhesion and metabolism (Hoffmann *et al.*, 2008). They are a basic helix loop helix leucine zipper transcription factor which forms heterodimers with MAX, another transcription factor, and together they bind to E box sequences in promoter regions in target genes, directly driving transcription of genes which participate in multiple cellular pathways including cell division, apoptosis and differentiation (Grotzer *et al.*, 2009). They are among the most frequently affected genes in human cancers, including neuroblastoma. One member of this family, c-Myc, has been shown to play a critical role in the apoptotic response by either inducing apoptosis directly or by sensitising cells to apoptosis. Normally a cell with aberrant Myc expression will be eradicated by induction of apoptosis whilst in cells with defective apoptosis, overexpression of Myc may promote tumourigenesis (Hoffman *et al.*, 2008). Myc amplification has been shown to transform cells though a number of mechanisms such as induction of angiogenesis, increased DNA instability, an increase in cell growth, metabolism and protein synthesis, through upregulation of several proteins, including EIF2A and EIF4A, and repression of adhesion proteins integrin and N-cadherin, allowing for anchorage-independent growth (Grzmil *et al.*, 2012).

Amplification of MYCN, mapping to 2p24.1, was first identified in neuroblastoma patient samples by Schwab *et al.,* (1989) and to this day remains one of the most important prognostic indicators with amplification correlating with disease progression, development of drug resistance and poor prognosis (Huang *et al.*, 2013). Since this initial discovery, amplification has been defined as the presence of more than 10 gene copies per diploid genome. Like other members of the MYC family, this 60-63 kDa transcription factor heterodimerises with MAX and binds to E box sequences in promoter regions of target genes supporting tumour progression through increased proliferation, angiogenesis and metastasis, while simultaneously suppressing apoptosis. *In vivo* studies

have provided evidence to support the role of MYCN amplification in the tumourigenesis of neuroblastoma. Ectopic expression of MYCN was sufficient to drive tumourigenesis in zebrafish (Zhu *et al.*, 2012) while overexpression of MYCN in the neural crest cells of transgenic mice lead to the development of neuroblastoma within several months (Weiss *et al.*, 1997).

The mechanism underlying amplification is still unknown. High levels of amplification are observed in approximately 5% of stage 1 and 2 patients, 10% stage 4S and 30% of stage 3 and 4 patients with an overall incidence of approximately 20-25% of cases of neuroblastoma (Althoff *et al.*, 2014). Amplification is associated with advanced disease with an unfavourable outcome. The 3-year event-free survival (EFS) of infants whose tumours lacked *MYCN* amplification was 93% but was only 10% for those with tumours that had *MYCN* amplification (Schmidt *et al.*, 2000). Currently there are no clinical trials targeting the MYCN protein directly in neuroblastoma due to the difficulties associated with developing therapies that directly target transcription factors.

1.1.4.3 p53

p53, commonly referred to as the guardian of the genome, is a tumour suppressor protein encoded by the TP53 gene. It is a nuclear phosphoprotein which has a pivotal role in the regulation of cell growth, apoptosis, DNA stability and inhibition of angiogenesis (Lane *et al.*, 1992); therefore, it is a critical anti-cancer protein. Normally present at low levels in the cell in response to stresses such as DNA damage, it accumulates in the nucleus and binds to DNA to activate the transcription of a number of target genes involved in various cellular pathways such as apoptosis, cell cycle arrest and DNA damage repair (Muller *et al.*, 2013). The activity of p53 is regulated though interaction with mouse double minute homolog 2 (Mdm2); binding of Mdm2 to the N-terminus transactivation domain blocks p53's transcriptional activity, transports it from the nucleus to the cytoplasm and targets it for degradation by the proteasome creating an autoregulatory feedback loop to tightly regulate p53 levels. MDM2 binding to p53 may be inhibited by $p14^{ARF}$ to maintain p53 in its active state. $p14^{ARF}$ binds to the central domain of Mdm2, keeping Mdm2 in the nucleolus leading to inhibition of the Mdm2-p53 interaction (Muller *et al.*, 2013). The release of p53 from MDM2 results in p53 accumulation and activation of

the p53 pathway leading to potent antitumor effects such as cell cycle arrest, apoptosis and cellular senescence (van Maerken *et al.*, 2014).

p53 is mutated in over 60% of cancers offering a selective advantage to tumour cells, as induction of p53 can activate DNA repair and apoptotic pathways following treatment with chemotherapeutic drugs (Petroni *et al.*, 2012). Expression of wild-type p53 generally correlates with response to chemotherapy and a more favourable prognosis. MYCN drives transcription of Mdm2 in neuroblastoma cells (Slack *et al.*, 2005; Chen *et al.*, 2009) resulting in inhibition of p53. In contrast to many other cancers, in neuroblastoma p53 is rarely mutated at diagnosis but has been found to be inactive (Petroni *et al.*, 2012). Studies of relapsed neuroblastoma patient samples found p53 to be inactivated in one third of cases (Carr-Wilkinson *et al.*, 2010). 49% of relapsed neuroblastoma tumour samples exhibited abnormalities in the p53 pathway at diagnosis, while p53 was mutated in 65% of these cases. Inactivation occurred through a variety of mechanisms including amplification of Mdm2 or inhibition of $p14^{ARF}$ activity. Furthermore, studies have found that the incidence of mutation increases after chemotherapy (Petroni *et al.*, 2012). Neuroblastoma patients tend to respond to therapy initially and later develop drug resistance. This initial response to chemotherapy may be attributed in part to functional p53.

Restoration of p53 has already been proved to be effective in promotion regression of tumours in *in vivo* models, while strategies aimed at restoration of p53 function are currently undergoing clinical trials (Cheok *et al.*, 2011; Khoo *et al.*, 2014). These strategies include p53 gene therapy, wild type p53 restoration via small molecule/Mdm2-antagonists and mutant-p53 folding restoration. As discussed above, Mdm2 is a negative regulator of p53 whose transcription is driven by MYCN in neuroblastoma. Nutlins are a family of *cis*-imidazoline compounds that have been developed to selectively and potently disrupt the p53–Mdm2 interaction (Vassilev *et al.*, 2004). Inhibition of the MDM2/p53 interaction by Nutlin-3 is currently under investigation (Chen *et al.*, 2014). In a panel of 18 neuroblastoma cell lines treated with Nutlin-3, Gamble *et al.*, (2012) found that the cell lines which were MYCN amplified had increased caspase 3/7 activity compared with the non-MYCN-amplified group of cell lines, but p53 mutant cell lines were resistant to the antagonists regardless of MYCN status. They concluded that amplification or

overexpression of MYCN sensitises neuroblastoma cell lines with wild-type p53 to MDM2-p53 antagonists, and that these compounds may therefore be particularly effective in treating high-risk MYCN-amplified disease.

1.1.4.4 1p Loss of Heterozygosity

Cytogenetic analysis has identified a loss of heterozygosity (LOH) at chromosome 1, occurring in 20-35% of primary neuroblastoma tumours, (van Noesel *et al.*, 2004) involving a deletion or unbalanced translocation resulting in the loss of genetic material from the distal short arm of chromosome 1.

This aberration is frequently associated with amplification of *MYCN* and is found in approximately 70% of aggressive neuroblastomas (Fong *et al.*, 1989). 1p LOH can also serve as a prognostic indicator as it not only is associated with advanced disease but also with a decrease in EFS (Attiyeh *et al.*, 2005). It has been established that the presence of 1p LOH correlates with a metastatic disease in comparison to localised tumours with an intact 1p. Fong *et al.*, (1989) found that 62% of tumours that had the 1p deletion were MYCN amplified compared with only 3% of 1p intact tumours.

Several potential tumour suppressor genes in the 1p LOH genetic subtype have been identified. One of the first was the chromodomain helicase DNA binding domain 5 (*CHD5*), mapping to 1p36.31 (Thompson *et al.*, 2003). Analysis of CHD5 in primary tumours and cell lines found very low levels of CDH5 which correlated with 1p LOH, *MYCN* amplification and advanced disease. Later *in vivo* studies supported these reports where overexpression of CHD5 inhibited tumour growth (Fujita *et al.*, 2008). More recently it has been suggested that loss of CHD5 contributes to tumour formation by preventing neuroblasts from undergoing terminal differentiation (Egan *et al.*, 2013). Other potential tumour suppressor genes mapping to this region include the transcription factors *CAMTA*1 (Heinrich *et al.*, 2011) and *CASZ1* (Liu *et al.*, 2011).

1.1.4.5 11q deletion

Another common structural chromosomal aberration associated with poor prognostic outcome is 11q LOH which occurs in approximately 40–45 % of cases, (Guo *et al.*, 1999)

with a small subset of patients exhibiting both 11q LOH and MYCN amplification. Plantaz *et al.,* (2001) performed comparative genomic hybridisation analysis on 50 patients with stage 4 neuroblastoma and found a high incidence of the 11q deletion, while only 15% of patients were also MCYN amplified. This was in contrast to 59% without the amplification suggesting that *MYCN* amplification and 11q LOH are independent markers of disease progression. Maris *et al.,* 2005 found that the deletion correlated with acquisition of metastasis, a marker of late stage aggressive disease. Since 2009, LOH at 11q has been included in the INRG classification system (Cohen *et al.*, 2009).

Similar to 1p LOH, efforts have been made to identify genes on the 11q chromosome which contribute the pathology of neuroblastoma but to date few genes have been identified. Cell adhesion molecule 1 (*CADM1*) has been identified as a novel tumour suppressor gene in neuroblastoma. This gene maps to 11q23 and encodes a cell adhesion protein which has a role in neural cell development (Michels *et al.*, 2008). Loss of *CADM1* expression has been described in many malignancies, including liver, pancreatic, breast, brain and prostate cancers, particularly in those showing invasion or metastasis (Heller *et al.*, 2007). In neuroblastoma, loss of *CADM1* expression has been found in disseminated tumours with adverse outcome (Nowacki *et al.*, 2008; Ando *et al.*, 2008). Overexpression of *CADM1* in neuroblastoma cells resulted in significant reduction of proliferation, viability and colony formation in soft agar suggesting that downregulation of *CADM1* tumour suppressor gene expression is crucial for tumour progression and unfavourable prognosis (Nowacki *et al.*, 2008).

1.1.5 Familial Neuroblastoma

A small percentage of cases of neuroblastoma have a familial origin due to a genetic predisposition. Mutations in Anaplastic lymphoma kinase (*ALK*) gene, located on chromosome 2 at position p23 and Paired-like homeobox 2b (*PHOX2B*) gene, located on chromosome 4 at position p12 are the two most common genetic changes associated with familial neuroblastoma with alterations in *ALK* being the most common (Mosse *et al.*, 2004; 2008; Chen *et al.*, 2008). Both of these genes are critical for normal nervous system development; *ALK* encodes a receptor tyrosine kinase which is widely expressed in the nervous system. *ALK* related susceptibility occurs in people who are heterozygous for a germline mutation in *ALK* (Hallberg *et al.*, 2013) in the kinase domain to promote *ALKs*

kinase activity leading to cellular transformation. Mutations that result in oncogenic activation can be acquired through somatic changes in between 5-15% of neuroblastoma patients. Phase 1 clinical trials have recently been completed which investigated the use of Crizotinib, a small molecule inhibitor of *ALK*, for the treatment of patients harbouring the ALK mutation (Mosse *et al.*, 2013). Patients displayed minimal toxicity despite high doses of the drug while 50% of patients with the *ALK* mutation entered remission.

1.2 Current Treatments

Most cases of neuroblastoma are treated by conventional means e.g. surgery, radiation therapy and chemotherapy with treatment regime being dependent on the stage of the disease (Table 1.3). Recently a trend has emerged which has seen a reduction in therapeutic intensity for patients with early stage low risk disease; tumours may regress without therapeutic intervention or differentiate into a benign ganglioneuroblastoma (Zage *et al.*, 2011). Doctors may employ the 'wait and see' approach employing screening and observation while avoiding surgical intervention, therefore, thwarting any possible complications of surgery in the newborn (Cozzi *et al.*, 2013). This approach is supported by studies which have reported that 81% of early stage, low risk patients undergo spontaneous regression without surgical intervention, while the three year EFS was 97% and overall survival (OS) was 100% (Hara., 2012). In cases where surgery fails to eliminate the tumour completely, patients undergo low dose chemotherapy including etoposide, doxorubicin, and carboplatin (Strother *et al.*, 2012). Radiation therapy is introduced if chemotherapy is not successful. Chemotherapy for intermediate risk patients encompasses four to eight cycles of multiple chemotherapeutics. It is generally started before the patient undergoes surgery and involves chemotherapeutics including carboplatin, cyclophosphamide, doxorubicin, and etoposide. More recently topoisomerase I inhibitors have shown efficacy in the clinic with a 30-50% response rate in newly diagnosed patients (Hara., 2012).

The current treatment of high risk neuroblastoma patients involves induction therapy consisting of 4–9 months of high dose myeloablative chemotherapy, surgical tumour removal, autologous stem cell transplantation and 6–12 months maintenance therapy. The aim of chemotherapy is to achieve a complete and lasting remission through

reduction of tumour burden at the primary and metastatic sites. Treatment can be divided into three phases; induction, consolidation of remission and maintenance of remission. The primary tumour is generally resected during or shortly after the induction phase while patients receive radiation therapy at the primary and if necessary metastatic sites. The aim of the consolidation phase is to reduce the tumour burden as much as possible before the tumour cells acquired multidrug resistance. Finally, the aim of the maintenance phase is to eradicate any remaining malignant cells as the patient enters remission. In addition to conventional chemotherapy patients with high risk neuroblastoma may undergo radiation therapy, stem cell or bone marrow transplantation or retinoic acid therapy. Retinoids are derivatives of vitamin A, and include all trans-retinoic acid (ATRA), 13-cis-retinoic acid, (13-cis-RA), and fenretinide (4-HPR) which induce neuroblastoma cell differentiation.

Stage	Treatment Options
Low-Risk Neuroblastoma	Surgery followed by observation.
	Chemotherapy with or without surgery (for symptomatic disease or unresectable progressive disease after surgery).
	Observation without biopsy (for perinatal neuroblastoma with small adrenal tumours).
Intermediate-Risk Neuroblastoma	Chemotherapy with or without surgery.
	Surgery and observation (in infants).
	Radiation therapy (only for emergent therapy).
High-Risk Neuroblastoma	A regimen of chemotherapy, surgery, SCT, radiation therapy, and anti-GD2 antibody ch14.18, with interleukin-2/GM-CSF and isotretinoin.
Stage 4S Neuroblastoma	Observation with supportive care (for asymptomatic patients with favourable tumour biology).
	Chemotherapy (for symptomatic patients, very young infants, or those with unfavourable biology).

Table 1.3 Treatment strategies for neuroblastoma

Although the immune system can recognise and eliminate malignant cells, cancers such as neuroblastoma can often escape immune surveillance, allowing them to spread and ultimately cause death (Cheung *et al.*, 2013). Immunotherapy is a strategy being employed for the treatment of neuroblastoma which aims to redirect the immune system to target tumours and tumour-associated antigens, leading to the elimination of malignant cells. Multiple forms of immunotherapy are being used in the clinic. GD_2 is a

surface glycolipid antigen that is ubiquitously expressed on neuroblastoma cells and neuroblastoma patient samples (Ritter *et al.*, 1991) while expression of this antigen in non-malignant cells is limited to neurons and peripheral pain fibers which are protected from the effects of anti-GD_2 therapy by the blood brain barrier (Svennerholm *et al.*, 1994). Murine IgG3 monoclonal antibody 3F8 was the first monoclonal anti-GD_2 antibody to undergo pre-clinical testing in neuroblastoma patients (Cheung *et al.*, 1998). It was shown to target neuroblastoma cells particularly metastatic cells within the bone marrow while other murine anti-GD2 mAbs Ch14.18 and Ch14.G2 have also been developed (Kowalczyk *et al.*, 2009; Yu *et al.*, 2010).

Antibodies can mediate destruction of tumour cells through complement mediated cytotoxicity (Esser *et al.*, 2012). The variable region of the antibody binds to antigen on the tumour cell; the Fc portion of the antibody can bind to the Fc receptor on immune cells such as monocytes, macrophages, neutrophils and natural killer (NK) cells and stimulate tumour cell lysis via antibody-dependent cell-mediated cytotoxicity (ADCC). In order to kill a malignant cell, an antibody must recognise and bind to the tumour cell for long enough to avoid internalisation allowing adequate immune signalling. The activated immune cell must be able to create a destructive signal such as activation of ADCC (Sondel *et al.*, 2001). However, ADCC is often compromised in cancer patients due to immune suppression from metastatic cancer and/or chemotherapy (Marleau *et al.*, 2012). Therefore cyctokines such as interleukin-2 (IL-2) or granulocyte–macrophage colony-stimulating factor (GM-CSF) that activate cells to mediate enhanced ADCC may enhance the efficacy of immunotherapy. Ch 14.18 is a chimeric human–murine anti-GD2 monoclonal antibody, which has undergone clinical testing as both a single agent and in combination with GM-CSF or IL-2 to enhance antibody-dependent cell-mediated cytotoxicity. Results from a recently completed phase two clinical trial indicate that the inclusion of immunotherapy resulted in significantly superior EFS and OS when compared with standard chemotherapy (66% versus 42% for EFS) (Yu *et al.*, 2010). Future development of immunotherapy is warranted to identify more effective and less toxic ways to stimulate ch14.18-mediated antibody-dependent cell-mediated cytotoxicity, and to identify more efficacious GD_2-targeted monoclonal antibodies.

For children with high-risk neuroblastoma, with the current treatment strategies employed long term survival rates stand at approximately 54% (Maris *et al.*, 2010) while children with aggressively treated, high-risk neuroblastoma have approximately a 60% chance of relapse within 5 years after completion of therapy. Therefore, it is clear there is a need for new treatment strategies to improve mortality rates.

1.3 Novel treatment strategies

Conventional treatment regimes although successful for low risk neuroblastoma have not achieved the desired survival rates for high risk patients, where clinical outcome remains poor and chemoresistant relapse is frequent following high-intensity conventional therapy. Additional use of combination chemotherapy generally results in a temporary control of this cancer. It is clear novel treatment strategies are necessary to improve survival rates of these high risk patients.

One approach currently under investigation is immunotherapy; the conjugation of monoclonal antibodies to agents for site directed delivery of toxins, chemotherapeutic agents, radioactive isotopes, and immunological agents to the tumour site. Radiolabeled monoclonal antibodies have been used for both disease detection and targeted treatment of a variety of adult cancers but very few childhood malignancies. However, radioimmunotherapy is an attractive strategy due to the tendency of this cancer to be radiosensitive (Modak *et al.*, 2005). By employing this approach, high dose radiation can be delivered to the tumour while sparing the surrounding tissues from the toxic effects of radiation. A phase I clinical trial has demonstrated the feasibility of radioimmunotherapy for patients with GD_2-expressing neoplasms using the anti-GD2 murine monoclonal antibody 3F8 labelled with ^{131}I (Kramer *et al.*, 2007). Another murine monoclonal antibody, 8H9, is specific for 4Ig-B7H3, a 58 kDa surface immunomodulatory glycoprotein that inhibits natural killer cells and T cells. This B7-H3 protein is preferentially expressed on a number of paediatric and adult solid tumours when compared to normal human tissues (Modak *et al.*, 2001). When radiolabeled with ^{131}I, 8H9 can deliver therapeutic doses of radiation to solid tumours and suppress tumour cell growth in established xenografts (Modak *et al.*, 2005). Treatment with ^{131}I-3F8 has been shown to be well tolerated with no serious delayed toxicities observed (Bhandari *et al.*, 2010). Kramer *et*

al., (2010) evaluated the addition of radioimmunotherapy in patients with recurrent metastatic neuroblastoma and found it to improve the survival of this cohort of patients.

Natural killer (NK) cells represent one of the most promising anti-tumour strategies against neuroblastoma (Moretta *et al.*, 2011). Tumour cells express cell surface molecules which can engage NK cells to regulate their activity. Tumours which express human leukocyte antigen (HLA class I molecules negatively regulate NK function while NK cells may be activated by expression of non-MHC class I 'danger' molecules on tumour cells (Bottino *et al.*, 2014). Tumour cells have little to no HLA expression rendering them susceptible to NK mediated killing. Liu *et al.*, (2013) has reported efficient *ex vivo* growth and activation of NK cells from the blood of neuroblastoma patients which maintain potent anti-neuroblastoma activity. It has been suggested that repeated infusion of NK cells and anti-tumour antibodies may potentially treat minimal residual disease. A phase I clinical trial investigating the feasibility of treating neuroblastoma with chemotherapy (cyclophosphamide, vincristine and topotecan) and infusion of NK cell and 3F8 is currently being undertaken (ClincalTrials.gov: NCT00877110).

As discussed above, neuroblastomas can escape immune surveillance through downregulation of MHC molecules which are required for antigen presentation (Neefjees *et al.*, 2011). Few clinical trials have been conducted to determine whether an immune response could be exploited to fight neuroblastoma due to the limited number of because potential tumour antigens. Cancer-testis (CT) antigens are a category of tumour antigens which are normally expressed on male germ cells in the testis but are also commonly expressed on a number of solid tumours including neuroblastoma. Members of this family include MAGE-A1, MAGE-A3, and NY-ESO-1. Many cell lines have been shown to downregulate expression of these antigens therefore in order for cancer-testis antigens to be a viable therapeutic target; expression of these antigens would need to be pharmacologically enhanced. Decitabine (5-aza-2'-deoxycytidine [DAC]), a homomethylating agent which inhibits DNA methyltransferase (Klco *et al.*, 2013) has been shown to upregulate the expression of CT antigens in a number of tumour cell lines (Adair *et al.*, 2009) potentially making these tumours more susceptible to MAGE-A1–, MAGE-A3–, and NY-ESO-1–mediated killing. Bao *et al.*, (2011) recently demonstrated decitabine mediated upregulation of CT antigens in neuroblastoma cells. Krishnadas *et al.*, (2012)

investigated a combination of demethylating chemotherapy followed by a cancer antigen vaccine in a relapsed neuroblastoma patient. Decitabine was employed to upregulate cancer testis antigen expression, followed by a dendritic cell vaccine targeting the cancer testis antigens MAGE-A1, MAGE-A3, and NY-ESO-1. The patient had persistent tumour infiltration of the bone marrow after completion of standard therapy for neuroblastoma, including multi-agent chemotherapy, tumour resection, stem cell transplantation, radiation therapy, and anti-GD_2 monoclonal antibodies which persisted despite chemotherapy. After 3 cycles of decitabine and vaccine, this patient achieved a complete remission with no evidence of relapse in the bone marrow or other sites highlighting the potential of chemotherapy in combination with a cancer vaccine as a novel therapeutic strategy.

Genomic profiling has not revealed a high incidence of mutations in any significant number of therapeutically targeted genes with two exceptions, amplification of the *MYCN* oncogene and point mutations in *ALK*, thus presenting possibilities for targeted therapy. *ALK* mutations drive constitutive phosphorylation of *ALK* which are critical for growth of neuroblasts (Bresler *et al.*, 2011). *ALK* mutations or amplifications occur in up to 15% of newly diagnosed neuroblastoma (Maris *et al.*, 2010); approximately 6–10% of sporadic neuroblastomas carry somatic *ALK*-activating mutations, while an additional 3–4% have a high frequency of *ALK* gene amplification (Cheung *et al.*, 2013). These reports indicate *ALK* is an oncogenic driver in both familial and sporadic neuroblastoma and thus a promising therapeutic target. As previously discussed Crizotinib, a small molecule inhibitor of ALK is undergoing clinical investigations. Results from a phase 1 clinical study revealed promising findings; patients displayed minimal toxicity despite high doses of the drug while 50% of patients with the *ALK* mutation entered remission (Mosse *et al.*, 2013). A combination trial of crizotinib with chemotherapy is currently ongoing (clinicalTrials.gov: NCT01606878) while several second-generation ALK inhibitors with increased potency and specificity are currently in early phase clinical trials (Mehra *et al.*, 2012; Seto *et al.*, 2013).

1.4 Analysis of drug interactions

Combination chemotherapy has proved to be an effective therapeutic strategy for the treatment of multiple cancers including neuroblastoma. Pre-clinical investigations are employed to identify drug combinations which may interact to produce additive or synergistic effects. Numerous strategies may be used to quantitatively measure the dose-effect relationship of each drug alone and in combination and to determine whether a given combination produces a synergistic, additive or antagonistic effect. One of the most widely employed methods to evaluate whether a combination is effective is the median-drug effect analysis method (Chou and Talalay., 1984). This method is based on the median-effect equation, derived from the mass-action law principle. It is the unified theory which provides a common link between single entity and multiple entities, and first order and higher order dynamics (Chou., 2010). This general equation encompasses the Michaelis-Menten, Hill, Henderson-Hasselbalch, and Scatchard equations.

This method uses the combination index (CI) as a quantitative measure of an additive, synergisticor antagonistic effect. A CI value greater than 1 indicates antagonism, equal to 1 indicating an additive effect and less than 1 indicating synergism. To calculate the CI value, the computer programme Calcusyn may be employed. Data can be entered for individual drugs and for constant-ratio or non-constant-ratio combinations of drugs. Calcusyn graphs the data and produces reports summarising the drug interactions including the CI value. The plots drawn by Calcusyn include dose-effect, median-effect and isobolograms. The isobologram analysis can evaluate the nature of interaction between two drugs, i.e., drug A and drug B. The concentrations required to produce the given effect, for example the IC_{50} value, are determined for each drug i.e. drug A ($IC_{x, A}$) and drug B ($IC_{x, B}$) and are indicated on the x and y axes of a two-coordinate plot, forming two points ($IC_{x, A}$, 0) and (0, $IC_{x, B}$). The line which connects these two points is the line of additivity. The concentrations of the combination of drug A and drug B are denoted as ($C_{A, x}$, $C_{B, x}$), and are placed on the same plot. If these points are located above the line, this indicates antagonism, on the line indicates an additive combination and a point located below the line of additivity indicates a synergistic combination (Chou., 2010).

1.5 Multidrug resistance

Despite both advances in understanding the biology of the cancer and aggressive treatment strategies, neuroblastoma continues to be one of the most difficult paediatric cancers to successfully treat. A major barrier in the effective treatment of neuroblastoma is the development of multidrug resistance (MDR) to a broad range of cytotoxic drugs (Keshelava *et al.*, 1998; 2000), which limits the effectiveness of these chemotherapeutics to successfully treat neuroblastoma. MDR is classified as the cross resistance to multiple structurally and functionally unrelated cytotoxic drugs. These include vinca alkaloids (vincristine, vinblastine), alkylating agents (cyclophosphamide), platinum compounds (cisplatin, carboplatin) and anthracyclines (doxorubicin, danorubicin) (Saraswathy *et al.*, 2013). Several MDR mechanisms may be simultaneously at play in a cell thereby increasing the degree of drug resistance. In neuroblastoma this MDR phenotype often includes amplification of the proto-oncogene MYCN, mutation/deletion of p53 deletion of loci at 1p or 11q and overexpression of MDR proteins leading to altered drug transport and increased drug efflux.

MDR may be intrinsic, in that a cell displays resistance from the initial exposure to chemotherapy, or acquired. The ABC (ATP binding cassette) transporters are a family of transmembrane proteins that use ATP hydrolysis to perform a number of functions; namely the exportation of molecules such as lipids, hydrophobic drugs and proteins. More than 48 MDR genes have been identified in humans while only ten are postulated to play a role in drug resistance (Saraswarthy *et al.*, 2013). The normal function of these proteins is to detoxify cytotoxic chemicals (Alisi *et al.*, 2013). Two of the best studied multidrug resistant genes of the ABC family are MDR-1 (also called ABCB1, multidrug resistant protein or p-glycoprotein (P-gp)) and MRP-1 (also called ABCC1). P-gp is a 170 kDa plasma membrane protein normally expressed in certain cell types in the liver, pancreas, kidney, colon, and jejunum (Thiebaut *et al.*, 1987), consisting of 1280 amino acids with twelve membrane spanning domains made up of two halves each containing six transmembrane regions with a large cytoplasmic tail that contains the ATP binding cassette (Liu *et al.*, 2010). Binding of a chemotherapeutic drug to this transporter results in the activation of the ATP domains; hydrolysis of ATP induces a conformational change in P-gp and finally expulsion of the bound drug from the cell. P-gp is expressed in the

intestinal epithelium where it plays an important role in the extrusion of many drugs from the blood into the intestinal lumen and may prevent drugs from entering the blood stream therefore the expression and activity of P-gp may reduce absorption and bioavailability of those drugs which bind to P-gp.

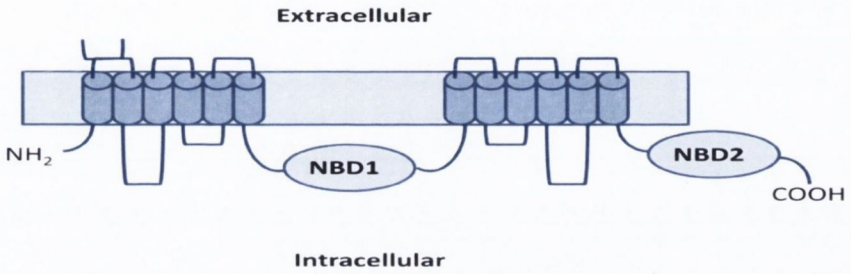

Figure 1.2 Structure of P-glycoprotein

P-gp is a twelve transmembrane domain protein; the N-terminal half of the molecule contains six transmembrane domains, followed by a cytoplasmic domain with an ATP-binding site, another six transmembrane domains and a second ATP-binding site. When ATP binds at the cytoplasmic side to the nucleotide binding domain (NBD), this induces dimerisation of the NBDs stimulating a structural change which results in the outward facing conformation.

Increased cellular expression of P-gp has been reported in many cancers including liver, pancreatic, myeloma and neuroblastoma (Coley *et al.*, 2010) and has been proposed as an independent prognostic marker (Schaich *et al.*, 2005). The exact role of P-gp in neuroblastoma remains controversial; early studies noted a correlation between overexpression of P-gp and poor outcome in patients (Chan *et al.*, 1991; Goldstein *et al.*, 1990) with expression of P-gp increasing after exposure to chemotherapeutics in primary neuroblastoma (Bourhis *et al.*, 1989). A more recent large scale study of P-gp expression in neuroblastoma was not shown to be predictive of outcome in primary untreated neuroblastoma (Haber *et al.*, 2006). Although the precise role of P-gp in acquired MDR is unresolved, it is clear the contribution of this transporter to the development of MDR should not be disregarded. P-gp is upregulated in drug resistant neuroblastoma CHLA-90 and SK-N-FI cell lines. Flahaut *et al.*, (2009) generated two MDR chemoresistant neuroblastoma cell lines by prolonged exposure to doxorubicin and noted the acquired chemoresistance was not restricted to P-gp overexpression as sensitivity could only partially be restored by the addition of the P-gp inhibitor, verapamil. This study suggests

P-gp has a role in MDR but other factors may be at play.

Expression of P-gp has been proposed to be regulated by p53, a tumour suppressor protein which is often mutated in cancer. Mutant p53 has been reported to upregulate P-gp in osteocarcinoma and colon carcinoma cell lines (Sampath *et al.*, 2001). Interestingly nutlin-3, an inhibitor of Mdm2 (the negative regulator of p53), which is currently in preclinical development for the treatment of neuroblastoma, has been shown to reverse P-gp mediated drug resistance in a panel of MDR neuroblastoma cell lines (Michaelis *et al.*, 2009). Non-toxic nutlin-3 concentrations were found to significantly decrease the IC_{50} for vincristine (and other P-gp substrates structurally unrelated to vincristine) in different p53-mutated, P-gp–expressing cell lines (92- to 3,434-fold).

Another member of the ABC family of transporters, MRP-1 (multidrug resistance associated protein), may be contributing to MDR. This is a 190kDa protein that shares 15% homology with P-gp; while they share a low level of homology, MRP-1 also mediates cellular resistance to a wide range of structurally and pharmacologically distinct chemotherapeutic drugs including vinca alkaloids, anthracyclines and epipodophyllotoxins (Pajic *et al.*, 2005). Bordow *et al.*, (1994) first reported a correlation between MRP-1 expression and MYCN amplification. A high level of MRP-1 expression in primary tissue samples has been reported to correlate with poor patient outcome (Peaston *et al.*, 2001).

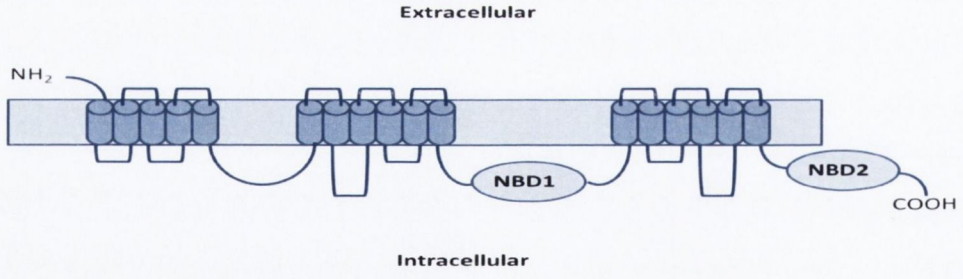

Figure 1.3 Structure of multidrug resistance protein-1

The structure of MRP-1 is similar to P-gp. This protein possesses two ATP binding sites, twelve transmembrane domains and an additional five transmembrane domains at the amino terminal end. When ATP binds at the cytoplasmic side to the nucleotide binding domain (NBD), this induces dimerisation of the NBDs stimulating a structural change which results in the outward facing conformation.

Following analysis of 209 neuroblastoma patient samples, Haber *et al.,* (2006) found that high levels of MRP-1 expression were associated with poor prognosis. They observed that after chemotherapy aggressive tumours increase expression of MRP-1. Using MRP-1 antisense oligonucleotides in an *in vivo* mouse model, Kuss *et al.,* (2002) were able to decrease MRP-1 levels to 40% resulting in an increased chemosensitivity to etoposide, a substrate of MRP-1 leading to decreased tumourigenicity. A report describing a correlation between the expression of MRP1 and MYCN amplification in primary NB tumours (Manohar *et al.*, 2004) and cell lines (Bordow *et al.*, 1994) suggested MYCN mediated regulation of MRP1. Bordow *et al.*, (1994) provided the first evidence of an association between high levels of MRP1 expression in primary tumours and amplification and overexpression of MYCN. The authors also found that the treatment of NB cell lines with retinoic acid resulted in coordinated down-regulation of MYCN and MRP1. Later studies identified MRP1 as a direct transcriptional target of MYCN in neuroblastoma (Porro *et al.*, 2010) and as a consequence MRP1 is highly expressed in MYCN amplified tumours. More recently, Henderson *et al.,* demonstrated that MRP1 contributes to the development of neuroblastoma in an *in vivo* mouse model (Henderson *et al.*, 2011). Homozygous deletion of the *MRP1* gene in primary murine neuroblastoma tumours resulted in increased sensitivity to MRP1 substrate drugs (vincristine, etoposide, doxorubicin), compared to tumours containing both copies of wild-type MRP1. Reversan, a small molecule inhibitor of MRP1, was found to increase the efficacy of both vincristine and etoposide in murine models of neuroblastoma (Burkhart *et al.*, 2009) demonstrating the potential of MRP1 inhibition for the treatment of MDR neuroblastoma. Although it should be noted at present there are no MRP1 inhibitors undergoing clinical trials for the treatment of neuroblastoma, a phase 1 clinical trial of sulindac, an MRP-1 inhibitor has been carried out in patients with advanced cancer (breast, lung, bowel, melanoma, renal and ovarian) (O'Connor et al., 2007).

As the intensity of high dose chemotherapy for advanced stage neuroblastoma is already at or approaching the limits of tolerance, it is clear the need for new therapeutics is vital, in particular more targeted treatments which can bypass or overcome MDR.

1.6 Apoptosis

Apoptosis is the programmed series of events culminating in the death of a cell which is essential for the normal development of an organism, maintenance of cellular homeostasis (Danial & Korsmeyer., 2004) and for the elimination of excess or potentially harmful cells that would otherwise threaten an organism's survival. Apoptosis proceeds through two distinct yet interconnected pathways; the intrinsic (or mitochondrial) or extrinsic (or death receptor) pathway both involving the activation of a series of cysteine proteases called caspases, also known as the death executioners of the cell. As approximately 50 to 70 billion cells are made per day, equal numbers must undergo apoptosis in order to maintain cellular homeostasis (Cotter *et al.*, 2009).

Apoptosis is characterised by a distinct set of physiological and biochemical processes beginning with cleavage of nuclear lamins which causes the cell to shrink (Wyllie *et al.*, 1980). Cells lose contact with neighbouring cells, cytoskeletal proteins are cleaved resulting in loss of cell shape (Rao *et al.*, 1996) and the cell begins to bleb. Cytoplasmic swelling leads to membrane rupture and cell lysis. The hallmark feature of apoptosis is DNA 'laddering' (Wyllie *et al.*, 1980). Within the nucleus, DNA is cleaved by caspase activated DNAse and the chromatin undergoes compaction. Chromatin aggregates into nucleosomal units of 180 bp. The cell continues to bleb and form apoptotic bodies which are eliminated by macrophages.

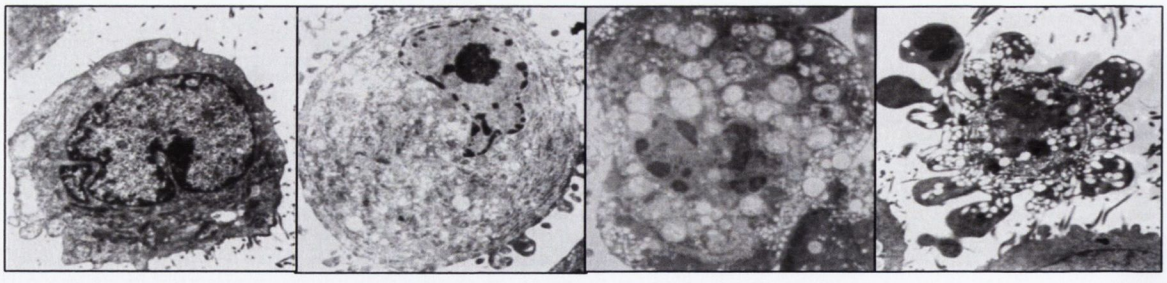

Figure 1.4 Morphological changes during apoptotic cell death in PC-2 cells in response to hypoxia. Adapted from Dai *et al.*, (2012).

1.6.1 Caspases

Caspases, often referred to as the death executioners of apoptosis, are a family of cytosolic cysteine proteases that are specifically activated and cleave particular intracellular substrates as a cell undergoes apoptosis (Alnemri *et al.*, 1986). They are synthesised as zymogens with weak proteolytic activity containing an N-terminal prodomain, a large subunit (p20) and a C-terminus small subunit (p10) (Walker *et al.*, 1994). When cleaved at internal aspartate residues between the prodomain and the large subunit, they mature and acquire increased proteolytic activity (Fig. 1.5). Their catalytic activity is dependent on a cysteine residue within a conserved pentapeptide motif (QACXG) in the large subunit (Cohen *et al.*, 1997). When activated, the prodomain is cleaved off; the mature enzyme is a heterotetramer of two p20 and p10 heterodimers in which the active site of each heterodimer is composed of residues from both the small and large subunit. Caspases are activated by cleavage at Asp-X sites between the p10 and p20 and between the prodomain and p20 (Thornberry *et al.*, 1997). These internal proteolytic sites are themselves caspase consensus sites. This allows one caspase to activate another leading to the initiation of caspase cascades. Twelve caspases have been identified to date, eleven of which are found in humans (Chai *et al.*, 2014). Caspases can be categorised into two classes, initiator and effector, based on their position in apoptotic signalling cascade. Anti-cancer therapy such as chemotherapy, immunotherapy or radiation therapy exert their effects partly though activation of apoptosis for the most part through activation of caspases.

Although caspases have been proven to play a crucial role in the execution of apoptosis, there is evidence to support caspase-independent cell death. Furthermore a subset of caspases (1, 4 and 5) mediate inflammatory responses by cleaving precursor forms of inflammatory cytokines such as interleukin-18 and are not implicated as having a role in apoptosis (McIlwain *et al.*, 2013).

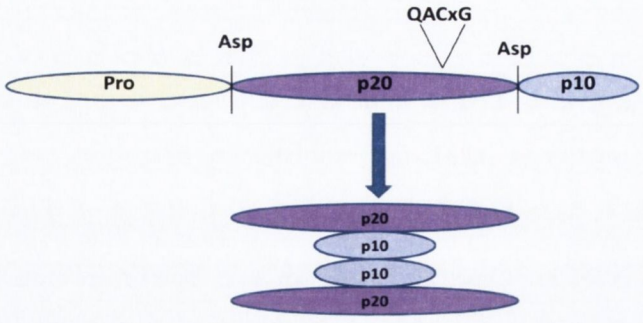

Figure 1.5 Activation of caspases

Capases are activated upon cleavage at internal aspartate residues between the pro-domain and the large subunit. Their catalytic activity is dependent on a cysteine residue within a conserved pentapeptide motif (QACXG) in the large subunit. The pro-domain is cleaved off; the mature enzyme is a heterotetramer of two p20 and p10 heterodimers. Caspases are activated by cleavage at Asp-X sites between the p10 and p20 and between the pro-domain and p20.

1.6.2 Intrinsic Pathway

Also referred to as the mitochondrial pathway, the intrinsic pathway is activated by internal stress signals such as DNA damage, growth factor withdrawal or cytotoxic drugs (Tait & Green., 2010). These signals induce perturbations in the mitochondrial membrane resulting in release of proteins such as the pro-apoptotic mitochondrial protein cytochrome c (Green & Reed., 1998; Saelens *et al.*, 2004). Cytochrome c binds to APAF-1 (apoptotic protease activating factor-1) via the WD40 repeats (Zou *et al.*, 1997; Saelens *et al.*, 2004) inducing a conformational change that exposes the CARD domains (caspase recruitment domains). In mammalian cells internal stress induces mitochondrial outer membrane permeabilisation (MOMP) leading to the release of cytochrome-c and other pro-apoptotic proteins. Once released cytochrome c binds to the cytosolic protein APAF-1 to facilitate formation of a multimeric complex, the apoptosome (Li *et al.*, 1997). Pro-caspase-9 is recruited to the CARD motif within the apoptosome (Srinivasula *et al.*, 1998). Initiator caspase-9 is cleaved and activated leading to activation of a cascade of downstream effector caspases 3, 6 and 7 (Zou *et al.*, 1999) which subsequently cleave cellular proteins such as the DNA repair enzyme PARP (poly ADP ribose polymerase) resulting in cell death (Fig. 1.6). Permeabilisation of the mitochondrial membrane, the central event in the execution of the intrinsic pathway, is controlled by the Bcl-2 family of

proteins which will be discussed in the section below. Other pro-apoptotic factors such as AIF and Smac/DIABLO may be released from the mitochondria. Following release, Smac/DIABLO antagonises inhibitor of apoptosis proteins (IAPs) relieving their inhibitory effects on caspases (Martinez-Ruiz *et al.*, 2008).

1.6.3 Extrinsic pathway

The extrinsic pathway is activated by ligation of a member of the tumour necrosis factor (TNF) receptor family also referred to as 'death receptors'. Members of this family include tumour necrosis factor (TNFα), Fas/CD95, TNFR1 and TNF related apoptosis inducing ligand (TRAIL) receptors all of which share structural similarity. These receptors posses a cysteine rich extracellular domain essential for recognition of their ligands and a cytoplasmic region called a 'death' domain (DD) which is critical for propagation of death signalling. The DD binds to the DD of adaptor molecules such as TRADD or FADD (Walczak *et al.*, 2000) forming the death inducing signalling complex (DISC) to which pro-caspase-8 is recruited via interaction of the death effector domains (DED) of FADD (Kischkel *et al.*, 1995). Pro-caspase-8 is activated by autocatalytic activation leading to the subsequent activation of effector caspases such as caspase-3 (Scaffidi *et al.*, 1998). This is referred to as type I signalling (Fig. 1.6). In type II cells, activation of casapase-8 is not sufficient to induce cell death alone and requires amplification of death signalling though activation of the intrinsic pathway. Activated caspase-8, cleaves Bid, a pro-apoptotic member of the Bcl-2 family, to tBid which then translocates to the mitochondria where it interacts with other pro-apoptotic proteins, Bak and Bax to form pores in the mitochondria leading to the release of cytochrome c and consequently processing of pro-caspase-9 to active caspase-9 (Lou *et al.*, 1998).

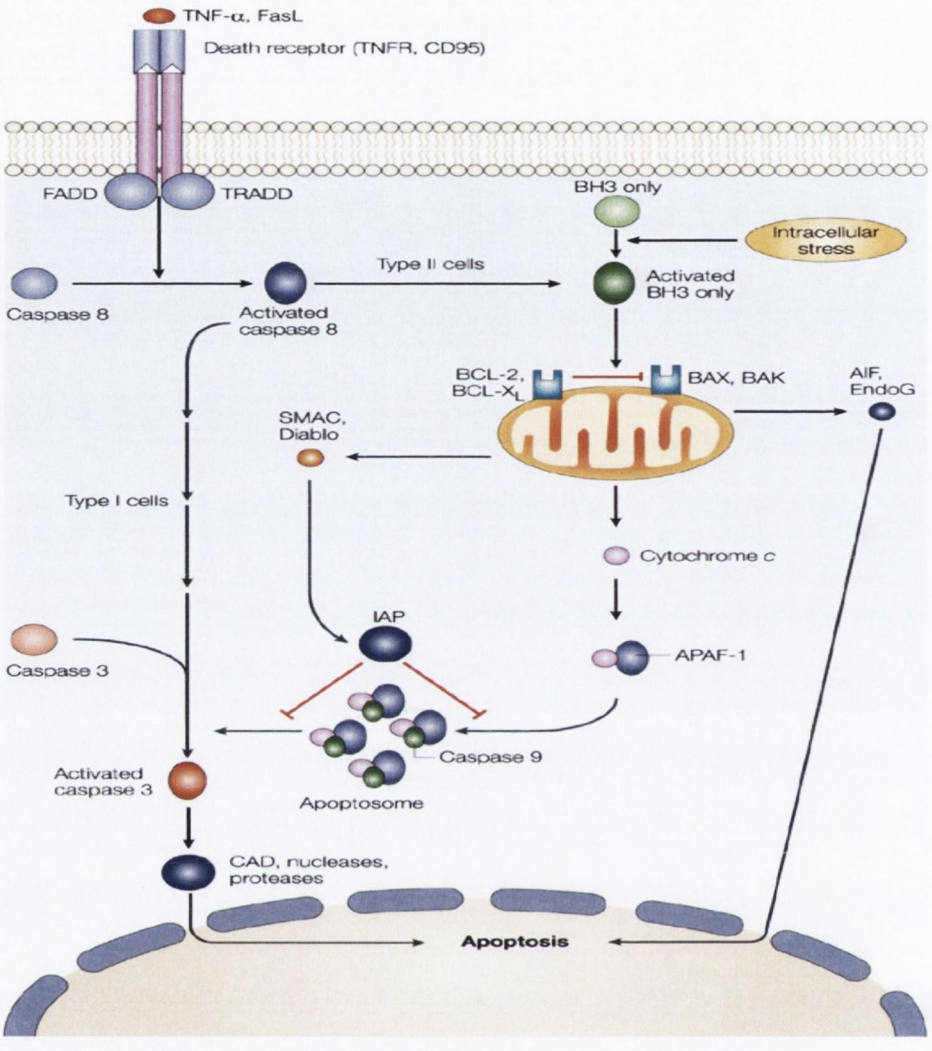

Figure 1.6 The extrinsic and intrinsic pathways of apoptosis.

The intrinsic pathway is activated by internal stress signals which produce perturbations in the mitochondria resulting in the release of pro-apoptotic proteins such as cytochrome c which binds to APF-1 via the CARD domains forming the apoptososome. Pro-caspase-9 is recruited and activated which subsequently activates caspase-3. The extrinsic pathway is activated by ligation of a TNF receptor. These receptors possess cysteine rich death domains (DD) in their cytosolic region which recognise and bind to the DD of adaptor molecules such as FADD forming the death inducing signalling complex (DISC). Procaspase-8 is recruited via interaction of the death effector domains and activated resulting in subsequent activation of caspase-3. Taken from Byrne *et al.*, (2004).

Caspase-8 has been shown to be inactivated in neuroblastoma through deletion or silencing by DNA methylation. Inactivation of this gene was found by Teitz *et al.*, (2000) in

63% of patients with MYCN amplification. In this study caspase-8 null cells were shown to be resistant to doxorubicin mediated apoptosis indicating that caspase 8 works as a tumour suppressor in MYCN amplified tumours. A link has also been established between loss of caspase-8 and the metastatic potential of neuroblastoma cells. Stupack *et al.*, (2006) found that suppression of caspase-8 expression occurs *in vivo* during the establishment of metastases. Restoration of caspase-8 expression suppressed metastases while the use of shRNA to knockdown caspase-8 expression doubled the incidence of metastases. More recently Teitz *et al.*, (2013) found that mice with a caspase-8 deficiency develop advanced neuroblastoma with bone marrow metastases. Additionally amplification of MYCN in caspase-8 deficient mice was found to significantly increase the presence of metastases.

1.6.4 The Bcl-2 family

These are a family of structurally similar proteins which are categorised based on their ability to either inhibit or activate apoptosis (Fig. 1.7). Bcl-2 was the first member to be identified when it was discovered as an oncogene in follicular lymphocyte lymphoma (Tsujimoto *et al.*, 1985). Normally present on chromosome 18, a translocation occurs which places the *Bcl-2* gene next to the immunoglobulin heavy chain locus on chromosome 14 (Bakhshi *et al.*, 1985) resulting in the overexpression of Bcl-2.

The Bcl-2 family is composed of three functionally distinct groups with each member containing one or more BH domains. Group 1 family members are those which inhibit apoptosis, in addition to four BH domains, they also contain a C terminal transmembrane domain which allows them to preferentially tether themselves to the outer mitochondrial although they may also anchor to other organelles (Juin *et al.*, 2013). Members include Bcl-2, Mcl-1, Bcl-xL, Bcl-W and Bcl-2A1. Group 2 members promote apoptosis; they share a similar structure to group one with the exception of one less BH domain. Members include Bax, Bak and Bok. The final group 3 possess a single BH3 domain; they bind to anti-apoptotic members to promote Bcl-2 proteins and are thought to control the permeability of the mitochondrial membrane (Youle *et al.*, 2008). Group 1 proteins inhibit permeabilisation while group 2 and 3 promote it. Members of the group 3 family include Bim, Bid, Puma, Bad, Noxa and BMF (Czabator *et al.*, 2014).

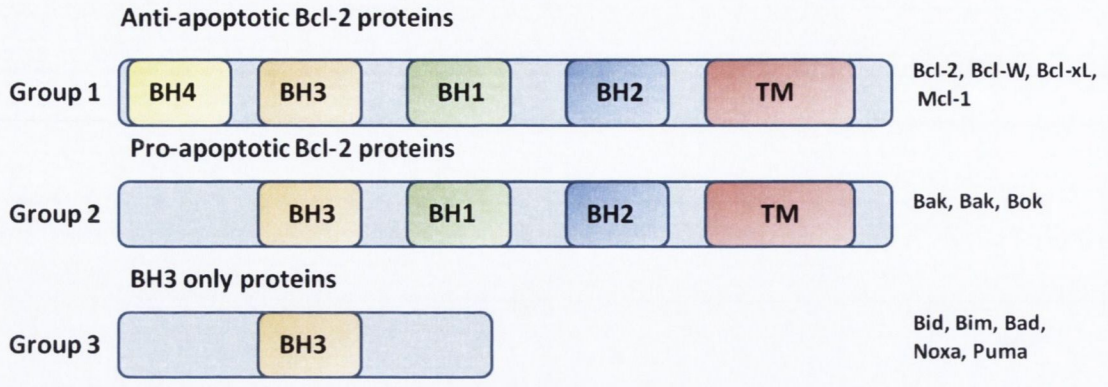

Figure 1.7 Structure of Bcl-2 family members

Bcl-2 family members are classified into three groups based on structure as well as sequence homology. Group 1 have four BH3 helices while group 2 have three. Group 3, the BH3-only proteins, contain a single BH3 amphipathic helix, which mediates their interaction with the groove of anti-apoptotic Bcl-2 proteins. Group 1 and 2 members have a transmembrane domain which allows Bcl-2 proteins to anchor to cellular membranes such as the mitochondria.

These proteins can interact with one another to either promote or inhibit apoptosis. Bax and Bak dimerise, insert into the mitochondrial membrane to form pores through which pro-apoptotic proteins are released (Czabator *et al.*, 2014). Two models have been proposed to account for the pro-apoptotic activities of these proteins (Fig. 1.8). The first, the indirect activator model, describes interaction of constitutively active Bax/Bak with anti-apoptotic Bcl-2 proteins. This inhibitory interaction may be relieved though competitive binding of BH3 only proteins. The second model, the direct activator-depressor model proposes that anti-apoptotic Bcl-2 proteins prevent cell death through direct interaction with Bax and Bak thus inhibiting their function. This model also proposes anti-apoptotic members prevent mitochondrial outer membrane permeabilisation (MOMP) by sequestering BH3 only proteins. A second set of BH3 proteins, termed sensitisors, are thought not to directly activate Bak or Bak but function to neutralise anti-apoptotic Bcl-2 protein binding (Czabator *et al.*, 2014). The current consensus is that both models may apply in many circumstances.

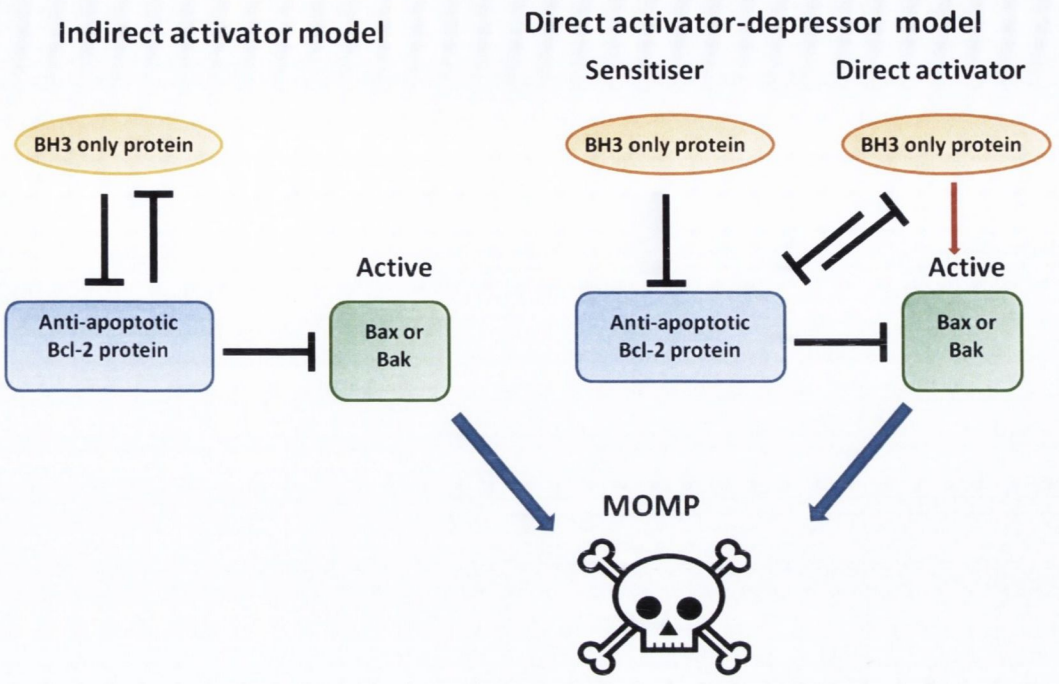

Figure 1.8 Proposed models to explain the control of MOMP by Bcl-2 proteins.

In the indirect activation model as well as sequestering BH3 only proteins, anti-apoptotic Bcl-2 proteins must sequester any Bax or Bak molecule that becomes activated and exposes its BH3 domain. According to this model, Bax and Bak are only free to induce MOMP if all anti-apoptotic proteins are neutralised by BH3-only proteins. In the direct activation model, certain BH3-only proteins, namely Bid, Bim and PUMA interact directly with pro-apoptotic Bcl-2 proteins, Bak and Bax to activate them. BH3-only proteins that lacking this direct 'activator' function, such as Bad, are referred to as ' sensitisors' as they bind pro-survival Bcl-2 family members, thereby releasing any bound BH3-only activator proteins.

1.6.4.1 Bcl-2

The first member of the family of proteins to be identified, Bcl-2 is a 26 kDa protein which is localised to the cytoplasmic face of the mitochondrial outer membrane, the endoplasmic reticulum and the nuclear envelope (Vaux *et al.*, 1988). Bcl-2 functions as an anti-apoptotic protein preventing oligomerisation of Bak and Bax and the formation of a pore in the outer mitochondrial membrane leading to inhibition of cytochrome c release, caspase activation, and ultimately cell death (Youle *et al.*, 2008). It has been shown that the binding of Bcl-2 to Bax is an essential step in its ability to prevent cell death (Murphy

et al., 2000). BH3 only proteins, such as Puma and Noxa, have been shown to exert their pro-apoptotic role by competitively binding to Bcl-2 and preventing binding of Bax or Bak. Bcl-2 expression has also previously been shown to correlate with poor prognosis in primary neuroblastoma samples, although the exact contribution of Bcl-2 to the malignant phenotype of neuroblastoma remains controversial. Castle *et al.*, (1993) found that Bcl-2 expression was associated with MCYN expression, unfavourable histology and marginally poorer prognosis, while Ramani *et al.*, (1994) found no correlation between Bcl-2 expression in primary neuroblastoma samples and the stage of the tumour. Beltinger *et al.*, (2002) demonstrated that overexpression of Bcl-2 in the SHEP neuroblastoma cell line prevented TRAIL induced apoptosis by inhibiting TRAIL induced mitochondrial changes.

Bcl-2 has been proposed as a therapeutic target in neuroblastoma. At present several Bcl-2 inhibitors are undergoing clinical trials for a number of cancers (Vogler *et al.*, 2009) such as ABT263, a small molecule mimetic of the BH3 domain of Bad. This inhibitor has not proven to be successful in several *in vitro* neuroblastoma studies, as most cell lines were found to be resistant. One approach to overcome this resistance, is combination therapy; norcantharidin (NCTD), a small-molecule anticancer drug derived from a traditional Chinese medicine, has been found to significantly enhance ABT-263-mediated apoptosis induction, cell viability inhibition and inhibit clonal formation in neuroblastoma SH-SY5Y and CHLA-119 neuroblastoma cell lines (Wang *et al.*, 2014). An upregulation in Noxa expression was noted in response to this novel combination. Notably, knockdown of Noxa significantly attenuated cell death induction by cotreatment with ABT-263 and NCTD, indicating Noxa essentially contributes to the combination anticancer effect. Other reports have supported the use of combination therapy. Lamers *et al.*, (2012) has shown that a combination with multiple chemotherapeutics which are currently used to treat neuroblastoma was an effective strategy to maximise cell death. Each chemotherapeutic tested was found to synergistically enhance the effects of Bcl-2 inhibition. To support these findings, combinations of ABT263 and etoposide or vincristine have been shown to be synergistic in other cancers such as ALL (High *et al.*, 2010) and B cell lymphoma (Ackler *et al.*, 2010).

1.6.4.2 Mcl-1

Mcl-1 (myeloid lymphocyte leukaemia sequence-1) was the second member of the *Bcl-2* family to be discovered. It was identified as a gene which is induced during early differentiation of the myeloid lymphocyte line ML-1 (Kozopas *et al.*, 1993). Structurally Mcl-1 differs from other anti-apoptotic Bcl-2 proteins; the 170 amino acid N-terminus is larger in Mcl-1 than other members and contains two PEST (proline/glutamic acid/serine/threonine) sequences which are subject to modification, namely ubiquitination, phosphorylation and caspase cleavage (Thomas *et al.*, 2010). Initially Mcl-1 was reported to possess three BH domains but more recent studies have identified a forth BH domain between BH3 and the PEST region (Mojsa *et al.*, 2014). This N terminus has been shown to be important for function and localisation, promoting its association with the mitochondria. Germain *et al.*, (2007) showed that cellular localisation is regulated by the first 79 amino acids in this region (Fig. 1.9).

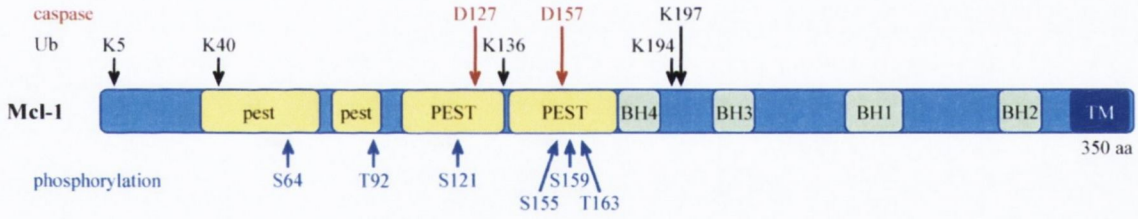

Figure 1.9 Structure of anti-apoptotic Mcl-1

Schematic representation of Mcl-1 showing the transmembrane region (TM), Bcl-2 homology domains (BH1-4) and PEST sequences of ubiquitination, caspase cleavage and phosphorylation. Taken from Mojsa *et al.*, (2014).

Mcl-1 is a highly regulated protein with a short half life of less than one hour (Stewart *et al*, 2010). The PEST sequences have been implicated in the regulation of Mcl-1. Mcl-1 can be cleaved by caspases and granzyme B, which proteolytically degrade Mcl-1 during cell death (Clohessy *et al.*, 2004) or undergo phosphorylation or ubiquitination. Phosphorlyation of Thr ^{92} by ERK increases the half life of Mcl-1 while phosphorylation of Ser^{155} by GSK-3 marks it for degradation by ubiquitination. Three E3 ubiquitin ligases have been identified which can target Mcl-1 for proteasomal destruction; SCF^{FBW7} (Inzuka *et al.*, 2011), SCF$^{\beta TRCP}$ (Ding *et al.*, 2007) and Mcl-1 ubiquitin ligase E3 (Mule). SCF (Skp1-Cullen1-F-box) is a multi component E3 ligase which is active from late G1 to G2. It

mediates the destruction of G1 cyclins and CDK inhibitors by ubiquitination. It is composed of Skp-1, an adaptor protein, Cul1, a scaffold protein, Rbx1, a ring finger protein and F box protein. The F box protein is responsible for substrate recognition therefore this component of the complex is variable. SCF^{FBW7} functions as a tumour suppressor by mediating the degradation of several proto-oncogenes including Myc. Deletion of SCF^{FBW7} in mouse T cells was shown to result in an accumulation of Mcl-1 leading to T- cell ALL (T-ALL) and resistance to chemotherapeutics confirming its tumour suppressor function (Inuzuka *et al.*, 2007; Wertz *et al.*, 2011). In contrast, reintroduction of wild type SCF^{FBW7} dramatically reduced Mcl-1 levels and decreased its stability. Loss of this tumour suppressor function has been reported in multiple cancers (Wood *et al.*, 2007).

Mcl-1 blocks the progression of apoptosis by binding and sequestering the pro-apoptotic proteins Bak and Bax, which are capable of forming pores in the mitochondrial membrane, allowing the release of cytochrome c. Antagonism of Mcl-1 has been shown to have anti-cancer activity in a range of malignancies including lymphoma and melanoma (Nguyen *et al.*, 2007). Small molecule antagonists of Mcl-1 are currently in development. Recently, a stapled BH3 peptide inhibitor (Joseph *et al.*, 2012) and a small-molecule antagonist (Cohen *et al.*, 2012) have been reported. Cohen *et al* identified an Mcl-1 inhibitor molecule that selectively targets the BH3-binding groove of Mcl-1, this small-molecule antagonist binds to Mcl-1 with poor affinity, but can release Bax from Mcl-1, triggering caspase activation and cell death. It was also shown to synergize with ABT-737, a small molecule inhibitor of Bcl-2, to kill cells that express both Mcl-1 and Bcl-2.

There is indirect evidence that points to *Mcl-1* acting as an oncogene in neuroblastoma. The *MCL-1* gene maps to 1q21, a region which is amplified in many neuroblastoma cell lines and patient samples (Mosse *et al.*, 2005; Janoueix-Lerosey *et al.*, 2009). In the most aggressive forms of neuroblastoma, Mcl-1 is overexpressed; increased levels of a deubiquitase USP9X, causes stabilisation of the protein resulting in higher than normal levels of Mcl-1 (Schwickart *et al.*, 2010) contributing to the survival of malignant cells. Stabilisation of Mcl-1 by a stress protein BAG3 has recently been shown to promote survival of neuroblastoma cells *in vitro* and resistance to ABT-737 (Boiani *et al.*, 2013). In contrast, knockdown of Mcl-1 by siRNA sensitises neuroblastoma cell lines to ABT-737

(Lestini *et al.*, 2009), while siRNA-mediated knockdown of Mcl-1 has also been shown to sensitise neuroblastoma cells to cytotoxic drugs including etoposide and doxorubicin, both of which are currently used in the clinic (Karami *et al.*, 2014). Numerous other studies have shown a correlation between a decrease in Mcl-1 expression and induction of apoptosis in neuroblastoma cells (Bettayab *et al.*, 2010; Rapino *et al.*, 2013; Löschmann *et al.*, 2013), indicating that inhibition of Mcl-1 expression and/or neutralisation of its anti-apoptotic function increases susceptibility to apoptosis and provides a viable target for therapeutic intervention in both neuroblastoma and multiple other cancers.

1.6.4.3 Bcl-xL

A third anti-apoptotic member of the Bcl-2 family, Bcl-xL is a 30 kDa protein located on the outer mitochondrial membrane, which prevents apoptosis through heterodimerisation with pro-apoptotic proteins such as Bax and Bak, inhibiting the formation of mitochondrial outer membrane pores (Youle *et al.*, 2008). It interacts with other Bcl-2 proteins through its BH1 and BH2 domains while the BH4 domain is essential for its anti-apoptotic function. When Bcl-xL is cleaved during apoptotic cell death, the cleaved protein lacks the BH4 domain and can no longer prevent cell death (Sugioka *et al.*, 2003).

Expression of Bcl-2 proteins has been shown to be associated with increased survival of malignant cells and development of resistance to therapy. Dole *et al.,* (1995) determined the expression levels of Bcl-xl in a panel of neuroblastoma cell lines and investigated their role in the cells response to a number of chemotherapeutic drugs. A high percentage (88%) of the cell lines were positive for Bcl-xl expression. Cytotoxicity assays revealed that overexpression of Bcl-xl in SHEP-1 neuroblastoma cells leads to an inhibition of drug-induced apoptosis, conferring a survival advantage to these cells. Additional studies of this nature have been carried out. Yuste *et al.,* (2002) stably transfected Bcl-xl in SHSY5Y cells and showed resistance to staurosporine-induced cytochrome c release. These cells survived for up to 15 days in 1M staurosporine. Prevention of apoptosis by overexpression of Bcl-xL in neuroblastoma cells has been postulated to be due to effective inhibition of cytochrome c release.

1.6.4.4 Pro-apoptotic Bcl-2 family members

Multiple proteins are contained within the mitochondria which if released initiate a signalling cascade resulting in the survival or death of a cell. The integrity of the mitochondrial membrane is controlled by the Bcl-2 family. Loss of MOMP leads to the release of pro-apoptotic proteins and activation of apoptosis through the intrinsic pathway. Two proteins central to controlling this process are Bax and Bak (García-Sáez *et al.*, 2010). Evidence for the role of Bak and Bax in initiating the intrinsic pathway has been provided by knock out studies. Bak- and Bax deficient mice are resistant to stimuli that induce the intrinsic pathway and are unable to activate initiator caspases (Wei *et al.*, 2001; Hutchinson *et al.*, 2005).

Under normal physiological conditions these monomeric proteins are found in a latent form; Bax residing primarily in the cytosol and Bak at the outer mitochondrial membrane. Both are globular proteins comprising of nine helices. The alpha 9 helix at the C-terminus mediates interaction with the mitochondrial outer member by acting as a transmembrane domain (Suzuki *et al.*, 2000). Once activated through either the direct or indirect model as discussed above, Bax and Bak undergo a conformational change; they dimerise through interaction of the exposed BH3 domains of one molecule with the hydrophobic groove of another forming BH3: groove dimers (Westphal *et al.*, 2011). These dimers may then oligomerise to form a complex which inserts into the mitochondrial membrane leading to the formation of pores through which pro-apoptotic proteins such as cytochrome-c may be released. In both the inactive forms of Bak and Bax (Dewson *et al.*, 2009), an N-terminal amino acid sequence is buried in the folded protein. Once activated and a change in conformation occurs, this sequence is exposed. This structural change may be exploited as this amino acid sequence is now accessible as an epitope for antibody binding allowing monitoring of Bak and Bak activation.

Bid is another pro-apoptotic protein, in healthy cells it is unable to interact with anti-apoptotic proteins as it is sequestered in the cytoplasm. Caspase-8 is activated in the extrinsic pathway and cleaves Bid to generate tBid, a truncated form of Bid (Luo *et al.*, 1998). tBid translocates to the site where Bcl-2 resides and inhibits its function. tBid also functions to activate Bax by inducing its oligomerisation.

1.7 Reactive oxygen species-mediated induction of apoptosis

The aim of chemotherapy is to selectively induce cell death in cancer cells whilst causing minimum effects on non- malignant cells. Numerous chemotherapeutics have been shown to induce apoptosis mediated by production of reactive oxygen species (ROS). ROS is the term which describes the by-products of metabolism formed during the conversion of oxygen to water (Simon *et al.*, 2000). As electrons pass through the electron transport chain, an electron is passed from cytochrome c oxidase to oxygen resulting in the production of O_2, which is then converted to hydrogen peroxide (H_2O_2) and oxygen (O_2) by superoxide dismutase (SOD). H_2O_2 and O_2 can be further converted to H_2O and O_2 by the detoxifying enzyme catalase. These reactive oxygen species may act as second messengers in signalling cascades or during times of oxidative stress oxidise DNA, lipids and proteins (Marchi *et al.*, 2012).

At physiological levels, ROS functions as redox messengers in cell signalling while in malignant cells increases in ROS production may induce apoptosis. Multiple investigations have supported the role of ROS in apoptotic signalling; firstly, through identification of elevated levels of ROS in cells undergoing apoptosis (Alexandre *et al.*, 2006); secondly, through demonstration of the ability of exogenous ROS to induce apoptosis in multiple cell types (Conde de la Rosa *et al.*, 2005); thirdly, through identification of the role of antioxidants in inhibiting apoptosis (Chan *et al.*, 2005), and finally, through demonstration that inhibition of intracellular anti-oxidant levels promotes apoptosis (Pirlich *et al.*, 2002).

In contrast to normal cells, cancer cells exhibit increased levels of ROS production. Otto Warburg first observed that cancer cells actively metabolise glucose, and produce excessive lactic acid, while at the same time consuming oxygen via mitochondrial oxidative phosphorylation in a process termed 'aerobic glycolysis' or the so called 'Warburg Effect' (Warburg *et al.*, 1931, 1956) in contrast to normal cells which convert glucose to pyruvate when limited amounts of oxygen are available (anaerobic glycolysis) (Fig. 1.10) (Cairns *et al.*, 2011). In addition to the normal energy requirements of a non-malignant cell, rapidly dividing cancer cells must generate surplus energy supplies to sustain division. These cells reprogramme their metabolism to undergo anaerobic glycolysis; glucose is catabolised to lactate rather than directing it to the mitochondria to undergo oxidative phosphorylation. This lactate is exported to the microenvironment of

cancer cells causing acidosis and creation of a toxic environment surrounding the cell. In normal cells, glucose is metabolised into pyruvate, a potent anti-oxidant which is not transported out of the cell, thus enhancing the anti-oxidant capacity of normal cells. Normal cells and weak cancer cells are unable to survive the toxic environment and this may lead to selection of a more aggressive, often MDR and metastatic cancer cell (Dhuo *et al.*, 2012).

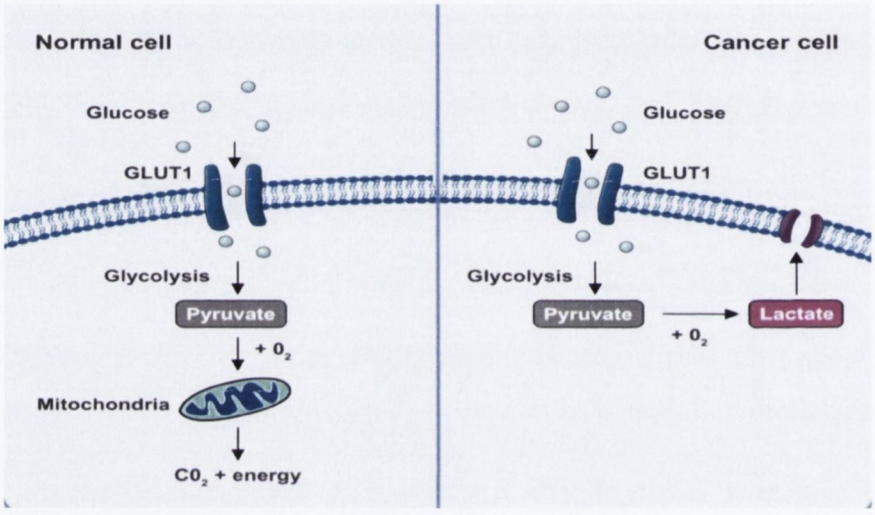

Figure 1.10 The 'Warburg' effect

Normal cells undergo oxidative phosphorylation to produce ATP as a source of energy. Cancer cells reprogram energy metabolism; they convert available glucose to pyruvate and lactate irrespective of the availability of oxygen. Taken from Marie *et al.*, (2011).

As cancer cells are often under oxidative stress, they have a relatively high level of ROS which renders them more susceptible to oxidative stress–induced cell death, and can be exploited for selective cancer therapy (Noguiera *et al.*, 2013). For example a drug which causes even a small increase in ROS, may push the level of ROS over a given threshold and induce cell death, in contrast to a normal cell which can better tolerate the drug-induced increase due to its superior anti-oxidant capacity. Therefore, development of cancer therapies which either directly increase ROS production to a toxic level and/or inhibit ROS scavenging systems, represent a promising means for selectively killing cancer cells.

1.8 5'AMP-activated protein kinase

Oxidative stress is defined as an imbalance between the production of ROS and their elimination by antioxidants (Noguiera *et al.*, 2013). As previously discussed, cancer cells are under increased oxidative stress which can result in activation of MAP kinases such as 5'AMP-activated protein kinase (AMPK). AMPK, a master regulator of homeostasis, is a kinase which becomes activated in response to stresses which inhibit the anabolic consumption of ATP such as a decrease in glucose levels, ischameia or hypoxia (Hardie *et al.*, 2011). AMPK senses fluctuations in cellular energy status by monitoring the ratios of AMP/ATP and ADP/ATP (Fig. 1.10). As ATP is consumed by the cells, levels of AMP and ADP increase. ATP competes with ADP and AMP for binding to the regulatory sites on AMPK preventing activation of this enzyme. As the cell undergoes metabolic stress, ADP and AMP will replace ATP bound to AMPK. A decrease in ATP leads to AMPK activation, resulting in the inhibition of anabolic pathways which consume ATP, such as protein synthesis, and the switching on of catabolic pathways which produce ATP such as autophagy resulting in restoration of cellular energy homeostasis (Kim *et al.*, 2011). AMPK may also be regulated by the upstream calmodulin-dependent protein kinase kinase (CaMKK) in response to increases of intracellular Ca(2+) levels (Gormand *et al.*, 2011).

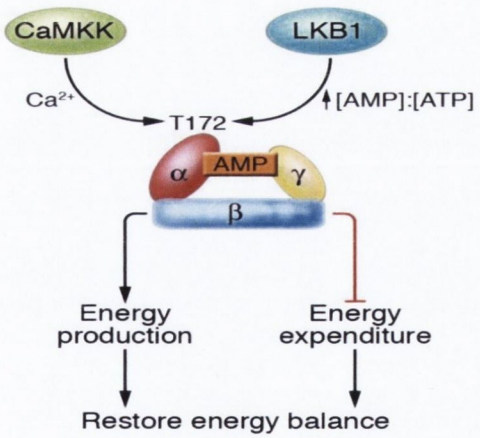

Figure 1.11 Regulation of AMPK

AMPK can be activated by increases in cellular AMP: ATP or ADP:ATP ratio. Binding of AMP or ADP to AMPK causes a conformational change that promotes phosphorylation by upstream kinase LKB1 while also inhibiting protein phosphatases. Taken from Long *et al.*, (2006).

AMPK activity is regulated by phosphorylation; an upstream AMPK kinase, liver kinase B1 (LKB1) directly phosphorylates Thr-172 in the activation loop of the α subunit (Hardie., 2011). Upon activation AMPK activates/inactivates a multitude of signalling pathways including protein synthesis, glucose and lipid metabolism and autophagy (Fig. 1.12). AMPK has been shown to be activated in response to numerous drugs such as the metformin, a drug which is used to treat diabetes, and numerous other natural plant products such as resveratrol, garlic and gallatte (Baur *et al.*, 2006; Lee *et al.*, 2011).

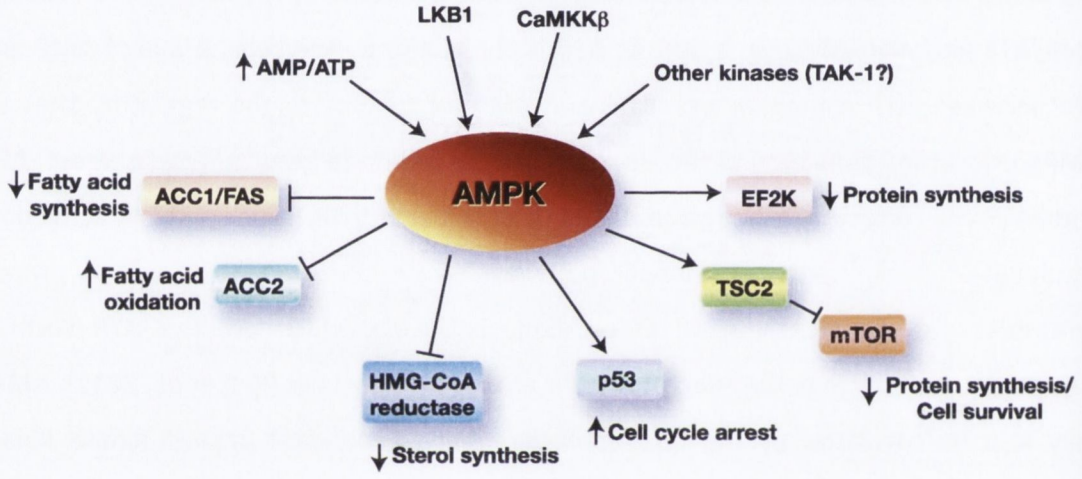

Figure 1.12 The AMPK signalling pathway. Taken from Fay *et al.*, (2008).

AMPK functions to allow cells to cope with stress, by activating catabolic pathways and inhibiting anabolic metabolism. This role is not compatible with cell proliferation and cancer progression; studies have demonstrated that activation of AMPK causes cell cycle arrest associated with stabilization of p53 and the cyclin-dependent kinase inhibitors $p21^{WAF1}$ and $p27^{CIP1}$ (Jones *et al.*, 2005; Liang *et al.*, 2007) whilst inhibiting the synthesis of the majority of cellular macromolecules, proteins, ribosomal RNA, cholesterol and glycogen (Hardie *et al.*, 2007; 2011; 2012). These findings are consistent with AMPK playing a tumour suppressor role. AMPK is situated at the centre of a signal transduction pathway, which has been shown to regulate cell growth and proliferation in response to stress (Faubert *et al.*, 2014), where it signals to multiple other tumour suppressor proteins such as upstream LKB1, TSC2 and p53 (Inoki *et al.*, 2006). For example, it has recently been shown that loss of AMPK accelerates Myc-induced lymphomagenesis.

Inactivation of AMPK resulted in a shift to aerobic glycolysis; cells exhibited increased glucose uptake, glycolytic flux, a flow of carbon into the tricarboxylic acid (TCA) cycle, suggesting that a loss of function promotes tumour progression, in part by regulating cellular metabolic pathways that support cell growth and proliferation (Faubert *et al.*, 2013). In melanoma, suppression of AMPK activation has been attributed to a mutation in B-RAF (Zheng *et al.*, 2009), causing deregulation of the signalling pathway leading to phosphorylation of LKB1 by extracellular signalling related kinase (ERK) and ribosomal S6 kinase (Rsk), reducing LKB1s ability to bind and activate AMPK. Furthermore, Zheng *et al.*, found that expression of a phosphorylation deficient LKB1 resulted in activation of AMPK and subsequent inhibition of melanoma cell growth.

If the LKB1-AMPK pathway is in fact a tumour-suppressing pathway, then it could be hypothesised that AMPK-activating drugs such as metformin and phenformin may protect against the development of cancer. Hardie *et al.*, (2003) reported that type 2 diabetics treated with the AMPK-activating drug metformin had a significantly reduced incidence of all forms of cancer, a finding which has been reproduced in multiple subsequent studies of different diabetic populations. An overall risk reduction of 30% was determined, with specific risk reductions being found for colon and liver cancers (Decensi *et al.*, 2010).

However, there is speculation that AMPK may also play a role in promoting cancer cell survival. In order to continuously divide, malignant cells have increased energy demands to allow them to replicate their protein, lipid and DNA content. As tumours grow, accessibility to nutrients and oxygen decreases, and in order to survive cells must adapt to hypoxia and nutrient deprivation by engaging in alternative metabolic pathways such as increasing glycolysis. It is possible that AMPK can provide the cell with a 'metabolic flexibility' to survive periods of stress through numerous mechanisms such as induction of autophagy (Egan *et al.*, 2011; Kim *et al.*, 2011) or an increase in fatty acid oxidation (McFadden *et al.*, 2009). Previous studies have found that the expression of AMPK correlates with their ability to tolerate stress such as glucose deprivation. Knock down of AMPK in pancreatic cells lines; PANC-1 and AsPC-1, significantly reduced their ability to tolerate glucose deprivation (Duong *et al.*, 2012). Similarly stable transfection of AMPK inhibited tumour growth in nude mice indicating that expression of AMPK in tumour cells may facilitate tolerance to nutrient deprivation (Kato *et al.*, 2002).

A pro- or anti-tumourogenic role for AMPK could depend on a number of factors such as the degree of activation, the expression of particular AMPK isoforms, the subcellular localisation or the activity of other signalling networks such as the mammalian target of rapamycin (mTOR) pathway (which will be discussed in detail below). Similarly, it is possible that AMPK inhibition may lead to deregulation of other signalling cascades which could reduce the effects of AMPK inhibitors. Whether AMPK acts as a tumour suppressor or has an oncogenic function is contentious and requires further investigation.

1.9 Mammalian target of rapamycin

To survive in times when nutrient availability is variable, a cell must be able to turn off anabolic ATP consuming pathways, and turn on catabolic ATP-producing pathways and maintain control of the switch between the processes. As discussed above, AMPK is activated when ATP levels decrease; activation of this kinase leads to activation/inactivation of a number of downstream signalling pathways such as mTOR. mTOR (mammalian target of rapamycin) is a serine/threonine kinase that plays a role in multiple cellular pathways including cell growth, proliferation and metabolism. mTOR is a 290 kDa protein belonging to the phosphatidylinositol kinases related kinase family. It is present in eukaryotes in two distinct complexes; mTORC1 and mTORC2. mTORC1 is composed of five subunits; Raptor, Deptor, mLST, PRAS40 and mTOR. mTORC2 is composed of Rictor, Deptor, Protor 1/2, SIN1, mLST8 and mTOR (Fig.1.13).

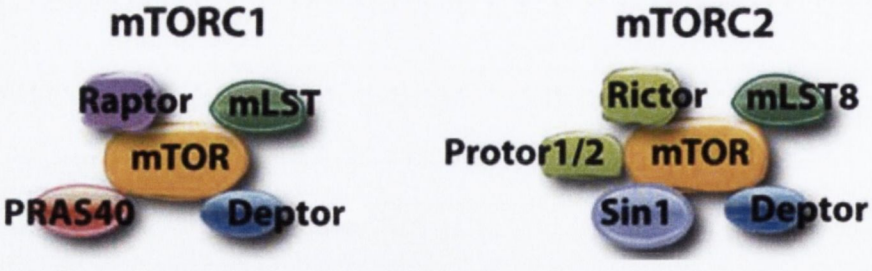

Figure 1.13 Structure of mTORC1 and mTROC2. Adapted from Limon *et al.*, (2012).

The mTOR pathway integrates signals from multiple sources including growth factors, oxygen, stress, energy status and amino acid availability to control protein and lipid synthesis (Fig. 1.14). The mTORC1 pathway regulates protein synthesis through one of

two mechanisms; firstly by phosphorylation and inactivation of eukaryotic initiation factor 4E-binding protein (4E-BP1), the repressor of mRNA translation, and, secondly, through the phosphorylation and activation of p70 ribosomal S6 kinase (p70 S6K). These mechanisms will be discussed in further detail below. In contrast, mTORC2 plays a role in the regulation of actin. Regulation of translation plays a vital role in the control of cell growth and proliferation (Loayza-Puch *et al.*, 2013), as an increase in the rate of translation is required for entry into the G_1 phase of the cell cycle. Deregulation of this process is associated with aberrant growth and tumourigenicity (Silvera *et al.*, 2010), therefore, drugs which target this pathway may provide a therapeutic opportunity to control aberrant cell growth and the development of malignant cells.

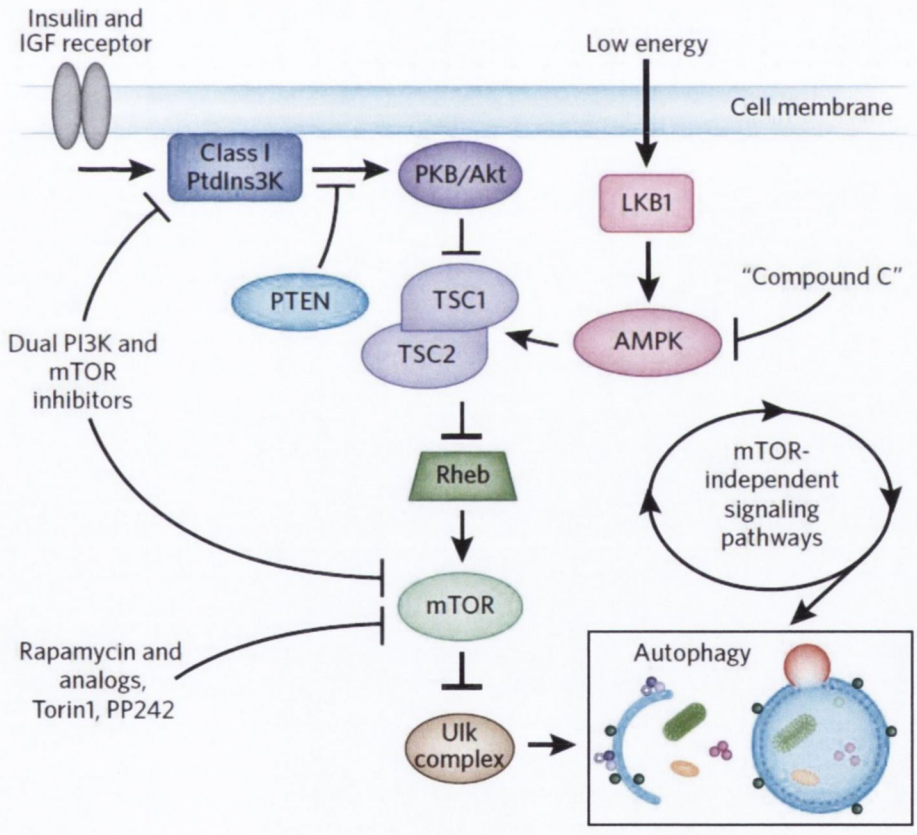

Figure 1.14 The mTOR signalling pathway. Taken from Fleming *et al.*, (2010).

Protein translation in eukaryotes is regulated primarily though the recruitment of the small ribosomal subunit to mRNA (Shveygert *et al.*, 2010). eIF4E recruits 40S ribosomal subunits to the 5′ end of mRNA. The eIF4F subunit eIF4E interacts directly with the mRNA

5' cap structure. 4E-BP1 is a repressor of translation; through binding to eIF4E it inhibits cap dependent translation. Activity of 4E-BP1 is regulated by phosphorylation; hypophosphorylated 4E-BP1 interacts strongly with eIF4E, whereas hyperphosphorylated 4E-BP1 does not (She *et al.*, 2010). In quiescent cells, 4E-BP1 is hypophosphorylated but becomes hyperphosphorylated on multiple sites in response to stimuli which activate the mTOR signalling pathway. For example, rapamycin, an inhibitor of mTOR signalling, inhibits phosphorylation of 4E-BP1, preventing translation.

The second target of mTOR is p70 S6 kinase is a serine/threonine kinase which regulates protein synthesis though phosphorylation of ribosomal S6 kinase. p70 S6 kinase is activated by phosphorylation on a number of serine/threonine residues; Thr^{389} in the linker domain has been identified as being essential for p70 S6 kinase activity (Dufner *et al.*, 1999). Phosphorylation releases the catalytic domain from the C terminal allowing Thr^{389} to be phosphorylated (Le *et al.*, 2003). When p70 S6 kinase is active and phosphorylates its downstream target, ribosomal s6 kinase, this leads to an increase in the translation of 5' terminal oligopyrimidine (TOP) mRNAs that encode ribosomal proteins and translation factors resulting in an increase in protein translation (Meyuhas & Dreazen., 2009).

mTOR is regulated by a number of upstream pathways including phosphatidylinositol-4,5-bisphosphate 3-kinase (PI3K) and protein kinase B (also referred to as Akt) (Yang *et al.*, 2013). When insulin binds to the insulin receptor, PI3K interacts with the insulin receptor and phosphorylates phosphatidylinositol-4,5-bisphosphate (PIP_2) to generate phosphatidylinositol-3,4,5-trisphosphate (PIP_3). PIP3 recruits Akt and PDK1 through binding of their pleckstrin homology (PH) domains. Activated Akt may phosphorylate a range of substrates, including TSC2 resulting in inhibition. mTORC1 is inhibited by TSC2; TSC2 has GTPase activating protein (GAP) activity towards Rheb, a small GTP-binding protein. TSC2 forms a complex with TSC1 and acts as a GAP converting Rheb from its active GTP bound form to an inactive GDP-bound form which leads to suppression of mTOR. Akt-mediated phosphorylation impairs the ability of TSC2 to inhibit Rheb and mTORC1 (Chalhoub *et al.*, 2009). mTOR may also be regulated by the upstream protein AMPK through inhibition of mTOR phosphorylation and phosphorylation of downstream

targets p70 S6 kinase and 4E-BP1, resulting in an inhibition of protein translation (Zhu *et al.*, 2012).

In addition to p70 S6 kinase and 4E-BP1, the mTOR signalling pathway also regulates the translation elongation process through the phosphorylation of eukaryotic elongation factor 2 (eEF2). eEF2 is a GTP-binding protein that mediates the translocation step of elongation. Similar to E4-BP1, binding of eEF2 is regulated by phosphorylation (Sengupta *et al.*, 2010). When eEF2 is phosphorylated at Thr^{56} within the GTPase binding domain, it loses its ability to bind to the ribosomes and is therefore inactivated, leading to a stop in translation. eEF2 is phosphorlyated and inactivated by eEF2K. eEF2K is regulated by the upstream protein p70 S6 kinase. p70 S6 kinase phosphorylates eEF2K leading to inactivation of eEF2K which consequently results in a dephosphorylation and activation of eEF2 thus allowing translation to proceed.

Translational control is crucial to the development and progression of cancer, controlling both protein synthesis and the selective translation of specific mRNAs, which may promote tumour cell survival through upregulation of angiogenesis and an increase in the invasive and metastatic potential of the cell. Numerous studies have found this pathway to be deregulated in multiple cancers. Initiation of translation is regulated by eIF2 proteins which dictate whether a specific mRNA will be translated and the speed at which it will occur (Sonenberg & Hinnebusch., 2009). Expression of eIF2 proteins have been reported to be increased in numerous cancers including melanoma (Rosenwald *et al.*, 2003), colon (Rosenwald *et al.*, 2003), stomach (Chen *et al.*, 2004), colorectal (Xie *et al.*, 2008) and bladder cancer (Luo *et al.*, 2009). At present it is unclear whether this increase in eIF proteins leads to an overall increase in protein synthesis or alteration of expression of specific mRNAs, although both may contribute to the development and progression of cancer. The loss of translational control is thought to contribute to metastasis; for example, eIF5A2 expression has been reported to increase in colon cancer from benign tumours to primary carcinomas to metastatic lesions (Xie *et al.*, 2008), while metastatic cells may survive periods of stress by increasing expression of anti-apoptotic proteins Bcl-2 and XIAP (Silvera *et al.*, 2009).

Control of this process could prove to be an effective means of controlling cancer cell survival. For example drug-induced activation of AMPK may lead to downstream inhibition of the mTOR pathway with potential therapeutic benefits. mTOR-mediated regulation of the cell cycle is controlled in part by an increase in translation of mRNAs encoding positive regulators of the cell cycle and a decreased translation of negative regulators such as p27, a cyclin dependent kinase inhibitor (Dalvai *et al.*, 2010). For instance, mTOR regulates the synthesis of cyclin D1 which controls progression though the G1/S phase of the cell cycle. Oncogenic activation of the mTOR pathway drives proliferation via increases in cyclin D1 and cyclin E and loss of the restraining effects of p21 and p27 on cell cycle (Wander *et al.*, 2011). Similarly inhibition of mTOR has been shown to decrease expression of the angiogenic protein VEGF (Yu et al., 2009).

1.10 Autophagy

Autophagy, an evolutionary conserved pathway, is a cellular degradation system which allows for the delivery of cytoplasmic material to the lysosomes for degradation (Codogno *et al.*, 2014). Cytoplasmic components become enclosed in a double membrane structure which fuses with the lysosomes where the contents are hydrolysed. Amino acids and other biomolecules are transported back to the cytosol where they can be reused. In this way autophagy allows for the recycling of cellular material to maintain homeostasis. Numerous studies have provided evidence to support the housekeeping role of autophagy. Tissue specific deletions of Atg genes were shown to result in ubiquitinated protein aggregates leading to tissue specific dysregulation (Fig. 1.15).

This is a process which occurs both at a basal level in healthy cells and aberrant levels in malignant cells (Yang *et al.*, 2011). It is a multi-step process involving firstly initiation followed by autophagasome formation, maturation and finally degradation. These processes are controlled by a family of ATG genes of which more than 30 have been identified. There are two Atg protein conjugation systems which are primarily responsible for autophagasome formation, namely the Atg 12- Atg-5 and Atg 8-phosphatidylethanolamine (PE) conjugation systems. Atg 12 is activated by Atg 7, a ubiquitin like protein which is conjugated to Atg 5. Atg 5 binds to Atg 16 to form a multimeric complex which aids the formation and elongation of the phagophore in autophagasome formation. This complex dissociates after autophagasome formation is

complete. Atg 8 (also referred to as LC3) PE conjugate also assists in formation possibly by enhancing membrane fusion. Finally the autophagasome fuses with the lysosome to form the autophagolysosome. Autophagy is primarily controlled by two energy sensing pathways; the AMPK pathway which is activated during hypoxia or during times of energy depletion, and the mTOR pathway which is a negative regulator of autophagy (Jung *et al.*, 2009).

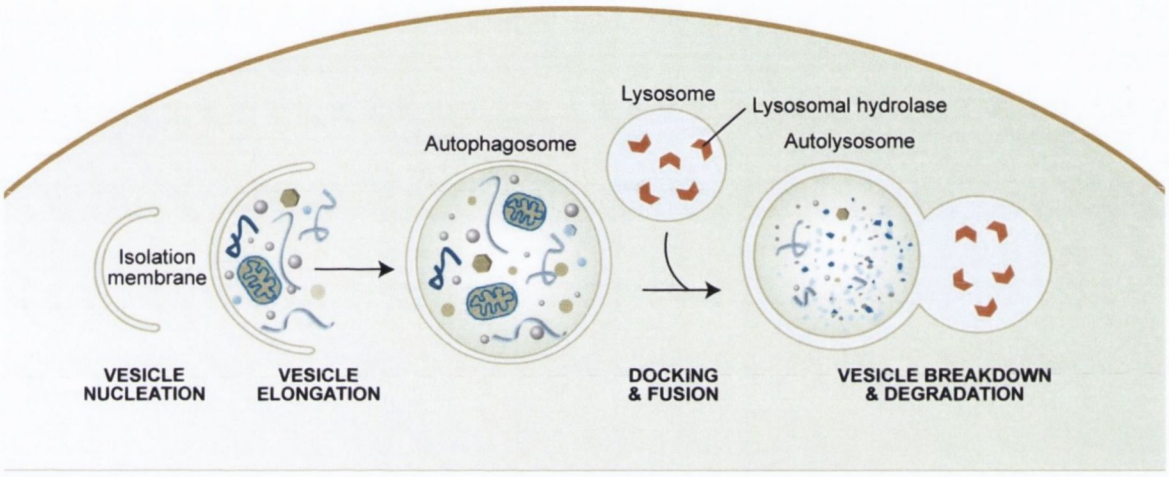

Figure 1.15 Schematic diagram of the steps of autophagy.

Autophagy begins with the formation of the phagophore which expands to form the autophagasome. The autophagosome can engulf bulk cytoplasm non specifically, including entire organelles, or specifically target cargo. When the outer membrane of the autophagosome fuses with an lysosome to form the autophagasosome in which the sequestered material is degraded and recycled. Taken from Melendez *et al.*, (2009).

Autophagy may function at a basal level to eliminate old or unwanted proteins while providing the building blocks to cellular growth to maintain homeostasis; although mounting evidence points to a role in cancer with evidence showing autophagy may be induced under certain conditions such as hypoxia, unfolded protein response and nutrient deprivation. Loss of Atg 5 or 7 in the brain was shown to result in neurodegeneration (Hara *et al.*, 2006; Komatsu *et al.*, 2006). A direct link between autophagy and cancer was established by the discovery that Beclin-1, the mammalian ortholog of yeast Atg 6 could function as a tumour suppressor (Liang *et al.*, 2006). Multiple cancers such as breast carcinoma and prostate cancer exhibit decreased levels of Beclin-1 while disruption of the

BECN1 gene leaves mice prone to the development of spontaneous tumours (Qu *et al*, 2003). Taken together these studies indicate that autophagy plays a tumour suppressor role in cancer; although there is also evidence to contradict these findings. Both *in vivo* and *in vitro* data support a tumour promoting role for autophagy in cancer (Yu *et al.*, 2008; Chen *et al.*, 2010; Yang *et al.*, 2011). As autophagy is activated in response to stress to facilitate cell survival, it is plausible that this process may contribute to the survival of an established tumour (Levine & Yuan., 2005). As a tumour grows it becomes poorly vascularised leading to a decrease in the availability of oxygen and nutrients often resulting in a hypoxic environment. Cells in the hypoxic core of a tumour can induce autophagy enabling them to survive in these harsh conditions (Mazure *et al.*, 2010). This allows the most aggressive, drug resistant cells with a higher metastatic potential to survive, furthermore this scenario is more likely to result in a failure to respond to treatment and overall a poorer prognosis. The ability of a tumour to cope with stress by activating survival pathways may offer tumours a selective advantage allowing them to metastasis and dessiminate. Many chemotherapeutic drugs have been shown to induce autophagy and may contribute to the development of drug resistance (Sui *et al.*, 2013). If autophagy is indeed working as a tumour promoter, then inhibition of this process though genetic manipulation such as the use of siRNA of shRNA or the use of chemical inhibitors such as bafilomycin-A1, 3-methyladenine or chlorquine may be able to resensitise cells to chemotherapy and could be exploited to prevent the development of MDR.

1.11 The Cell Cycle

This is the highly regulated series of events resulting in the division of a single cell into two daughter cells each with identical copies of the genome. The cycle may be divided into two phases; mitosis in which the cell divides, and interphase, the stage between two M phases. Mitosis may be further subdivided into prophase, metaphase, anaphase and telophase during which time the cells genetic material is replicated and divided into two identical sets of chromosomes which separate into two identical but entirely separate daughter cells. Interphase may also be subdivided into separate phases, namely G_1, S and G_2. During G_1 the cells are growing and preparing the chromosomes for replication. In S phase the DNA is synthesised. G_2 provides a gap between DNA synthesis and division.

Some cells may exit the cell cycle and enter a phase a resting period termed G_0, in which the cells are quiescent. This stage may be temporary or permanent.

To ensure two genetically identical cells are produced, the cell cycle is highly regulated by cyclins and the cyclin dependent kinases (CDKs), serine/threonine protein kinases that are activated at specific points during the cell cycle and phosphorylate specific proteins to activate downstream signalling pathways. The activity of CDKs are controlled though binding of cyclins which are synthesised and destroyed at different points during the cell cycle leading to fluctuations in their expressions; this is in contrast to the levels of CDKs which remain constant (Fig. 1.16).

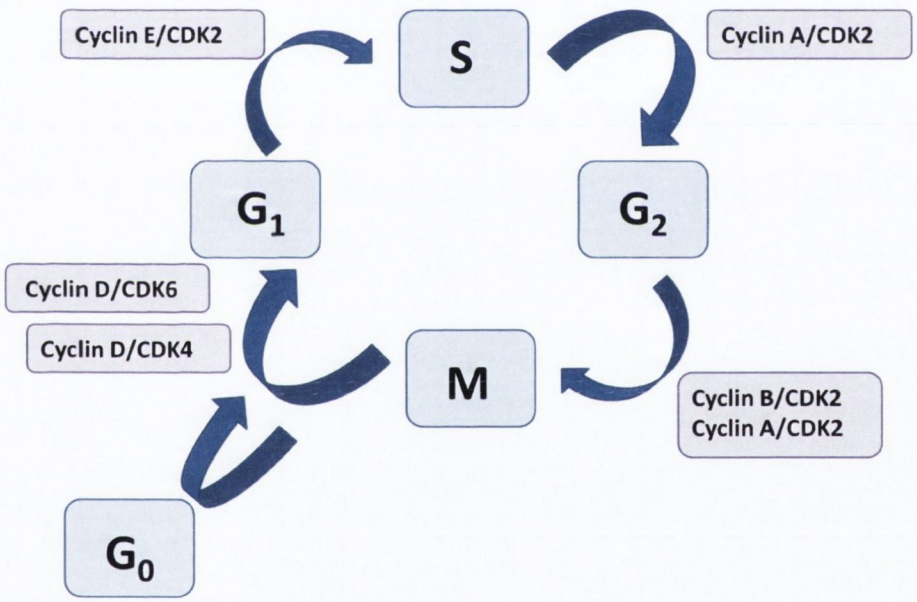

Figure 1.16 The stages of the cell cycle.

Progression though the cell cycle is maintained by checkpoints that detect defects in proper DNA replication and chromosomal division thus preventing the inheritance of faulty genetic material. These checkpoints are controlled by CDKs. For example, if DNA damage has occurred, the cell must be given time to repair this damage before continuing into S phase (G1-S checkpoint) or after DNA replication (G2-M checkpoint), consequently levels of CDKs fall preventing cell cycle progression. The spindle assembly checkpoint (SAC), also called the mitotic checkpoint, verifies that all conditions for chromosome

segregation have been met allowing segregation to proceed. The SAC will stall segregation until kinetochores of the sister chromotids are attached to polar microtubules (Musacchio and Salmon., 2007). Once completed the anaphase promoting complex (APC) mediates the ubiquitination of securin resulting in the release of separin which in turn cleaves the sister-chromatin cohesion complex triggering the release of the sister chromatids (Nasymth *et al.* 2000).

Dysregulation of the cell cycle is a hallmark of multiple cancers including neuroblastoma. Increased expression of spindle assembly checkpoint regulatory genes has been reported to be associated with MYCN amplification and 1p deletion in neuroblastoma (Westermann *et al.*, 2007; Ooi *et al.*, 2012). MYCN amplified tumours fail to arrest cells at the G1-S checkpoint after exposure to DNA damaging drugs such as doxorubicin. Gogolin *et al.*, (2013) have recently shown that several MYCN amplified neuroblastoma cell lines harbour mutations which result in an increase in CDK4 expression. Inhibition of CDK4 by siRNAs or selective small molecule inhibitors partly restored G1-S arrest, delayed progression into S phase and lead to a reduction in cell viability after exposure to doxorubicin. Cyclin D1 forms complexes with CDK4 and CDK6 to allow progression through the G1 checkpoint. Similarly expression of CDK2, a regulator of the S-phase checkpoint has also been shown to be increased in MYCN amplified tumours. Molenaar *et al.*, (2009) have demonstrated that inhibition of CDK2 induces apoptosis in MYCN amplified tumours advocating its role as a target for therapeutic intervention.

1.12 Microtubules

The cytoskeleton, the protein network which gives structure to the eukaryotic cell and allows for various types of cell movement, is composed of actin, intermediate filaments and microtubules. The three broad functions are as follows, to spatially organise the contents of the cell; to connect the cell physically and biochemically to the external environment; and to generate coordinated forces that enable the cell to move and change shape (Fletcher *et al.*, 2010).

Microtubules are polymers of α- and β- tubulin bound to microtubule-associated proteins (MAPs) which regulate the stability and distribution of the microtubule. Each tubulin molecule is a heterodimer of two globular subunits, α- and β- tubulin each with very

similar structure. Each monomer is formed by a pair of central beta sheets surrounded by helices, has a molecular weight of approximately 50 kDa and is characterised by a sequence of approximately 450 amino acids (Nogales *et al.*, 1998). Dimers of α- and β-tubulin dimers polymerise into protofilaments by joining end to end. The microtubule is formed when 13 linear protofilaments assemble in parallel with the same polarity around a hollow core. In each protofilament, α- tubulin is exposed at one end and β- at the other (Fig. 1.17). Microtubules are polar structures; the microtubule grows more rapidly at the positive end than the negative. The polarity of the microtubule determines the direction of movement.

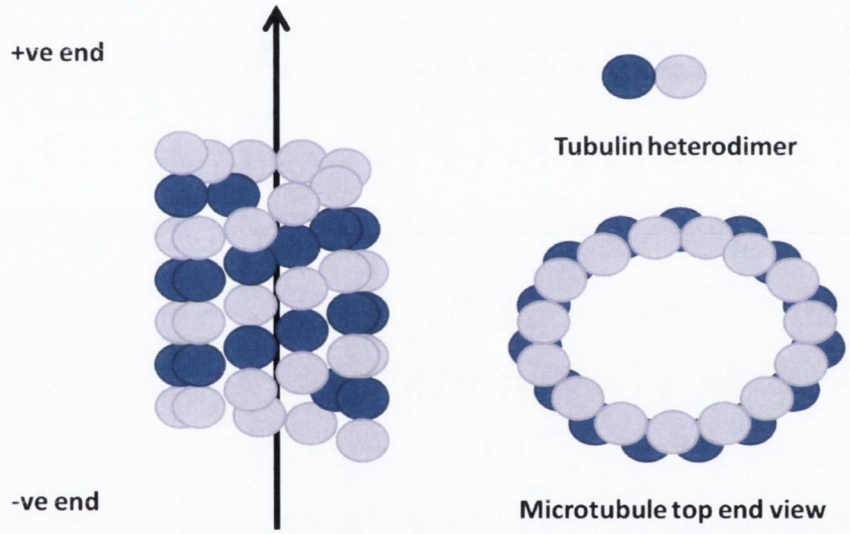

Figure 1.17 The structure of microtubules.

They are composed of dimers of α- and β-tubulin that polymerise to form microtubules, which are composed of 13 protofilaments assembled around a hollow core.

Microtubules are dynamic structures which undergo assembly/disassembly through polymerisation/depolymerisation (Fig. 1.18). This constant growing and shrinking is mediated by the hydrolysis of GTP. Both α- and β- tubulin can bind GTP; binding to α-tubulin is nonexchangeable as the site is trapped between two monomers of the heterodimer (known as the N site) whereas GTP can bind to β-tubulin in the 'E' site. During polymerisation GTP bound to β tubulin is hydrolysed. This weakens β- tubulins affinity for adjacent molecules resulting in depolymerisation. Tubulin with bound GDP are repetitively lost from the minus end and replaced at the plus end with GTP bound tubulin.

The microtubule will continue to grow as long as there is an excess of GTP bound tubulin. If the rate of GTP hydrolysis becomes faster than the rate of addition, the GDP bound tubulin at the end will dissociate and disassembly occurs. This switch between phases of growth and shrinkage is referred to as dynamic instability (Van der Vaart *et al.*, 2009). The microtubule will continue to grow as long as the concentration of tubulin remains above a critical level. At the minus end the critical concentration is slightly higher than the plus end so it tends to stop growing first. Although the critical level may not be reached, the microtubule may stop growing and begin to shrink; this is termed 'catastrophe'. If the microtubule begins to grow again this is called 'rescue'.

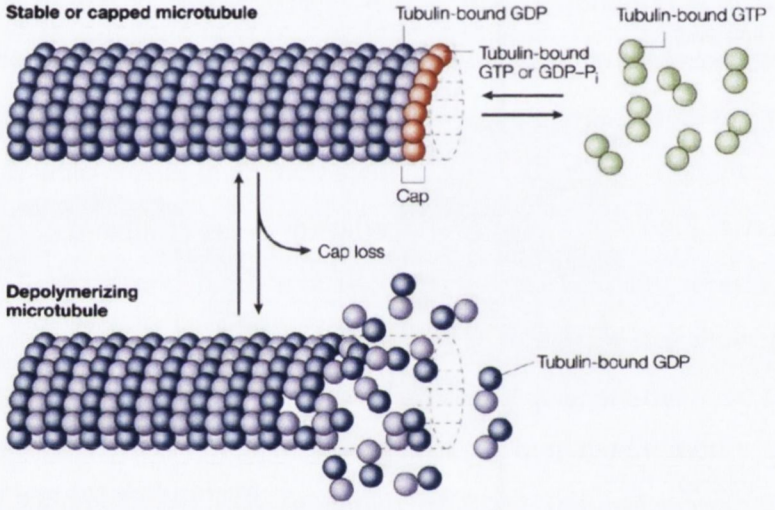

Figure 1.18 Polymerisation dynamics of microtubules.

GTP bound to tubulin is hydrolysed to GDP and inorganic phosphate (P_i) at the time that tubulin adds to the microtubule ends. The P_i dissociates from the microtubule. This leaves a microtubule consisting of tubulin with stoichiometrically bound GDP. A microtubule end is stable when containing tubulin-bound GTP or GDP–P_i and will not depolymerise. When GTP is hydrolysed a conformational change alters the tubulin molecules so that the polymer is destabilised. This results in catastrophe and shortening of the microtubule. Taken from Jordan *et al.*, (2001).

Microtubules play an essential role in mitosis; namely in the separation of sister chromatids. The microtubule organising centre (MTOC) is the anchoring point near the centre of the cell from which the microtubules extend out (Tanaka *et al.*, 2005). In interphase cells the MTOC is located at the centrosome. During mitosis the microtubules disassemble from this form and reassemble to form the mitotic spindle. After the nuclear

envelope is broken down, the chromosomes are condensed; the spindle microtubules ensure they are correctly attached to the spindle via their kinetochores. During metaphase, microtubules align the chromosomes along the metaphase plate. Subsequently during anaphase and later telophase, microtubules aid the movement of chromosomes to opposite poles to ensure they are in the proper position when the cell divides into two daughter cells.

1.13 Microtubule Targeting Agents

The cell cycle has a number of checkpoints which can become faulty in cancerous cells allowing for uncontrolled proliferation. Therefore, one approach to combating these defective cells is to use drugs that target certain processes or proteins that impinge on the cell cycle machinery. As discussed above, microtubules play a critical role in cell division therefore making them an attractive candidate for cancer therapy. Microtubule targeting agents (MTAs) inhibit cell division by binding to microtubules and inhibiting microtubule dynamics during mitosis. Rapid dynamics is crucial for successful mitosis. During mitosis, microtubules that form the spindle become 4-100 times more dynamic than interphase microtubules (Rusan *et al.*, 2001). MTAs inhibit cell division by interfering with spindle microtubule dynamics. There are two classes of MTAs; microtubule destabilising drugs and microtubule stabilising drugs. Destabilisers inhibit polymerisation, e.g. vinca alkaloids, colchicine and combretastatin whereas stabilisers increase polymerisation, e.g. paxlitaxel and epothilones (Fig. 1.19). These agents may act directly on microtubules but also on soluble tubulin. Inhibition of dynamic instability decreases spindle tension and slows movement from metaphase to anaphase (Jordan *et al.*, 1996).

Vinca alkaloids were first isolated from the leaves of the periwinkle plant *Catharanthus roseu*. Since the 17th century the leaves of this plant had been known for its medicinal properties. The anti-cancer potential of these drugs were discovered in the 1950s (Noble *et al*, 1958). It was initially used as a single treatment for solid and haematological malignancies in children and later in adults. Side effects include myelosuppression caused by inhibition of proliferation of bone marrow cells and peripheral neuropathy (Moudi *et al.*, 2014). Vinca alkaloids bind at the *vinca* binding domain in the β subunit of tubulin

dimers (Fig. 1.19). They can also bind directly to microtubules. Binding is rapid and reversible (Jordan *et al*, 1992). At low concentrations, vinca alkaloids such as vinblastine can block mitosis but it is only at higher concentrations that depolymerisation occurs (Jordan *et al.*, 1992). Vinblastine affects the mitotic spindle such that it cannot assemble as it should, reducing tension at the kinetochores. Chromosomes become trapped in a metaphase like state, unable to enter anaphase. These cells then die by apoptosis.

In 1967, Paclitaxel was isolated from the bark of the yew tree (Wall *et al.*, 1967) and is now used to treat several malignancies including cancers of the breast and ovaries. Unlike vinca alkaloids it binds poorly to soluble tubulin but strongly to β-tubulin along the length of the microtubule. Binding stabilises the microtubule surface and polymerisation increases. It is thought that binding induces a conformational change in the tubulin which increases its affinity for neighbouring tubulin (Nogales *et al.*, 2001).

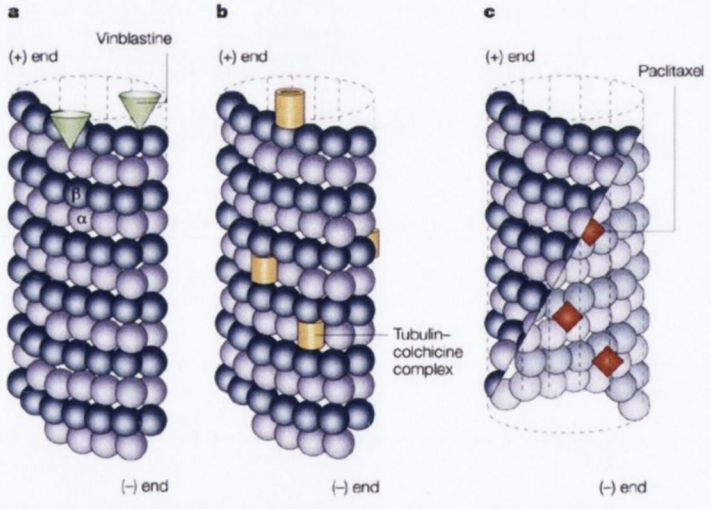

Figure 1.19 The binding sites of vinblastine, colchicine and paclitaxel on the tubulin polymer. Taken from Jordan *et al.*, (2001).

1.14 The PBOX Compounds

Pyrrolo-1,5-benzoxazepines (PBOXs) are a series of novel microtubule targeting agents originally designed as high affinity ligands for the peripheral type benzodiazepine receptor (PBR), an 18 kDa protein primarily found on the outer mitochondrial membrane. The PBR was initially identified as a receptor for benzodiazepines and has been shown to

be expressed in multiple locations in the body including the heart, liver and lymphatic system (Casellas *et al.*, 2002). Its exact physiological role has not yet been identified but multiple biological roles including cell proliferation, the transport of cholesterol, modulation of the immune system and steroidogenesis (Papadopoulos., 1997) has been postulated. A number of both antagonistic and agonist ligands have been identified including the agonist, diazepam binding inhibitor (DBI), an 11 kDa neuropeptide which stimulates steroidogenesis *in vivo* (Veenman *et al.*, 2012). Additionally PBR ligands, like the PBOXs have been shown to have a role in apoptosis although PBOX induced apoptosis has been shown to be independent of PBR. The PBOX were found to induce apoptosis in HL-60 (PBR expressing) and Jurkat (PBR deficient) cells with similar potency whereas the PBOXs were unable to induce apoptosis in PBR rich R2C Leydig cells (Zisterer *et al.*, 2000). PBOX compounds can be divided into two classes, those which arrest cells in G1 such as PBOX-21 and those which induce apoptotic cell death, for example PBOX-6 (Fig. 1.20).

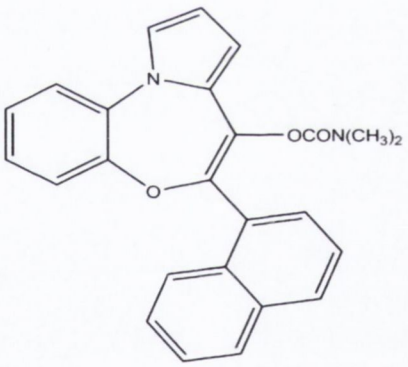

PBOX-6

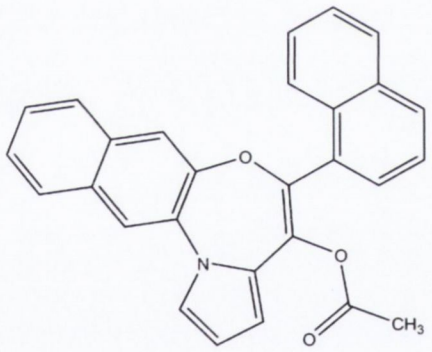

PBOX-15

Figure 1.20 Structure of two representative pro-apoptotic members of the PBOX family, PBOX-6 and PBOX-15.

Tubulin has been identified as the molecular target of the PBOXs (Mulligan *et al.*, 2006). Mulligan *et al.,* observed an accumulation of cells in G2/M in response to PBOX-6. PBOX-6 was found to induce prometaphase arrest and an accumulation of cyclin B1 levels and activation of cyclin B1/CDK1 kinase in a similar manner to that of nocodazole and paclitaxel. Both PBOX-6 and -15, another pro-apoptotic member of this family of novel MTAs, were shown to induce microtubule depolymerisation in MCF-7 cells, in contrast to

PBOX-21, a non-apoptotic PBOX compound which was found to have no effect on the cellular microtubule network or on the assembly of purified tubulin. Although it is known that disruption of the microtubule network is caused by PBOX binding to tubulin subunits, the PBOX binding site on tubulin is as yet unidentified.

Two of the more potent pro-apoptotic PBOXs, PBOX-6 and 15, have been shown to potently induce apoptosis in a number of cancer cell lines including, Jurkat and Hut-78 T lymphoma cells (Zisterer *et al.*, 2000), MCF-7 breast cancer cells (Greene *et al.*, 2005), HL-60, a promyelocytic leukaemia cell line (Mulligan *et al.*, 2006), A2780 ovarian cancer cells (Nathwani *et al.*, 2010) and K562S and LAMA84, chronic myeloid leukaemia cell lines (Bright *et al.*, 2009; 2010). Additionally, the PBOXs have been shown to induce apoptosis in a number of drug-resistant cell lines, for example the highly drug-resistant chronic myeloid leukaemia (CML), K562 cell line (McGee *et al.*, 2004). While it is important for anti-cancer drugs to induce apoptosis in malignant cells, it is crucial they do not have adverse effects on non-cancerous cells. The PBOXs fulfil these requirements; they elicit minimal toxicity to normal peripheral bone marrow cells (PMBC) (McGee *et al.*, 2004). Inhibition of proliferation of normal B-cells and bone marrow progenitor cells has been found to be minimal (McElligott *et al.*, 2009).

One characteristic common to a number of chemotherapeutics used in the treatment of neuroblastoma is that they are substrates for MDR proteins such as MDR1 and BCRP, which can result in resistance to these drugs. Previously, Nathwani *et al.*, (2010) demonstrated that the PBOXs are not substrates for these drug efflux proteins. In contrast to other MTAs including vincristine and paclitaxel, which displayed resistance in cell lines expressing MDR1 and BCRP, the PBOXs were equally potent in both the parental and resistant cell lines.

Ex vivo studies have demonstrated PBOX-induced apoptotic cell death is not limited to *in vitro* cell lines. McElligott *et al.*, (2009) reported that PBOX-15 induced apoptosis both in *ex vivo* B-cell lymphocytic leukaemia (CLL) cells harbouring poor prognostic indicators and fludarabine resistance-associated p53 deletions. The effects of the PBOXs have been investigated in *ex vivo* CML patient samples. CML is a cancer of the white blood cells characterised by the presence of the Philadelphia chromosome which is formed by a reciprocal translocation between two genes, Bcr and Abl forming an aberrantly expressed

Bcr-Abl oncogene. This gene codes for a constitutively active tyrosine kinase which phosphorylates proteins involved in growth factor signalling or cell adhesion (Deininger *et al.*, 2000). STI-571 (also called imatinib mesylate), a tyrosine kinase inhibitor is currently the front line treatment used in the clinic. PBOX-6 and -15 were shown to induce apoptosis in primary CML patient samples including those resistant to STI-571 (Bright *et al.*, 2010). Additionally the effects of the PBOXs have been investigated in a number of animal models. PBOX-6 inhibited tumour growth in both a mouse 4T1 breast cancer model (Greene *et al.*, 2005) and a mouse CML xenograph model (Bright *et al.*, 2010).

Similar to neuroblastoma, development of resistance to chemotherapeutics is a major obstacle in the successful treatment of CML. A substantial number of CML patients develop resistance to STI-571 particularly during the advanced stages of the disease when resistant cells express a mutant form of *Bcr-Abl* that demonstrates decreased binding to STI-571 when compared with the unmutated protein. As in neuroblastoma, the development of resistance to conventional chemotherapy demonstrates the need for alternative treatment strategies. Bright *et al.,* (2010) investigated the potential for PBOX-6 to synergistically enhance the anti-cancer effects of flavopiridol in drug-resistant CML cells. Flavopiridol is a potent CDK1 inhibitor which has shown activity in a wide variety of malignancies both *in vitro* and in *in vivo* animal models and is currently under clinical investigation for the treatment of CML (ClinicalTrials.gov: NCT00278330). It was demonstrated by flow cytometric analysis, that K562 CML cells underwent a dose-dependent increase in apoptosis when treated for 18 hours with PBOX-6 or PBOX-15 followed by a 24 hour treatment with flavopiridol when compared to either agent alone. Similar enhancements of PBOX-induced apoptosis were also seen in another CML cell line (LAMA84) after the addition of flavopiridol. Additionally, PBOX-6 was shown to enhance the apoptotic effects of flavopiridol in both native and Bcr-Abl mutated cells (Bright *et al.*, 2010) which could be attributed to an accelerated exit from the G2/M phase of the cell cycle resulting in an enhanced decrease cyclin B1/CDK1 activity. As this complex is a regulator of survivin, a pro-survival IAP protein, Bright *et al.*, reported a resultant decrease in survivin expression. This was further supported by additional studies showing an siRNA-mediated decrease in survivin expression increased PBOX-6 induced apoptosis in K562 cells. Other studies have shown PBOX enhancement of apoptosis in combination with other non MTA drugs in several malignant cell lines. Greene *et al.,* (2007)

demonstrated the capacity of PBOX-6 to enhance the apoptotic effect of STI-571 in both drug sensitive and resistant CML cell lines. PBOX-21 was also shown by Bright *et al.*, (2009) to work in combination with STI-571, to synergistically enhance the apoptotic effects of this tyrosine kinase inhibitor. Co-treatment of CML cells with PBOX-21 and STI571 induced more apoptosis than either drug alone in parental (K562S and LAMA84) and STI571-resistant cells lines (K562R). Apoptosis induced by PBOX-21/STI571 resulted in cleavage of the DNA repair enzyme PARP, downregulation of pro survival Bcl-xL and Mcl-1, upregulation of pro-apoptotic Bim and activation of caspase-8.

These findings would indicate the potential for the PBOXs to work in combination with other cytotoxic drugs to enhance their apoptotic effects. To date the anti-cancer effects of the PBOX compounds in human neuroblastoma cells have not been studied. However, the microtubule targeting agent, vincristine, is currently used to treat neuroblastoma, so tubulin is a valid therapeutic target in this type of cancer. Vincristine is a substrate of P-gp which may limit its efficacy in the treatment of neuroblastoma, thus novel tubulin depolymerising agents which are not substrates of P-gp may be more efficacious.

1.15 Objectives of the project

The objective of this study was to determine the ability of novel PBOXs to induce apoptosis in a panel of drug sensitive and resistant neuroblastoma cell lines. The effects of the PBOXs were compared to those currently used for the treatment of neuroblastoma including vincristine, doxorubicin, etoposide and carboplatin. The effect of the PBOXs alone and in combination with these chemotherapeutics was compared and any additive or synergistic effects were determined. Additionally the molecular basis for this enhancement in neuroblastoma cell lines was determined. The ability of PBOX-6 to induce apoptosis in primary neuroblastoma cells isolated from *ex vivo* patient samples, and to inhibit tumour formation in an *in vivo* neuroblastoma model was also determined.

Chapter 2

Materials and Methods

2.1 Materials and Suppliers

Alamar blue	Invitrogen
Anti actin monoclonal antibody	Calbiochem
Anti-Bak	Merck
Anti Bak-NT	Cell signalling technology
Anti-Bax	Cell signalling technology
Anti-Bcl-2	Cell signalling technology
Anti-caspase-3	Cell signalling technology
Anti-caspase-9	Cell signalling technology
Anti- caspase-8	Cell signalling technology
Anti-cytochrome c	BD Pharmingen
Anti-GAPDH	Calbiochem
Anti-Mcl-1	Calbiochem
Anti-mouse IgG secondary Ab	Merck
Anti-PARP	Merck
Ammonium persulfate	Sigma
BCA protein reagents A and B	Pierce
BSA powder	Sigma
BSA protein standards	Pierce
Carboplatin	Tocris
Cryogenic tubes	Nalgene
Crystal violet	Sigma
Doxorubicin	Tocris
DMEM+Glutamax	Biosciences
DMEM low glucose	Biosciences
DMEM/F12	Biosciences
DMSO	Sigma
Dithiothreitol	Sigma
ECL detection agents A and B	Sigma
Ethanol	Lennox
Etoposide	Sigma
FACs flow	BD Biosciences
FACS tubes	BD Biosciences
Fetal bovine serum	Invitrogen
Filter paper	Whatman
Glycerol	Sigma
Glycine	Sigma
HEPES	Sigma
Iscove's Modified Dulbecco's Medium	Biosciences

Iso-propanol	Lennox
Kodak-X-omat LS film	Sigma
Methanol	Lennox
N-acetylcysteine	Sigma Aldrich
Phosphate buffered saline	Biosera
Penicillin	Biosciences
Ponseau S	Sigma
Protogel	Sigma
Prism graphpad	Graphpad software,Inc
Propidium iodide	Sigma
PBS tablets	Dulbecco
Protein molecular weight marker	Thermo Fisher
PVDF	Millipore
RNAse	Sigma
RPMI 1640	Biosciences
siRNA-Mcl-1	Thermo Fisher
Sodium dodecyl sulphate	Sigma
Streptomycin	Biosciences
TEMED	Sigma
Trizma-base	Sigma
Triton-X-100	SIgma
Tween-20	Sigma
Vincristine	Sigma

All sterile tissue culture flasks, pipettes, plates, pipette tips and universal tubes were from Greiner Bio-one Ltd with the exception of CellBIND six well plates which were from Corning. PBOX-6 and 15 were synthesised by Professor Guiseppe Campiani, University of Siena, Italy. SHSY5Y, Kelly and SK-N-BE(1) cells were a kind gift from Professor Raymond Stallings, RCSI, Dublin. The SK-N-FI and CHLA-90 cell lines were received from the Childrens Oncology Group, Cell Culture and Xenograft Repository, Cancer Center, Texas Tech University Health Sciences Center School of Medicine, Lubbock, TX 79430, U.S.A. The SK-N-BE(2)c cell line was kindly provided by Doctor Sétha Douc-Rasy, Enseignante-chercheur, Université Paris.

2.2 Postal and email addresses of suppliers/ distributors

ATCC: LGC Standards, Queens Road, Teddington, Middlesex TW11 OLY, U.K
atcc@lgcpromochem.com

BD Bioscience: 21 Between Towns Road, Cowley. OX4 3LY Oxford, U.K
BDUK_customerservice@europe.bd.com

Biosciences: 3 Charlemont Terrece, Crofton Road, Dun Laoghaire, Co. Dublin, Ireland
orders@biosciences.ie

Biosoft: 20 Dolphin Way, Stapleford, Cambridge CB2 5DW, U.K
info@biosoft.com

Calbiochem: P.O Box 12087, La Jolla, California 92-39-2087, U.S.A
CUSTOMER.SERVICE@MERCKBIOSCIENCES.CO.UK

Cell Signalling Technology: 3 Trask Lame, Danvers, Massachusetts 01923, U.S.A
enquiries@brennanco.ie

GraphPad Software Inc: 2236 Avenida de la Playa, La Jolla California 92037, US.A
sales@graphpad.com

Grenier Bio-One Ltd: Brunel way, Stroudwater Business Park Stonehouse, Gloustershire GL10 3SX, U.K
orders@cruinn.ie

Harlan Laboratories U.K Ltd: Blackthorn, Oxon 0X25 ITP U.K
orders@harlan.com

Invitrogen Ltd: 3 Fountain Drive, inchinnan Business Park, Paisley PA4 9RF, U.K
orders@biosciences.ie

Lennox Laboratory Supplies Ltd: John. F. Kennedy Drive, Naas Road, Dublin 12, Ireland
sales@lennox.ie

Millipore Ireland B.V: Tullagreen Carrigtwohill, Co. Cork, Ireland
eiorders@europe.sial.com

Pierce Biotechnology, Inc: P.O Box 117, Rockford, Illinois 61105, U.S.A
Info"medical-supply.ie

R&D Systems Europe Ltd: 19 Barton Lane, Abingdon Sciences Park, Abingdon, Oxon OX14 3NB U.K
info@RnDSystems.co.uk

Roche Diagnostics Ltd: Charles Avenue, Burgess Hill, West Sussex RH159RY U.K

Uk.biochem@roche.com

Sigma Aldrich Ltd: Airton Road, Tallaght, Dublin 24, Ireland

eiorders@europe.sial.com

Thermo Fischer Scientific: Plaza 212, Blanchardstown Corporate Park 2, Ballycoolin, Dublin 15

Fsie.sales@thermofisher.com

Tocris: Tocris House, IO Centre, Moorend Farm Avenue, Bristol, BS11 0QL, United Kingdom

info@tocris.com

Whatman International Ltd: Springfiels Mill, James Whatman Way, Maidstone, Kent, ME14 2LE U.K

information@whatman.com

2.3 Cell maintenance

SHSY5Y and SK-N-BE(1) cells were cultured in DMEM/F12+GlutaMAX medium supplemented with 10% (v/v) foetal bovine serum (FBS) and 1% (v/v) penicillin/streptomycin. Kelly and SK-N-BE(2)c cells were grown in RPMI 1640 + GlutaMAX medium supplemented with 10% (v/v) (FBS) and 1% (v/v) penicillin/streptomycin. SK-N-FI cells were grown in DMEM+Glutamax medium supplemented with 10% FBS and 1% penicillin/streptomycin. CHLA-90 cells were grown in IMDM medium supplemented with 1% (v/v) insulin/transferrin/selenium, 10% (v/v) (FBS) and 1% (v/v) penicillin/streptomycin. Cells were incubated in a humidified environment at 95% O_2 and 5% CO_2 and passaged twice a week depending on levels of clonfuency. Medium was decanted and the flask was washed in 2-3 mls sterile phosphate buffered saline (PBS). PBS was discarded and cells were trypsinised in 1 ml of 1X trypsin/EDTA (10X trypsin/EDTA diluted 1:10 in PBS) at 37°C for 3 mins. Cells were rinsed in 9 mls of medium, transferred to a 30 ml universal tube and centrifuged at 300 xg for 5 mins in a Sorvall Legend T centrifuge. The supernatant was discarded, the pellet was resusupended in 10 mls medium and the cells were counted using a haemocytometer.

2.3.1 Cell counting

Cells were counted using a bright light haemocytometer, a glass microscope slide with a rectangular indentation that creates a chamber 0.1 mm high. This chamber is engraved with grid of perpendicular lines. Each grid consists of 9 large squares, eight of which contain 16 smaller squares and the central square containing 25. The chamber is designed so that both the area bounded by the lines and the depth of the chamber is also known. This facilitates counting of cells in a specific volume of fluid and thereby calculation of the concentration of cells in the fluid overall.

When in use a cover slip is placed over the haemocytometer. A 10 µl cell suspension is pipetted into an indentation at the edge. The cell suspension moves across the chamber by capillary action. The number of cells in each of the four large squares is counted and the mean number of cells per square is calculated. The volume of each large square is 1 x

10^{-4} ml so the total cell concentration of the sample can be determined by multiplying the mean number of cells counted by 10^4.

2.3.2 Cryopreservation of cells

Stocks of cells were prepared at low passage numbers. Cells were subcultured as previously described. After centrifugation, the pellet was resuspended in 10% DMSO and 90% FBS, transferred to a labelled cryotube and placed in a polycarbonate container containing iso-propanol. Cells were left overnight in a -80 °C freezer after which time they were stored in liquid nitrogen. When required an aliquot of cells was removed from liquid nitrogen, quickly thawed at 37°C and added to a 9 mls medium in a 30 ml universal tube. Cells were centrifuged at 300 xg for 5 mins. The pellet was resuspended in 1ml medium. Cells were added to 7mls medium in a T25cm^2 flask. The media was changed after 24 hours to remove any dead cells.

2.4 Reagents

The pyrrolo-1,5-benzoxazepine compounds, 7-[(N,N-dimethylcarbamoyl)oxy]-6-(naphth-1-yl)pyrrolo[2,1-d][1,5]benzoxazepine (PBOX-6) and 4-acetoxy-5-(1-(naphthyl)naphtho[2,3-b]pyrrolo[2,1-d][1,4]oxazepine (PBOX-15) were synthesised as described previously (Campiani *et al.*, 1996) and dissolved in ethanol. Vincristine (Tocris), doxorubicin (Sigma Aldrich) and carboplatin (Sigma Aldrich) were dissolved in dH_20 and sterile filtered. Etoposide (Sigma Aldrich) was reconstituted in DMSO (Sigma Aldrich). Anti-AMPK, p-AMPK, ACC, p-ACC, mTOR, p-mTOR, p70 S6kinase, S6 ribosomal protein, p-eEF2k, caspase-8 and caspase-9 antibodies were purchased from Cell Signalling Technologies. Cytochrome c was sourced from BD Bioscience while Bax and Bak antibodies were sourced from Santa Cruz. All other antibodies were obtained from Millipore. Caspase inhibitors were purchased from Millipore. All media and FBS were obtained from Invitrogen. The enhanced chemiluminescence reagents were supplied by Amersham Biosciences. The BCA reagents were from Pierce, the polyvinylidene difluoride membranes from Millipore, while the protease inhibitors were obtained from Roche. Unless otherwise stated all chemicals were obtained from Sigma-Aldrich. Cell culture materials were sourced from Greiner Bio-One GmbH.

2.5 Preparation of stock solutions

A 10 mM stock solution of PBOX-6 and a 1 mM stock solution of PBOX-15 were prepared by dissolving the drugs in ethanol and storing at -20^{0}C. A 1 mM stock of vincristine, a 10 mM stock of doxorubicin and a 100 μM stock of carboplatin were prepared by dissolving the drugs in dH_20 and sterile filtering. A 10 mM stock of etoposide was prepared by dissolving the drug in DMSO and heating gently until dissolved. Serial dilutions were made up in medium. All dilutions were prepared fresh on day of experiment. Working concentrations of each drug were made by serial dilution from the principle stock and stored at -20 ^{0}C.

2.6 AlamarBlue viability assay

AlamarBlue can be utilised to determine the effects of a drug on cell viability. The assay uses the natural reducing power of living cells to convert resazurin, a non toxic cell permeable compound, to the fluorescent molecule, resorufin. Reazurin is blue in colour and virtually nonfluorescent; upon entering cells, resazurin is reduced to resorufin, which produces very bright red fluorescence. Resazurin is continuously converted to resorufin in healthy cell thereby generating a quantitative measure of viability and cytotoxicity.

Cells were seeded at densities varying from 2.5 x 10^4 - 8.0 x 10^4 cells/ml in a 96 well plate in a volume of 200 μl medium, left overnight to attach and treated with a range of concentrations of PBOX-6, PBOX-15, vincristine, doxorubicin, etoposide, carboplatin or the appropriate vehicle up to 72 hours. AlamarBlue (final concentration 10% (v/v)) was added to each well and left to incubate in the dark at 37^{o}C for 5 hours. Fluorescence was measured using a SpectraMax Gemini plate reader (Molecular Devices, Sunnyvale, CA) at excitation and emission wavelengths of 544 nm and 590 nm respectively. The mean of each triplicate was calculated. Vehicle treated wells were set at 100% viability and treated wells were calculated as a percentage of the vehicle control. Dose response curves were plotted and IC_{50} values obtained using Prism GraphPad 4.

2.7 Flow cytometry

Following the required treatment, floating and adherent cells were harvested and fixed in 70% ethanol/PBS. Fixed samples were stored at -20 °C until required. Ethanol was removed by centrifugation and pellets were incubated in 400 µl FACS flow sheath fluid supplemented with 10 µg/ml RNase A (Sigma Aldrich, St Louis, MO, USA) and 100 µg/ml propidium iodide (Sigma Aldrich, St Louis, MO, USA). Cells were incubated in the dark at 37°C for 30mins. Analysis was performed on a FACScalibur Fluorescence Associated Cell Sorter (FACS) (Becton–Dickinson, San Jose, CA, USA) using Cell Quest and Quanti-Quest software. Samples were first gated using a vehicle control to eliminate debris and cell aggregates from analysis. 1 X 10^5 cells from each sample were counted and results were visualised on histograms (Fig. 2.1).

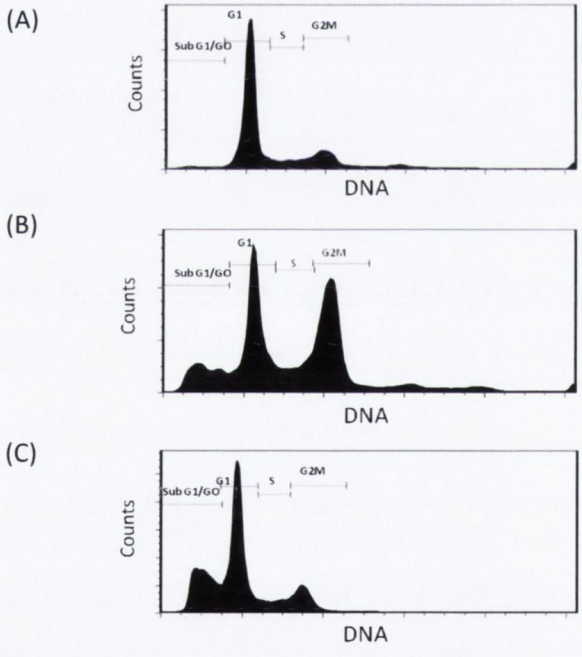

Figure 2.1 Representative flow cytometric histograms of propidium iodide stained SHSY5Y cells.

Representative histogram showing (A) vehicle treated cells, (B) cells undergoing G2/M arrest and (C) induction of apoptosis.

Mitochondrial membrane potential was analyzed using 5,5,6,6-tetrachloro-1,1,3,3-tetraethylbenzimidazolcarbocyanineiodide (JC-1) (Invitrogen), an aggregate forming lipophilic dye. It selectively enters into mitochondria and reversibly changes colour from green to red as the membrane potential increases. In healthy cells with high mitochondrial potential, JC-1 spontaneously forms aggregates known as J-aggregates with intense red fluorescence. In an apoptotic cell with a decrease in mitochondrial potential, JC-1 remains in the monomeric form, which shows only green fluorescence. Therefore a decrease in the red (~590 nm) to green (~529 nm) fluorescence intensity ratio is indicative of mitochondrial depolarisation. JC-1 was stored as a 200 μM solution in DMSO and added to cells at a final concentration of 5 μM for 20 mins at 37 °C. Cells were collected by centrifugation at 300 × *g* for 5 mins and the pellets were re-suspended in 400 μL PBS. Cells were treated with 50 mM Carbonylcyanide m- chlorophenylhydrazone (CCCP), a mitochondrial membrane depolarisor, for 5 mins as a positive control for depolarisation. Flow cytometry analysis was then performed within 10 min by using a FACScalibur Fluorescence Associated Cell Sorter (FACS) (Becton–Dickinson, San Jose, CA, USA) using Cell Quest and Quanti-Quest software. Cells were gated to exclude debris and standard compensation was performed using the positive control. The red:green fluorescence ratio was measured using the FITC and PE channels. Complete depolarization was defined by a gate setting the CCCP control as 98–100% depolarized. Response to each treatment was listed as the percentage of cells within the depolarized gate.

2.8 Determination of reactive oxygen species production

2.8.1 ROS-Glo H_2O_2 assay

ROS production was determined using the ROS-Glo H_2O_2 assay, a luminescent assay that measures the level of the reactive oxygen species, hydrogen peroxide (H_2O_2). A H_2O_2 substrate is employed that reacts directly with H_2O_2 to generate a luciferin precursor. Upon addition of the detection reagent which contains Ultra-Glo recombinant luciferase and D-Cysteine, the precursor is converted to luciferin by the D-Cysteine, and the luciferin reacts with Ultra-Glo recombinant luciferase to generate a luminescent signal which is proportional to the concentration of H_2O_2.

Number of Wells	H_2O_2 Substrate Dilution Buffer	H_2O_2 Substrate
10	200 µl	2.5 µl
50	1 ml	12.5µl
100	2 mls	25 µl

Table 2.1 Preparation of the H_2O_2 Substrate solution

Cells were seeded at a density of 6.0 x 10^4 cells/ml in 80 µl of medium in a 96-well plate and allowed to adhere overnight. The substrate dilution buffer was thawed and placed on ice. H_2O_2 was added to the substrate dilution buffer as described in Table 2.1 and 20 µl of H_2O_2 substrate solution was added to the cells in addition to the required test compound. The 96 well plate was placed in the incubator for the desired time. After such time, 100 µl of the ROS-Glo detection reagent (Table 2.2) was added to each well. The plate was left to incubate for 20 mins at room temp after which time luminescence was read on the spectraMAX Gemini plate reader.

Number of Reactions	Luciferin Detection	Reagent D-Cysteine	Signal Enhancer Solution
10	1 ml	10 µl	10 µl
50	5 ml	50 µl	50 µl
100	10 ml	100 µl	100 µl

Table 2.2 Preparation of ROS-Glo™ Detection Solution

2.8.2 DCFH-DA staining

SHSY5Y cells were seeded at a density of 1.0 X 10^5 cells/ml in a six well plate and left to adhere overnight. The following day cells were treated with a range of concentrations of PBOX-6 (2.5, 5 and 10 µM) for 4 hours. After this time, cells were incubated in phenol free media containing 10 µM DCFH-DA for 30 mins at 37^0C. Cells were washed, trypsinised and resuspended in 400 µl ice cold PBS. Cells were analysed on by flow cytometry; the 488 nm laser was used for excitation and DCFH-DA was detected in the FL-2 channel (535 nm). Cell analysis was performed on the CyAn using the appropriate gates, counting 10,000 cells and ensuring the necessary compensations were made to exclude the dead cells. The

percentage of mean fluorescence within the cells was analysed using Flow Jo software to generate histograms plots.

2.9 Clonogenic Assays

2.9.1 Optimisation of seeding density

SHSY5Y cells were seeded at varying densities (250, 500, 750, 1000 and 1250 cells/well) in 6 well CellBIND plates and left for 8-10 days (Table 2.3). Plates were regularly viewed under the microscope to monitor colony formation. A colony is considered to be 50 cells or more. Colonies had to be distinct and not in contact with any other colonies to be accurately counted. After the required time, plates were washed in 1 ml PBS and fixed in 70% methanol. Colonies were stained with 0.5% crystal violet and colonies were counted using the Colcount^{TM}. The Colcount is a colony counter for adherent mammalian cell colony forming assays. This system uses the CHARM (Compact Hough and Radial Map) image processing algorithm for accurate counting, including diffuse, irregular and overlapping colonies. The plating efficiency was calculated as the ratio of the number of colonies counted over the number of cells plated. Experiments were performed in triplicate.

PBOX-6 (μM)	Seeding density (cells/ml)	PBOX-15 (μM)	Seeding density (cells/ml)
0	1250	0	1250
1	1450	0.05	1875
2.5	3675	0.1	3750
5	7350	0.25	9500
10	14700	0.5	18750

Table 2.3 Varying seeding densities employed to determine the optimimum conditions for the clonogenic assay.

2.9.2 Treatment of colonies

The optimum seeding density was determined for SHSY5Y cells. Cells were seeded at a density of 1250 cells per ml in control wells and increasing densities with increasing drug concentration. For example for a concentration equal to the IC_{50}, twice the control

density was plated (2500 cells/ml). Seeding densities are described in Table 2.3. Cells were left overnight to attach. The following day cells were treated with various concentrations of PBOX-6/15. Cells were incubated at 37 °C for 7 days after which time the drug containing media was removed. Cells were washed in 1 ml sterile PBS and 2 mls fresh media was added to each well. Cells were left for 8-10 days to allow for colony recovery. Cells were then fixed in methanol, stained in 0.5% crystal violet and counted using a ColCount™. Percentage clonogenicity was determined for each treatment.

2.10 Western Blot

2.10.1 Preparation of cell lysates

Cells were seeded at a density of 3.5 x 10^4 cells in T25cm^2 flasks in 5 mls of media and left to adhere overnight. The following day cells were treated with the required volume of each drug. Following the required incubation time, cells were detached from each flask using a cell scraper. Cells and media were transferred into a universal tube and centrifuged at 600 xg for 10 mins. The supernatant was discarded and the pellet was washed in 1 ml non sterile PBS. The resuspended pellet was centrifuged as above. The PBS was removed and the pellets were stored at -80 °C until required. The cell lysates were removed from storage and kept on ice. Lysates were pelleted at 600 xg for 10mins and any remaining PBS was removed. Lysates were resuspended in PBS and 2 X laemmli buffer (1X= 30mM Tris-base pH6.2, 2% (v/v) SDS, 10%, 10% (v/v) glycerol in dH_20) with the exception of AMPK and ACC lysates which were resuspended in AMPK lysis buffer (50 mM Tris/HCl, pH 7.4 at 4^{0}C, 50 mM NaF, 5 mM Na pyrophosphate, 1 mM EDTA, 1 mM EGTA, 250 mM mannitol, 1% (v/v), Triton X-100, 1 mM DTT and the protease inhibitors) and mTOR, p70 S6Kinase, S6 ribosomal protein and eEF2K samples which were prepared in mTOR lysis buffer (10 mM Tris pH7.5, 50 mM NaCl, 30 mM sodium pyrophosphate, 50 mM sodium fluoride, 5 µM zinc chloride, 10% glycerol, 0.5% triton-X-100, 1 µM DTT and protease inhibitors). Samples were sonicated for 10 secs to degrade DNA. Following sonication, 10µl was removed for protein quantification using the BCA assay (see below). DTT (to a final concentration of 50 mM) and bromophenol blue were added to each sample. AMPK, ACC, mTOR, p70 S6Kinase, S6 ribosomal protein and eEF2K lysates were snap frozen in liquid nitrogen and stored at -80^{0}C until required. All other lysates were

boiled on a heating block for 3 mins at 100^{0}C and stored at-80^{0}C until required.

2.10.2 Preparation of cytosolic fractions

Following the required incubation time, media was removed from the flask and cells were washed in 1 ml PBS. Cells were trypsinised and pelleted at 600 xg for 5 mins. The pellet was washed in 1 ml ice cold PBS and incubated in 100 µl isotonic buffer (0.2 M mannitol, 0.07 M sucrose, 1 mM EGDTA, 10 mM HEPES, 1 mM DTT in dH_20) for 10 mins on ice. The resuspended pellet was drawn though a 21 G needle approximately 30 times and incubated on ice for a further 15 mins. Cells were pelleted at 1000 xg for 10 mins and the supernatant was removed. The supernatant was pelleted at 12,000 xg for 20 mins at 4^{o}C to produce the cytosolic fractions which were stored at -80^{0}C until required.

2.10.3 Determination of protein concentration

Standards were prepared as described in Table 2.4. Fresh standards were prepared on the day of the experiment. BCA working reagent was prepared by a 1:50 dilution of BCA reagent B in BCA reagent A. 200 µl of this working reagent was added to each well in a 96 well plate followed by 20 µl of each standard or unknown. This was performed in triplicate. The plate was wrapped in aluminium foil and left for 30 mins. Absorbance was read at 562 nm using the Molecular Devices microplate reader and the mean of the standards was determined and a standard curve was constructed. The standard curve was used to determine the protein concentration of each sample and the volume of sample required to add 30 µg protein per well was determined (Fig. 2.2).

Vial	Volume of Dilutent (µl)	Volume and Source of BSA (µl)	Final BSA concentration
A	0	300 of stock	2,000 µg/ml
B	125	375 of stock	1500 µg/ml
C	325	325 of stock	1000 µg/ml
D	175	175 of vial B dilution	750 µg/ml
E	325	325 of vial C dilution	500 µg/ml
F	325	325 of vial E dilution	250 µg/ml
G	325	325 of vial F dilution	125 µg/ml
H	400	100 of vial G dilution	25 µg/ml
I	400	0	Blank

Table 2.4 Preparation of BSA standards

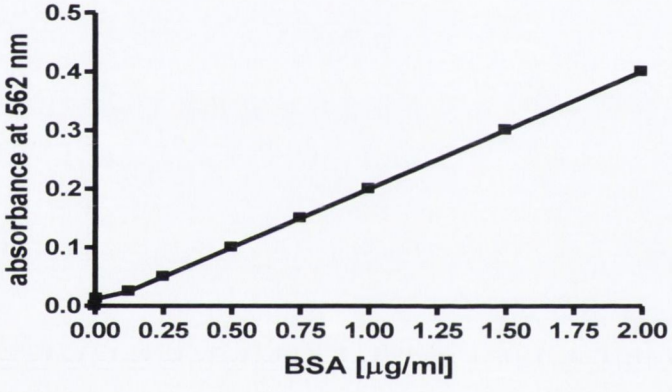

Figure 2.2 BSA standard curve used to determine protein concentration of cellular lysates.

2.10.4 Sodium Dodecylsulphate-Polyacrylamide Gel Electrophoresis

Glass plates were washed in methanol and assembled. Resolving gel was prepared as described in Table 2.4 and poured between the glass plates. 200 µl methanol was added to the top of the gel to eliminate air bubbles. The stacking gel was prepared as described in Table 2.5. When the resolving gel had set, the methanol was poured off, the stacking gel was poured on top and a comb was added. The gel was left to set for 30 mins. Prior to use, the gel was placed into a chamber filled with 1X running buffer (5X= 125 mM Tris, 1 M glycine, 0.5% (v/v) SDS in dH_2O) and the comb was removed to create the wells. 30 µg of sample was loaded into each well. 8µl of a molecular weight marker was loaded into

the last well of each gel. The chamber was filled with running buffer and the gel was run at 80 V until the samples passed through the stacking gel and the current was increased to 140 V until the samples had passed to the end of the resolving gel.

Acylamide percentage	6%	8%	10%	12%	15%	5% stacking gel
dH_2O	5.2 ml	4.6 ml	3.8 ml	3.2 ml	2.2 ml	3.4 ml
Acrylamide mix	2 ml	2.6 ml	3.4 ml	4 ml	5 ml	0.83 ml
1.5M Tris (pH 8.8)	2.6 ml	2.6 ml	2.6 ml	2.6 ml	2.6 ml	-
1M Tris (pH 6.8)	-	-	-	-	-	0.63 ml
10% (w/v)SDS	0.1 ml	0.1 ml	0.1 ml	0.1 ml	0.1 ml	0.05 ml
10% (w/v) APS	100 µl	100 µl	100 µl	100 µl	100 µl	50 µl

Table 2.5 Composition of resolving and stacking gels used in SDS-PAGE.

2.10.5 Western Blotting

The gel was removed from the chamber and rinsed in dH_20. Two pieces of blotting paper and one PVDF membrane per gel were soaked in transfer buffer (1X=25 mM Tris, 200 mM glycine, 10% (v/v) methanol in dH_20) for 30 mins. Two pieces for blotting paper were placed in the transfer cassette followed by the membrane. The gel was removed from the cassette and placed on top of the membrane. Two additional pieces of blotting paper were placed on top of the gel and air bubbles were eliminated. The cassette was placed in the transfer apparatus and filled with transfer buffer. The gel was transferred to the membrane for 1 hour at 150 mV. To ensure transfer to the membrane was successful it was stained with ponceau S. The membrane was then rinsed in dH_20. Non-specific binding sites on the membrane were blocked using 5% Marvel at room temp for 1 hour. The 5% Marvel solution was changed three times during the hour. Following blocking the membrane was washed three times in PBS-tween (PBST) and incubated with the primary antibody overnight. The following day, membranes were washed three times for 30 mins in PBST prior to incubation in secondary antibody conjugated to HRP for 60 mins. Membranes were washed for a further 30 mins in PBST and placed in ECL detection reagent for 5 mins before being transferred to the development cassette. Kodak X-Omat LS film was placed on top of the membrane within the cassette and developed using an

automated Fuji x-ray processor. Western blot analysis was performed using antibodies directed against the protein of interest as described in Table 2.6 followed by incubation with a horseradish peroxidase-conjugated anti-mouse or anti-rabbit antibody (Promega, Madison, WI, USA). All blots were probed with anti-GAPDH to confirm equal loading.

Antibody	Mr (kDa)	% Gel	Distributor	Product code	Host	1^0 Ab Dilution
PARP	116, 89	10	Millipore	AM30	Mouse	1 in 500
Bcl-2	28	12	Millipore	OP60	Mouse	1 in 500
Mcl-1	42	12	Millipore	AM50	Mouse	1 in 1000
Bax	25	12	Cell signalling	5023	Rabbit	1 in 2500
Bak	25	12	Abcam	32371	Rabbit	1 in 500
Bak-NT	28	12	Millipore	06535	Rabbit	1 in 2500
Caspase-3	32	12	Millipore	AM39	Mouse	1 in 500
Caspase-8	57, 28	10	Cell Signalling	9746S	Mouse	1 in 1000
Caspase-9	46, 35	12	Cell Signalling	9508	Mouse	1 in 1000
Cytochrome c	60, 15	10	BD	556433	Mouse	1 in 1000
GAPDH	38	10	Millipore	CB1001	Mouse	1 in 5000
AMPK	62	10	Cell Signalling	5831	Rabbit	1 in 500
Phospho-AMPK	62	10	Cell Signalling	2535	Rabbit	1 in 500
ACC	289	6	Cell Signalling	3676	Rabbit	1 in 500
Phospho-ACC	289	6	Cell Signalling	11818	Rabbit	1in 500
mTOR	290	6	Cell Signalling	2983	Rabbit	1 in 1000
Phospho-mTOR	290	6	Cell Signalling	5536	Rabbit	1 in 1000
p70 S6 Kinase	70	10	Cell Signalling	9234	Rabbit	1 in 1000
S6 ribosomal kinase	70	10	Cell Signalling	4858/5364	Rabbit	1 in 1000
Phospho-eEF2K	32	10	Cell signalling	3691	Rabbit	1 in 500

Table 2.6 Western blotting details for specific proteins

2.10.6 Densitometric analysis

Western blots were analysed by using the Imagej. This software programme calculates area and pixel value statistics of defined selections i.e. a protein band on a western blot (analysis was performed as follows: the X-ray film was scanned and saved as a JPEG file. This file was opened in the imageJ programme and the background was subtracted. The percentage of measurable pixels in the image was set by using the adjust image threshold command. The number of square pixels in the section selected i.e. the protein bands were then counted by measuring the area in the binary or thresholded image.

2.11 siRNA knockdown of Mcl-1

SHSY5Y and CHLA-90 cells in the log phase of growth were seeded at a density of 3.0×10^6 cells in six well plates. The following day cells were trypsinised, pelleted and transfected using the neon transfection system (Invitrogen, Paisley U.K) with 200 nM siRNA validated to target Mcl-1 (Invitrogen, Paisley U.K) Transfection conditions were optimised to ensure maximum knockdown of protein expression; five conditions were analysed to determine the optimum pulse voltage, pulse width and pulse number in each cell line transfected as described in Table 2.7).

Protein expression was assessed by SDS-PAGE up to 72 hours post transfection to ensure knockdown was successful. Transfected cells were treated with varying concentrations of carboplatin and the levels of apoptosis were analysed by flow cytometric analysis of propidium iodide stained cells.

Condition no.	Pulse voltage	Pulse width	Pulse no.
1	0	0	0
2	1500	20	1
3	1700	20	1
4	1200	30	1
5	1400	30	1
6	1100	40	1

Table 2.7 Conditions for Neon transfection optimisation.

2.12 Immunomagnetic separation of neuroblastoma cells from bone marrow aspirates

Ethical approval for all work in patient samples was obtained from Our Lady's Children's Hospital, Crumlin incorporating the National Children's Hospital Ethics Committee. Samples were depleted of red blood cells by red cell lysis. 14 mls of red cell lysis buffer (0.15 M NH_4Cl, 10 mM $KHCO_3$ and 0.1 mM EDTA in dH_20) was added per 1 ml of bone marrow and placed on a roller for 5mins. The sample was pelleted at 300 xg for 5 mins. The supernatant was discarded and the sample was washed in 1 ml cold PBS. The resusupended pellet was centrifuged at 300 xg. The pellet was resuspended in 1 ml BSA and 0.1% FBS and the cell number was determined. The pellet was centrifuged at 300 xg and resuspended in 80 µl MACs buffer (2mM Tris/PBS+0.01% FBS), 20 µl FcR blocking reagent and anti-GD_2 antibody (0.5µg/10^6 cells) was added to the pellet. This was thoroughly mixed and incubated at 4^0C for 30 mins. The sample was then resuspended in 2 mls MACs buffer and pelleted at 300 xg for 5 mins. The supernatant was discarded and the pellet was resupended in 80 µl MACs buffer prior to the addition of 20 µl anti-mouse IgG microbeads. The sample was vortexed and incubated for 15 mins at 4^0C. The sample was washed in 2 mls MAC buffer.

The column was placed in the magnet (Miltenyi Biotech) and prepared by rinsing with 3 mls of MACs buffer three times. The cell suspension was added to the column and the flow through collected. The column was washed three times with 3 mls of MACs buffer and the unlabelled cells were collected. The column was removed from the magnet, 5 mls of MACs buffer was added to the column and the piston was applied. The GD_2 positive cells were collected in a 30 ml universal tube and centrifuged at 300 xg for 5 mins. The supernatant was discarded and the pellet was resusupended in 1 ml DMEM supplemented with 20% (v/v) FBS and 1% (v/v) Pen/strep. Cells were counted and seeded at a density of 5 x 10^5 cells/ml in a 48 well plate. Half the media was removed every 3 days and replaced with fresh media. When the cells were confluent they were detached using 1x trypsin. The effect of PBOX-6 on the viability of primary neuroblastoma cells was determined using the alamarBlue viability assay.

2.13 *In vivo* tumour model of neuroblastoma

2.13.1 Mice

Specific pathogen-free 4- to 6-week-old adult female BALB/c-nu/nu mice were purchased from Harlan Laboratories (Cambridgeshire, UK). Mice were housed in sterile individually ventilated cages; food and water were provided *ad libitum*, in accordance with the standard operating procedures set down in the EC Directive 86/609. Mice were acclimatised for 1 week before the initiation of any *in vivo* experiments. Animals were killed by CO_2 followed by cervical dislocation if the tumour exceeded 15 mm in diameter or the volume exceeded 10% of mouse bodyweight or if found to be in distress (hunching, failure to groom etc.). Ethical approval and licence was obtained by the BioResources Committee, Trinity College, Dublin and the Irish Medicines Board.

2.13.2 *In vivo* tumour study

The *in vivo* antitumour efficacy of PBOX-6, carboplatin and a combination of the two was examined using an SHSY5Y xenograft in a BALB/c mouse model. Female BALB/c-nu/nu mice were inoculated subcutaneously (s.c.) into the right flank with 2×10^6 SHSY5Y cells in the log phase of growth. After 35 days, when tumours of approximately 3 mm in diameter were observed, mice were randomly divided into four groups (5 mice per group). A stock solution of PBOX-6 was prepared at a concentration of 15 mg ml^{-1} in 1:1 ethanol/cremophor EL. When required, this was then diluted 1 in 5 in sterile PBS to give a final concentration of 7.5 mg kg^{-1} or 0.15 mg per mouse. A stock solution of carboplatin was prepared at a concentration of 9 mgs/ml in dH_20 to give a final concentration of 60 mg/ kg^{-1} or 1.2 mg per mouse. The PBOX-6 treatment group (n=5) received an intratumoural (i.t.) injection (Williams *et al.*, 2007; Shah *et al.*, 2009; Bright *et al.*, 2010) of PBOX-6 (100 µl) once every two days for the duration of the experiment starting on day 35, the carboplatin treatment group (n=5) received an intraperitoneal (i.p) injection of carboplatin (100 µl) once every two days for the duration of the experiment starting on day 35 while the combination group (n=5) received both an i.t injection of PBOX-6 and and i.p injection of carboplatin every two days for the duration of the experiment. Control mice (*n*=5) received an i.t or i.p injection of 50 µl of the equivalent vehicle also starting on day 35. Tumour growth was measured every second day with a sterile vernier calliper. The long (*L*) and short (*S*) axes were recorded, and tumour volume (*V*) was calculated

using the following equation as described previously (Beck *et al.*, 2003) (Fig. 2.3). Mice were weighed every two days. Mice were killed by CO_2 asphyxiation followed by cervical dislocation at the experimental end point or if found to be under any distress.

$$V = \frac{S^2 \times L}{2}$$

Figure 2.3 Calculation of tumour volume.

2.14 Analysis of drug interactions

Using the software programme Calcusyn (Biosoft), median dose analysis was undertaken to study interactions between different drugs. This method is based on the drug effect equation of Chao and Talalay (Chou & Talalay., 1984) providing quantitative determination for synergism (CI < 1), additive effect (CI = 1) and antagonism (CI > 1). The lower the combination index value (CI), the greater the degree of synergism. A CI value of 0.1-0.3 indicates strong synergism (++++), 0.3-0.7 indicates synergism (+++), 0.7-0.85 indicates moderate synergism (++) and 0.85-0.9 indicates slight synergism (+).

Range of CI	Symbol	Description
<0.1	+++++	Very strong synergism
0.1-0.3	++++	Strong synergism
0.3-0.7	+++	Synergism
0.7-0.85	++	Moderate synergism
0.85-0.9	+	Slight synergism
0.9-1.10	+-	Nearly additive
1.10-1.20	-	Slight antagonism
1.20-1.45	--	Moderate antagonism
1.45-3.3	---	Antagonism
3.3-10	----	Strong antagonism
10	-----	Very strong antagonism

Table 2.8 Recommended symbols for describing synergism or antagonism in drug combination studies analysed with the CI method. (Taken from Calcusyn manual, 2005)

2.15 Statistics

The statistical analysis of experimental data was performed using the computer program Prism GraphPad 4. Results were presented as mean ± S.E.M. For comparison of two groups, values were determined using a Student's paired *t* test. For comparison of more than two groups, one way Anova followed by Tukey's multiple comparison test was employed. A value of $P < 0.05$ was deemed to be significant.

Chapter 3

Investigation into the anti-cancer effects of novel PBOX-6 in drug sensitive and multidrug resistant neuroblastoma cell lines

Chapter 3

3.1 Introduction

The paediatric malignancy neuroblastoma is both the most commonly diagnosed tumour in the first year of life and the most common extra cranial solid tumour in early childhood, accounting for 15% of cancer deaths in young children (Maris *et al.*, 2010). Prognosis is largely dependent on the stage at the time of diagnosis with low risk patients having an approximately 90% survival rate. Yet this is a cancer that is extremely heterogeneous in terms of biology, response to treatment and survival and, despite both advances in understanding the biology of this cancer and intense treatment strategies, it continues to be one of the most difficult paediatric cancers to successfully treat with more than 60% of patients presenting at diagnosis with adverse features. Less than 40% of these patients achieve disease free long term survival (Mattany *et al.*, 2009). In contrast to other childhood cancers, survival rates for neuroblastoma have only marginally improved in recent times. Between 20-50% of patients do not respond sufficiently to high dose chemotherapy.

A major obstacle in the effective treatment of neuroblastoma is the development of multidrug resistance (MDR) to a broad range of cytotoxic drugs (Keshelava *et al.*, 1998; 2000a; 2000b) including vinca alkaloids, alkylating agents, platinum compounds and anthracyclines. This MDR phenotype often includes amplification of the proto-oncogene MYCN, mutation/deletion of p53, deletion of loci at 1p or 11q and over expression of MDR proteins leading to altered drug transport and an increase in drug efflux (Maris *et al.*, 2010). There is, therefore, an urgent need for alternative approaches to treatment.

MDR proteins are members of a family of transmembrane ABC (ATP binding cassette) transporters that use ATP hydrolysis to mediate the export of hydrophobic drugs from the cell. Some of the best studied multidrug resistant proteins of the ABC family are multidrug resistance protein (MDR-1) (also called ABCB1 or P-glycoprotein (P-gp)), ABCC1 (also called multidrug resistance associated protein (MRP-1)) and breast cancer resistance protein (BCRP) (Sakadi *et al.*, 2008). The 170kDa P-gp is a transmembrane efflux pump with low substrate specificity which has been shown to be overexpressed in neuroblastoma patients where it predicts poor outcome (Chan *et al.*, 1998), indicating that there is a need for alternative chemotherapeutic agents which are not substrates for

these transporters.

Some PBOX compounds have been identified as novel microtubule-targeting agents (MTAs) (Mulligan *et al.*, 2006) that possess the ability to potently induce cell cycle arrest and apoptosis in a number of cancer cell lines derived from both solid tumours and haematological malignancies (Greene *et al.*, 2006; McElligott *et al.*, 2009; Bright *et al.*, 2009; Nathwani *et al.*, 2010; Bright *et al.*, 2010; Maginn *et al.*, 2011; Greene *et al.*, 2013). Additionally these compounds have been shown to be efficacious in *ex vivo* studies (McElligot *et al.*, 2009; Bright *et al.*, 2010) and *in vivo* chronic myeloid leukaemia (CML) (Bright *et al.*, 2010) and breast cancer animal models (Greene *et al.*, 2005). It has previously been demonstrated that PBOX-15 induces apoptosis both in *ex vivo* B-cell lymphocytic leukaemia (CLL) cells harbouring poor prognostic indicators and fludarabine resistance-associated p53 deletions (McElligot *et al.*, 2009), and in primary CML patient samples including those resistant to STI-571, the current frontline treatment for CML (Bright *et al.*, 2009). Unlike many chemotherapeutic agents, the PBOX compounds are not substrates for many MDR drug efflux pumps (Nathwani *et al.*, 2010). PBOX-6 and 15 were shown to induce comparable levels of apoptosis in both drug sensitive and MDR human promyelocytic leukaemia and ovarian carcinoma cell lines expressing either P-gp or BCRP, two of the main ABC transporters associated with MDR, indicating that they may possess advantages over standard chemotherapy which is currently in clinical use.

In this chapter, the effects of two of the more potent pro-apoptotic members of the PBOX family, PBOX-6 and -15, on a panel of both drug sensitive and drug resistant neuroblastoma cell lines were determined. Both PBOX compounds were shown to reduce the viability of all cell lines with similar potency indicating a lack of resistance to these novel compounds. The effects of multiple chemotherapeutic drugs, which are currently used to treat neuroblastoma, were also tested on the panel of neuroblastoma cell lines. The PBOXs exhibited a lower fold resistance in MDR cells when compared to other chemotherapeutics. The effect of PBOX-6 and -15 on clonogenic survival of SHSY5Y cells and primary neuroblastoma cells isolated form bone marrow aspirates was also investigated while part of the molecular mechanism through which the PBOX-6 induces apoptosis in neuroblastoma cells was delineated.

3.2 Results

3.2.1 Validity of the AlamarBlue viability assay in determining the effects of cytotoxic drugs on SHSY5Y cell viability.

The alamarBlue assay was employed to measure the decrease in viability of cells 72 hours post drug treatments in SHSY5Y cells. The validity of the assay was determined before commencing experiments; SHSY5Y cells were seeded at a number of densities (10-50 x 10^5 cells/ml) and the fluorescence was read after 72 hours on the SpectraMax Gemini plate reader at excitation and emission wavelengths of 544 nm and 590 nm respectively. As shown in Figure 3.1 there was a linear correlation between cell density and fluorescence demonstrating the validity of the assay.

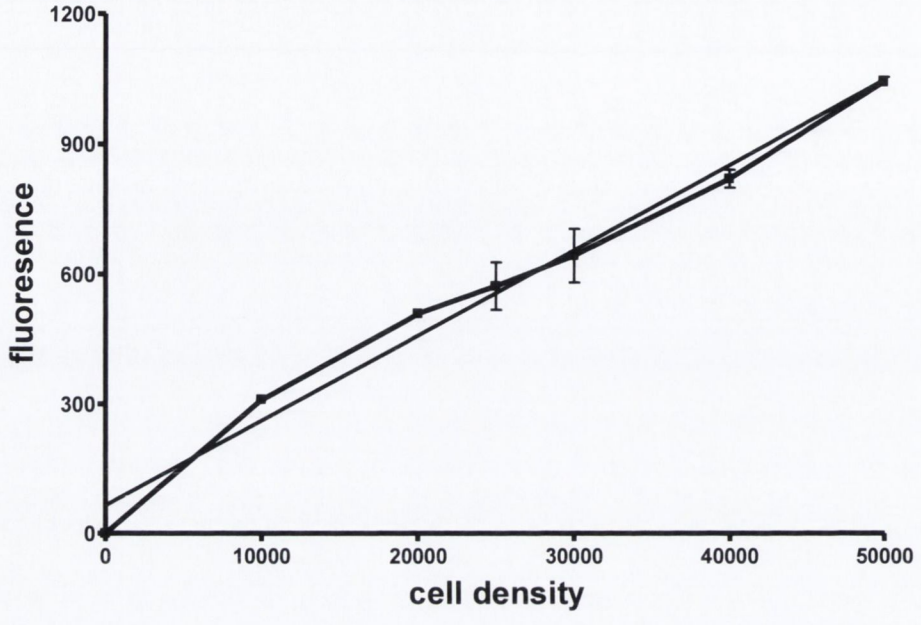

Figure 3.1 The linear relationship between SHSY5Y cell density and fluorescence.

SHSY5Y cells were seeded at a number of densities (10-50 x 10^5 cells/ml) in 96 well plates and left for 72 hours after which time 20 µl alamarBlue was added to each well. The plate was incubated at 37^0C for 5 hours and the fluorescence was read on the SpectraMax Gemini plate reader at excitation and emission wavelengths of 544 nm and 590 nm respectively. Values represent the mean ± S.E.M of three independent experiments.

3.2.3 Effect of vehicles, DMSO and ethanol, on viability of SHSY5Y cells.

In order to distinguish between the effects of a given drug and any potential cytotoxic effects of a vehicle, the effects of each vehicle on cell viability must be determined. It was necessary to determine the concentration of a given vehicle which could be used without causing a reduction in cell viability. Doxorubicin, vincristine and carboplatin were reconstituted in dH_20, etoposide in DMSO while PBOX-6 and 15 were reconstituted in ethanol. SHSY5Y cells were treated with varying concentrations of ethanol (1-5%) or DMSO (0.1-0.5%). After 72 hours 20 µl alamarBlue was added to each well and fluorescence was measured on the Spectromax Gemini plate reader at 562 and 590 nm. As can be seen from Figure 3.2, some of the higher concentrations of both vehicles exhibited significant effects on cell viability; however, 1% (v/v) ethanol (A) and 0.1% (v/v) DMSO (B) did not affect cell viability (Fig. 3.2) therefore, these concentrations were used in all future experiments.

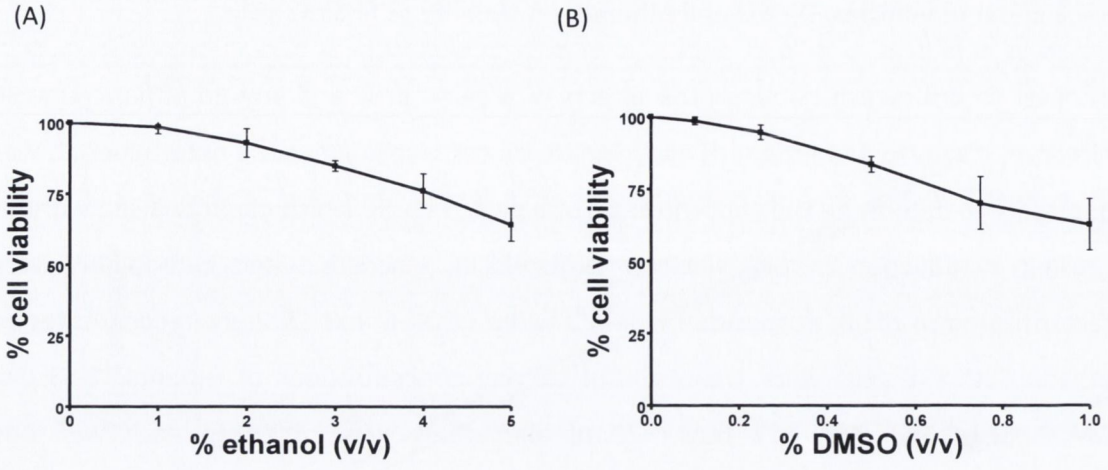

Figure 3.2 Effect of ethanol and DMSO on viability of SHSY5Y cells.

SHSY5Y cells were seeded at a density of 2.5 x 10^5 cells/ml in a 96 well plate and left to adhere overnight. The following day cells were treated with increasing concentrations of (A) ethanol (0-5% v/v) or (B) DMSO (0-1% v/v). After 72 hours 20 µl alamarBlue was added to each well and incubated for 5 hours. Fluorescence was measured on the Spectromax Gemini plate reader at 562 and 590 nm. Values represent the mean ± S.E.M of three independent experiments.

3.2.4 PBOX-6 and -15, doxorubicin, etoposide, carboplatin and vincristine reduce the viability of neuroblastoma cell lines.

The alamarBlue viability assay was employed to investigate the effects of PBOX-6 and 15 on viability of both drug-sensitive and resistant neuroblastoma cell lines. Cells were treated with a range of concentrations of PBOX-6 (0.01-10 μM) or PBOX-15 (0.001-1 μM) for 72 hours. Both PBOXs reduced the viability of all cell lines tested in a dose-dependent manner. The IC_{50} value of PBOX-6 and 15 was determined in each cell line (Fig. 3.3 and 3.4) and were of similar value in all cell lines, both drug sensitive and resistant. For PBOX-6 this ranged from 1.73 μM to 2.10 μM in the sensitive (SHSY5Y, Kelly and SK-N-BE(1)) and 1.08 μM to 3.73 μM in the resistant (SK-N-FI, Kelly and SK-N-BE2(C)). Similarly the IC_{50} value for PBOX-15 was consistent between the sensitive and resistant cell lines analysed. This value ranged from 0.06 μM to 0.11 μM (sensitive) and 0.04 μM to 0.11 μM (resistant).

The alamarBlue viability assay was also used to assess the effect of four chemotherapeutic drugs which are currently used for the treatment of neuroblastoma, on the viability of both drug-sensitive and resistant neuroblastoma cell lines. Cells were treated with a range of concentrations of vincristine (Fig. 3.5) doxorubicin (Fig. 3.6), etoposide (Fig. 3.7) or carboplatin (Fig. 3.8) for 72 hours. Results show that all drugs reduced the viability of all cell lines tested in a dose-dependent manner. The IC_{50} value of vincristine in the drug sensitive cell lines was in a similar range to PBOX-15 (0.02-0.07 μM) in the sensitive cell lines but significantly higher in the resistant CHLA-90 cell line (0.92 μM). The IC_{50} value for etoposide, doxorubicin and carboplatin was several fold higher than PBOX-15 in all sensitive and resistant cell lines ranging from 0.18-0.1.83 μM for doxorubicin and 0.34->20 μM for etoposide while carboplatin had the highest IC_{50} value in all cell lines tested (15->100 μM) significantly higher than both PBOX-6 and -15. In two out of three of the resistant cell lines, no resistance to PBOX-6 or 15 was observed while a slight resistance was noted in the SK-N-FI cells. This was in contrast to all four other chemotherapeutics which displayed substantially higher IC_{50} values in all three resistant cell lines. The IC_{50} value of all drugs in all six cell lines is summarised in Table 3.1.

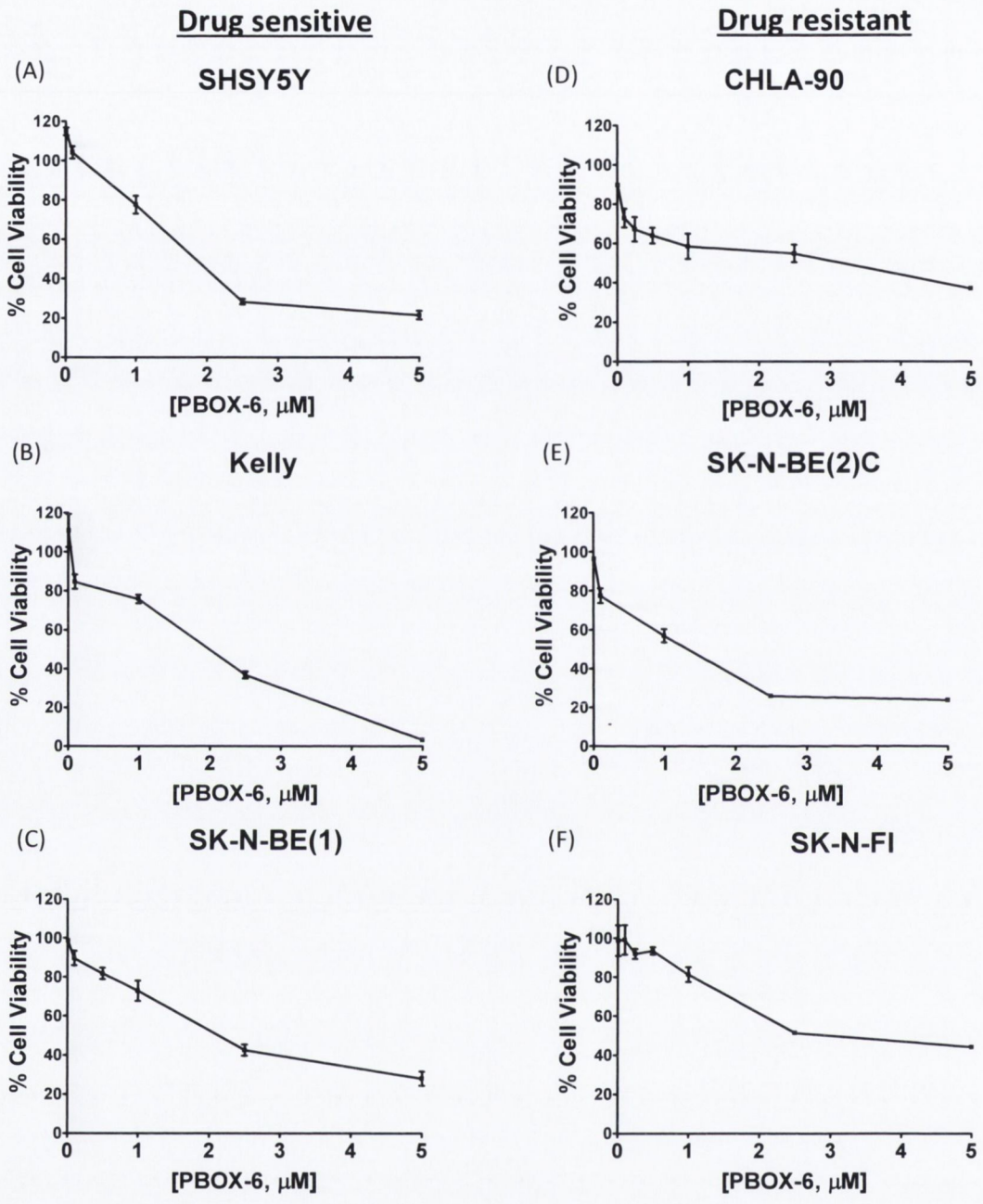

Figure 3.3 PBOX-6 reduces the viability of neuroblastoma cell lines.

Neuroblastoma cell lines (A) SHSY5Y, (B) Kelly, (C) SK-N-BE(1), (D) CHLA-90, (E) SK-N-BE(2)c and (F) SK-N-FI cells) were seeded at varying densities in 96 well plates and left for 24 hours to attach. Cells were treated with a vehicle (1% (v/v) ethanol) or a range of concentrations of PBOX-6. After 72 hours cells were harvested, and 20 µl alamarBlue was added to each well. Plates were incubated in the dark for up to 5 hours until a colour change was observed. Fluorescence was measured using a SpectraMax Gemini plate reader at excitation and emission wavelengths of 544 nm and 590 nm respectively. Values represent the mean ± S.E.M of three independent experiments.

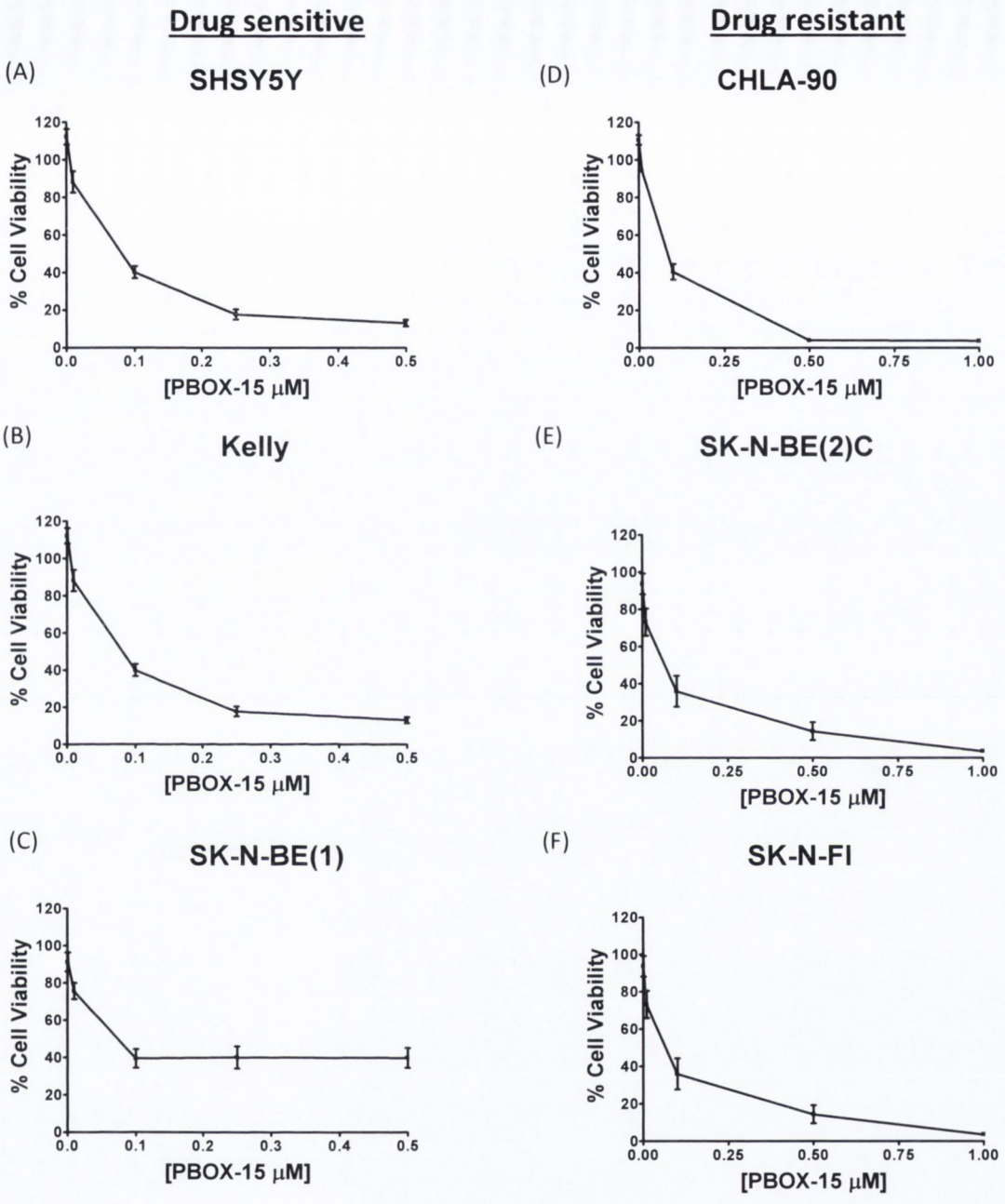

Figure 3.4 PBOX-15 reduces the viability of neuroblastoma cell lines.

Neuroblastoma cell lines (A) SHSY5Y, (B) Kelly, (C) SK-N-BE(1), (D) CHLA-90, (E) SK-N-BE(2)c and (F) SK-N-FI cells) were seeded at varying densities in 96 well plates and left for 24 hours to attach. Cells were treated with a vehicle (1% (v/v) ethanol) or a range of concentrations of PBOX-15. After 72 hours cells were harvested, and 20 μl alamarBlue was added to each well. Plates were incubated in the dark for up to 5 hours until a colour change was observed. Fluorescence was measured using a SpectraMax Gemini plate reader at excitation and emission wavelengths of 544 nm and 590 nm respectively. Values represent the mean ± S.E.M of three independent experiments.

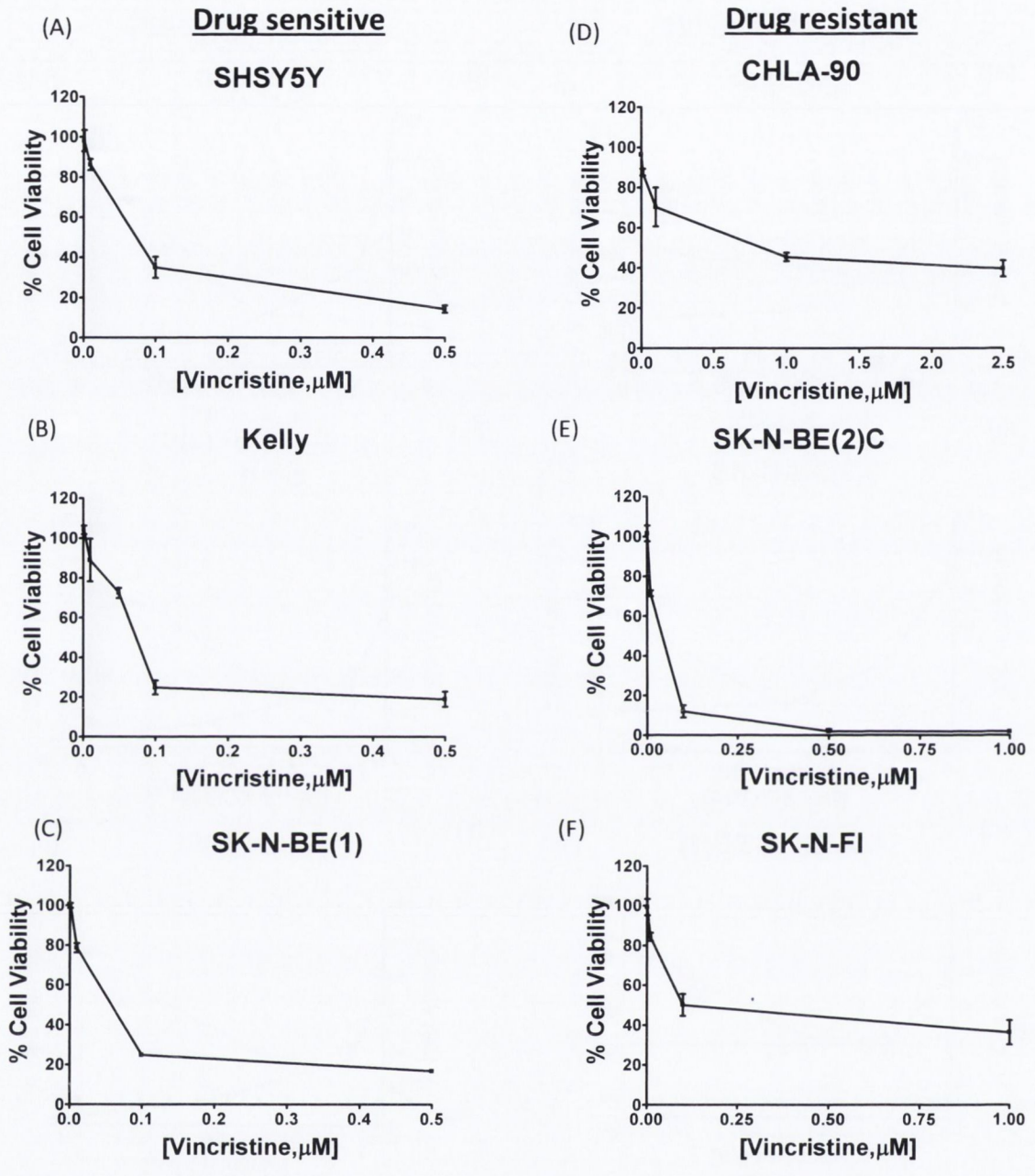

Figure 3.5 Vincristine reduces the viability of neuroblastoma cell lines.

Neuroblastoma cell lines (A) SHSY5Y, (B) Kelly, (C) SK-N-BE(1), (D) CHLA-90, (E) SK-N-BE(2)c and (F) SK-N-FI cells) were seeded at varying densities in 96 well plates and left for 24 hours to attach. Cells were treated with a vehicle (1% (v/v) ethanol) or a range of concentrations of vincristine. After 72 hours cells were harvested, and 20 µl alamarBlue was added to each well. Plates were incubated in the dark for up to 5 hours until a colour change was observed. Fluorescence was measured using a SpectraMax Gemini plate reader at excitation and emission wavelengths of 544 nm and 590 nm respectively. Values represent the mean ± S.E.M of three independent experiments.

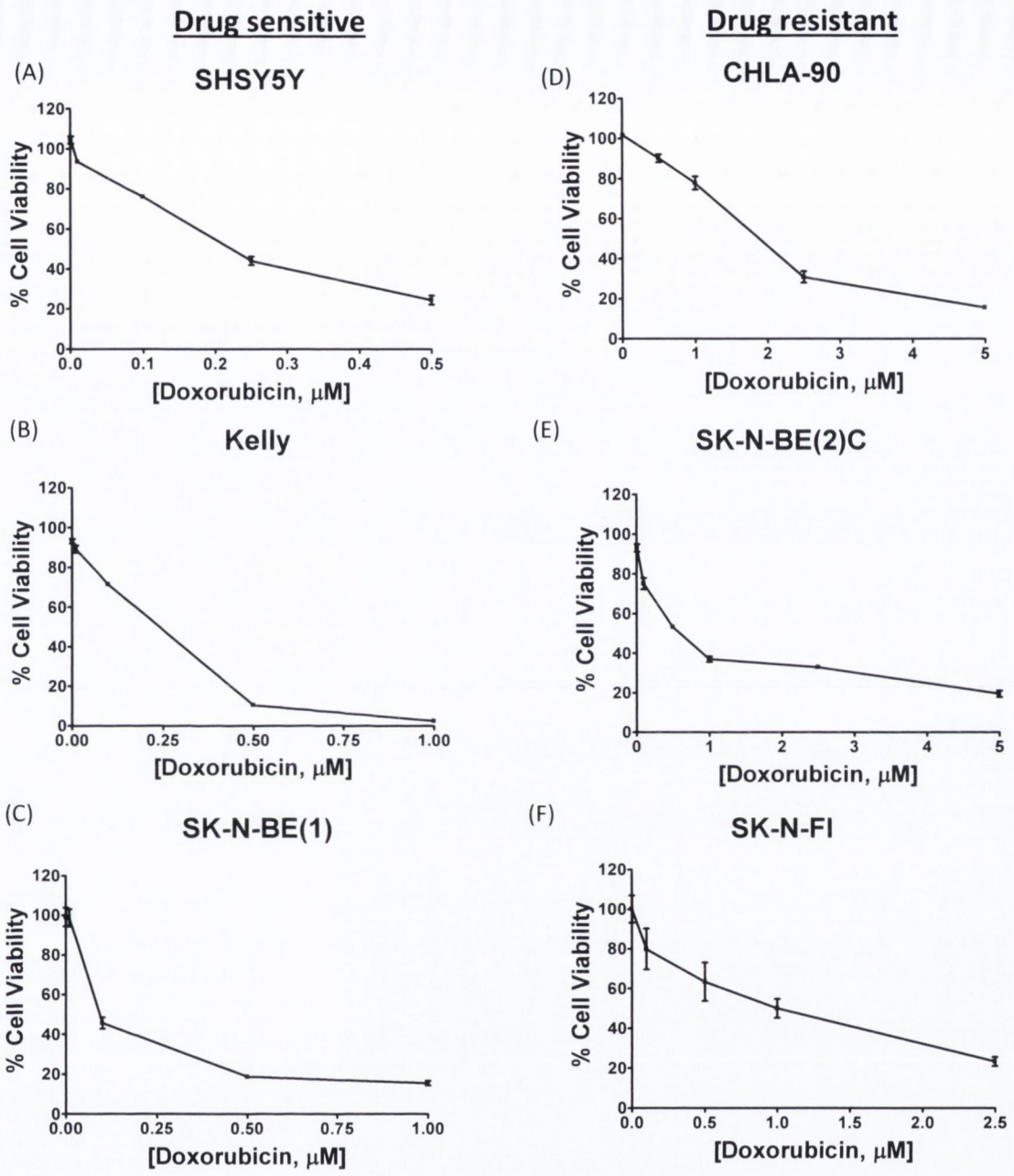

Figure 3.6 Doxorubicin reduces the viability of neuroblastoma cell lines.

Neuroblastoma cell lines (A) SHSY5Y, (B) Kelly, (C) SK-N-BE(1), (D) CHLA-90, (E) SK-N-BE(2)c and (F) SK-N-FI cells) were seeded at varying densities in 96 well plates and left for 24 hours to attach. Cells were treated with a vehicle (1% (v/v) ethanol) or a range of concentrations of doxorubicin. After 72 hours cells were harvested, and 20 µl alamarBlue was added to each well. Plates were incubated in the dark for up to 5 hours until a colour change was observed. Fluorescence was measured using a SpectraMax Gemini plate reader at excitation and emission wavelengths of 544 nm and 590 nm respectively. Values represent the mean ± S.E.M of three independent experiments.

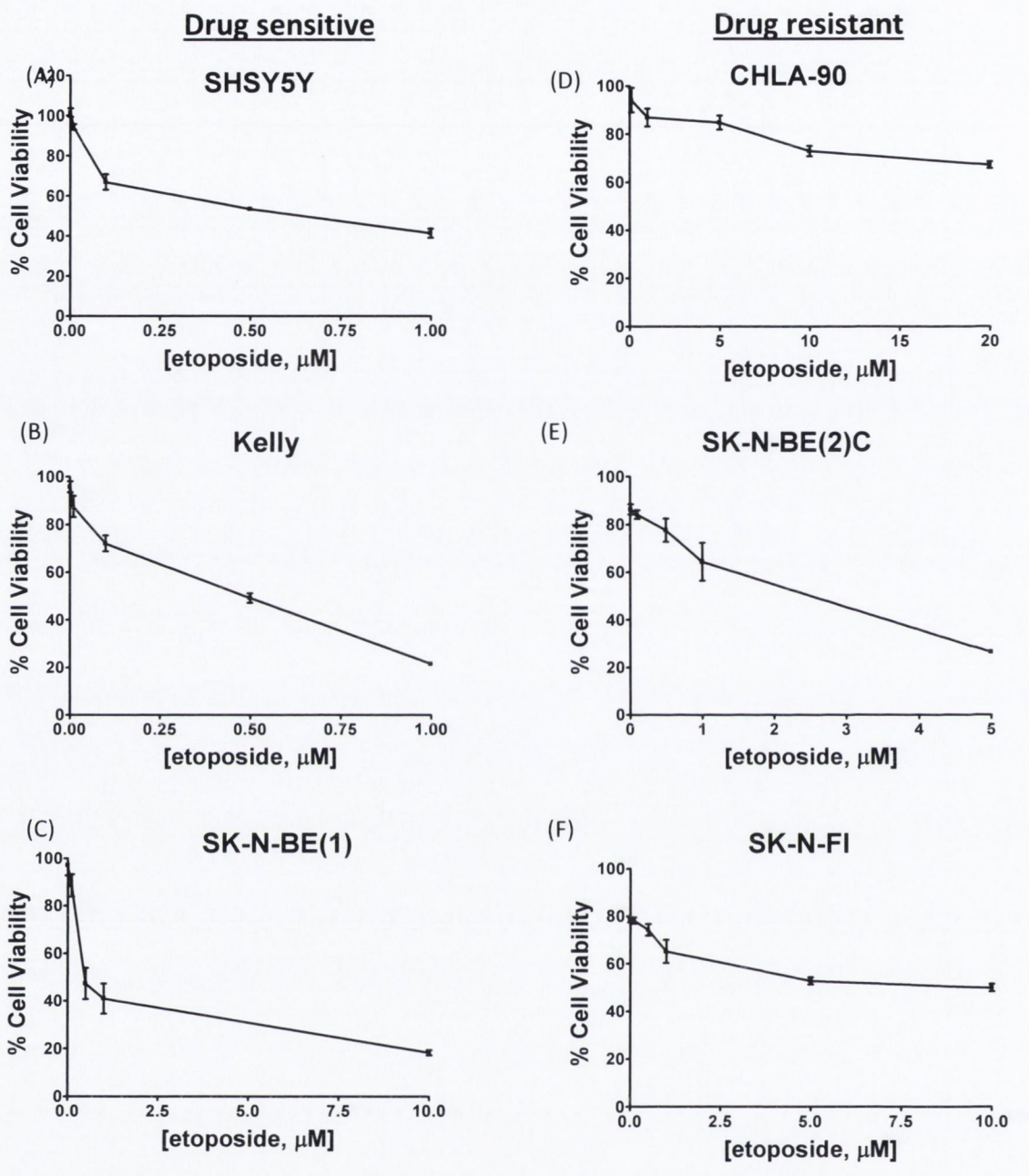

Figure 3.7 Etoposide reduces the viability of neuroblastoma cell lines.

Neuroblastoma cell lines (A) SHSY5Y, (B) Kelly, (C) SK-N-BE(1), (D) CHLA-90, (E) SK-N-BE(2)c and (F) SK-N-FI cells) were seeded at varying densities in 96 well plates and left for 24 hours to attach. Cells were treated with a vehicle (1% (v/v) ethanol) or a range of concentrations of etoposide. After 72 hours cells were harvested, and 20 µl alamarBlue was added to each well. Plates were incubated in the dark for up to 5 hours until a colour change was observed. Fluorescence was measured using a SpectraMax Gemini plate reader at excitation and emission wavelengths of 544 nm and 590 nm respectively. Values represent the mean ± S.E.M of three independent experiments.

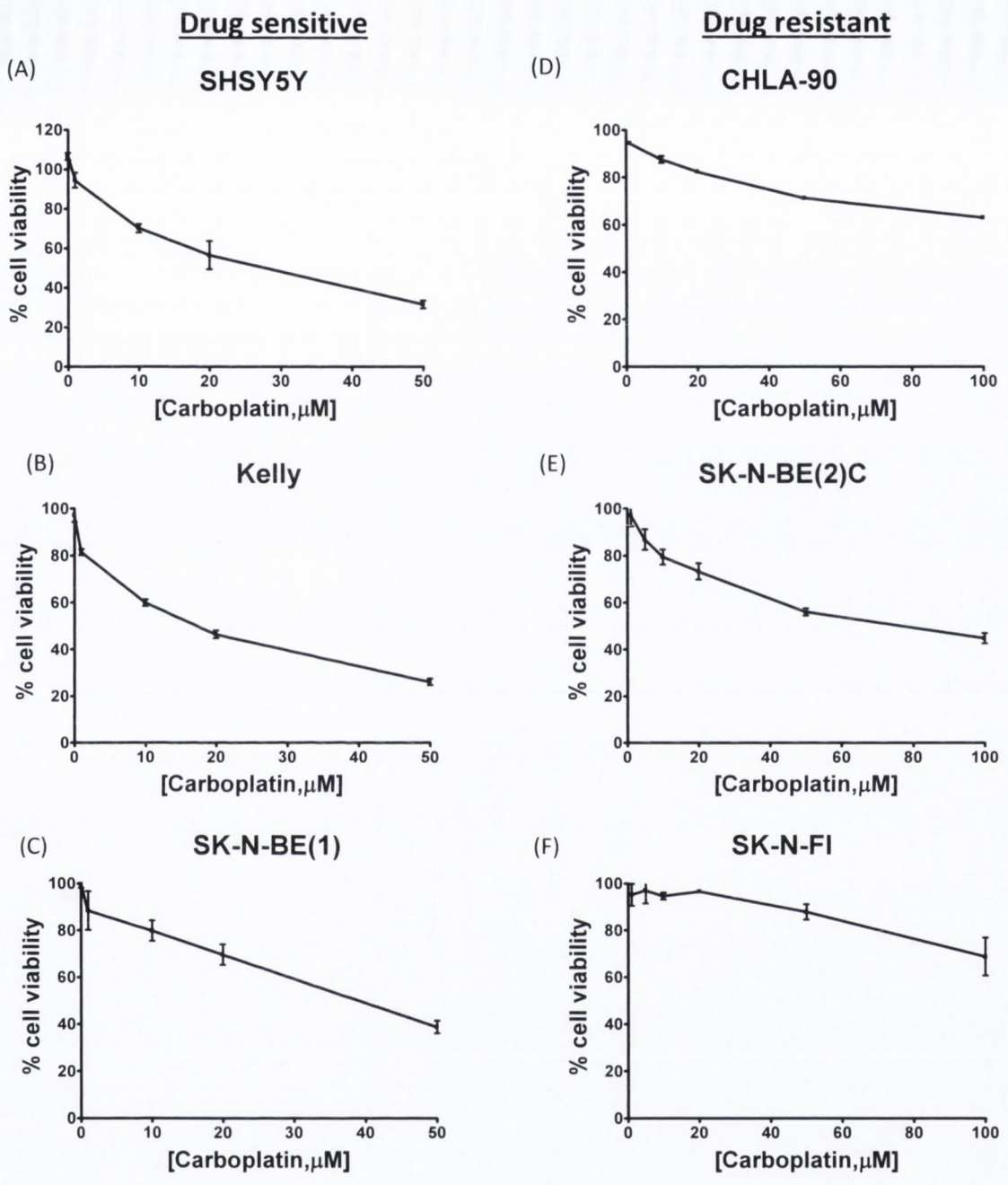

Figure 3.8 Carboplatin reduces the viability of neuroblastoma cell lines.

Neuroblastoma cell lines (A) SHSY5Y, (B) Kelly, (C) SK-N-BE(1), (D) CHLA-90, (E) SK-N-BE(2)c and (F) SK-N-FI cells) were seeded at varying densities in 96 well plates and left for 24 hours to attach. Cells were treated with a vehicle (1% (v/v) ethanol) or a range of concentrations of carboplatin. After 72 hours cells were harvested, and 20 µl alamarBlue was added to each well. Plates were incubated in the dark for up to 5 hours until a colour change was observed. Fluorescence was measured using a SpectraMax Gemini plate reader at excitation and emission wavelengths of 544 nm and 590 nm respectively. Values represent the mean ± S.E.M of three independent experiments.

Cell lines	IC_{50} (μM)					
	PBOX-6	PBOX-15	Vincristine	Doxorubicin	Etoposide	Carboplatin
SHSY5Y	1.73 ± 0.08	0.06 ± 0.06	0.07 ± 0.01	0.21 ± 0.03	0.51 ± 0.06	24.35 ± 0.04
Kelly	1.47 ± 0.09	0.06 ± 0.06	0.02 ± 0.05	0.18 ± 0.07	0.34 ± 0.05	15.75 ± 0.04
SK-N-BE(1)	2.10 ± 0.03	0.11 ± 0.09	0.03 ± 0.06	0.10 ± 0.05	0.60 ± 0.07	40.5 ± 0.05
SK-N-BE(2)c	1.08 ± 0.05	0.04 ± 0.09	0.06 ± 0.05	0.65 ± 0.05	1.70 ± 0.05	62.42 ± 0.04
CHLA-90	1.58 ± 0.01	0.06 ± 0.07	0.92 ± 0.01	1.83 ± 0.07	>20	>100
SK-N-FI	3.73 ± 0.05	0.11 ± 0.1	0.15 ± 0.09	0.91 ± 0.06	9.76 ± 0.10	>100

Table 3.1 IC_{50} values of PBOX compounds and standard chemotherapeutic drugs in a range of neuroblastoma cell lines

3.2.5 Determination of fold resistance of PBOX-6 and 15, etoposide, carboplatin, doxorubicin and vincristine in drug resistant neuroblastoma cell lines.

Development of drug resistance is a major obstacle for the successful treatment of neuroblastoma. Many mechanisms of resistance have been proposed including amplification of MYCN, mutated or deleted p53 and overexpression of drug efflux pumps. SK-N-FI, CHLA-90 and SK-N-BE(2)C are three representative resistant neuroblastoma cell lines. All three cell lines have mutated p53, both the CHLA-90 and SK-N-BE(2)c are MYCN amplified, while the SK-N-FI and CHLA-90 cells overexpress the MDR protein, P-gp (Dijkhuis *et al.*, 2003).

The alamarBlue assay was used to determine the effects of the PBOXs and the four other chemotherapeutics on these three resistant cell lines. The fold resistance of each drug in the three multidrug resistant cell lines was determined as the ratio of the IC_{50} of an MDR cell line to the IC_{50} of a sensitive cell line (Table 3.2, 3.3, 3.4). A cell line with a higher IC_{50} value than the clinically achievable levels is considered to be resistant (Keshelava *et al.*, 1998).

In comparison to all sensitive cell lines, SK-N-BE(2)C cells displayed no resistance to PBOX-6 and 15 (Table 3.2). The IC_{50} values were in a similar range to those observed in the three sensitive cell lines while the IC_{50} value of PBOX-15 was lower in this resistant cell line than in all three sensitive cell lines. Indeed this was in contrast to the fold resistance observed with etoposide, doxorubicin and carboplatin which showed increased IC_{50} values indicating drug resistance. This is with the exception of vincristine in which no difference in the SK-N-BE(2)c cells in comparison to the SHSY5Y was observed while a small fold increase was noted in comparison to the Kelly and SK-N-BE(1) cells.

In the CHLA-90 cell lines the IC_{50} of PBOX-6 was in a similar range to all other drug sensitive lines indicating that this MDR cell line is not resistant to this novel drug (Table 3.3). In comparison to the three drug sensitive cell lines, the IC_{50} value of PBOX-15 was slightly elevated but was within a range consistent with previous PBOX studies. It is important to note that although the IC_{50} value of PBOX-15 increased in the MDR CHLA-90 cell line, the fold resistance was lower than with all the other chemotherapeutics tested. Following treatment with etoposide, the IC_{50} value was greater than 20 μM. The exact

value could not be determined as it exceeded the limits of solubility, although it is clear this cell line is extremely resistant to this drug. Similarly, the IC_{50} value of carboplatin could not be determined in this cell line as it also exceeded the limits of solubility although it was greater than 100 μM again indicating resistance. The microtubule targeting agent vincristine also demonstrated elevated levels of resistance in comparison to the PBOX compounds. An IC_{50} value 23 times higher was evident in CHLA-90 cells in comparison to the drug sensitive SK-N-BE(1) cell line.

The effects of PBOX-6 and -15 were tested in a third drug resistant cell, SK-N-FI. One mechanism of resistance in this cell line is the expression of the drug efflux pump P-gp. It has been previously demonstrated that PBOX-6 and 15 are not substrates for this protein. Again in this cell line both PBOX-6 and -15 showed a lower fold resistance than all other chemotherapeutics tested (Table 3.4). In particular no difference in the IC_{50} value was found for PBOX-15 in the drug sensitive SK-N-BE(1) as in the multidrug resistant SK-N-FI. Once again the fold resistance of etoposide was considerably higher than both PBOXs; with up to a 28 fold resistance in comparison to the drug-sensitive Kelly cell line. Similar to the CHLA-90 cells, the exact IC_{50} value for carboplatin could not be determined as it exceeded the limits of solubility therefore an exact value for fold resistance could not be determined, although it is clear that the cell line displayed a higher fold resistance than both PBOXs. Vincristine, another MTA, was more than 7 times more resistant in comparison to the Kelly cell line. These results demonstrate the potential of the PBOXs for the treatment of resistant neuroblastoma.

		Fold resistance		Fold resistance
	IC_{50} PBOX-6 (μM)		**IC_{50} PBOX-15 (μM)**	
SHSY5Y	1.73	None	0.066	None
Kelly	1.47	None	0.067	None
SK-N-BE(1)	2.10	None	0.115	None
		Fold resistance		**Fold resistance**
	IC_{50} vincristine (μM)		**IC_{50} doxorubicin (μM)**	
SHSY5Y	0.074	None	0.214	3.04
Kelly	0.021	2.85	0.185	3.51
SK-N-BE(1)	0.039	1.53	0.105	6.20
		Fold resistance		**Fold resistance**
	IC_{50} etoposide (μM)		**IC_{50} carboplatin (μM)**	
SHSY5Y	0.519	3.20	24.35	2.56
Kelly	0.346	4.90	15.75	3.96
SK-N-BE(1)	0.603	2.82	40.5	1.54

Table 3.2 Fold resistance of PBOX-6, PBOX-15 vincristine, doxorubicin, etoposide and carboplatin in SK-N-BE(2)c cells in comparison to drug sensitive neuroblastoma cell lines.

The alamarBlue assay was used to determine the effects of the PBOXs and the four other chemotherapeutics on these three resistant cell lines. The fold resistance of each drug in the three multidrug resistant cell lines was determined as the ratio of the IC_{50} of an MDR cell line to the IC_{50} of a sensitive cell lines.

		Fold resistance		Fold resistance
	IC_{50} PBOX-6 (μM)		**IC_{50} PBOX-15 (μM)**	
SHSY5Y	1.73	None	0.066	3.25
Kelly	1.47	None	0.067	3.20
SK-N-BE(1)	2.10	None	0.115	1.86
		Fold resistance		**Fold resistance**
	IC_{50} vincristine (μM)		**IC_{50} doxorubicin (μM)**	
SHSY5Y	0.074	12.4	0.214	8.55
Kelly	0.021	13.78	0.185	9.85
SK-N-BE(1)	0.039	23.66	0.105	17.4
		Fold resistance		**Fold resistance**
	IC_{50} etoposide (μM)		**IC_{50} carboplatin (μM)**	
SHSY5Y	0.519	N.D	24.35	N.D
Kelly	0.346	N.D	15.75	N.D
SK-N-BE(1)	0.60	N.D	40.5	N.D

Table 3.3 Fold resistance of PBOX-6, PBOX-15 vincristine, doxorubicin, etoposide and carboplatin in CHLA-90 cells in comparison to drug sensitive neuroblastoma cell lines.

The alamarBlue assay was used to determine the effects of the PBOXs and the four other chemotherapeutics on these three resistant cell lines. The fold resistance of each drug in the three multidrug resistant cell lines was determined as the ratio of the IC_{50} of an MDR cell line to the IC_{50} of a sensitive cell lines. N.D = not determined.

		Fold resistance		Fold resistance
	IC_{50} PBOX-6 (μM)		**IC_{50} PBOX-15 (μM)**	
SHSY5Y	1.73	2.10	0.066	1.7
Kelly	1.47	2.5	0.067	1.7
SK-N-BE(1)	2.10	1.77	0.115	None
		Fold resistance		**Fold resistance**
	IC_{50} vincristine (μM)		**IC_{50} doxorubicin (μM)**	
SHSY5Y	0.074	2.13	0.214	4.35
Kelly	0.021	7.52	0.185	5.08
SK-N-BE(1)	0.039	4.05	0.105	8.71
		Fold resistance		**Fold resistance**
	IC_{50} etoposide (μM)		**IC_{50} carboplatin (μM)**	
SHSY5Y	0.519	18.80	24.35	N.D
Kelly	0.346	28.2	15.75	N.D
SK-N-BE(1)	0.603	16.1	40.5	N.D

Table 3.4 Fold resistance of PBOX-6, PBOX-15 vincristine, doxorubicin, etoposide and carboplatin in SK-N-FI cells in comparison to drug sensitive neuroblastoma cell lines.

The alamarBlue assay was used to determine the effects of the PBOXs and the four other chemotherapeutics on these three resistant cell lines. The fold resistance of each drug in the three multidrug resistant cell lines was determined as the ratio of the IC_{50} of an MDR cell line to the IC_{50} of a sensitive cell lines. N.D=not determined.

3.2.6 Optimisation of cell seeding density for clonogenic assay

Conventional cell viability assays such as the alamarBlue viability assay do not allow for long term treatment times so the prolonged effects of a given drug on a cell population cannot be ascertained by this method. The clonogenic assay overcomes this obstacle; cells can be treated for longer periods permitting investigation into the effects of a given drug over a prolonged duration. After the treatment period, cells are left for a number of days to allow for colony formation.

The clonogenic assay was employed to study the longer term effect of the PBOXs on neuroblastoma cells. It was necessary to optimise the cell seeding density before commencing the clonogenic survival assays therefore five seeding densities, ranging from 250-1250 cells/ml were tested. It is necessary that all wells, both controls and drug treated contain at least 100 colonies at the endpoint of the assay. It is also essential that the plating efficiency is approximately 10% (Forde *et al.*, 2011). This is determined by dividing the average number of colonies per well by the original plating density and multiplying by one hundred. The optimum density for SHSY5Y cells was identified as 1250 cells/well (Fig. 3.9). This density was chosen as although the plating efficiency was closer to 10% in the 750 and 1000 cells/well, these wells contained less than 100 colonies and were therefore deemed to be unsuitable.

(A)

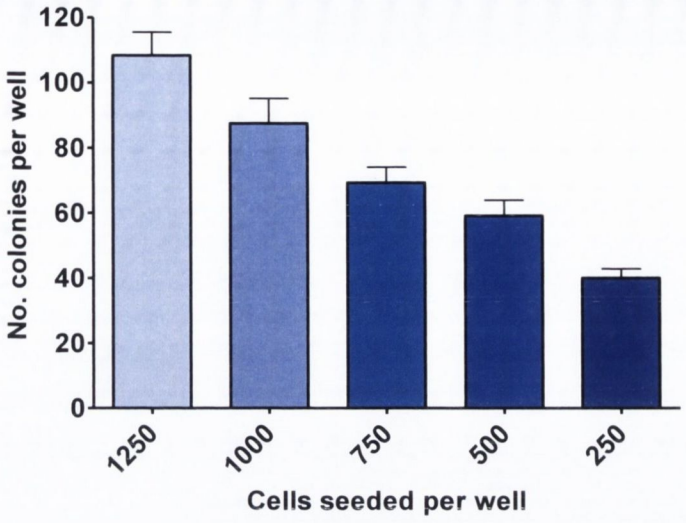

(B)

Seeding density	Plating efficiency (%)
1250	8.6
1000	8.7
750	9.2
500	11.8
250	16.0

Figure 3.9 Optimisation of seeding density of SHSY5Y cells for clonogenic assay.

Cells were seeded at 250, 500, 750, 1000 and 1250 cells/ CellBIND well and left for 10 days. After this time wells were washed with 1ml PBS fixed in ice cold methanol and stained with 0.5% crystal violet. (A) The number of colonies per well were quantified using a ColCount™ (Oxford Optronix, U.K). (B) Plating efficiency was calculated as the ratio of the number of colonies counted over the number of cells plated. Values represent the mean ± S.E.M of three independent experiments preformed in triplicate.

3.2.7 PBOX-6 and 15 inhibits the clonogenicity of SHSY5Y cells in a dose-dependent manner.

The seeding density of each plate was dependent on the concentration of drug treatment. The control plates were seeded at 1250 cells/well. This number was doubled if cells were treated with a concentration equal to the IC_{50} value i.e. plates were seeded at 2500 cells/well if they were to be treated with a concentration of 1.7 μM PBOX-6. Both PBOX-6 and -15 inhibited the clonogenicity of SHSY5Y cells in a dose-dependent manner (Fig. 3.10). After treatment with 1 μM PBOX-6, the percentage clonogenicity decreased to 85%. This further decreased to 30% after treatment with 2.5 μM PBOX-6. Treatment with both 5 μM and 10μM PBOX-6 completely inhibited the cells ability to produce colonies. A similar trend in decreasing clonogenic potential was noted following treatment with PBOX-15 although the concentration which inhibited clonogenic survival was found to be significantly lower, indicative of PBOX-15 being the more potent member of this family of novel MTAs. The IC_{50} of each drug was established; the values were comparable to those determined by the alamarBlue viability assays.

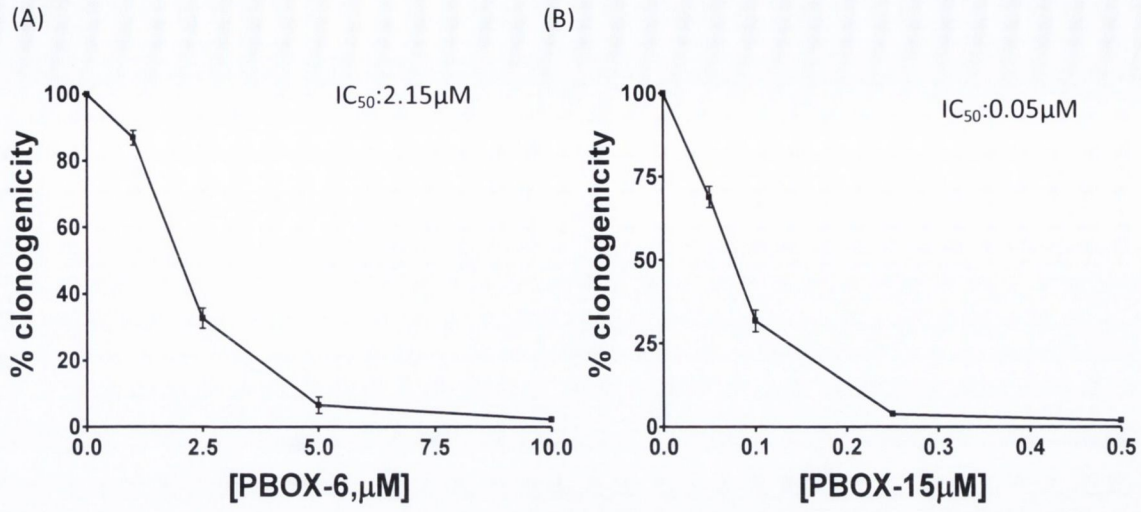

Figure 3.10 PBOX-6 and 15 inhibit the clonogenicity of SHSY5Y cells.

SHSY5Y cells were seeded at densities dependent on concentration of treatment. Cells were left to adhere overnight and treated with a range of concentrations of (A) PBOX-6 or (B) PBOX-15. After 7 days media containing drug was removed, cells were washed in PBS and fresh media was added to each well. Cells were left for 10 days to allow for recovery of colonies. After 10 days cells were fixed in methanol and stained using crystal violet. Colonies were counted using a Colcount™. Values represent the mean ± S.E.M of three independent experiments performed in triplicate.

3.2.8 PBOX-6 decreases the viability of neuroblastoma cells isolated from primary bone marrow samples

Anti-cancer research is dependent on cell lines to screen for activity of compounds and determine the mechanism of action of drugs. They are an indispensible tool and provide a wealth of valuable information allowing for exploration of all aspects of cancer, from the role of individual molecules, to cellular processes involved in invasion and metastasis within animal models. They have the advantage of being easy to use, grow rapidly, produce reproducible results and have a strong track record of use in cancer research (Holliday *et al.*, 2011). There are some disadvantages to their use, over time a cell line may undergo selection to the extent that it no longer truly represents a particular malignant phenotype. Cell lines are adapted to grow in conditions far different to the original tumour and become dependent on particular growth factors and nutrients (Pan *et al.*, 2009). Therefore primary cell culture is an essential component of any drugs development (Eglan *et al.*, 2011)

Approximately 70% of neuroblastoma patients present with a metastatic disease at the time of diagnosis with bone marrow involvement being extremely common in children with metastatic disease (Maris *et al.*, 2010). Approximately 60-65% of stage 4 patients test positive for metastasis in this area. Despite an intensive programme of therapy combining surgery, chemotherapy, and radiotherapy, patients who present with bone marrow involvement have a poor prognosis and higher mortality rates with the probability of remission lasting longer than three years less than 10% (London *et al.*, 2011). Neuroblastoma cells present in the bone marrow represent the most advanced, aggressive form of this cancer that have demonstrated the capacity to metastasise and invade distant organs. These are the cells which become resistant to chemotherapy and so are an important population to consider when examining new therapeutic strategies for this cancer. GD_2 is a cell surface antigen which is widely expressed on neuroblastoma cells (Yang *et al.* 2010). This principle can be exploited to separate neuroblastoma cells from a bone marrow sample (Scaruffi *et al.*, 2011). Neuroblastoma cells were isolated from bone marrow samples by immunomagnetic separation based on the positive selection of GD_2 expressing cells, and cultured. Not all isolated cells are capable of being grown in culture. Some cells will not adhere to the cell culture dish and will die

immediately. Others will adhere to the cell culture dish but will not undergo cell division (personal communication with Dr. David Betts, Our Lady's Children's Hospital, Crumlin, Dublin). As samples were received prior to diagnosis all samples were separated regardless of stage. The characteristics of all patient samples received to date are summarised in Table 3.5. Only six samples were positive for metastasis and were subsequently cultured. If culturing was successful, viability assays were performed. The effect of PBOX-6 on viability of primary neuroblastoma cells isolated from patient 3 was determined using the alamarBlue viability assay (Fig. 3.11). Cells were treated with varying concentrations of PBOX-6 (1-10μM) for 72 hours and the IC_{50} was determined. The IC_{50} value of PBOX-6, (6.04 ± 2.15μM) although slightly elevated, was in the same range as those established in *in vitro* studies. Previously it has been shown that to induce apoptosis in *ex vivo* CML samples, cells were treated with a higher concentration of both PBOX-6 and 15 than used in *in vitro* studies (Bright *et al.*, 2010). The IC_{50} value for patient 19 could not be determined as viability did not fall below 50% after treatment with PBOX-6 although it should be noted that the trend is similar to that observed in patient 3 suggesting PBOX-6 is having a similar effect on primary cell viability. Due to the limited number of cells available it was not possible to determine the effects of PBOX-15 in these primary cells.

Number	Sex	Bone marrow	Grew in culture	Date received
1	F	Negative	-	26/1/11
2	M	Negative	-	4/5/11
3	F	Positive	Yes	14/9/11
4	F	Negative	-	27/9/11
5	M	Negative	-	24/10/11
6	M	Negative	-	11/11/11
7	M	Positive	Contamination	22/12/11
8	F	Negative	-	28/11/11
9	F	Negative	-	4/5/12
10	F	Negative	-	11/5/12
11	F	Positive	No	5/6/12
12	M	Positive	No	16/7/12
13	M	Negative	-	30/11/12
14	F	Negative	-	7/1/13
15	F	Negative	-	13/2/13
16	F	Negative	-	22/3/13
17	F	Positive	Contamination	9/8/13
18	M	Positive	Yes	25/10/13

Table 3.5 Characteristics of neuroblastoma patient samples in *ex vivo* study.

Bone marrow samples were obtained from Dr. Anne O'Meara in Our Lady's Children's Hospital Crumlin. All patients' guardians signed a written consent allowing the use of samples and clinical data for research purposes. Relevant medical data was obtained including patient's sex and presence of metastasis in the bone marrow. M-Male, F-Female.

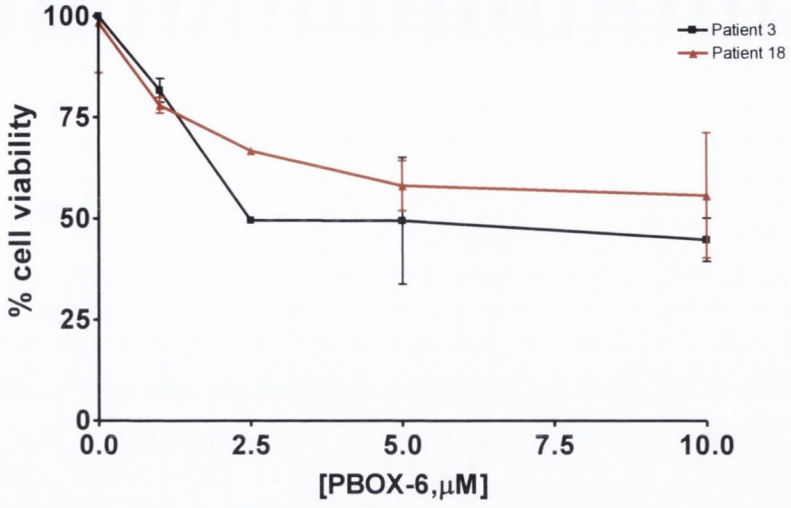

Figure 3.11 PBOX-6 decreases the viability of primary neuroblastoma cells.

Primary cells were isolated from bone marrow aspirate of a stage 4 neuroblastoma patients. Cells were seeded at a density of 1.5 x 10^5 cells/ml in a 96 cell plate and left to adhere overnight. The following day cells were treated with varying concentrations of PBOX-6 (1 μM, 2.5 μM, 5 μM and 10 μM). After 72 hours cells were harvested, 20 μl alamarBlue was added to each well and incubated in the dark for up to 5 hours until a colour change was observed. Fluorescence was measured using a SpectraMax Gemini plate reader at excitation and emission wavelengths of 544 nm and 590 nm respectively. Values represent two independent experiments.

3.2.9 The effect of PBOX-6 and 15 on SHSY5Y cell cycle progression and induction of apoptosis.

Results from the alamarBlue assays showed a decrease in cell viability following treatment with the novel PBOX compounds. It was then necessary to determine whether this observed decrease in cellular viability was due to apoptosis, cell cycle arrest or a combination of the two. Flow cytometric analysis of propidium iodide-stained cells was therefore employed. Flow cytometry, a more thorough quantitative method to establish the effect of a drug on cell viability, was used to assess the effects of the drugs on cell cycle progression. The percentage of cells undergoing apoptosis and/or cell cycle arrest was determined. Dose and time-dependent studies were performed; a range of concentrations of both PBOX-6 (1 μM, 2.5 μM, 5 μM and 10 μM) and PBOX-15 (0.01 μM, 0.1 μM, 0.25 μM, 0.5 μM and 1 μM) were examined at five time points (6, 16, 24, 48 and 72hours).

PBOX-6-induced apoptosis in SHSY5Y cells in a time-dependent manner. The effect of 5 μM and 10 μM PBOX-6 on cell cycle progression and induction of apoptosis was investigated over a 72 hour period (Fig. 3.12). Apoptosis induction by PBOX-6 was first observed between 6 and 16 hours. At 16 hours 5 μM PBOX-6 induced 5.97±0.7% which continued to increase to a maximum of 21.76±5.2% at 72 hours. In a similar manner after 16 hours, 10 μM PBOX-6 induced 12.75±1.2% apoptosis which also continued to rise to a maximum of 47.77±1.0% at 72 hours. Similar results were obtained with the more potent analogue PBOX-15 (Fig. 3.12). At 0.5 μM PBOX-15 induced apoptosis in SHSY5Y cells between 6 and 16 hours post treatment with a maximum level of 23.94±1.1% apoptosis being reached after 72 hours. Furthermore 72 hours after treatment with 1 μM PBOX-15 a maximum of 48.57±1.2% apoptosis was induced. Additionally a dose response analysis was undertaken. SHSY5Y cells were treated with varying doses of PBOX-6 (1 μM, 2.5 μM, 5 μM or 10 μM) or -15 (0.1 μM, 0.25 μM, 0.5 μM or 1 μM) for 72 hours. Both PBOX-6 and -15 induced apoptosis in SHSY5Y cells in a dose-dependent manner (Fig. 3.13).

The effect of the PBOX compounds on cell cycle progression was also established (Fig. 3.14). PBOX-6 (5 μM) induced a G2/M arrest which peaked at 24 hours. After 48 hours the cells exited mitosis and the percentage of cells in the G2/M phase fell to less than 20%

(17.98 ± 2.5%) with a further decrease to 11.05 ± 1.1% after 72 hours. As cells exited the G2/M phase at 16 or 24 hours, the percentage of cells undergoing apoptosis increased. 10 μM PBOX-6 induced a transient G2/M arrest which peaked at the earlier time of 16 hours (36.56 ± 4.9%) and decreased to 10.83 ± 1.9% after 48 hours and 6.14 ± 3.9% after 72 hours. These levels were significantly lower than the controls which remained constant at approximately 18% over all time points. A concentration of 10 μM PBOX-6 more potently induces both the G2/M arrest and apoptosis in SHSY5Y cells. Similar to 10 μM PBOX-6, 0.5 μM PBOX-15 induced a transient G2/M arrest which peaked at 16 hours (30.84 ± 4.9%) and decreased to 17.34 ± 1.9% after 72 hours (Fig. 3.14). In contrast to PBOX-6, cells treated with 1 μM PBOX-15 exhibited a more sustained G2/M arrest which peaked at 24 hours and was maintained until 48 hours post treatment. An apoptotic cell population was observed from 16 hrs post treatment, increasing with time (Fig. 3.12). A substantial decrease in the G2/M population was noted between 48 and 72 hours which could be accounted for by the increase in the sub G1/GO population after 48 hours. The observed G2/M arrest induced by both these drugs was in agreement with previous reports demonstrating that the PBOX's target the microtubules (McGee *et al.*, 2006).

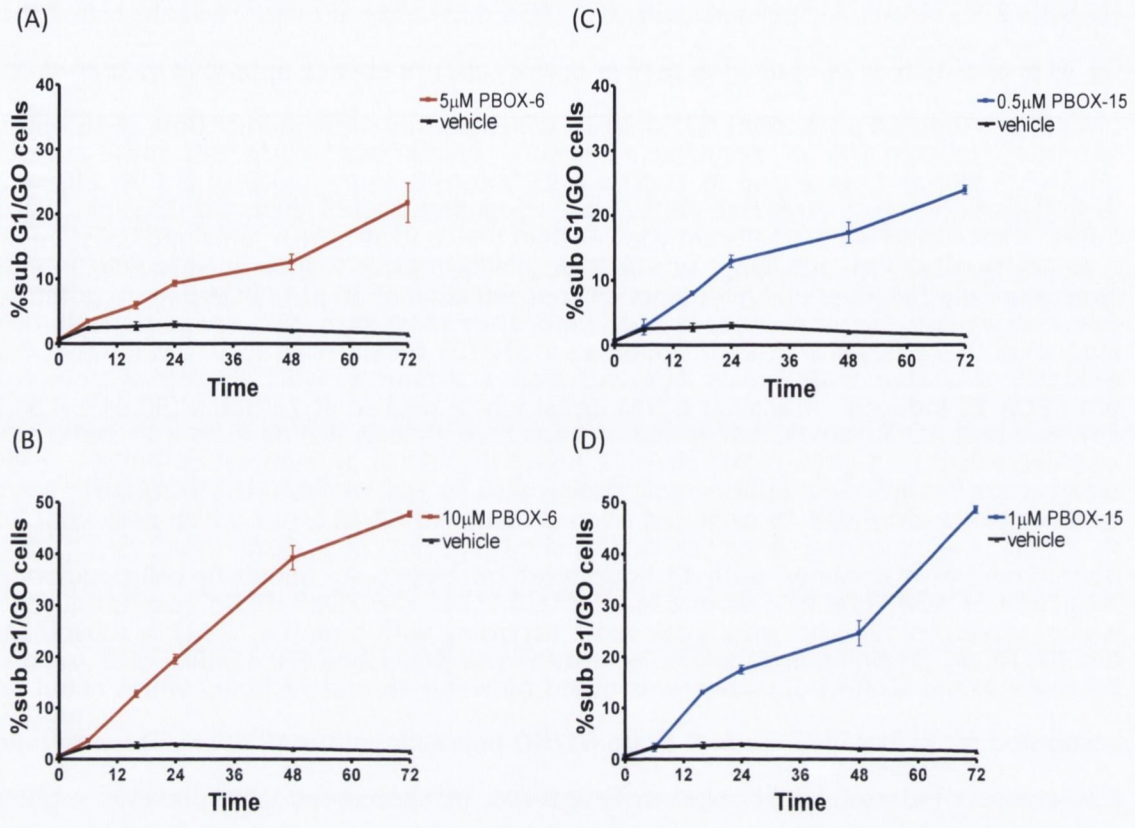

Figure 3.12 PBOX-6 and -15 induces apoptosis in SHSY5Y cells in a time-dependent manner.

SHSY5Y cells were treated for up to 72 hours with a vehicle (1% (v/v) ethanol), (A) 5 μM PBOX-6, (B) 10 μM PBOX-6, (C) 0.5 μM PBOX-15 or (D) 1 μM PBOX-15. After the required incubation time (6 hours, 16 hours, 24 hours, 48 hours or 72 hours), cells were harvested, fixed in 2 mls ethanol and stained with propidium iodide. Cells were analyzed by flow cytometry for the percentage of cells undergoing apoptosis and determined by quantification of the sub G1/GO peak. Values represent the mean ± S.E.M of three independent experiments.

(A) (B)

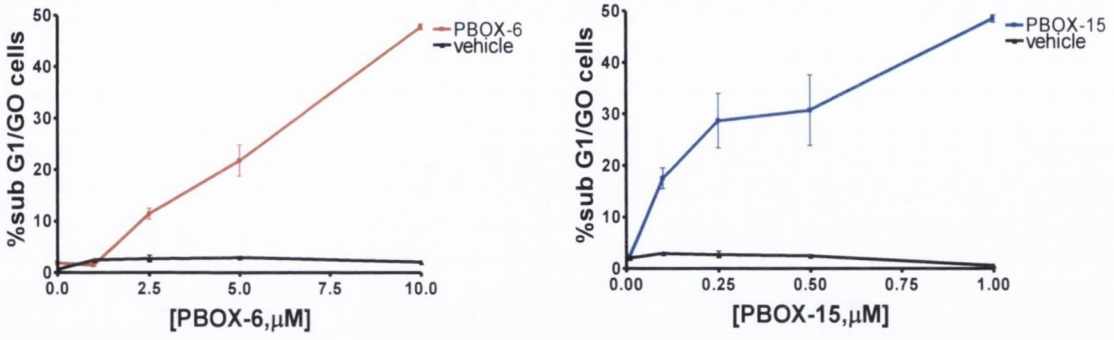

Figure 3.13 PBOX-6 and -15 induces apoptosis in SHSY5Y cells in a dose-dependent manner.

SHSY5Y were seeded at 1 x 10^5 cells/ml in a 6 well plate and left to adhere overnight. The following day, cells were treated for 72 hours with a vehicle (1% (v/v) ethanol), (A) up to 10 μM PBOX-6 or (B) up to 1 μM PBOX-15. After 72 hours cells were harvested, fixed in 2 mls ethanol and stained with propidium iodide. Cells were analysed by flow cytometry for the percentage of cells undergoing apoptosis and determined by quantification of the sub-G1/G0 peak. Values represent the mean ± S.E.M of three independent experiments.

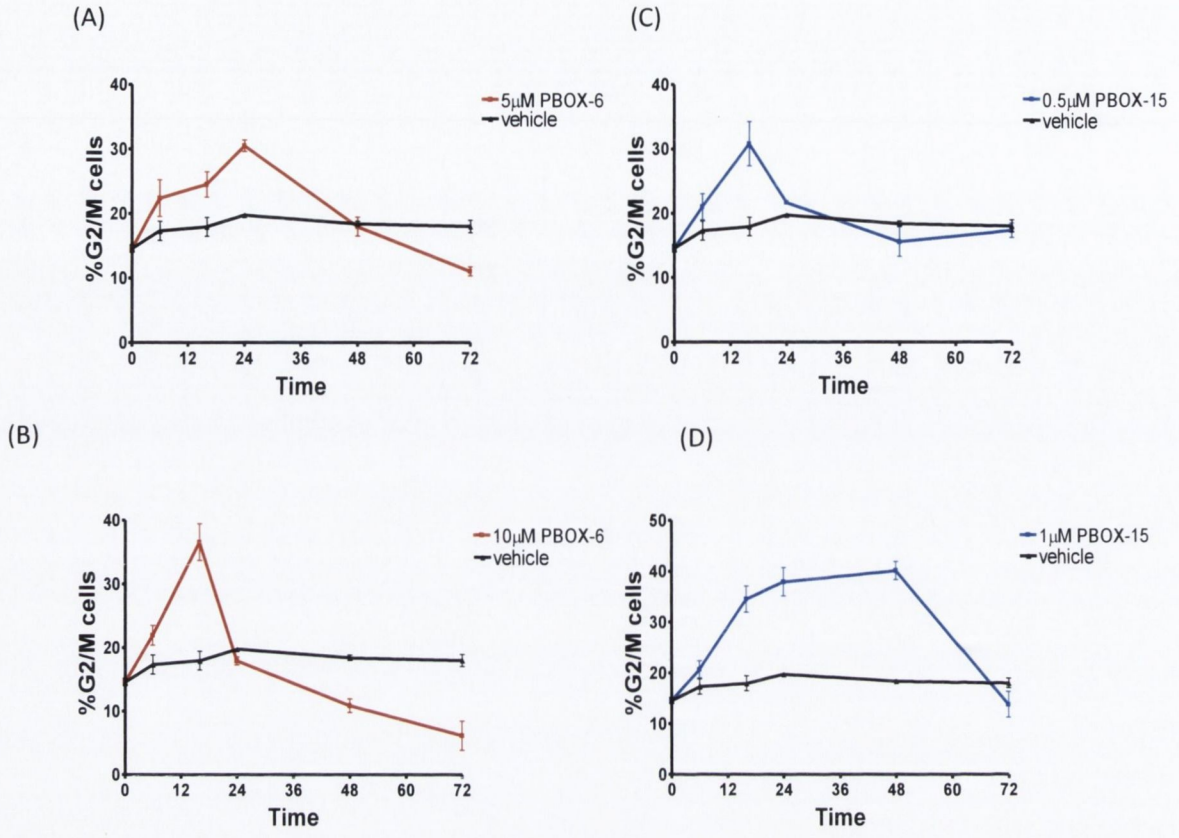

Figure 3.14 PBOX-6 and -15 induces G2/M arrest in SHSY5Y cells.

SHSY5Y were seeded at 1 x 10^5 cells/ml in a 6 well plate and left to adhere overnight. The following day cells were treated for up to 72 hours with a vehicle (1% (v/v) ethanol), (A) 5 μM PBOX-6, (B) 10 μM PBOX-6, (C) 0.5 μM PBOX-15 or (D) 1 μM PBOX-15. After the required incubation time (6 hours, 16 hours, 24 hours, 48 hours or 72 hours) cells were harvested, fixed in 2 mls ethanol and stained with propidium iodide. Cells were analyzed by flow cytometry for the percentage of cells in the G2/M phase of the cells cycle. The percentage of cells undergoing G2/M arrest was determined by quantification of the G2/M peak. Values represent the mean ± S.E.M of three independent experiments.

3.2.10 PBOX-6 induces PARP cleavage in SHSY5Y cells.

Poly (ADP) ribose polymerase PARP is a 116kDa nuclear protein which plays a role in the detection and repair of DNA damage. During apoptosis this protein is cleaved between Asp^{214} and Gly^{215} by caspase-3 and it loses enzymatic repair function (Chaitanya *et al.*, 2010). PARP cleavage has been shown in almost all forms of apoptosis so is a powerful indicator of cell death. Western blot analysis of PARP cleavage was undertaken to confirm that the sub GO/GI peaks observed by flow cytometric analysis was representative of an apoptotic cell population. Consistent with results from flow cytometric analysis, PARP was cleaved in a time and dose dependent manner in SHSY5Y neuroblastoma cells. Cleavage of PARP was first observed between 6 and 16 hour treatment with the appearance of faint bands at 89kDa. Cleavage was found to increase with concentration and time. The full length form representing the fully functional repair enzyme was observed in the vehicle control at all time points (Fig. 3.15).

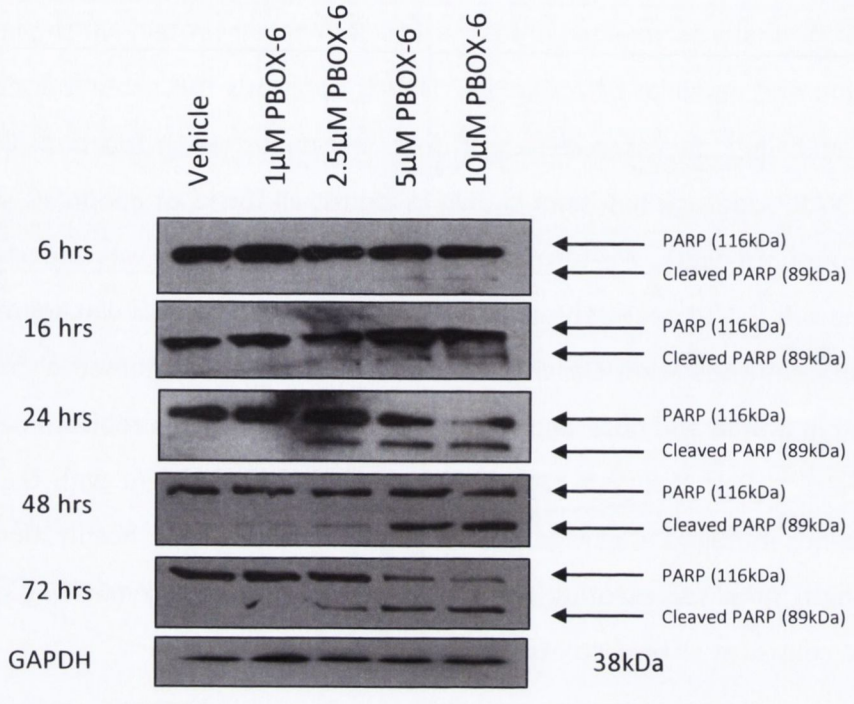

Figure 3.15 PBOX-6 induces PARP cleavage in SHSY5Y cells.

SHSY5Y cells were seeded at a density of 3.0 x 10^5 cells in T25cm^2 flasks and left to adhere overnight. The following day, cells were treated with either vehicle (1% v/v) ethanol) or varying concentrations of PBOX-6 (1 μM, 2.5 μM, 5 μM and 10 μM). After the required time cells were harvested and lysates were prepared for western blot analysis. 30 μg of protein was separated on a 10% resolving gel with 5% stacking gel, transferred to a PVDF membrane and probed with an anti-PARP antibody. Membranes were also probed for GAPDH as a loading control. Results are representative of three separate experiments.

3.2.11 The effect of PBOX-6 on the Bcl-2 family of proteins.

Determination of the molecular mechanisms through which PBOX-6 mediates apoptosis was next undertaken. As the Bcl-2 family of proteins control the induction or inhibition of apoptosis by exerting either pro or anti-apoptotic affects on the cell, analysis of the expression levels of different members of this family and determination of their role in inhibition or induction of apoptosis was undertaken.

Overexpression of the anti-apoptotic protein Mcl-1 is a major determinant of drug resistance in many cancers including neuroblastoma where it has been suggested to serve as a putative oncogene (Boiani *et al.*, 2013). Primary neuroblastoma tumours have been shown to heterogeneously express Mcl-1, with high expression correlating to high-risk phenotype (Lestini *et al.*, 2009). Downregulation of Mcl-1 expression has been shown to sensitise neuroblastoma cells to chemotherapy (Lestini *et al.*, 2009). Therefore we first sought to establish the effects of PBOX-6 on this anti-apoptotic protein. Cells were treated with a vehicle, or various concentrations of PBOX-6 (1-10μM) for up to 72 hours. It was found that PBOX-6 decreased anti-apoptotic Mcl-1 expression in a time-dependent manner (Fig. 3.16). No change in Mcl-1 expression was observed after a 6 hour treatment with PBOX-6. A decrease was first noted after treatment for 16 hours and continued to decrease with time. Additionally Mcl-1 expression was found to decrease in a dose-dependent manner.

Expression of the anti-apoptotic Bcl-2 protein in untreated neuroblastoma tumours has been shown to correlate with poor prognosis (Dole *et al.*, 2003). Silencing of Bcl-2 was found to sensitise neuroblastoma cells to chemotherapy with a number of small molecule inhibitors of Bcl-2 currently undergoing clinical trials (Lamers *et al.*, 2012) indicating this is a valid therapeutic target in neuroblastoma. Following a 16 hour treatment with PBOX-6 there was no discernible change in Bcl-2 expression (Fig. 3.17). After 24 hour treatment PBOX-6 induced cleavage of Bcl-2 in a dose-dependent manner. This cleaved fragment represents a form of the Bcl-2 protein which has lost its anti-apoptotic activity (Cheng *et al.*, 1999; Kirsch *et al.*, 1999).

Next the effect of PBOX-6 on expression of pro-apoptotic Bcl-2 proteins was examined; Bak was chosen as a representative member of this family (Fig. 3.18). It has been reported that therapies which shift the balance of protein expression from an anti-apoptotic to a pro-apoptotic state, prime neuroblastoma cells for apoptotic cell death (Bender *et al.*, 2011). No change in Bak expression after a 6 or 16 hour treatment with PBOX-6 was observed. An increase in expression was noted after 24 hours and continued to increase with time with the highest level of Bak expression being observed after a 72 hour treatment with PBOX-6. Expression of pro-apoptotic Bax in SHSY5Y cells was monitored; no change in expression was noted (Fig. 3.19). This is consistent reports showing that although PBOX-6 induced phosphorylation and inactivation of several anti-apoptotic proteins in CML cells, Bax expression was not affected (McGee *et al.*, 2004).

Pro-apoptotic cytochrome c is released though pores which form in the outer mitochondrial membrane in an apoptotic cell. These pores have been postulated to form when Bak and Bax oligomerise and insert into the membrane. This oligomerisation requires a conformational change that involves exposure of N-terminal epitopes. Therefore, we sought to determine whether the increase in Bak expression observed after treatment with PBOX-6 represented an activated form of Bak which was capable of forming pores and consequently the release of cytochrome c. An anti-Bak antibody specific for the conformationally active form of Bak was utilised and expression was analysed by western blot. After a 72 hour treatment Bak was activated in a dose-dependent manner by PBOX-6 (Fig. 3.18). No expression was observed in the vehicle-treated lane or with the 1 μM PBOX-6 treatment. Bands were visible in the lanes representing the 2.5-10 μM PBOX-6 treated cells with expression increasing in a dose-dependent manner.

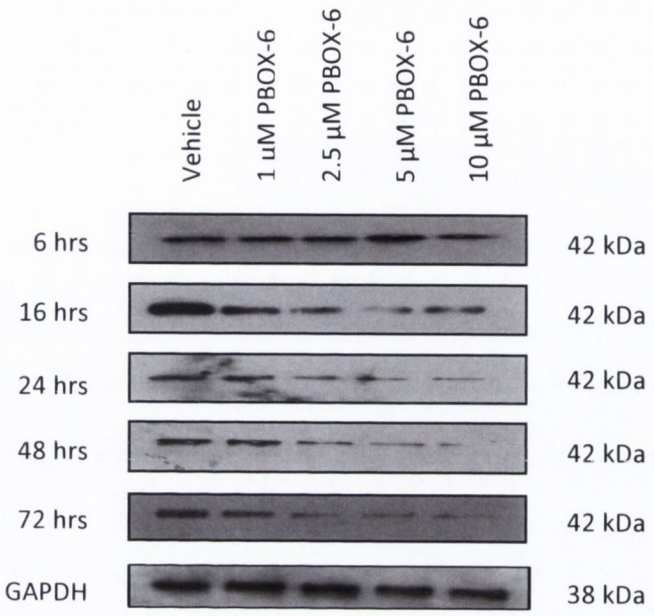

Figure 3.16 PBOX-6 decreases the expression of anti-apoptotic Mcl-1 in a time and dose-dependent manner.

SHSY5Y cells were seeded at a density of 3.0 x 10^5 cells in T25cm^2 flasks and left to adhere overnight. The following day, cells were treated with varying concentrations of PBOX-6 (1 µM, 2.5 µM, 5 µM and 10 µM). After the indicated time, cells were harvested and lysates were prepared for western blot analysis. 30 µg of protein was separated on a 12% resolving gel with 5% stacking gel, transferred to a PVDF membrane and probed with an anti-Mcl-1 antibody. Membranes were also probed for GAPDH as a loading control. Results are representative of three separate experiments.

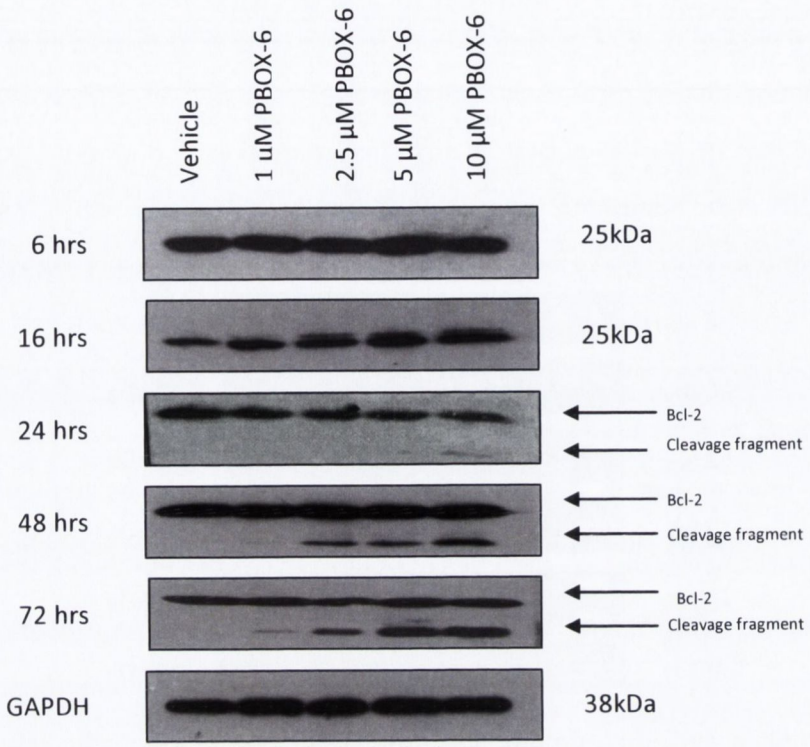

Figure 3.17 PBOX-6 induces cleavage of anti-apoptotic Bcl-2 in SHSY5Y cells.

SHSY5Y cells were seeded at a density of 3.0 x 10^5 cells in T25cm^2 flasks and left to adhere overnight. The following day, cells were treated with varying concentrations of PBOX-6 (1 µM, 2.5 µM, 5 µM and 10 µM). After the indicated time, cells were harvested and lysates were prepared for western blot analysis. 30 µg of protein was separated on a 12% resolving gel with 5% stacking gel, transferred to a PVDF membrane and probed with an anti-Bcl-2 antibody. Membranes were also probed for GAPDH as a loading control. Results are representative of three separate experiments.

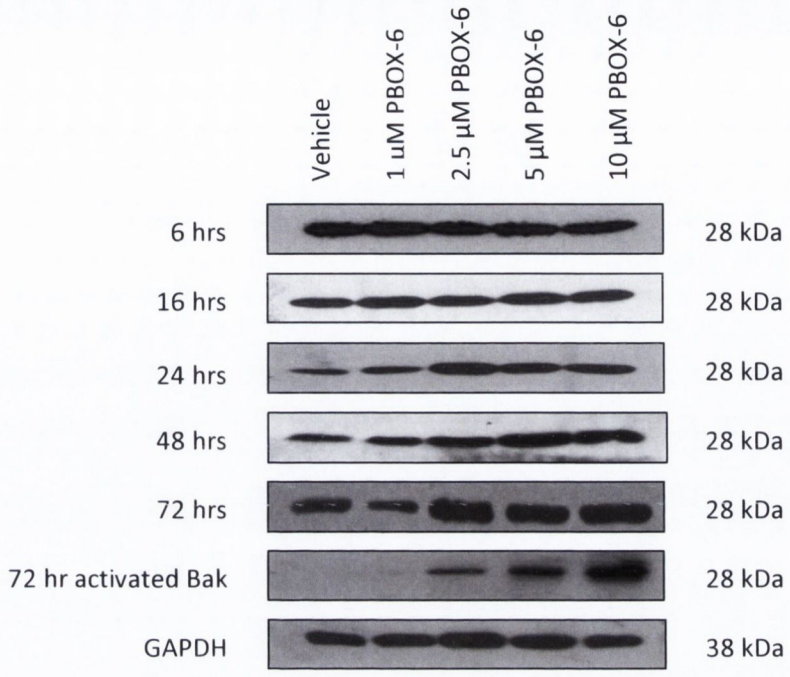

Figure 3.18 PBOX-6 increases the expression of pro-apoptotic Bak in SHSY5Y cells.

SHSY5Y cells were seeded at a density of 3.0 x 10^5 cells in T25cm^2 flasks and left to adhere overnight. The following day, cells were treated with varying concentrations of PBOX-6 (1 µM, 2.5 µM, 5 µM and 10 µM). After the indicated time, cells were harvested and lysates were prepared for western blot analysis. 30 µg of protein was separated on a 12% resolving gel with 5% stacking gel, transferred to a PVDF membrane and probed with an anti-Bak or anti-Bak-NT (activated Bak) antibody. Membranes were also probed for GAPDH as a loading control. Results are representative of three separate experiments.

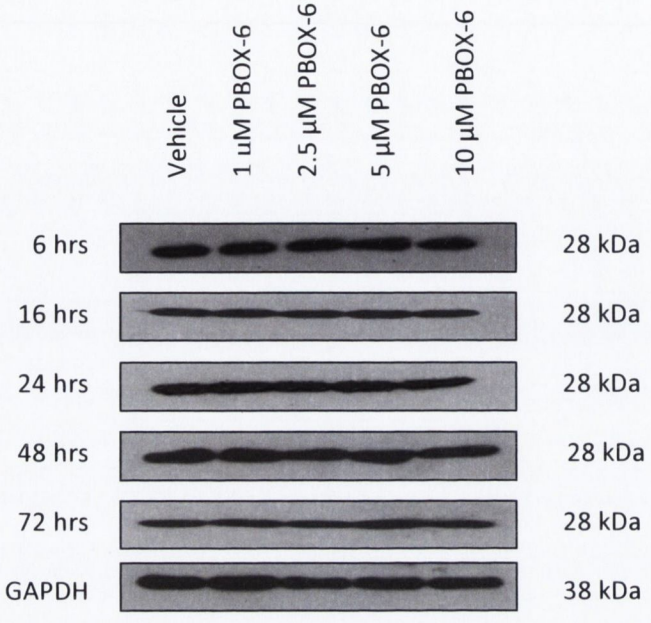

Figure 3.19 Bax expression is unaltered upon treatment with PBOX-6 in SHSY5Y cells.

SHSY5Y cells were seeded at a density of 3.0 x 10^5 cells in T25cm^2 flasks and left to adhere overnight. The following day, cells were treated with varying concentrations of PBOX-6 (1 µM, 2.5 µM, 5 µM and 10 µM). After the indicated times, cells were harvested and lysates were prepared for western blot analysis. 30 µg of protein was separated on a 12% resolving gel with 5% stacking gel, transferred to a PVDF membrane and probed with an anti-Bax antibody. Membranes were also probed for GAPDH as a loading control. Results are representative of three separate experiments.

3.3 Discussion

Neuroblastoma, a paediatric malignancy caused by aberrant development of the sympathetic nervous system, is the most fatal solid tumour in children. Although patients with low risk disease have a very favourable outlook (>90% survival rate), children who are diagnosed late with a metastatic disease have a very poor prognosis (10-40% survival rate) often suffering from recurrent relapses (Maris *et al.*, 2010). These patients have been shown to develop resistance to a broad range of chemotherapeutic drugs used in the treatment of this cancer (Keshelava *et al.*, 1998). Several mechanisms such as amplification of MYCN and p53 loss of function have been reported to contribute to the development of multidrug resistance (Cheung *et al.*, 2013). Some neuroblastoma cells become resistant through enhanced drug efflux caused by the overexpression of a family of ABC (ATP binding cassette) transporters which use ATP hydrolysis to pump drugs out of cells. This poses a problem as many chemotherapeutic drugs used in the treatment of neuroblastoma, are substrates for these transporters such as etoposide, vincristine and doxorubicin, all of which are substrates of P-gp (Balayssac *et al.*, 2005). P-gp has been shown to be overexpressed in a number of multidrug resistant neuroblastoma cell lines. Dijkhuis *et al.*, (2003) characterised the P-gp status of three neuroblastoma cell lines (SK-N-DZ, SK-N-AS and SK-N-FI) demonstrating that P-gp expression was highest in the SK-N-FI cell line. Consequently this study found that the IC_{50} values for all drugs tested correlated with P-gp expression with the highest IC_{50} values being recorded in SK-N-FI cells, the cell line with the highest levels of P-gp expression, concluding that expression of P-gp correlates with the level of resistance pointing to its role in drug resistance. Park *et al.*, (1990) have previously shown that high levels of P-gp mRNA are often associated with resistance to chemotherapeutics and these high levels may contribute to resistance. Similarly Chan *et al.*, (1991) found that the tumours of all relapsed patients studied had high expression of P-gp whereas it was not detected in low risk localised tumours. The expression of P-gp in pre-treatment samples was predictive of outcome with those patients who were negative for P-gp expression having superior rates of response to treatment. It is therefore clear that there is a need for new therapeutics which are not substrates for P-gp.

It has been previously shown that the novel microtubule targeting drugs, the PBOXs are

not substrates for these MDR proteins (Nathwani *et al.*, 2008). Although the PBOXs had not previously been tested in neuroblastoma cells, they have been shown to potently induce apoptosis in a number of cell lines, *ex vivo* leukaemia patient samples and in several mouse cancer models (Greene *et al.*, 2007; McElligott *et al.*, 2009; Nathwani *et al.*, 2010; Bright *et al.*, 2010; Maginn *et al.*, 2011). The aim of this work was the determine the effects of novel PBOXs on the viability of neuroblastoma cell lines, to identify if these compounds could induce apoptosis in NB cell lines and to establish the molecular mechanisms through which these drugs induce apoptosis.

The alamarBlue viability assay was employed to investigate the effects of the PBOXs on the viability of a panel of drug-sensitive and -resistant neuroblastoma cell lines. The IC_{50} value of PBOX-6 was found to be in a similar range in all six cell lines, both drug sensitive and resistant. This was in contrast to all four other chemotherapeutics tested which displayed increased fold resistance in the resistant cell lines when compared to the drug sensitive. This includes vincristine, another microtubule targeting agent which is currently used to treat neuroblastoma which displayed up to 23 fold resistance in the CHLA-90 cell line when compared to the SK-N-BE(1). The IC_{50} values obtained for PBOX-15 was lower in all cell lines tested when compared to PBOX-6 indicating that this is a more potent member of the PBOX family of compound, which is consistent with prior findings in several other cancer cell lines. Similarly the IC_{50} values obtained for both PBOX-6 and 15 were consistent with previous published results. Greene *et al.,* (2005) tested the effects of PBOX-6 in four breast cancer cell lines and determined the IC_{50} value to be in a range of 1-2.03μM. Similarly in human ovarian carcinoma A2780 cells and chronic myelogenous leukaemia K562 cells the IC_{50} values were found to be 3.58μM and 6.49μM respectively. Likewise the IC_{50} of PBOX-15 was consistent with previous studies in numerous malignant cell lines including the leukaemia cell line, HL60 (0.21μM) and lung adenocarcinoma cell line A2780 (0.24μM) (Nathwani *et al.*, 2008).

The IC_{50} of PBOX-6 has been determined in a number of other multi drug resistant cancer cell lines. Nathwani *et al.,* (2010) established the IC_{50} value of PBOX-6 in two multidrug resistant leukaemia cells lines, HL60-P-gp (expressing P-gp) and HL60-ABCG2 (expressing BCRP) and found no increase in this value between the parental and resistant cell lines. In contrast, two other microtubule targeting agents, vincristine and paclitaxel exhibited

substantially higher IC_{50} values when compared to the parental cell lines (>10 μM in HL60-MDR cells in contrast to 2.79 nM in the parental line for paclitaxel and 679 nM in contrast to 2.53 nM for vincristine). Flow cytometric analysis of propidium iodide stained cells showed that neither vincristine nor paclitaxel induced apoptosis in the MDR cell lines. A virtual molecular docking study was undertaken and determined that based on its structure PBOX-6 was not a substrate of P-gp. It was concluded that in contrast to other MTAs, PBOX-6 and 15 are not substrates for several MDR proteins which confer resistance to chemotherapeutic drugs. Comparable results were found in the present study in neuroblastoma cells lines. In the P-gp overexpressing SK-N-FI and CHLA-90 cell lines, the fold resistance was significantly lower in comparison to each of the other drugs tested. In the SK-N-FI cells, etoposide, a substrate of P-gp displayed a fold resistance of 9 to 15 in comparison to the three sensitive cell lines. Vincristine also exhibited an increased fold resistance in comparison to PBOX-6 and 15. The level of resistance was not as high as seen in the HL60-MDR cell line. It is possible that this could be due to a difference in level of expression of P-gp between these cell lines but this hypothesis would need to be tested. No difference was reported in the IC_{50} value of the PBOXs in the SK-N-BE(2)C cell line in comparison to all other chemotherapeutics. The fold increase of vincristine in CHLA-90 cells in comparison to SK-N-BE(1) was approximately 23, this was in contrast to PBOX-6 which displayed no resistance demonstrating the potential advantage of the PBOXs over current MTAs being used in the clinic. Wickstrom *et al.*, (2007) investigated the effects of six commonly used chemotherapeutic drugs on the viability of seven neuroblastoma cell lines (both drug-sensitive and resistant) and found increased IC_{50} values for each drug in the MDR cell lines. It is interesting to note that the IC_{50} values for vincristine, etoposide and carboplatin from the SK-N-FI cell line in the present study were in the same range as reported by Wickstom *et al.*, (2007).

Multiple cytotoxicity assays are vital for determining the response of a cell to a given therapy but also for the pre-clinical evaluation of novel drugs such as the PBOXs. Conventional cell viability assays such as the alamarBlue viability assay do not allow for the longer term effects of a given drug on a cell population to be established. The clonogenic assay overcomes this obstacle; cells can be treated for longer periods permitting investigation into the effects of a given drug over a prolonged duration.

Therefore in addition to the alamarBlue viability assay, clonogenic assays were employed. SHSY5Y cells were treated with increasing doses of PBOX-6 and -15 and the percentage clonogenicity was determined. It was found that PBOX-6 and -15 reduced the clonogenicity of SHSY5Y cells in a dose-dependent manner indicating that both PBOXs prevent recovery of SHSY5Y cells. This is the first time the effects of PBOX-6 on the clonogenic survival of a malignant cell line has been established. Previously Forde *et al.*, (2011) investigated the effect of PBOX-15 on the clonogenicity of several malignant cell lines including lung cancer, glioma and prostate cancer and found that PBOX-15 significantly reduced the surviving fraction of the cell lines at all concentrations tested. The sensitivity of PBOX-15 in these cancer cell lines was comparable to those observed in response to other microtubule disrupting agents, such as paclitaxel. To our knowledge the effects of other microtubule targeting agents on the clonogenic survival of neuroblastoma cell lines have not previously been reported in the literature.

Microtubule targeting agents have been reported to disrupt formation of the mitotic spindle blocking cells in the G2/M phase of the cell cycle, consequently resulting in apoptosis. Preliminarily results from the alamarBlue viability assays and clonogenic assays indicated that PBOX-6 and -15 reduce the viability of neuroblastoma cells although it was not clear whether this reduction in viability could be attributed to cell cycle arrest, induction of apoptosis or a combination of both. Therefore cell cycle analysis by flow cytometry was employed. It was found that PBOX-6 and -15 induced apoptosis in a time-dependent manner. Findings from flow cytometry were in agreement with those from viability assays which showed a dose-dependent decrease in cell viability. It was also demonstrated that G2/M arrest preceded apoptosis in neuroblastoma cells and was dependent on the concentration of PBOX used, with arrest peaking at 16 hours in the case of PBOX-6 and a more sustained arrest at 24 hours for cells treated with PBOX-15. Mulligan *et al.*, (2006) showed that PBOX-6 induced G2/M arrest and subsequently apoptosis in MCF-7 cells by binding to tubulin and disrupting tubulin polymerisation. Recently studies in multiple myeloma (MM) cell lines, U266 and NCI-H929, supported these earlier findings (Maginn *et al.*, 2011). Maginn *et al.*, demonstrated by direct immunoflourescent staining that PBOX-15 treatment resulted in complete disruption of the microtubule network in these two MM cell lines.

Chapter 3

One hallmark of neuroblastoma is heterogeneity at both a cellular and clinical level. Neuroblasts are present in tumours at different stages of differentiation therefore both neuroblastoma tumours and cell lines have a number of distinct cell types, the 'N' or neural type of a neuronal lineage, 'S' or schwannian of a glial lineage and the 'I' type which is an intermediate with the ability to progress towards a neuronal or glial lineage upon differentiation (Ross *et al.*, 2003). The difference in malignant properties between S- and N-type cell subtypes may have clinical relevance. It has been previously demonstrated that N and S type cells exhibit differences in response to treatment with MTAs. S type cells undergo mitotic arrest in contrast to N type cells which undergo apoptosis (Piacentini *et al.*, 1996). This would support our finding that N type cells (SHSY5Y, Kelly and SK-N-BE(1)) undergo apoptosis in response to our novel MTA.

Previously the PBOX compounds have shown efficacy in *ex vivo* CLL samples (McElligott *et al*, 2009) and *ex vivo* CML patients (Bright *et al*, 2010). It was necessary to confirm the response of primary neuroblastoma cells to this novel MTA in order to predict its potential clinical response. Metastasis is the main cause of death in patients with neuroblastoma with the bone marrow being the major site of metastasis. In spite of aggressive therapy children presenting with dissemination of malignant neuroblasts in the bone marrow have a poor prognosis, therefore cells isolated from the bone marrow are representative of the most advanced and drug resistant population.

Metastatic neuroblastoma cells were freshly isolated from patients' bone marrow by positive selection of GD_2 expressing cells using an anti-GD_2 monoclonal antibody. PBOX-6 was found to reduce the viability of primary neuroblastoma cells. As with all primary cell culture, there are numerous obstacles to overcome, including the low numbers of patient samples available. Prior to isolation the stage of the tumour was unknown so isolation of every sample was undertaken. In total eighteen samples have been received and isolated since commencement of this work; of these samples, six were positive for metastasis in the bone marrow and two were successfully grown in culture. PBOX-6 was shown to decrease the viability of these primary neuroblastoma cells in a dose dependent manner. As previously discussed primary neuroblastoma cells are not always amenable to culture; cells may die immediately after isolation or may not proliferate. Of the six GD_2 positive samples, two did not grow in culture while two could not be used due to bacterial

contamination. This study is therefore limited by the low number of samples available and as a result there is a need for further samples to validate our initial findings. Although no firm conclusion may be drawn from such a low sample number, this is a positive result and would support further investigation into the use of PBOXs for treatment of neuroblastoma. Due to the difficulty associated with culturing primary neuroblastoma cells, there are few reports in the literature detailing the effects of conventional or novel therapeutic strategies on these cells. One other study which successfully isolated and cultured primary neuroblastoma cells (Bender *et al.*, 2011) and demonstrated an enhancement of doxorubicin induced apoptosis in combination with PI3 kinase inhibitors.

To confirm that apoptosis observed by flow cytometric analysis was truly representative of an apoptotic cell population; western blot analysis of the repair enzyme PARP was carried out. The time-dependency of PARP cleavage correlated with flow cytometric results. After confirming the cells were undergoing apoptosis, the molecular mechanisms by which PBOX-6 enhances the apoptotic effect of other chemotherapeutic drugs in neuroblastoma cells was investigated. Entry into the mitochondrial pathway is controlled by binding of pro-death Bcl-2 proteins to pro-survival Bcl-2 proteins which can inhibit the pro-apoptotic activity of these proteins. Activation of anti-apoptotic members may tip the balance towards survival and contribute to chemoresistance. Therefore expression levels of several of these proteins in SHSY5Y cells was examined to see if they were altered upon treatment.

Bcl-2 has previously been shown to be expressed in a significant percentage of untreated neuroblastoma tumours, with expression correlating with poor prognosis (Dole *et al.*, 1994). Bcl-2 expression was also shown to inhibit chemotherapy induced apoptosis in neuroblastoma; therefore investigation into the effect of PBOX-6 on expression of this anti-apoptotic protein in SHSY5Y cells was undertaken. It was found that PBOX-6 induces a dose-dependent cleavage of Bcl-2 which results in the formation of a Bcl-2 cleavage fragment and the loss of its anti-apoptotic activity. Cleavage of Bcl-2 was previously observed by Nathwani *et al.*, (2010) in HL-60 cells after treatment with PBOX-6, while other MTAs have demonstrated similar activity (Srivastava *et al.*, 1998). Although Bcl-2 is an anti-apoptotic protein it has been reported in the literature that the cleavage product of this protein is pro-apoptotic (Cheng *et al*; Kirsch *et al.*, 1999). Cleavage results in

formation of a pro-apoptotic fragment lacking the N-terminal 34 amino acids of Bcl-2. Kirsch *et al.,* (1999) established that caspase-3 dependent cleavage of Bcl-2 promoted release of Bcl-2. This pro-apoptotic fragment was then shown to localise to the mitochondria and cause the release of cytochrome c. In this present study, these results indicate that PBOX-6 induced cleavage of Bcl-2 may promote apoptosis in a number of ways, by preventing inhibition of pro-apoptotic Bcl-2 proteins such as Bak and by formation of a pro-apoptotic fragment which induces cytochrome c release.

Mcl-1 is a pro-survival Bcl-2 protein which has been implicated to play a role in chemoresistance in a range of cancers. It is widely expressed in a number of tumour cells but expression is poor or completely absent in normal cells. As previously discussed Mcl-1 has been postulated to function as an oncogene in neuroblastoma and may contribute to pathogenesis though prevention of apoptosis. Antagonism of Mcl-1 has been shown to have anti-cancer activity in a number of different malignancies including sarcoma, myeloma, lymphoma and small and non small cell lung cancer (Lestini *et al.*, 2009). More recently a novel small molecule inhibitor of Mcl-1 has been found to block pancreatic cancer growth both *in vitro* and *in vivo* (Abulwerdi *et al.*, 2014). Mcl-1 has recently been postulated to be a critical regulator of apoptosis induced by MTAs. Wertz *et al.,* 2011 treated mouse embryonic fibroblasts (MEFs) with taxol and nocodazole and found that while both drugs induced mitotic arrest, they also decrease expression of Mcl-1. As PBOX-6 is a MTA, it was hypothesised that it may affect expression of Mcl-1 in neuroblastoma cells.

PBOX-6 induced a dose-dependent reduction in Mcl-1 with complete abolition of expression following 72 hour treatment. This is the first report of PBOX-6 alone decreasing the expression of Mcl-1. Previously Greene *et al.,* (2007) found that a combination of PBOX-6 and STI-571 caused a downregulation of Mcl-1 in CML cell lines. Similarly, treatment of CML cells (LAMA84) with a combination of ST1-571 and PBOX-21 was demonstrated to result in a decrease in expression of Mcl-1 (Bright *et al.*, 2008). In contrast to the findings presented herein, both of these previous reports found that PBOX-6 or -21 alone had no effect on Mcl-1 expression, suggesting that the apoptotic pathway by which PBOXs induce cell death may be cell line specific. Our results are in agreement with previous findings which found that PBOX-15 completely abolished Mcl-1

expression in MM cell lines (Maginn *et al*, 2011). This finding is of particular interest as downregulation of Mcl-1 has been shown to be an effective strategy to enhance neuroblastoma cells to Fas- or chemotherapy-induced apoptosis (Ammann *et al.*, 2009).

As levels of Mcl-1 expression were decreased after treatment with PBOX-6, work was then undertaken to identify how this decrease affects other pro-apoptotic members of the Bcl-2 family, namely expression of Bak and Bax. It has been proposed that some Bcl-2 proteins exert their anti-apoptotic function by inhibiting translocation of Bax to the mitochondria where it heterodimerises with Bak to form pores in the mitochondrial membrane (Czabator *et al.*, 2014). When Bcl-2, Bcl-xL and Mcl-1 levels are decreased or inactivated though cleavage or phosphorylation, Bax and Bak are free to heterodimerise allowing for the release of cytochrome c and consequent activation of caspases (Youle *et al.*, 2008). An increase in Bak expression was noted up to 72 hours post treatment with PBOX-6 while no increase in Bax was observed. One proposed mechanism of Bcl-2 function is inhibition of Bax translocation from the cytosol to the mitochondria, but treatment with PBOXs has previously been shown to occur through an alternative mechanism. McGee *et al.,* (2004) found that although PBOX-6 induced phosphorylation and inactivation of several anti-apoptotic proteins in CML cells, Bax expression was not affected. Additionally subcellular localisation studies showed that Bax expression was neither altered in the mitochondrial or cytosolic fractions. Other studies have shown that while Bcl-2, Bcl-xL and Mcl-1 expression may decrease after drug treatment Bax expression may not be effected. For example bortezomib treatment of neuroblastoma cells caused a decrease in Bcl-2 expression while levels of Bax were unaltered. (Combaret *et al.*, 2008).

Interestingly a time- and dose-dependent increase in Bak expression was observed upon treatment with PBOX-6. In contrast to the previous findings with Bax, it was shown that a decrease in Mcl-1 expression correlated with a simultaneous increase in Bak expression. This is the first report in the literature describing the effect of PBOX-6 treatment on expression of Bak. It has previously been shown that in healthy cells Bak is sequestered by Mcl-1 and not Bcl-2 (Willis *et al.*, 2005). It is only when BH3 only proteins such as Noxa are activated, the cell receives a cytotoxic signal, and they can engage with Mcl-1 and displace Bak from this complex allowing it to induce cell death. Release of Bak from this

complex precedes degradation of Mcl-1 by ubiquitination. Recently Bender *et al.*, (2011) investigated the effect of PI3K inhibitors on neuroblastoma cells, and found that cells become primed for chemotherapy induced apoptosis by shifting the balance from anti-apoptotic Bcl-2 proteins to pro-apoptotic members. In SH-EP neuroblastoma cells treated with a combination of doxorubicin and a PI3K inhibitor (LY294002), expression of Mcl-1 was decreased with a corresponding increase in Bak. In this study, it was hypothesised that a PBOX-6 induced reduction of Mcl-1 correlates with an increase in Bak expression in SHSY5Y cells due to release of Bak from the Mcl-1 complex. The shift in the ratio of these proteins initiates a conformational change in Bak (as demonstrated by western blot analysis of the conformationally active form of Bak), allowing for formation of pores in the mitochondrial membrane and release of pro-apoptotic proteins such as cytochrome c. Additional studies are warranted to further explore the events downstream of Bak activation, such as release of cytochrome c and activation of various initiator and effector caspases.

In conclusion this study has shown for the first time the anti-cancer effects of POX-6 and -15 family on neuroblastoma cells, demonstrating the ability of PBOX-6 to reduce the viability of neuroblastoma cells *in vitro* and in *ex vivo* neuroblastoma patient samples; induction of apoptosis while delineating part of the mechanism through which this occurs. This work supports the use of these novel compounds as a potential treatment for neuroblastoma.

Chapter 4

PBOX-6 synergistically enhances the anti-cancer effects of carboplatin, etoposide and doxorubicin in neuroblastoma cell lines

Chapter 4

4.1 Introduction

Drug design has evolved from a trial and error approach involving a large scale screening process of multiple natural and synthetic compounds to a targeted approach termed 'rational drug design' in which a specific cellular target is identified (Mavromoustakos *et al.*, 2011). A drug is generally synthesised to activate or inhibit the chosen target or cellular process to produce the required effect such as induction of cell death (Temirak *et al.*, 2012). Although this approach is more logical, efficient and cost effective it, due to the heterogeneous nature of cancer, a single target approach does not always achieve the desired effects therefore combining multiple drugs, each designed to target a specific cellular pathway is deemed to be the most therapeutically effective strategy (Kapse-Mistry *et al.*, 2014).

Since first pioneered in the 1950s as a novel therapeutic strategy for acute lymphoblastic leukaemia (ALL), combination chemotherapy has since been established as more effective than single agent therapy in multiple cancers. Combination chemotherapy is based on the idea that the use of multiple cytotoxic drugs may result in an increased therapeutic benefit, when compared to single agent therapy. The key principles of combination therapy are to firstly use drugs with non-overlapping toxicities, if necessary; the maximal doses of each drug may be used and secondly to use drugs with different mechanisms of actions so multiple cellular pathways can be targeted simultaneously, and finally to use drugs which have been previously shown to be effective when used alone (Mayer *et al.*, 2007).

This multimodal approach has a number of advantages; firstly combination chemotherapy offers the benefit of targeting multiple cellular pathways that induce apoptosis, and has proven in other paediatric cancers to be efficacious leading to higher rates of long term survival (Matthay *et al.*, 2012). For example, vincristine will target the microtubule network, while etoposide will target DNA replication. In addition, a combination of two drugs may reduce the possibility of the malignant cell developing resistance to each drug, while also reducing the chance of mutated cells evolving within the tumour. Combinations of drugs which will synergise may help to decrease the development of resistance, while maximising the anti-tumour effects on the cell (Furfaro *et al.*, 2014).

The aim of chemotherapy is to eliminate all traces of cancer from the body before the malignant cells may potentially evolve into resistant cells. Tumours may develop resistance through intrinsic mechanisms or by exposure to sub lethal concentrations of a given drug. Conventional chemotherapy can often target DNA, triggering events in the cell such as activation of p53, cell cycle arrest and apoptosis. Frequently in advanced tumours such as late stage neuroblastoma these pathways are defective, for example p53 may be mutated or deleted leading to ineffective induction of cell death by chemotherapeutics (Maris *et al.*, 2010). Similarly amplification of the transcription factor MYCN, may lead to suppression of apoptosis and promotion of cell proliferation and survival (Gogolin *et al.*, 2010). Lone chemotherapeutic drugs may provide insufficient toxicity to overcome these pro-survival mechanisms and cells may develop multidrug resistance.

Members of the PBOX family have previously been shown to work in combination with other drugs to synergistically enhance apoptosis. These include flavopiridol, a pan Cdk inhibitor and imatinib, a receptor tyrosine kinase inhibitor. Co-treatment of CML cells with PBOX-21 and STI571 was shown to induce more apoptosis than either drug alone in parental (K562S and LAMA84) CML and STI571-resistant CML cells lines (K562R) (Bright *et al.*, 2010). The Bcr-Abl translocation present in approximately 95% of CML patients has been identified as having a central role in CML pathology. This potentiation of apoptosis was specific to Bcr-Abl-positive leukaemia cells with no effect observed on Bcr-Abl-negative HL-60 acute myeloid leukaemia cells. Bright *et al.,* (2010) showed that combination therapy of the PBOX compounds and flavopiridol induced a sequence dependent, synergistic enhancement of apoptosis in the imatinib-resistant T315I mutant CML cells. A phase 1 clinical trial investigating the therapeutic potential of flavopiridol in neuroblastoma has recently been completed (ClinicalTrials.gov NCT00012181), while flavopiridol has also been reported to synergistically enhance the effects of HDAC inhibitors such virinostat, in MDR neuroblastoma cell lines with p53 loss of function (LOF). Huang *et al.,* (2010) found that a combination of vorinostat and flavopiridol was synergistic and significantly more cytotoxic in cell lines with p53-LOF, and in the clones stably transfected with dominant-negative p53 plasmids. These results support the

hypothesis that PBOX-6 and -15 have the potential to work in combination with other chemotherapeutics to enhance apoptosis in neuroblastoma cells.

In the case of many chemotherapeutic drugs, the mechanism through which individual drugs work has been extensively studied, while investigation into the means through which drugs work in combination has not been as thorough. Therefore, in this chapter, a study to identify any potential synergistic combinations between the PBOXs and current chemotherapeutic drugs, and examination into the molecular mechanisms through which these drugs work, was undertaken.

4.2 Results

4.2.1 PBOX-15 works in combination with other chemotherapeutics to reduce the viability of SHSY5Y cells.

The alamarBlue assay was employed to identify potential synergies between the novel microtubule targeting drugs, the PBOXs, and other chemotherapeutic drugs currently used in the clinic to treat neuroblastoma. An enhanced decrease in cell viability may point to the potential additive or synergistic interactions between two drugs. SHSY5Y cells were treated for 72 hrs with varying concentrations of either PBOX-15, carboplatin or a combination of the two. As shown in Fig 4.1 an enhanced decrease in viability was observed in the cells treated with the combination in comparison to either drug treatment alone. Cell viability decreased from 85% with PBOX-15 or 62% with carboplatin alone to 19% for a combination of the two. This indicated that PPBOX-15 may potentially work in combination with other chemotherapeutic drugs to produce additive or synergistic effects although further studies using flow cytometry were required to confirm this.

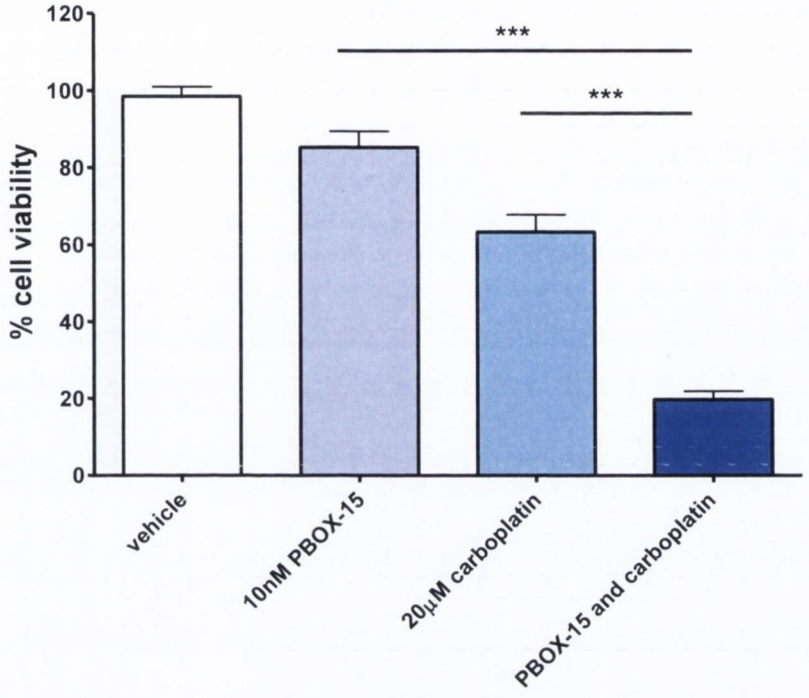

Figure 4.1 Combination of PBOX-15 and carboplatin enhanced the observed decrease in cell viability in SH5Y5Y cells.

SHSY5Y cells were seeded at 2.5x 10^5 cells per ml in 96 well plates and left for 24hrs to attach. Cells were treated with a vehicle (1% (v/v) ethanol), 10 nM PBOX-15, 20 μM carboplatin or a combination of both. After 72 hours cells were harvested and 20 μl alamarBlue was added to each well. Plates were incubated in the dark for up to 5 hours until a colour change was observed. Fluorescence was measured using a SpectraMax Gemini plate reader at excitation and emission wavelengths of 544 nm and 590 nm respectively. Values represent the mean ± S.E.M of three independent experiments. Statistical analysis was performed using one way ANOVA with Tukey's multiple comparison test. *** $p<0.001$.

4.2.2 The effect of PBOX-6 and -15 in combination with a number of current chemotherapeutics used to treat neuroblastoma.

Regardless of stage, all neuroblastoma patients that receive chemotherapy are treated by combination therapy. This indicated the potential for the novel microtubule targeting drugs, the PBOXs, to be used in combination with several chemotherapeutic drugs which are currently used in the clinic. It was proposed that the PBOXs may work in combination with doxorubicin, etoposide and carboplatin and may synergistically increase the apoptotic effects of these drugs on neuroblastoma cells. The percentage of apoptosis induced by these drugs alone and in combination was assessed by flow cytometric analysis of the sub G1/G0 peak of propidium iodide stained cells. SHSY5Y cells were initially treated for 48 hours with varying concentrations of PBOX-6, PBOX-15, etoposide, doxorubicin and carboplatin alone and in combination.

Findings from the viability assays indicated that PBOX-15 had the potential to synergise with carboplatin and possibly other cytotoxic drugs. A concentration of 0.5 μM PBOX-15 was chosen for further investigation as it induced an intermediate level of apoptosis in SHSY5Y cells (Fig. 3.12). Cells were then treated with 0.5 μM PBOX-15 or a range of concentrations of carboplatin (10, 20 and 50 μM) alone and in combination (Fig. 4.3). Apoptosis was significantly enhanced in cells treated with combinations of both drugs. Apoptosis increased from 12% with PBOX-15 alone to 18%, 26% and 28% in combination with 10 μM, 20 μM and 50 μM carboplatin respectively. CI values for each combination were identified using Calcusyn and all three combinations were shown to be synergistic with the 0.5 μM PBOX-15/20 μM carboplatin showing the highest degree of synergism (Table 4.1).

Given that PBOX-15 synergised with carboplatin it was hypothesised that PBOX-6 may also have additive or synergistic effects on this and potentially other chemotherapeutics. A concentration of 5 μM PBOX-6 was chosen as it was shown to induce an intermediate level of apoptosis in SHSY5Y cells 48 hours post treatment (Fig. 3.12). Cells that were treated for 48 hours with 5 μM PBOX-6 alone induced approximately 7% apoptosis, this increased to 21% in combination with 10 μM carboplatin, 27% with 20 μM carboplatin and 28% with 50 μM carboplatin (Fig. 4.2). Apoptosis was also induced by carboplatin

alone (8%, 11% and 17% for 10 μM, 20 μM and 50 μM respectively). In comparison to single treatments, combinations gave greater than additive effects. A CI value was determined for each combination using Calcusyn. Co-treatment with 5 μM PBOX-6 and 10 μM carboplatin gave a CI value which indicated a strong synergism. Likewise, a combination of 5 μM PBOX-6 and 20 μM carboplatin was shown to be strongly synergistic while co-treatment with 50μM carboplatin was determined to be synergistic (Table 4.2). Statistical analysis was performed using one way ANOVA with Tukey's multiple comparison test. All P values obtained were less than 0.05 indicating that results were statistically significant.

Although both drugs induced similar levels of apoptosis, a lower CI value was obtained with the PBOX-6/carboplatin combination than the PBOX-15/carboplatin combination. Therefore it was decided to continue to investigate this drug in combination with doxorubicin and etoposide, two other chemotherapeutics which are used to treat neuroblastoma. Apoptosis was significantly increased in cells treated with PBOX-6 and etoposide in comparison to treatment with each drug alone. Levels of apoptosis increased from 5% with 1 μM etoposide alone to 23% when treated with 5 μM PBOX-6. Similarly an enhancement of apoptosis was observed in cells treated with 2.5 μM and 10 μM etoposide in combination with PBOX-6 (Fig. 4.4). Analysis by Calcusyn confirmed that PBOX-6 was synergistically augmenting the apoptotic effects of etoposide (Table 4.3). Statistical analysis was performed using one way ANOVA with Tukey's multiple comparison test. All P values obtained were less than 0.05 indicating that results were significant.

Further synergies between doxorubicin and PBOX-6 were investigated. Initially cells were treated with 5μM PBOX-6 and varying concentrations of doxorubicin (0.5 μM, 1 μM and 5 μM). To confirm synergy, combinations must be deemed to be statistically significant. Analysis by calcusyn found all three of these combinations were shown to be synergistic; although following statistical analysis (one way ANOVA followed by students t test) one of these combinations (5 μM PBOX-6 and 1 μM doxorubicin) was not deemed to be statistically significant, therefore it was decided that concentrations of PBOX-6 would be varied. Three concentrations of PBOX-6 (1 μM, 2.5 μM and 5 μM) were used alone and in combination with 5 μM doxorubicin (Fig. 4.5). All three combinations were shown to be

synergistic but the synergism was not as strong when compared with other combinations tested previously (Table 4.4).

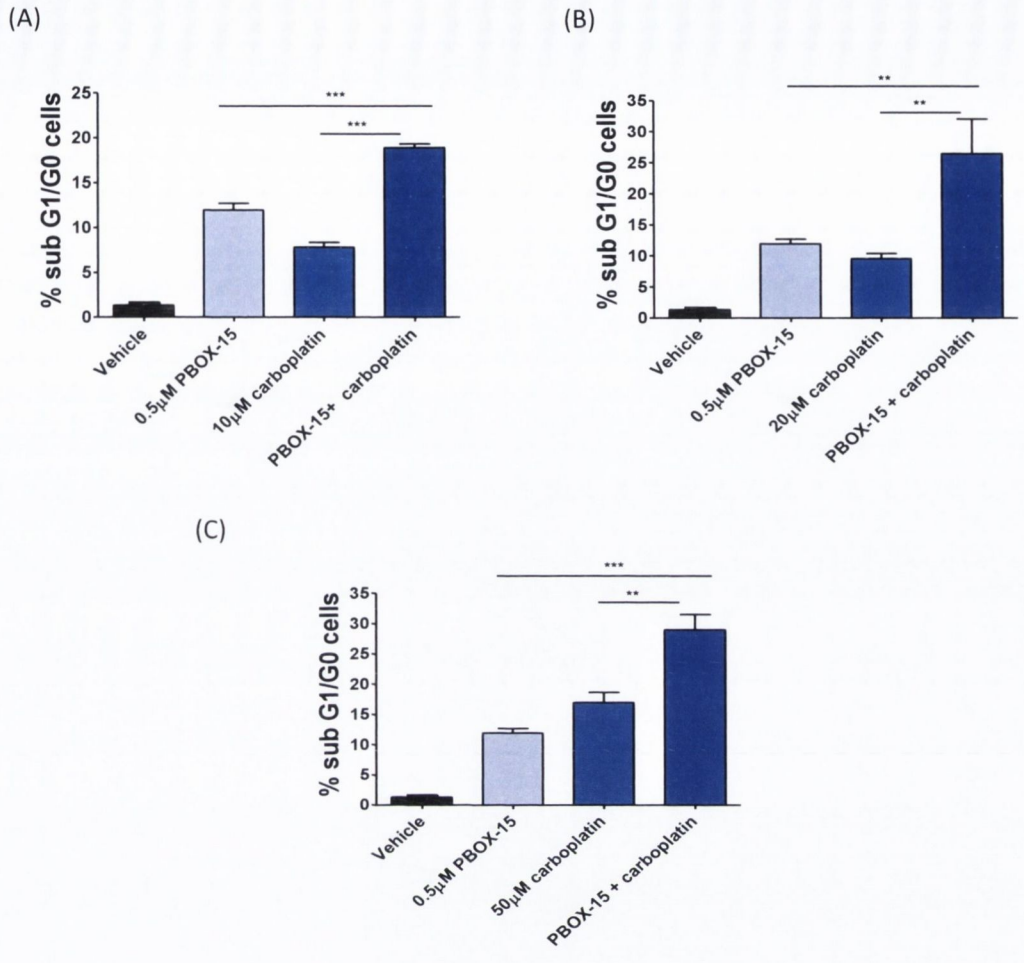

Figure 4.2 PBOX-15 enhances the apoptotic effects of carboplatin in SHSY5Y cells.

SHSY5Y cells were seeded at a density of 1.0 x 10^5 cells/ml in 6 well plates and left for 24hrs to attach. Cells were treated with a vehicle (1% (v/v) ethanol), 0.5μM PBOX-15, 10μM or a combination of both, (B) 0.5μM PBOX-15, 20μM or a combination of both or (C) 0.5μM PBOX-15, 50μM carboplatin or a combination of both. After 48 hrs cells were harvested, resuspended in 200μL PBS, fixed in 2mls ethanol and stained with propidium iodide. Cells were analysed by flow cytometry and the percentage of apoptotic cells was determined by quantification of the sub G/G0 peak. Values represent the mean ± S.E.M of at least three independent experiments. Statistical analysis was performed using one way ANOVA with Tukey's multiple comparison test. *** $p<0.001$, ** $p<0.01$.

PBOX-15	Carboplatin	% sub G1/GO cells	CI value	Rating
0.5	10	18.91	0.618	++
0.5	20	26.44	0.477	+++
0.5	50	28.97	0.569	+++

Table 4.1 CI values of PBOX-15 in combination with carboplatin in SHSY5Y cells.

Data from flow cytometry experiments was used to analyse the interactions between PBOX-15 and carboplatin using the isobologram method described by Chou and Talalay. The degree of synergism between PBOX-15 and carboplatin was determined by using combination index (CI) analysis at a non-constant ratio, i.e., drug combinations were made by varying the concentrations of one drug (carboplatin) while keeping the second drug (PBOX-15) concentration fixed. An average CI < 1 indicates synergism, >1 indicates antagonism and an average CI of 1 indicates additivity. CI values for each drug combination were calculated using Calcusyn software (Biosoft, U.K).

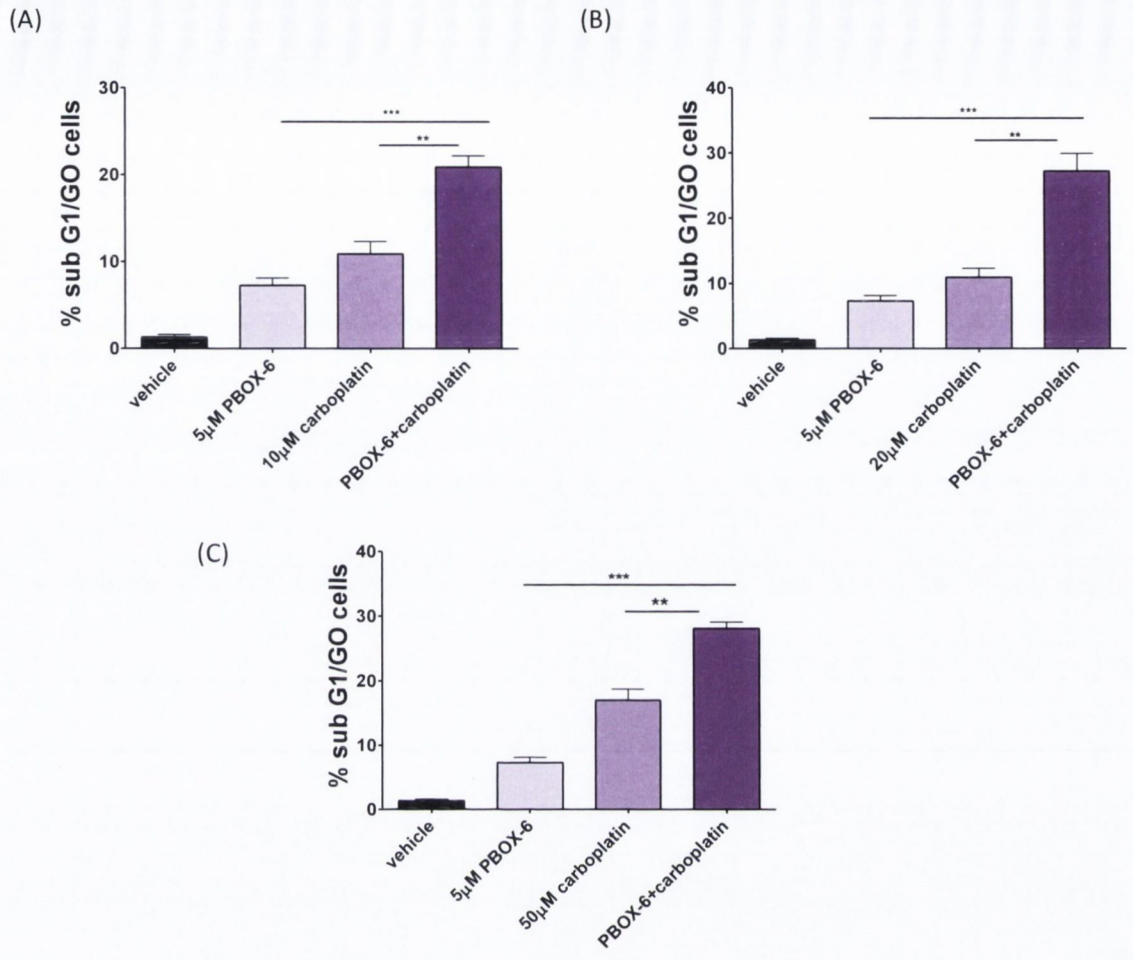

Figure 4.3 PBOX-6 enhances the apoptotic effects of carboplatin in SHSY5Y cells.

SHSY5Y cells were seeded at a density of 1.0 x 10^5 cells/ml in 6 well plates and left for 24 hours to attach. Cells were treated with a vehicle (1% (v/v) ethanol), (A) 5 μM PBOX-6, 10 μM carboplatin or a combination of both, (B) 5 μM PBOX-6, 20 μM carboplatin or a combination or (C) 5 μM PBOX-6, 50 μM carboplatin or a combination of both. After 48 hours cells were harvested, resuspended in 200μL PBS, fixed in 2mls ethanol and stained with propidium iodide. Cells were analysed by flow cytometry and the percentage of apoptotic cells was determined by quantification of the sub G1/G0 peak. Values represent the mean ± S.E.M of at least three independent experiments. Statistical analysis was performed using one way ANOVA with Tukey's multiple comparison test. *** $p<0.001$, ** $p<0.01$.

PBOX-6	Carboplatin	% sub G1/GO cells	CI value	Rating
5	10	20.88	0.299	++++
5	20	27.22	0.249	++++
5	50	28.08	0.430	+++

Table 4.2 CI values of PBOX-6 in combination with carboplatin in SHSY5Y cells.

Data from flow cytometry experiments was used to analyse the interactions between PBOX-6 and carboplatin using the isobologram method described by Chou and Talalay. The degree of synergism between PBOX-6 and carboplatin was determined by using combination index (CI) analysis at a non-constant ratio, i.e., drug combinations were made by varying the concentrations of one drug (carboplatin) while keeping the second drug (PBOX-6) concentration fixed. An average CI < 1 indicates synergism, >1 indicates antagonism and an average CI of 1 indicates additivity. CI values for each drug combination were calculated using Calcusyn software (Biosoft, U.K).

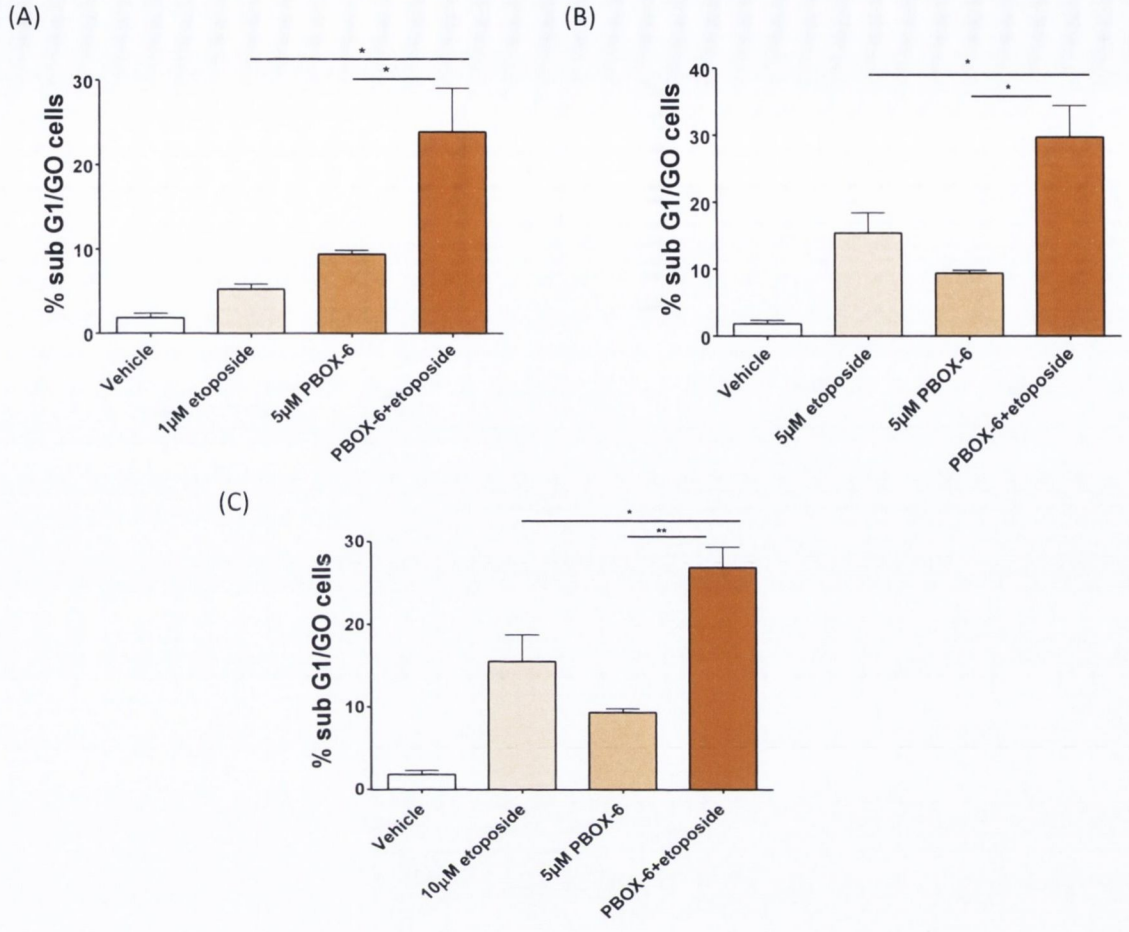

Figure 4.4 PBOX-6 enhances the apoptotic effects of etoposide in SHSY5Y cells.

SHSY5Y cells were seeded at a density of 1.0 x 10^5 cells/ml in 6 well plates and left for 24 hours to attach. Cells were treated with a vehicle (1% (v/v) ethanol), (A) 5 μM PBOX-6, 1 μM etoposide or a combination of both, (B) 5 μM PBOX-6, 5 μM etoposide or a combination or (C) 5 μM PBOX-6, 10 μM etoposide or a combination of both. After 48 hours cells were harvested, resuspended in 200 μL PBS, fixed in 2 mls ethanol and stained with propidium iodide. Cells were analysed by flow cytometry and the percentage of apoptotic cells was determined by quantification of the sub G1/G0 peak. Values represent the mean ± S.E.M of at least three independent experiments. Statistical analysis was performed using one way ANOVA with Tukey's multiple comparison test. ** $p<0.01$, * $p<0.05$.

PBOX-6	Etoposide	% sub G1/GO cells	CI value	Rating
5	1	23.8	0.194	+++++
5	5	29.7	0.281	++++
5	10	26.9	0.590	+++

Table 4.3 CI values of PBOX-6 in combination with etoposide in SHSY5Y cells.

Data from flow cytometry experiments was used to analyse the interactions between PBOX-6 and etoposide using the isobologram method described by Chou and Talalay. The degree of synergism between PBOX-6 and etoposide was determined by using combination index (CI) analysis at a non-constant ratio, i.e., drug combinations were made by varying the concentrations of one drug (etoposide) while keeping the second drug (PBOX-6) concentration fixed. An average CI < 1 indicates synergism, >1 indicates antagonism and an average CI of 1 indicates additivity. CI values for each drug combination were calculated using Calcusyn software (Biosoft, U.K).

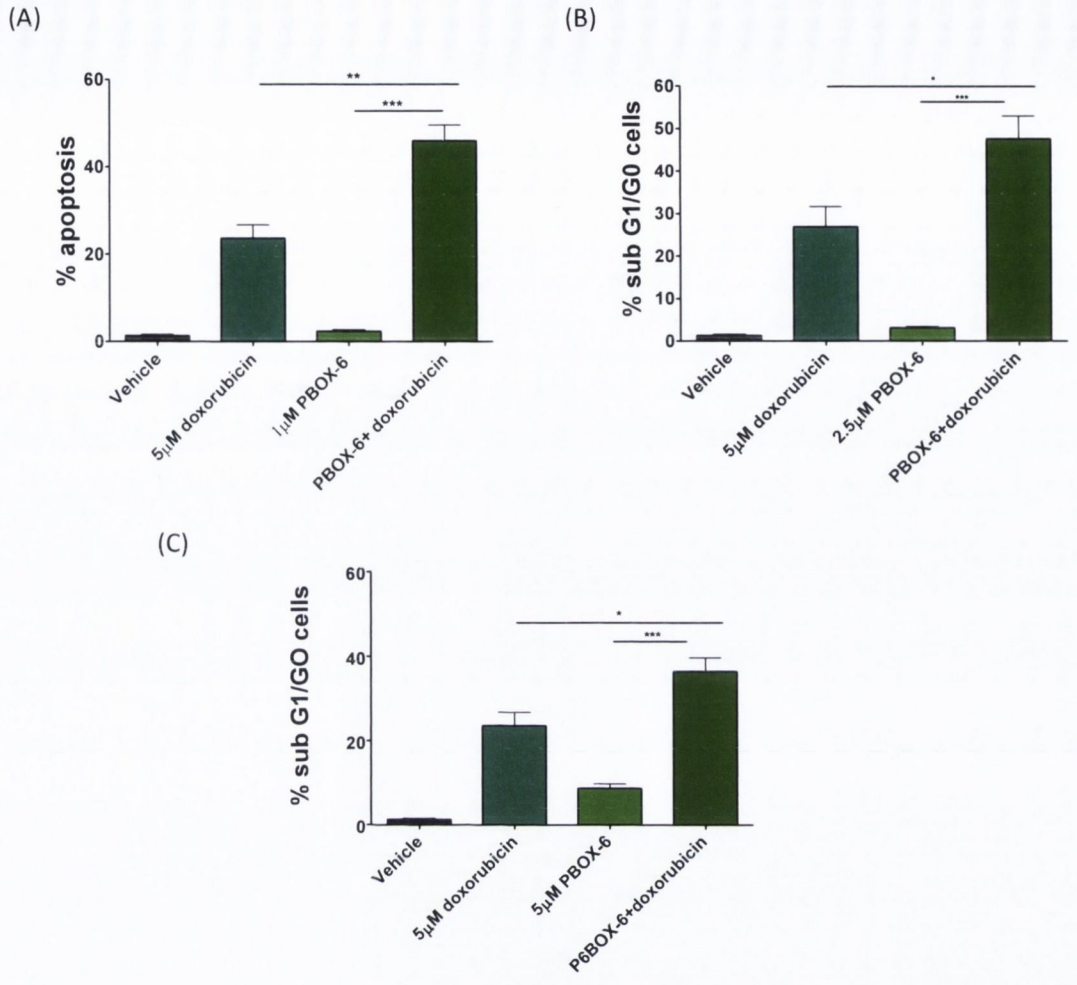

Figure 4.5 PBOX-6 enhances the apoptotic effects of doxorubicin in SHSY5Y cells.

SHSY5Y cells were seeded at a density of 1.0 x 10^5 cells/ml in 6 well plates and left for 24 hours to attach. Cells were treated with a vehicle (1% (v/v) ethanol), (A) 1 μM PBOX-6, 5 μM doxorubicin or a combination of both, (B) 2.5 μM PBOX-6, 5 μM doxorubicin or a combination of both or (C) 5 μM PBOX-6 or 5 μM doxorubicin or a combination of both. After 48 hours cells were harvested, resuspended in 200 μL PBS, fixed in 2 mls ethanol and stained with propidium iodide. Cells were analysed by flow cytometry and the percentage of apoptotic cells was determined by quantification of the sub G1/GO peak. Values represent the mean ± S.E.M of at least three independent experiments. Statistical analysis was performed using one way ANOVA with Tukey's multiple comparison test. *** $p<0.001$, ** $p<0.01$, *$p<0.05$.

PBOX-6	Doxorubicin	% sub G1/GO cells	CI value	Rating
1	5	45.99	0.398	+++
2.5	5	47.54	0.380	+++
5	5	36.49	0.700	++

Table 4.4 CI values of PBOX-6 in combination with doxorubicin in SHSY5Y cells.

Data from flow cytometry experiments was used to analyse the interactions between PBOX-6 and doxorubicin using the isobologram method described by Chou and Talalay. The degree of synergism between PBOX-6 and doxorubicin was determined by using combination index (CI) analysis at a non-constant ratio, i.e., drug combinations were made by varying the concentrations of one drug (PBOX-6) while keeping the second drug (doxorubicin) concentration fixed. An average CI < 1 indicates synergism, >1 indicates antagonism and an average CI of 1 indicates additivity. CI values for each drug combination were calculated using Calcusyn software (Biosoft, U.K).

4.2.3 PBOX-6 synergistically increases the apoptotic effect of carboplatin 72hrs hours post treatment in drug sensitive and multidrug resistant neuroblastoma cell lines.

Upon completion of the 48 hour combination studies it was decided to expand the combination studies to a 72 hour time point to establish if the synergism observed could be maintained or enhanced at this later time. Carboplatin was chosen as the representative chemotherapeutic as both PBOX-6 and 15 was shown to synergise with this drug and these combinations demonstrated the strongest synergism. Although PBOX-6 was shown to synergise with doxorubicin when treated at varying concentrations, these combinations proved to be less synergistic than carboplatin. While good CI values were obtained with etoposide it was deemed that these concentrations were high in comparison to carboplatin. A concentration of 10 μM etoposide which induced just 15% apoptosis alone is almost twenty times higher than the IC_{50} value for this drug in SHSY5Y cells. In contrast similar levels of apoptosis (8-17%) were induced with various concentrations of carboplatin in a range of its IC_{50} value in this cell line. Consequently it was decided to continue with the PBOX-6/carboplatin combination and investigate their effects on SHSY5Y cells 72 hours post treatment. SHSY5Y cells were treated with the same concentrations of PBOX-6 and carboplatin alone and in combination for 72 hours. Analysis by calcusyn confirmed that PBOX-6 synergistically increased the apoptotic effects of carboplatin 72 hours post treatment (Fig. 4.6). Statistical analysis was performed using one way ANOVA with Tukey's multiple comparison test. All p values obtained were less than 0.05 indicating that results were significant. CI values for each combination was less than 0.5 indicating synergism (Table 4.5).

The CHLA-90 cell line derived from an 8½ year old stage 4 post therapy and bone marrow transplantation neuroblastoma patient is p53 mutated, MYCN amplified and overexpresses the MDR protein, P-gp and has been shown to be resistant to multiple chemotherapeutics which are currently used in the treatment of neuroblastoma such as carboplatin, doxorubicin and etoposide (Huang *et al.*, 2010). This cell line was chosen as a representative MDR cell line to test the lead PBOX-6/carboplatin combination. SHSY5Y cells were treated with 5μM PBOX-6 and 10/20/50μM carboplatin alone and in combination for 48 (Fig.4.7) and 72 hours (Fig. 4.8). Analysis by calcusyn confirmed that that PBOX-6 synergistically increased the apoptotic effects of carboplatin at both time

points (Table 4.6). Statistical analysis was performed using one way ANOVA with Tukey's multiple comparison test. All p values obtained were less than 0.05 indicating that results were significant. CI values for each combination was less than 0.8 indicating synergism (Table 4.7).

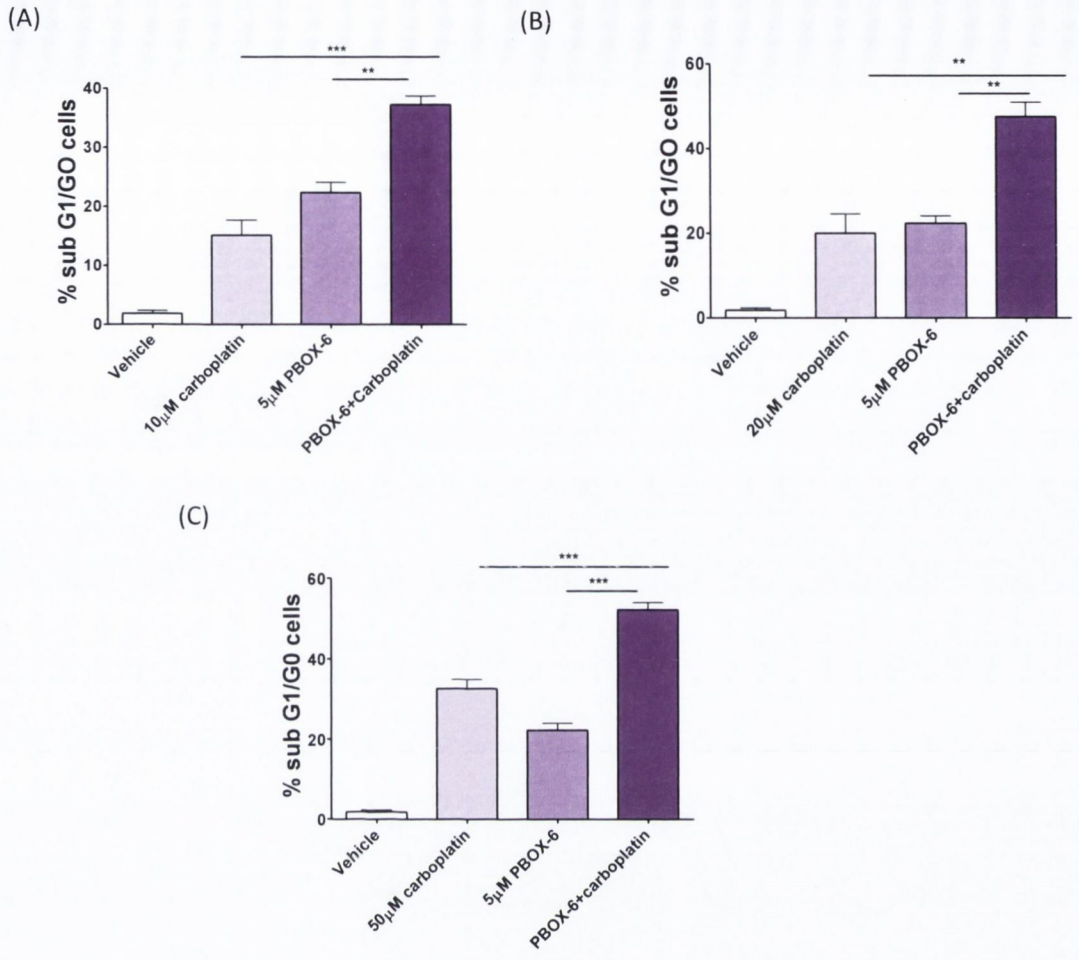

Figure 4.6 PBOX-6 enhances the apoptotic effects of carboplatin in SHSY5Y cells 72hrs post treatment.

SHSY5Y cells were seeded at a density of 1.0 x 10^5 cells/ml in 6 well plates and left for 24 hours to attach. Cells were treated with vehicle (1% (v/v) ethanol), (A) 5 μM PBOX-6, 10 μM carboplatin or a combination of both, (B) 5 μM PBOX-6, 20 μM carboplatin or a combination or (C) 5 μM PBOX-6, 50 μM carboplatin or a combination of both. After 72 hours cells were harvested, resuspended in 200 μL PBS, fixed in 2 mls ethanol and stained with propidium iodide. Cells were analysed by flow cytometry and the percentage of apoptotic cells was determined by quantification of the sub G1/G0 peak. Values represent the mean ± S.E.M of at least three independent experiments. Statistical analysis was performed using one way ANOVA with Tukey's multiple comparison test. *** $p<0.001$, ** $p<0.01$, *$p<0.05$.

PBOX-6	Carboplatin	% sub G1/GO cells	CI value	Rating
5	10	37	0.440	+++
5	20	47	0.359	+++
5	50	53	0.450	+++

Table 4.5 CI values of PBOX-6 in combination with carboplatin in SHSY5Y cells.

Data from flow cytometry experiments was used to analyse the interactions between PBOX-6 and carboplatin using the isobologram method described by Chou and Talalay. The degree of synergism between PBOX-6 and carboplatin was determined by using combination index (CI) analysis at a non-constant ratio, i.e., drug combinations were made by varying the concentrations of one drug (carboplatin) while keeping the second drug (PBOX-6) concentration fixed. An average CI < 1 indicates synergism, >1 indicates antagonism and an average CI of 1 indicates additivity. CI values for each drug combination were calculated using Calcusyn software (Biosoft, U.K).

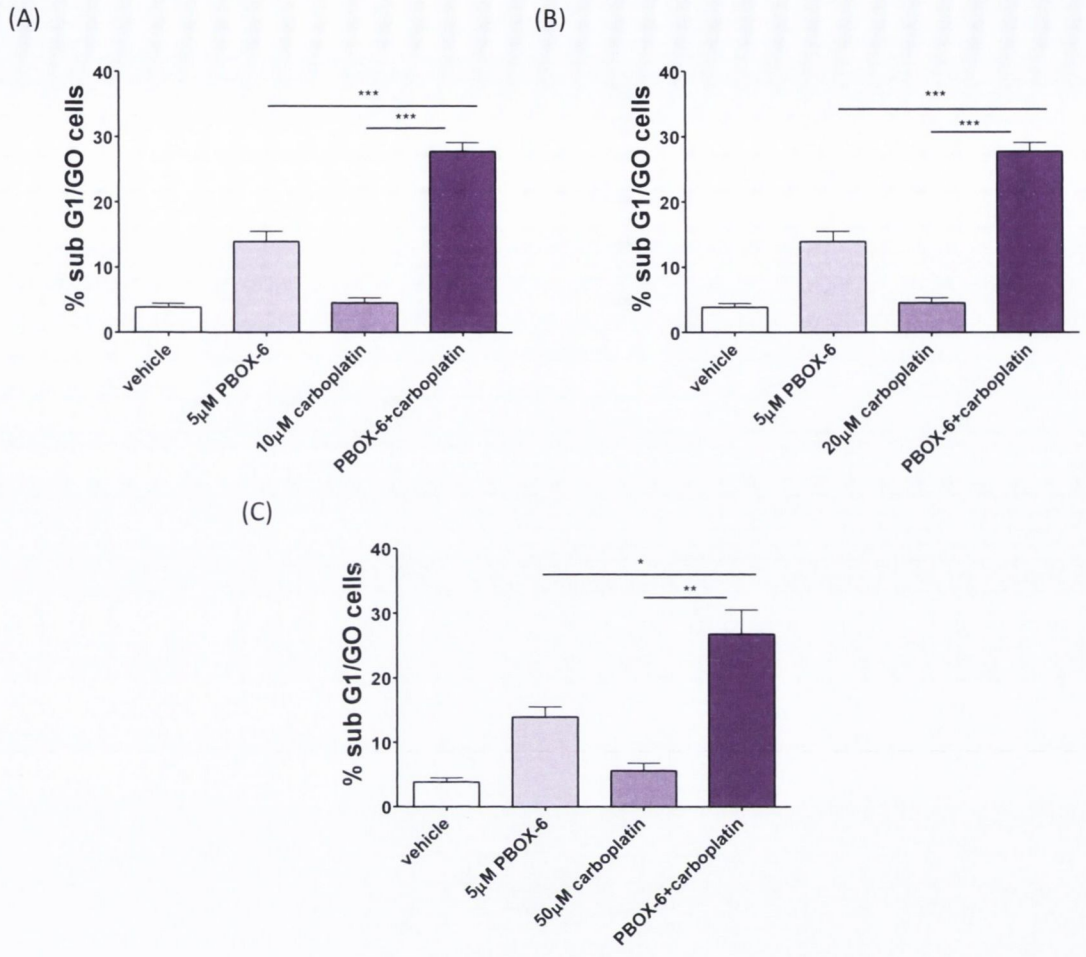

Figure 4.7 PBOX-6 enhances the apoptotic effects of carboplatin in CHLA-90 cells 48hrs post treatment.

CHLA-90 cells were seeded at a density of 1.0 x 10^5 cells/ml in 6 well plates and left for 24 hours to attach. Cells were treated with vehicle (1% (v/v) ethanol), (A) 5 μM PBOX-6, 10 μM carboplatin or a combination of both, (B) 5 μM PBOX-6, 20 μM carboplatin or a combination or (C) 5 μM PBOX-6, 50 μM carboplatin or a combination of both. After 48 hours cells were harvested, resuspended in 200 μL PBS, fixed in 2 mls ethanol and stained with propidium iodide. Cells were analysed by flow cytometry and the percentage of apoptotic cells was determined by quantification of the sub G1/G0 peaks. Values represent the mean ± S.E.M of at least three independent experiments. Statistical analysis was performed using one way ANOVA with Tukey's multiple comparison test. *** $p<0.001$, ** $p<0.01$, * $p<0.05$.

PBOX-6	Carboplatin	% sub G1/G0 cells	CI value	Rating
5	10	23.71	0.727	++
5	20	27.74	0.644	+++
5	50	27.47	0.657	+++

Table 4.6 CI values of PBOX-6 in combination with carboplatin in CHLA-90 cells.

Data from flow cytometry experiments was used to analyse the interactions between PBOX-6 and carboplatin using the isobologram method described by Chou and Talalay. The degree of synergism between PBOX-6 and carboplatin was determined by using combination index (CI) analysis at a non-constant ratio, i.e., drug combinations were made by varying the concentrations of one drug (carboplatin) while keeping the second drug (PBOX-6) concentration fixed. An average CI < 1 indicates synergism, >1 indicates antagonism and an average CI of 1 indicates additivity. CI values for each drug combination were calculated using Calcusyn software (Biosoft, U.K).

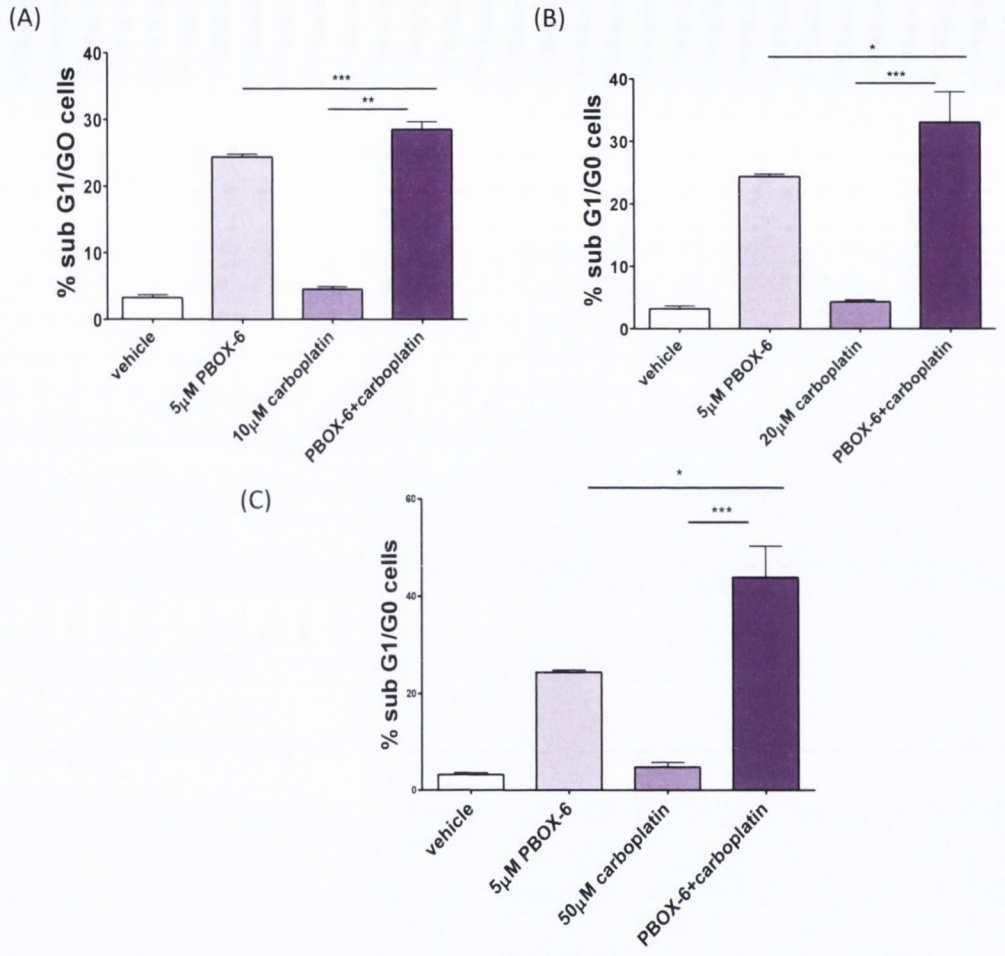

Figure 4.8 PBOX-6 enhances the apoptotic effects of carboplatin in CHLA-90 cells 72hrs post treatment.

CHLA-90 cells were seeded at a density of 1.0 x 10^5 cells/ml in 6 well plates and left for 24 hours to attach. Cells were treated with vehicle (1% (v/v) ethanol), (A) 5 μM PBOX-6, 10 μM carboplatin or a combination of both, (B) 5 μM PBOX-6, 20 μM carboplatin or a combination or (C) 5 μM PBOX-6, 50 μM carboplatin or a combination of both. After 72 hours cells were harvested, resuspended in 200 μL PBS, fixed in 2 mls ethanol and stained with propidium iodide. Cells were analysed by flow cytometry and the percentage of apoptotic cells was determined by quantification of the sub G1/G0 peak. Values represent the mean ± S.E.M of at least three independent experiments. Statistical analysis was performed using one way ANOVA with Tukey's multiple comparison test. *** $p<0.001$, ** $p<0.01$, *$p<0.05$.

PBOX-6	Carboplatin	% sub G1/G0 cells	CI value	Rating
5	10	28.50	0.771	++
5	20	32.90	0.642	+++
5	50	43.40	0.431	+++

Table 4.7 CI values of PBOX-6 in combination with carboplatin in MDR CHLA-90 cells.

Data from flow cytometry experiments was used to analyse the interactions between PBOX-6 and carboplatin using the isobologram method described by Chou and Talalay. The degree of synergism between PBOX-6 and carboplatin was determined by using combination index (CI) analysis at a non-constant ratio, i.e., drug combinations were made by varying the concentrations of one drug (carboplatin) while keeping the second drug (PBOX-6) concentration fixed. An average CI < 1 indicates synergism, >1 indicates antagonism and an average CI of 1 indicates additivity. CI values for each drug combination were calculated using Calcusyn software (Biosoft, U.K).

4.2.4 A combination of PBOX-6 and carboplatin enhances PARP cleavage in SHSY5Y cells.

In chapter 3, PBOX-6 was shown to induce cleavage of the DNA repair enzyme PARP, a hallmark of apoptosis. Having observed an enhancement of PBOX-6 mediated apoptosis in combination with carboplatin, it was next sought to establish the effects of these combinations on PARP. PARP was found to be cleaved in SHSY5Y cells after treatment with PBOX-6, carboplatin or a combination of the two after 48 hours (Fig. 4.9). The full length form was observed in the vehicle controls at both time points. Some cleavage is observed in single doses of each drug although residual full length bands are prominent in each of these lanes. The 89 kDa cleaved band increased in each of the three combinations with decreasing full length bands indicating a greater proportion of apoptotic cells while the full length band becomes increasingly faint. This was consistent with flow cytometric analysis demonstrating a potentiation of apoptosis.

One PBOX-6 and carboplatin combination was chosen as the lead combination to further investigate the molecular events associated with the enhancement of cell death. 10 μM carboplatin was chosen as the representative dose as it was decided to use the least toxic dose which induced an intermediate level of apoptosis alone, while in the combination with PBOX-6 at both 48 and 72 hours was shown to be highly synergistic. The effect of these drugs alone and in combination on PARP cleavage was determined. Comparable to Fig. 4.9, some cleavage is observed in single doses of each drug although residual full length bands were clearly observed, while the 89kDa cleavage band was shown to increase with the combination indicating an increase in the apoptotic cell population (Fig. 4.10). Similar results were observed after a 72 hour treatment, although the proform was entirely absent in the combination treated cells indicating an even greater enhancement of apoptosis (Fig. 4.10).

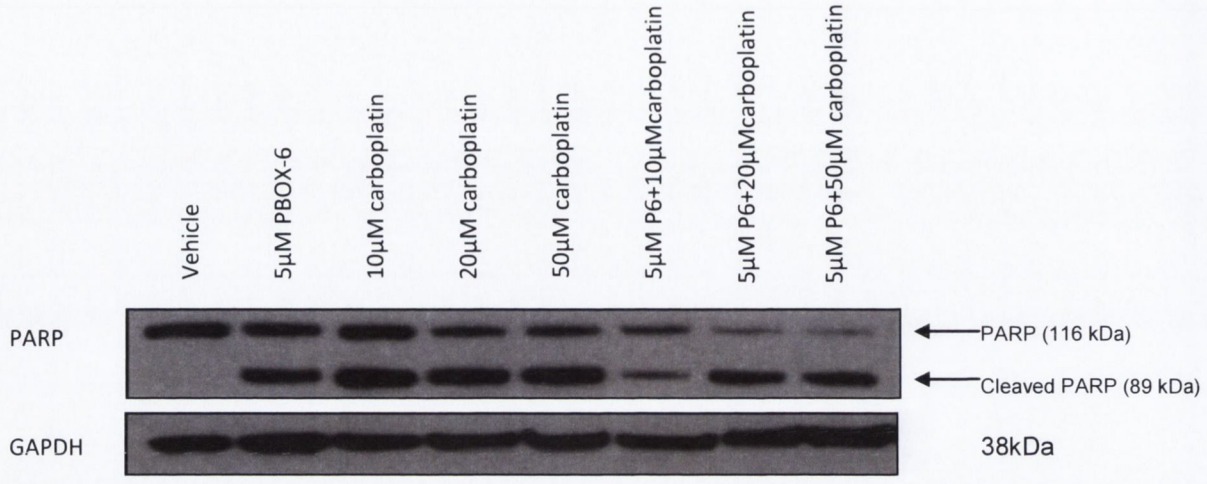

Figure 4.9 PBOX-6 and carboplatin alone and in combination induce cleavage of PARP.

SHSY5Y cells were seeded at a density of 3.0 x 10^5 cells in T25cm^2 flasks and left to adhere overnight. The following day, cells were treated with 5μM PBOX-6, 10μM, 20μM, 50μM carboplatin or a combination of both. After 48 hours cells were harvested and lysates were prepared for Western blot analysis. 30 μg of protein was separated on a 10% resolving gel with 5% stacking gel, transferred to a PVDF membrane and probed with an anti-PARP antibody. Membranes were also probed for anti-GAPDH as a loading control. Results are representative of three separate experiments.

(A)

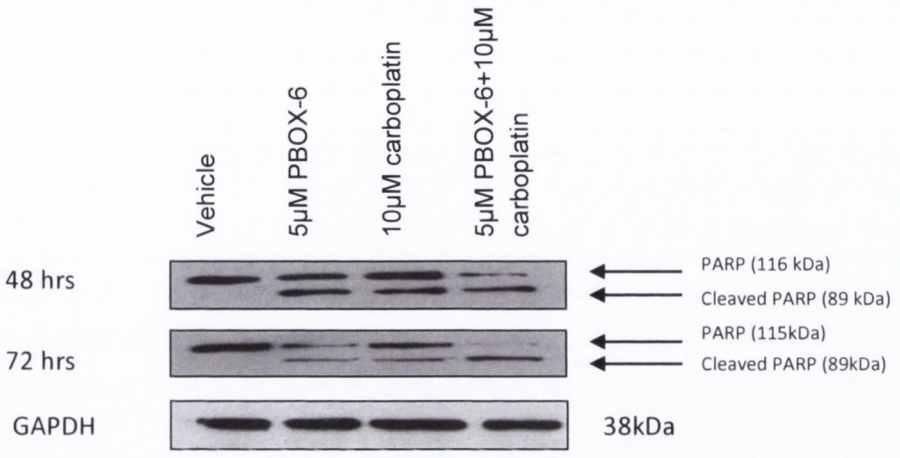

(B)

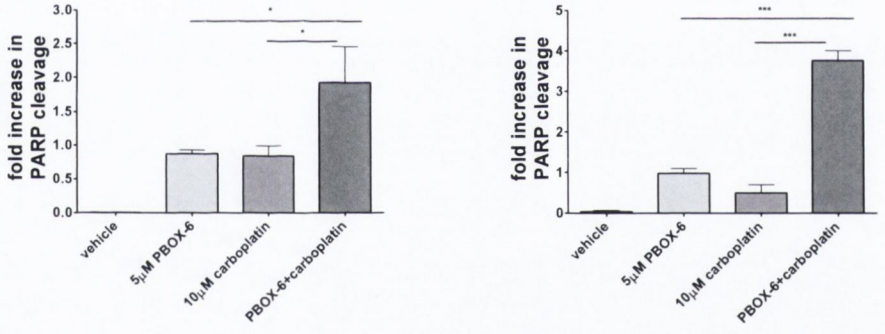

Figure 4.10 A combination of PBOX-6 and carboplatin enhances PARP cleavage in SHSY5Y cells. SHSY5Y cells were seeded at a density of 3.0 x 10^5 cells in T25cm^2 flasks and left to adhere overnight. The following day, cells were treated with 5 μM PBOX-6, 10 μM carboplatin or a combination of PBOX-6 and carboplatin. (A) After 48 or 72 hours cells were harvested and lysates were prepared for Western blot analysis. 30 μg of protein was separated on a 10% resolving gel with 5% stacking gel, transferred to a PVDF membrane and probed with an anti-PARP antibody. Membranes were also probed for GAPDH as a loading control. Results are representative of three separate experiments. (B) Western blots were normalised to total GAPDH as a control and densitometric analysis of bands was carried out with the imageJ software. Statistical analysis was performed using one way ANOVA with Tukey's multiple comparison test. *** $p<0.001$, *$p<0.05$.

4.2.5 The effect of PBOX-6/carboplatin combination of Bcl-2 family members.

Results from flow cytometric analysis of drug-sensitive SHSY5Y and drug-resistant CHLA-90 cell lines indicated that PBOX-6 synergistically enhanced the apoptotic effects of carboplatin. Western blotting showed that cleavage of PARP was increased in the combination in comparison to either agent alone (Fig. 4.10). It was next sought to determine the molecular events that underlie this enhancement of apoptosis. Members of the Bcl-2 family, namely Mcl-1 and Bcl-2 have been shown to be overexpressed in neuroblastoma with overexpression correlating with the development of drug resistance and poor prognosis. Small molecule inhibitors of Bcl-2 and Mcl-1 have been developed and have shown promising results in preclinical studies (Lestini *et al.*, 2009; Abulwerdi *et al.*, 2014), while there are currently four phase 1 clinical trials of ABT 263, a small molecular inhibitor of Bcl-2, ongoing for the treatment of multiple cancers. Due to the contribution of these proteins in the control of apoptosis and the development of drug resistance, determination of the effects of this novel drug combination of their expression in drug sensitive and resistant neuroblastoma cell lines was undertaken.

Western blotting analysis showed that expression of two anti-apoptotic Bcl-2 proteins, Mcl-1 and Bcl-2, and pro-apoptotic Bak were affected by treatment with 5μM PBOX-6 alone and in combination with 10μM carboplatin after 48 hours. The PBOX-6/carboplatin combination decreased expression of Mcl-1 (Fig. 4.11) and induced cleavage of Bcl-2 (Fig. 4.11), while expression of the conformationally active Bak was only present in cells treated with PBOX-6 alone and in combination with carboplatin (Fig. 4.12). This was in contrast to carboplatin which had no effect on the expression of any of these proteins. Mcl-1 and Bak expression were equivalent to the vehicle treated cells, while no cleavage of Bcl-2 was observed in the carboplatin treated cells. Comparable results were also found after 72 hour treatment (Fig. 4.11, 4.12).

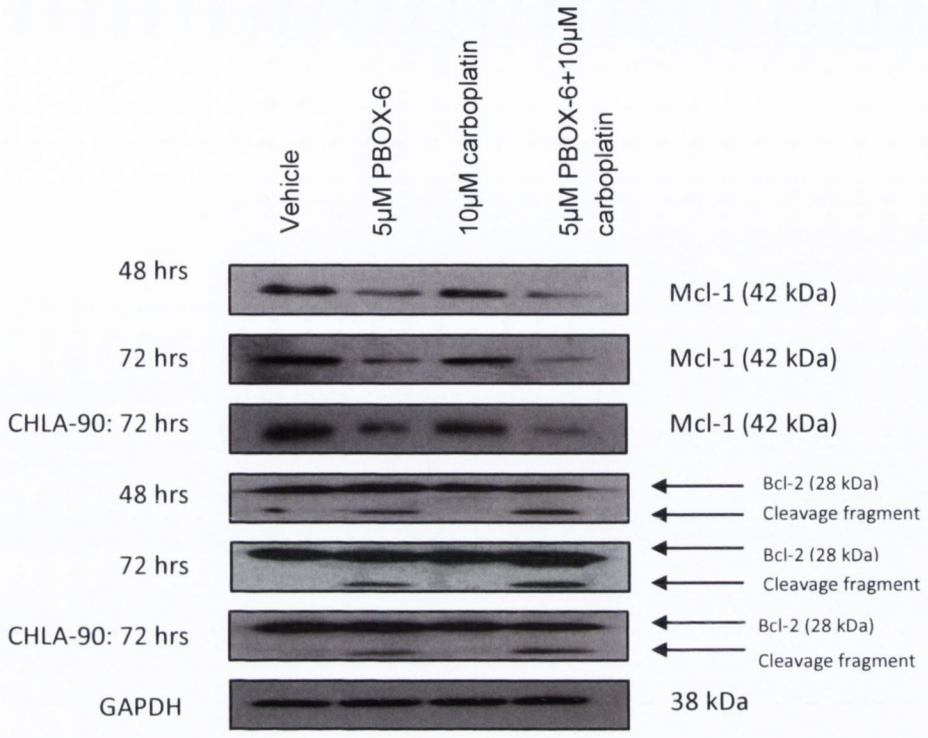

Figure 4.11 The PBOX-6/carboplatin combination reduces the expression of anti-apoptotic Mcl-1 and induces cleavage of Bcl-2 in drug sensitive and MDR neuroblastoma cell lines.

SHSY5Y and CHLA-90 cells were seeded at a density of 3.0 x 10^5 cells in T25cm^2 flasks and left to adhere overnight. The following day, cells were treated with 5 μM PBOX-6, 10 μM carboplatin or a combination of PBOX-6 and carboplatin. After 48 or 72 hours cells were harvested and lysates were prepared for Western blot analysis. 30 μg of protein was separated on a 12% resolving gel with 5% stacking gel, transferred to a PVDF membrane and probed with an anti-Mcl-1 or anti-Bcl-2 antibody. Membranes were also probed for GAPDH as a loading control. Results are representative of three separate experiments.

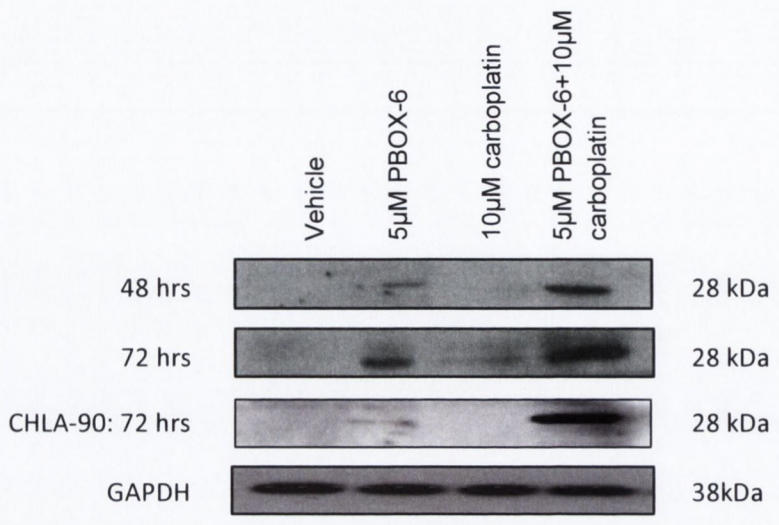

Figure 4.12 The PBOX-6/carboplatin combination induces activation of Bak in drug sensitive and MDR neuroblastoma cell lines.

SHSY5Y and CHLA-90 cells were seeded at a density of 3.0 x 10^5 cells in T25cm^2 flasks and left to adhere overnight. The following day, cells were treated with 5 μM PBOX-6, 10 μM carboplatin or a combination of PBOX-6 and carboplatin. After 48 or 72 hours cells were harvested and lysates were prepared for Western blot analysis. 30 μg of protein was separated on a 12% resolving gel with 5% stacking gel, transferred to a PVDF membrane and probed with an anti-Bak-NT antibody. Membranes were also probed for GAPDH as a loading control. Results are representative of three separate experiments.

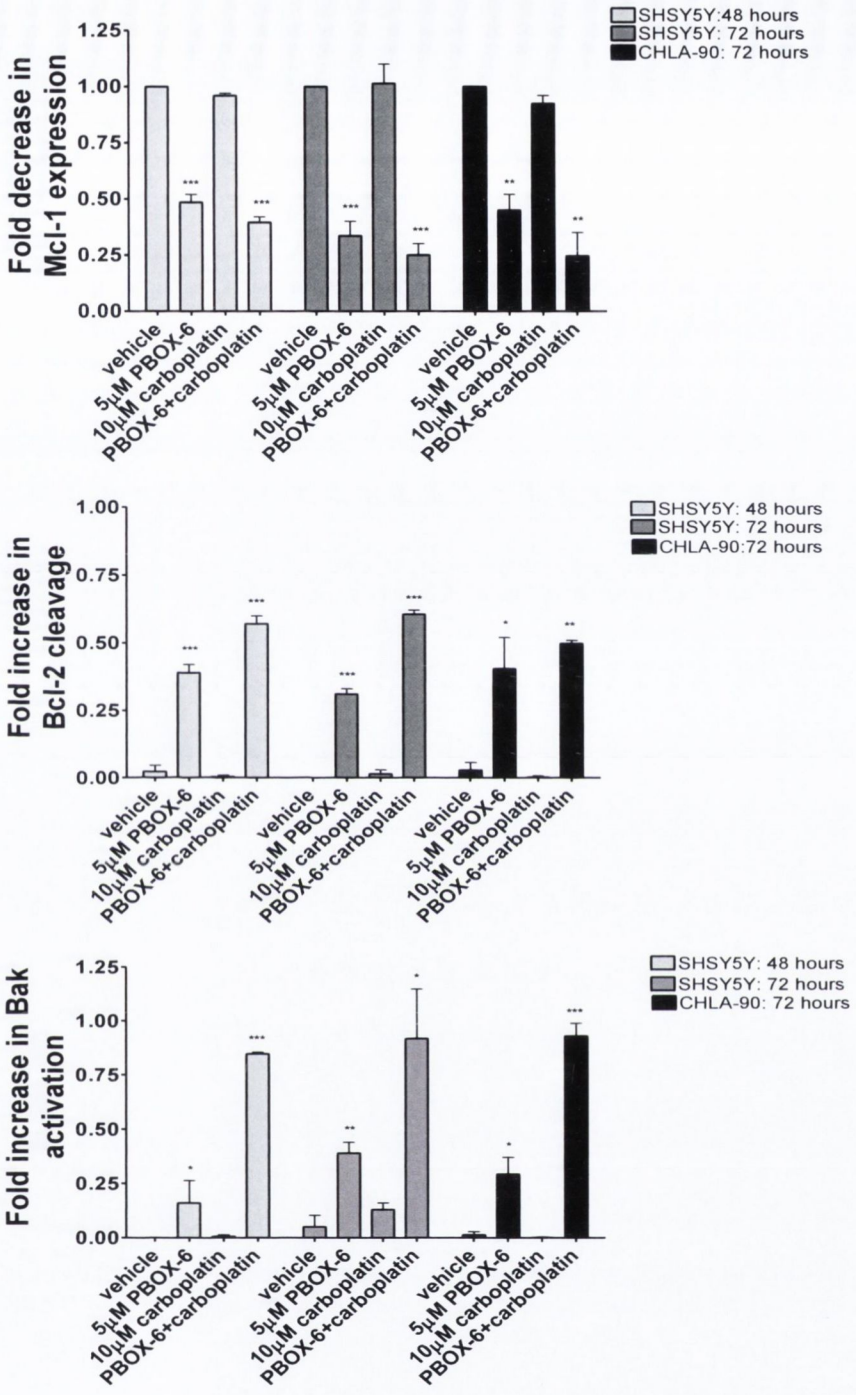

Figure 4.13 Densitometric analysis of Mcl-1, Bcl-2 and Bak expression following treatment with PBOX-6, carboplatin or a combination of PBOX-6 and carboplatin in SHSY5Y and CHLA-90 cells. Western blots were normalised to total GAPDH as a control and densitometric analysis of bands was carried out with the imageJ software. Statistical analysis was performed using one way ANOVA with Tukey's multiple comparison test. *** $p<0.001$, ** $p<0.01$ *$p<0.05$.

4.2.6 The PBOX-6/carboplatin combination induces depolarisation of the mitochondrial membrane and release of cytochrome c.

The mitochondria plays a fundamental role in the intrinsic apoptotic pathway allowing for the release of pro-apoptotic factors such as SMAC/DIABLO and cytochrome c through pores formed by Bak and Bax (Youle *et al.*, 2008). Cytochrome c is a small heme protein found in the inner membrane of the mitochondria. In addition to its pro-apoptotic role it is also a component of the electron transport chain where it transfers electrons between complexes 3 and 4 (Ow *et al.*, 2008). In non-apoptotic cells cytochrome c is anchored to the inner mitochondrial membrane preventing its release. The release of cytochrome c triggers formation of the apoptosome leading to the processing and activation of pro-caspase 9 and in turn cleavage and activation of executioner caspases 3 and 7 (Tait *et al.*, 2010).

The observed increase in conformationally active Bak would indicate that Bak is homodimerising and forming pores in the mitochondrial membrane. When this occurs the electrochemical gradient across the mitochondrial membrane collapses and the membrane is depolarised. This can be visualised by JC-1, a cationic dye which detects loss of mitochondrial membrane potential. As can be seen in Figure 4.14, depolarisation of the mitochondrial membrane 24 hours post treatment was observed.

Formation of pores and depolarisation enables the release of pro-apoptotic proteins such as cytochrome c. Previous studies have demonstrated that in response to some apoptotic stimuli, cytochrome c is released from the mitochondria and accumulates in the cytosol. Therefore cytosolic fractions were prepared and cytochrome c expression was analysed by Western blotting in both SHSY5Y and CHLA-90 cells. PBOX-6 alone and the PBOX-6/carboplatin combination triggered the release of cytochrome c into the cytosol which correlated with induction of apoptosis (Figure 4.14). In contrast, in cells treated with carboplatin alone, cytochrome c release was not observed in either cell line. The antibody utilised recognises both monomeric and polymeric cytochrome c. In the combination treated SHSY5Y cells, cytochrome c was observed in both the monomeric and polymeric form. Release of cytochrome c correlated with induction of apoptosis in this cell line (Fig. 4.14).

(A)

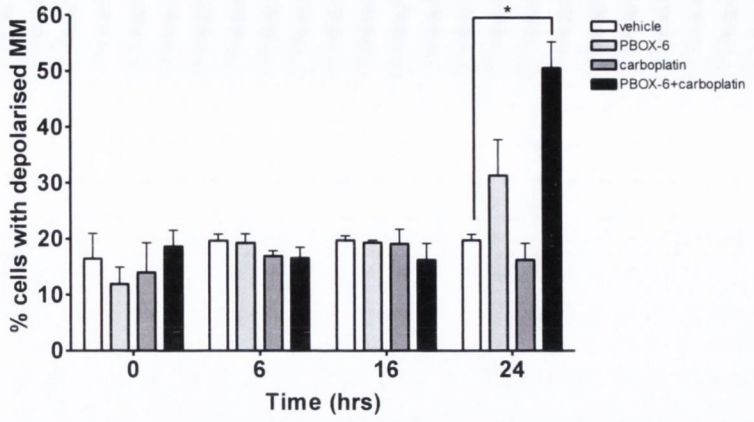

(B)

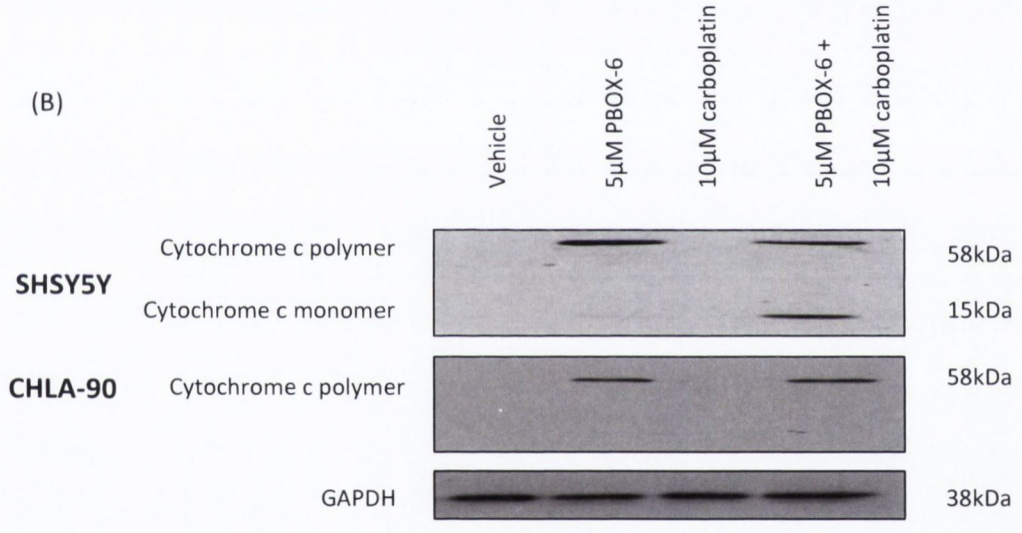

Figure 4.14 The PBOX-6/carboplatin combination evokes depolarisation of the mitochondrial membrane and the release of cytochrome c

(A) SHSY5Y cells were treated as indicated above and stained with JC-1 for 15mins. Depolarisation of the mitochondrial membrane was assessed by flow cytometry as described in materials and methods. (B) SHSY5Y and CHLA-90 cells were seeded at a density of 3.0 x 10^5 cells in T25cm^2 flasks and left to adhere overnight. The following day, cells were treated with 5 μM PBOX-6, 10 μM carboplatin or a combination of PBOX-6 and carboplatin. After 72 hours cells were harvested and lysates were prepared for Western blot analysis. Cytosolic lysates were prepared by subcellular fractionation for cytochrome c analysis. 30 μg of protein was separated on a 12% resolving gel with 5% stacking gel, transferred to a PVDF membrane and probed with an anti-cytochrome c antibody. Results are representative of three separate experiments.

4.2.7 Involvement of caspase-3, 8 and -9 in the apoptotic pathway induced by the PBOX-6/carboplatin combination

The release of cytochrome c triggers formation of the apoptosome leading to the processing and activation of pro-caspase-9 and in turn cleavage and activation of executioner caspases-3 and -7. It has been previously reported that PBOX-6 induced apoptosis may involve both caspase-dependent and -independent pathways (Zisterer *et al.*, 2000; McGee *et al.*, 2001). The involvement of caspases in the pathway initiated in neuroblastoma cells was therefore determined.

A series of pharmacologic inhibitors of caspase activity were utilised to determine the importance of the caspases in the apoptotic pathway. Pre-treatment of SHSY5Y and CHLA-90 cells with zVAD-fmk, a pan-caspase inhibitor, significantly inhibited PBOX-6/carboplatin-induced apoptosis indicating caspases play a role in the apoptotic pathway induced by the combination in both SHSY5Y and CHLA-90 cells (Fig. 4.15). The role of various caspases through the use of caspase inhibitors (Z-LEHD-fmk which inhibits caspase-9 and Z-IETD-fmk which inhibits caspase-8) was next investigated. Apoptosis was found to be significantly inhibited by pre-treatment with a caspase-9 inhibitor (Fig. 4.15 A,D). Activation of caspase-9 was investigated by Western blot analysis. In the pro-form, caspase-9 is present as a 47 kDa band which when activated through cleavage appears as a 37kDa band. As shown in Figure 4.16, treatment of cells with a combination of PBOX-6 and carboplatin resulted in a decrease of the pro-form and appearance of a lower molecular weight band at 37 kDa indicating cleavage and activation of caspase-9. Comparable results were observed in cells treated with PBOX-6 alone.

Similarly pre-treatment with a caspase-8 inhibitor significantly decreased apoptosis after treatment with the PBOX-6/carboplatin combination was observed, suggesting possible involvement of the extrinsic pathway in mediating apoptosis (Fig. 4.15 B,E). To confirm the involvement of caspase-8 in the apoptotic pathway, cleavage and activation was visualised by Western blot (Fig. 4.16). The pro-form was expressed at very low levels in the vehicle treated cells while expression of the proform was increased in cells treated with carboplatin alone with a slight cleavage band visible. Cleaved caspase-8 was present in lanes treated with PBOX-6 alone and in combination with carboplatin indicating

activation (Fig. 4.16). Previously, caspase-8 has been shown to be undetectable or present at very low levels in SHSY5Y cells but expression has been induced though various means such as after treatment with interferon γ (Tong *et al.*, 2009) or a combination of interferon γ and valproic acid (Hacker *et al.*, 2009). These results herein indicate that the PBOX-6/carboplatin combination restores caspases-8 expression in SHSY5Y cells as previously reported in the literature. Consequently activation of executioner caspase-3 was monitored and similar to caspase-8 and -9, caspase-3, was found to be activated in cells treated with PBOX-6 alone and in combination with carboplatin in both drug sensitive and resistant neuroblastoma cell lines (Fig. 4.16).

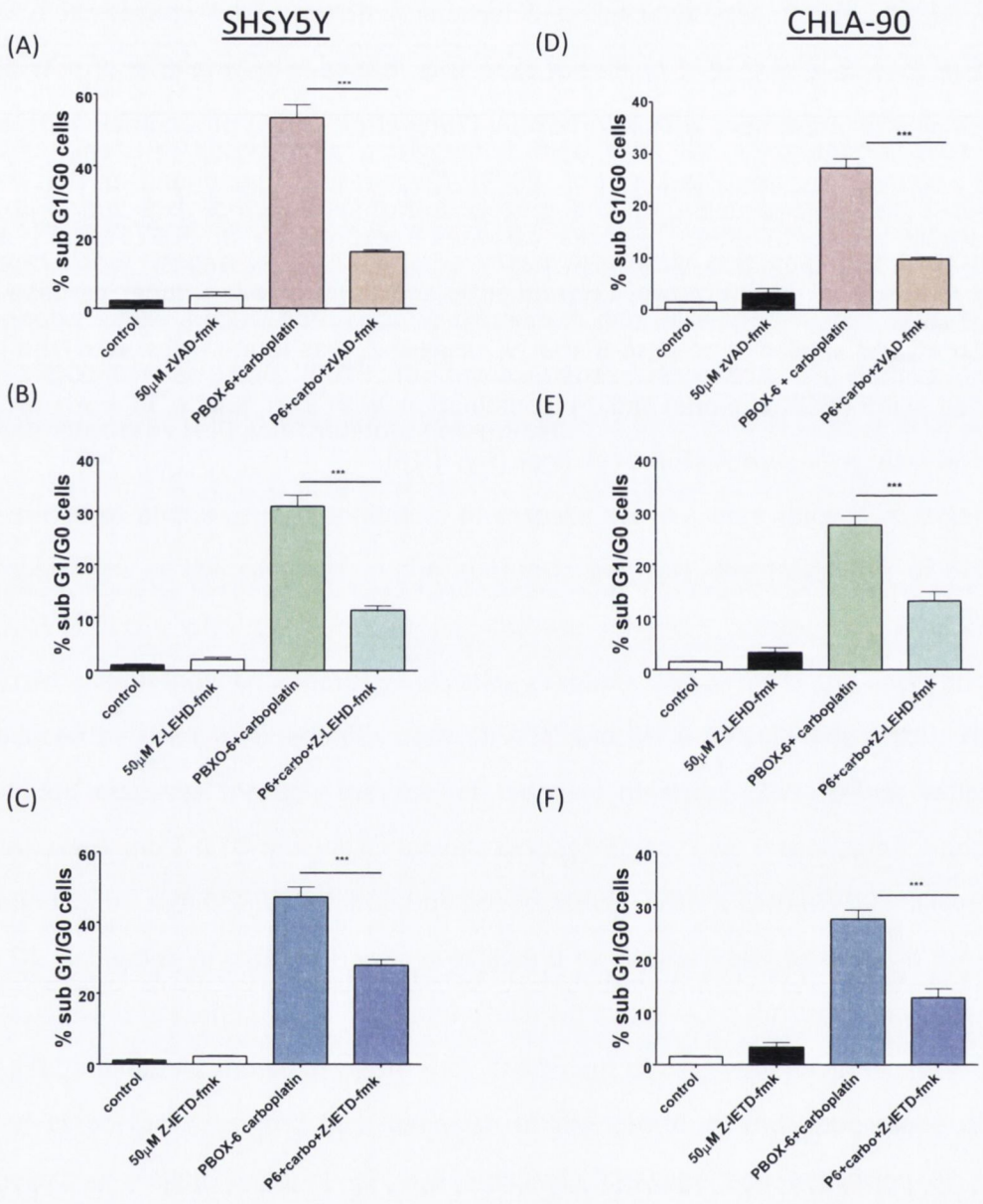

Figure 4.15 Apoptosis induced by the PBOX-6/carboplatin combination is caspase dependent in SHSY5Y and CHLA-90 neuroblastoma cell lines.

SHSY5Y and CHLA-90 cells were seeded at a density of 1 X 10^5 cells/ml in 6 well plates and left to adhere overnight. The following day cells were pre-treated with (A, D) 50μM zVAD-fmk, a general caspase inhibitor, (B, E) 50μM z-LEHD-fmk, a caspase-9 inhibitor or (C, F) 50μM z-IETD-fmk, a caspase-8 inhibitor before being treated with the PBOX-6/carboplatin combination. Apoptosis was measured by flow cytometric analysis of PI stained cells. Values represent the mean ± S.E.M. of three independent experiments. Statistical analysis was performed using one way ANOVA with Tukey's multiple comparison test. *** $p<0.001$.

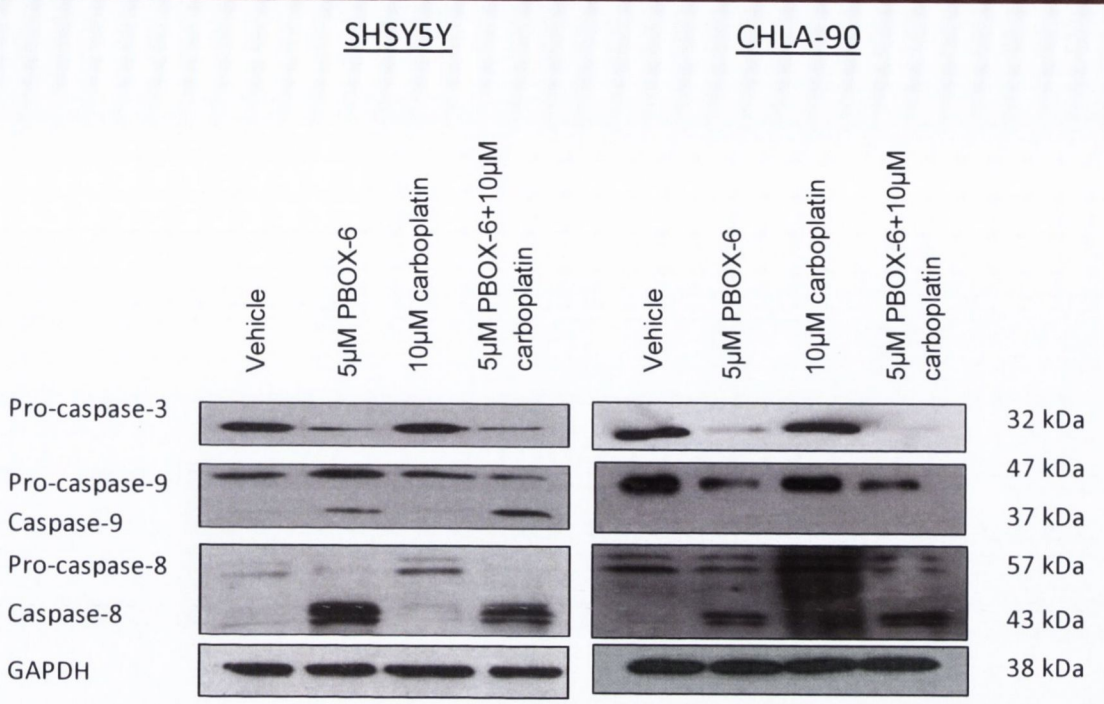

Figure 4.16 PBOX-6/carboplatin induces activation of caspase-3, -8 and -9.

Caspase-3, -8 and -9 activation was monitored by Western blot. SHSY5Y and CHLA-90 cells were seeded at a density of 3.0 x 10^5 cells in T25cm^2 flasks and left to adhere overnight. The following day, cells were treated with 5 μM PBOX-6, 10 μM carboplatin or a combination of PBOX-6 and carboplatin. After 72 hours cells were harvested and lysates were prepared for Western blot analysis. 30 μg of protein was separated on a 10% or 12% resolving gel with 5% stacking gel, transferred to a PVDF membrane and probed with an anti-caspase-3, -8 or -9 antibody. Results are representative of three separate experiments.

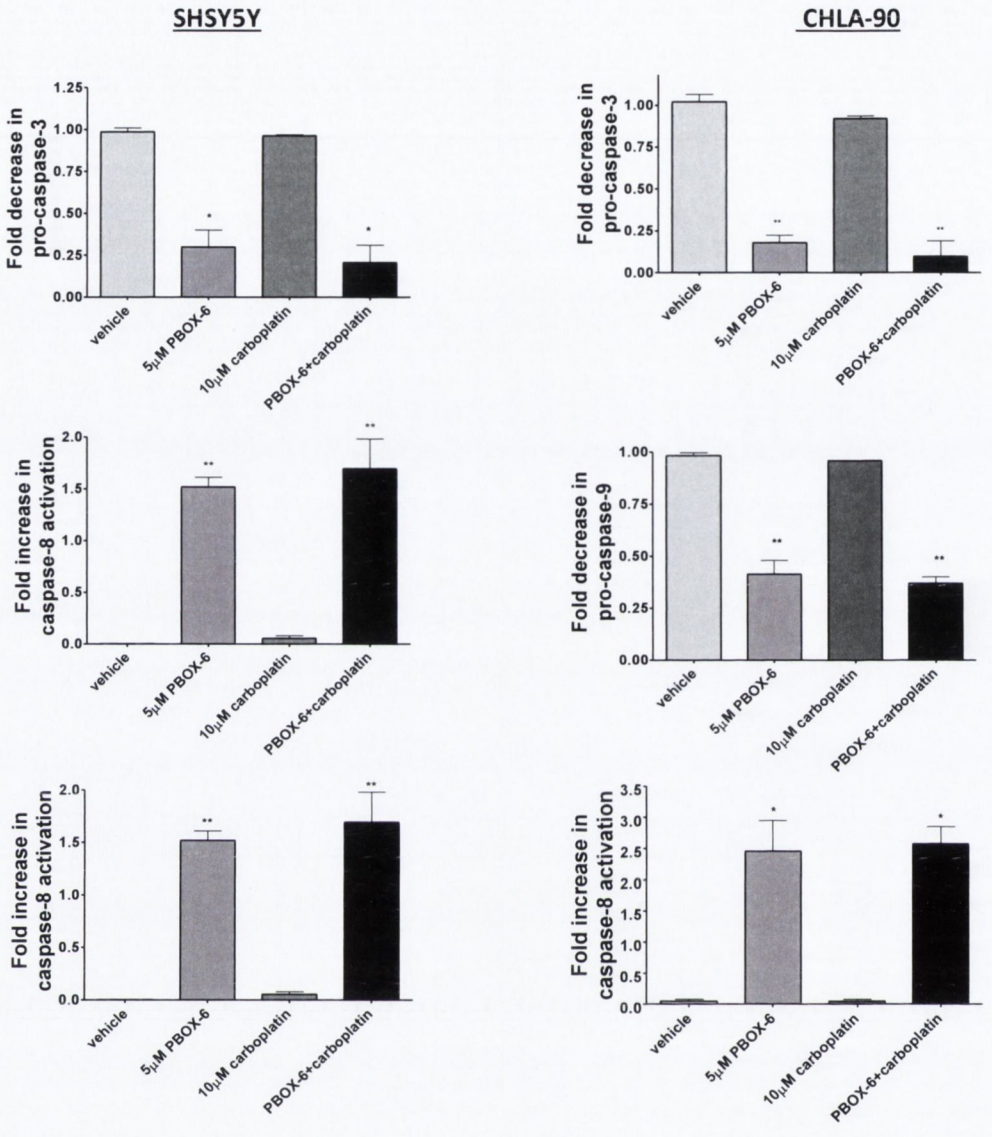

Figure 4.17 Densitometric analysis of caspase-3. -8 and -9 activation following treatment with PBOX-6, carboplatin or a combination of PBOX-6 and carboplatin in SHSY5Y and CHLA-90 cells. Western blots were normalised to total GAPDH as a control and densitometric analysis of bands was carried out with the imageJ software. Statistical analysis was performed using one way ANOVA with Tukey's multiple comparison test. ** $p<0.01$ *$p<0.05$.

4.2.8 Knockdown of Mcl-1 sensitises SHSY5Y and CHLA-90 cells to carboplatin

Finally the importance of Mcl-1 in the apoptotic pathway was investigated. Through the use of siRNA to knockdown Mcl-1, this study aimed to assess whether this could sensitise neuroblastoma cells to carboplatin. SHSY5Y and CHLA-90 cells were transfected with siRNA targeted against Mcl-1 using the Neon transfection system. Transfection conditions were optimised (Table 4.8) to determine the most effective knockdown of Mcl-1.Pulse voltage, pulse width and pulse number were varied, and the most effective downregulation of the expression levels of the Mcl-1 protein was confirmed by Western blot analysis (Fig. 4.18 A, B). Following knockdown, cells were treated with varying concentrations (10, 20 and 50 μM) of carboplatin and assessed by flow cytometry for induction of apoptosis after 48 hours (Fig. 4.19). We found that a knockdown of Mcl-1 expression sensitised both cell lines to carboplatin. There was a significant increase in the percentage of cells undergoing apoptosis following knockdown of Mcl-1 at all carboplatin concentrations examined, pointing to the importance of Mcl-1 in mediating apoptosis. As Mcl-1 overexpression has been shown to contribute to treatment failure in patients with neuroblastoma, drug combinations including PBOX-6/carboplatin which target this protein would appear to be a promising therapeutic strategy.

Condition no.	Pulse voltage	Pulse width	Pulse no.
1	0	0	0
2	1500	20	1
3	1700	20	1
4	1200	30	1
5	1400	30	1

Table 4.8 Conditions for Neon transfection optimisation

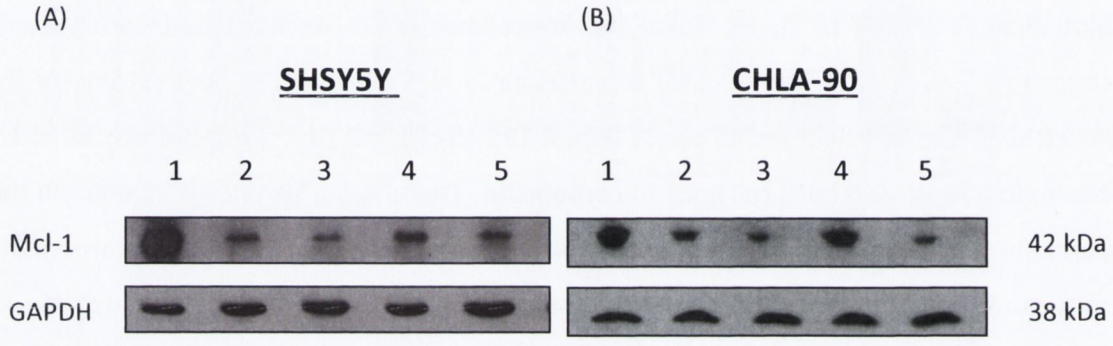

Figure 4.18 Optimisation of conditions for transfection efficiency in SHSY5Y and CHLA-90 cells.

SHSY5Y and CHLA-90 cells were seeded at 3.5 x 10^4 cells/ml in 10mm petri dishes and left to adhere overnight. The following day cells were transfected with 200nM siRNA targeting Mcl-1 using the varying pulse voltage, width and number as described in Table 4.8. The degree of knockdown was assessed by Western blotting analysis of Mcl-1 expression in (A) SHSY5Y and (B) CHLA-90 cell lines. Membranes were also probed with GAPDH to ensure even loading. Results are representative of three separate experiments.

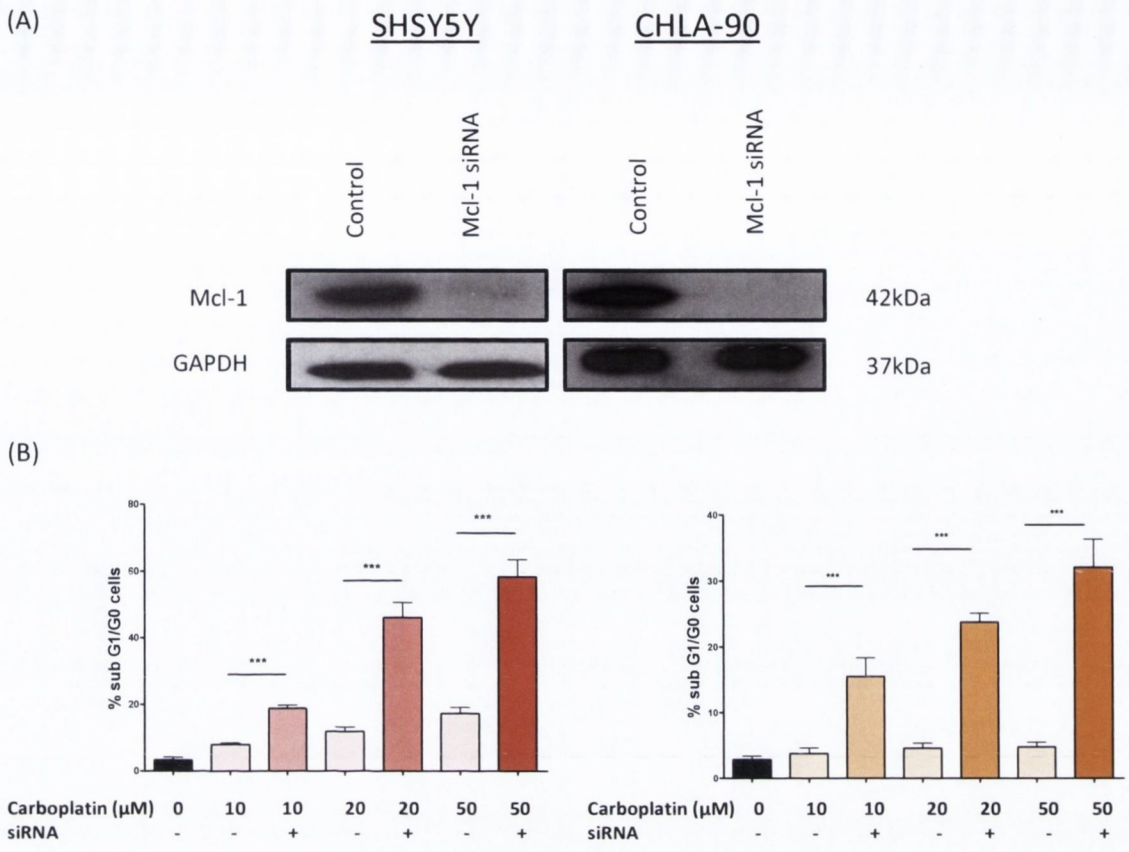

Figure 4.19 Knockdown of Mcl-1 sensitises SHSY5Y and CHLA-90 cells to carboplatin.

SHSY5Y and CHLA-90 cells were seeded at 3.5 x 10^4 cells/ml in 10mm petri dishes and left to adhere overnight. The following day cells were transfected with 5mM siRNA targeting Mcl-1 using the optimised voltage, pulse width and number. The degree of knockdown was assessed by Western blotting (A). Membranes were also probed with GAPDH to ensure even loading. Cells were subsequently treated with varying concentrations of carboplatin (10-50 μM) for 48 hours after which they were harvested, fixed in ethanol and stained with propidium iodide. Apoptosis was measured by quantification of the sub G1/G0 peak (B). Values represent the mean ± S.E.M. of three independent experiments. Statistical analysis was performed using one way ANOVA with Tukey's multiple comparison test. *** $p<0.001$.

4.2.8 PBOX-6 significantly decreases tumour volume in a mouse model of neuroblastoma.

Four-six week-old female BALB/c-nude mice received a subcutaneous injection of 2×10^6 SHSY5Y cells in the log phase of growth into the right flank. Tumours started to appear by day 30 and were measurable by day 35. Mice were randomly divided into four groups (n=5). The PBOX-6 treatment group (n=5) received an intratumoural (i.t.) injection of 7.5 mg kg^{-1} PBOX-6 once every two days for the duration of the experiment starting on day 35. PBOX-6 was administered by i.t. injection as previous studies have indicated that this is the most efficacious route of administration (Green *et al.*, 2005; Bright *et al.*, 2010). The carboplatin treatment group (n=5) received an intraperitoneal (i.p.) injection of 60 mg kg^{-1} carboplatin once every two days for the duration of the experiment starting on day 35 while the combination group (n=5) received both an i.t. injection of PBOX-6 and i.p. injection of carboplatin every two days for the duration of the experiment. Control mice (n=5) received an i.t. and i.p. injection of 50 µl of the equivalent vehicle (10% (v/v) ethanol and 10% (v/v) cremophor EL in PBS). Welfare was monitored every two days to ensure that no mouse suffered any form of distress such as failing to groom or hunching.

Tumour growth was measured every second day, the long (L) and short (S) axes were recorded, and tumour volume (V) calculated using the following equation: $V=(S^2 \times L)/2$ (Beck *et al.*, 2003). Injections were initiated on day 35 when there was no significant difference in tumour volume between the control and the PBOX-6-treated groups. By day 7, PBOX-6 had significantly reduced tumour growth when compared to control group (Fig. 4.20A). Tumour burden was continuously and significantly inhibited up until the experimental end point of the study (Fig. 4.20A). Statistical analysis was performed using an unpaired Student's t-test. At the experimental end point, day 13, mice were killed by CO_2 asphyxiation followed by cervical dislocation.

Mice were weighed every two days. Results indicate that neither the vehicle nor PBOX-6 adversely affected body weight. In fact, both groups put on a small amount of weight during the experiment (Fig 4.20B) which would be expected with healthy mice of this age. This was in contrast to carboplatin treated mice which suffered severe weight loss. In both the carboplatin and the carboplatin/PBOX-6 combination groups, the mice were

euthanized on day 5 of the study due to excessive weight loss and this aspect of the study could not be completed. Results for the effect of carboplatin or the carboplatin/PBOX-6 combination on tumour growth could therefore not be obtained.

(A)

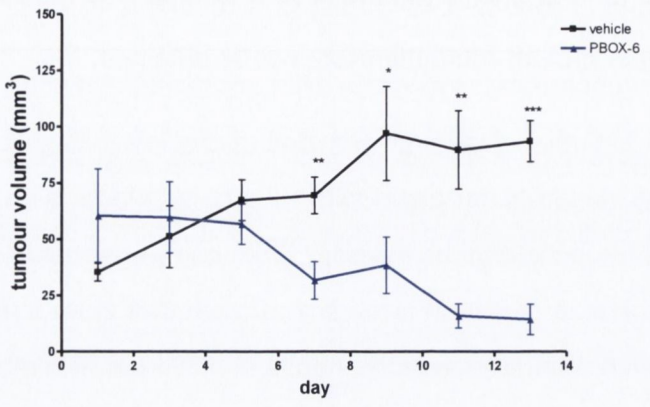

(B)

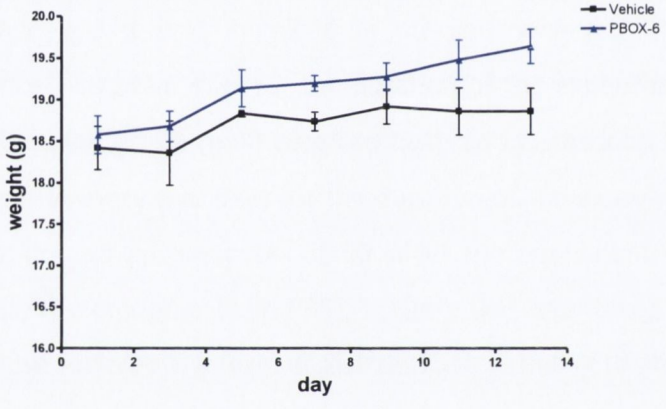

Figure 4.20 Administration of PBOX-6 significantly inhibits tumour growth in an *in vivo* mouse model of neuroblastoma.

Four-six week-old female BALB/c-nude mice received a subcutaneous injection of 2×10^6 SHSY5Y cells in the log phase of growth into the right flank. On day 35 when the tumour diameter was approximately 3 mm, mice were randomly divided into groups (n=5). (A) The PBOX-6 treatment group (n=5) received an intratumoural (i.t.) injection of 7.5 mg kg^{-1} PBOX-6 once every two days for the duration of the study. Control mice (n=5) received an i.t. injection of 50 μl of vehicle (10% (v/v) ethanol and 10% (v/v) cremophor EL in PBS). Tumour growth was measured every second day, the long (L) and short (S) axes were recorded, and tumour volume (V) calculated using the equation: $V=(S^2 \times L)/2$. Data shown represents the mean ± SEM of five mice per group. Statistical analysis was performed using the Student's unpaired t-test. *** p<0.001, p<0.01, *p<0.05. The tumour volume after PBOX-6 treatment was measured and was compared to the tumour volume after vehicle treatment on a day 2, 4,6,8,10,12 and 14. (B) Following commencement of the vehicle/PBOX-6 injections, animals were weighed once every two days for the duration of the study.

4.3 Discussion

An investigation was undertaken to assess the effects of PBOX-6 in combination with doxorubicin, etoposide and carboplatin on SHSY5Y cells, a representative drug sensitive cell lines, and PBOX-6 in combination with carboplatin in CHLA-90 cells, a representative MDR cell line. These cell lines were chosen as they are well established neuroblastoma cell lines which have been used extensively to study combination treatments (Bender *et al.*, 2009). PBOX-6 was shown to synergistically enhance the apoptotic effects of all three drugs investigated. PBOX-6 targets the microtubule network but each of the other drugs target different cellular pathways to induce apoptosis. Treatment of advanced neuroblastoma entails the incorporation of intensive courses of combination chemotherapy. Conventional chemotherapy can often target DNA triggering events in the cell such as activation of p53, cell cycle arrest and apoptosis. Frequently in advanced tumours, these pathways are frequently defective, for example p53 may be mutated or deleted leading to ineffective induction of cell death by chemotherapeutics. Single agent chemotherapy may provide insufficient toxicity and cells may develop MDR. Combination therapy offers the benefit of targeting multiple cellular pathways that induce apoptosis, and has proven to be efficacious in other paediatric cancers leading to higher rates of long term survival.

Members of the PBOX family have previously been shown to work in combination with other drugs to synergistically increase apoptosis. These include flavopiridol, a pan Cdk inhibitor, and Imatinib, a receptor tyrosine kinase inhibitor (Bright *et al.*, 2009). There have also been previous reports in the literature of other novel compounds potentiating the effects of standard chemotherapeutics via modulation of the Bcl-2 family of proteins. Mohan *et al.,* (2011) demonstrated that 2,3-DCPE (a small molecule inhibitor of the anti-apoptotic protein Bcl-xL) in combination with 4-HPR (a synthetic retinoid) works synergistically to significantly increase apoptosis in SK-N-DZ and SH-SY5Y neuroblastoma cells via downregulation of the anti-apoptotic proteins Bcl-xL, Bcl-2 and Mcl-1 and upregulation of the pro-apoptotic proteins Bax, p53, Puma and Noxa, ultimately causing activation of caspase-3. Similarly, Fang *et al.,* (2011) found that 4-HPR synergises with ABT-737, a small-molecule BH3-mimetic, in neuroblastoma cell lines. It was proposed that inhibition of anti-apoptotic Bcl-2 proteins induced by ABT-737 enhances 4-HPR activity in

neuroblastoma cell lines though an increase in pro-apoptotic Bcl-2 proteins, such as Bax, Bak and tBid. While PBOX-6 has been shown to target the microtubule network, doxorubicin, etoposide and carboplatin each mediate apoptosis though a number of different means.

Etoposide is an inhibitor of topoisomerase II (Ezoe., 2012). Topoisomerases are enzymes that regulate the relaxing and unwinding of DNA during replication. As DNA is a double helix, the two strands must be separated before they can be replicated. Topoisomerase II generates transient breaks in the DNA allowing it to unwind. When cells are treated with etoposide, the accumulation of cleavages generates permanent breaks in the DNA strands which triggers repair pathways, mutagenesis and chromosomal translocations (Chen *et al.*, 2013). If these breaks overpower the cell, apoptosis is induced. Etoposide switches topoisomerase II from an essential enzyme for successful DNA replication to a cellular poison that fragments the genome. As topoisomerase II is highly expressed in proliferating cells, especially at late S and G2/M phases of the cell cycle, cells are most sensitive to etoposide at these stages in the cell cycle (Chen *et al.*, 2013). The dose-limiting toxicity of etoposide is myelotoxicity while non-haematological toxicities are mild to moderate (Wolff *et al.*, 2008). In the present study, treatment with PBOX-6 in combination with etoposide synergistically enhanced apoptosis in neuroblastoma cells. The enhancement in apoptosis seen in the PBOX-6 combination was most likely caused by multiple pathways being targeted simultaneously. The combination of etoposide and paclitaxel, another microtubule targeting agent has previously been used to treat a number of cancers including, breast lung and colon (Cobleigh *et al.*, 2011; Loriot *et al.*, 2009). Unlike neuroblastoma, retinoblastoma another paediatric malignancy has a generally positive prognosis (a 5 year mean survival of 95.6% in the United States) with the exception of cases where diagnosis is late and the patient presents with an advanced, highly invasive disease similar to neuroblastoma. Kaliki *et al.,* (2011) found that a combination of vincristine, etoposide and carboplatin prevented metastasis in 100% of 52 retinoblastoma patients after a mean follow up time of 66 months. Combination chemotherapy with etoposide, vincristine, doxorubicin and dexamethasone has been proposed by Zhong *et al.,* (2012) to represent a new therapeutic approach for the

treatment of advanced AIDS-related Kaposi's sarcoma, for patients where first line treatment has failed.

Doxorubicin is an anthracycline antibiotic derived from *Streptomyces peucetius var. caesius*. which interacts with DNA, forming complexes by intercalation between base pairs. Topoisomerase II activity is inhibited by stabilizing the DNA-topoisomerase II complex, preventing the religation of DNA strands (Tacar *et al.*, 2013). Doxorubicin is an active drug in solid tumours such as neuroblastoma but its use is limited by development of resistance (mediated in part by overexpression of P-gp) and adverse side effects such as acute myelosuppression and cardiotoxicity (Sieczkowski *et al.*, 2010; Bao *et al.*, 2011; Ichikawa *et al.*, 2014). By combining doxorubicin with PBOX-6, this could potentially prevent the development of resistance. It is possible that the use of lower concentrations of doxorubicin may not elicit such toxic side effects. Similar to results with etoposide, PBOX-6 was shown to synergistically enhance doxorubicin mediated apoptosis.

PBOX-6 and -15 in combination with a third drug currently used to treat neuroblastoma was also investigated; carboplatin is an alkylating agent which induces apoptosis in malignant cells by a number of mechanisms. Firstly by attaching alkyl groups to DNA resulting in fragmentation of DNA by repair enzymes preventing DNA synthesis; secondly through formation of cross-links preventing separation of DNA strands, and lastly through introduction of mispaired nucleotides causing mutations which activate cell cycle checkpoints, triggering apoptosis (Bristow *et al.*, 2008). Carboplatin has become increasingly popular for the treatment of multiple cancers as it has displayed significantly lower toxicities when compared to its parent compound cisplatin. However, the efficacy of both drugs is limited by the development of resistance, which occurs through a number of mechanisms, including decreased uptake or increased efflux of the drug; increased repair of lesions in DNA, or by DNA tolerance through replication of DNA containing unrepaired damage (Stewart *et al.*, 2007). Therefore, a combination with another drug, which acts through an alternative pathway, provides a promising alternative treatment strategy.

Carboplatin is commonly used in combination with paclitaxel in a number of malignancies including ovarian, breast and non small cell lung cancer (Xiong *et al.*, 2007; Chen *et al.*,

2010; Pignata *et al.*, 2014). In addition, Huang *et al.,* (2012) found that a combination of carboplatin and paclitaxel showed a greater decrease in the survival of OS732 osteocarcinoma cell lines than either drug alone. A phase 1 clinical trial examining the efficacy of a combination of carboplatin and vinblastine for the treatment of recurrent glioma has recently been completed and found that combining carboplatin with vinblastine reduced the myelosuppressive effect experienced by patients when treated with vinblastine alone. Patients who received paclitaxel in combination with carboplatin experienced less thrombocytopenia than when carboplatin was administered alone (Jakacki *et al.*, 2009). In a recent trial of low grade glioma patients, a combination of vincristine and carboplatin was given as the first line treatment and after a mean follow time of 56 months all patients were alive with 68% of patients being progression free (Ronghe *et al.*, 2010). These published results would support the hypothesis that MTAs may enhance the apoptotic effects of carboplatin in malignant cells and the further investigation is warranted.

The effect of PBOX-6 with varying doses of carboplatin on SH5Y5Y and CHLA-90 cells was examined and it was found that PBOX-6 synergistically enhanced the apoptotic effects of carboplatin. There are checkpoints within the cell cycle which are activated in response to DNA damage or replication stress, that determine whether the cell cycle should progress, and as carboplatin is a DNA damaging agent these checkpoints may be activated. Ataxia telangiectasia and Rad3-related protein (ATR) and ataxia telangiectasia mutated protein (ATM) are two key players in the cellular response to carboplatin. They activate checkpoints which lead to arrest of the cell cycle at S, G2 or M phase, and cause activation of cell cycle kinases, chk1 and chk2, which regulate S phase progression and entry into mitosis, and the G1/S and G2/M checkpoints respectively (Bristow *et al.*, 2008). As carboplatin covalently crosslinks DNA, it causes the replication fork to stall activating the replication checkpoint at S phase. Chk1 phosphorylates cdc25C, a phosphatase which functions to remove phosphorylations which inhibit the activity of CDKs. Phosporylation of cdc25C prevents activation of cyclinE/CDK2 a complex which plays a vital role in progression from G1 to S phase. In contrast to carboplatin, PBOX-6 does not target the G1 or S phase of the cell cycle, it induces depolymerisation of microtubules, preventing formation of the metaphase spindles subsequently activating the mitotic spindle

checkpoint and several proteins such as BubR1 act to initiate a G2/M arrest (Greene *et al.*, 2008; Nathwani *et al.*, 2010). By 48 hours cells have undergone arrest and enter apoptosis. Acting alone each drug may not cause adequate damage to permanently arrest the cells at either S or G2/M and induce substantial amounts of apoptosis, as could be observed by the intermediate levels of apoptosis induced by each drug alone. By targeting multiple checkpoints, it is possible that the damage induced by both drugs in combination was too great for the cell to recover and consequently there was a significant induction of apoptosis.

Carboplatin was chosen as the representative chemotherapeutic for further investigation into the molecular basis for the enhancement of apoptosis, as both PBOX-6 and 15 were shown to synergise with this drug, while low CI values were obtained by both combinations indicating synergism. Although PBOX-6 was shown to synergise with doxorubicin when treated at varying concentrations, these combinations proved to be less synergistic than carboplatin. While good CI values were obtained with etoposide it was deemed that these concentrations were high in comparison to carboplatin. A concentration of 10μM etoposide which induced just 15% apoptosis alone is almost twenty times higher than the IC_{50} value for this drug in SHSY5Y cells. In contrast similar levels of apoptosis (8-17%) were induced with various concentrations of carboplatin in a range of its IC_{50} value in this cell line. To confirm that apoptosis observed by flow cytometric analysis was truly representative of an apoptotic cell population; Western blot analysis of the repair enzyme PARP was carried out. The time-dependency of PARP cleavage correlated with flow cytometric results. After confirming the cells were undergoing apoptosis, it was decided to investigate these findings further by identifying the molecular mechanisms by which PBOX-6 enhances the apoptotic effect of other chemotherapeutic drugs in neuroblastoma cells.

Having investigated the molecular events leading to PBOX-6-induced apoptosis in Chapter 3, it was next sought to identify the possible mechanism by which PBOX-6 enhances carboplatin induced apoptosis. Carboplatin treatment alone had no effect on the anti-apoptotic Bcl-2 and Mcl-1 proteins or the pro-apoptotic Bak, whereas the PBOX-6/carboplatin combination resulted in cleavage of Bcl-2, a downregulation of Mcl-1 and upregulation of Bak in both drug sensitive and MDR neuroblastoma cell lines. The

disturbance of the microtubule network induce signals that initiate cell death via the mitochondrial pathway indicating that microtubules, the mitochondria and cell death are very much linked. PBOX-6 in combination with carboplatin was found to provoke depolarisation of the mitochondria, release of cytochrome c and activation of caspase-9 and -3. Pre-treatment with caspase-9 inhibitors demonstrated the importance of caspase-9 activation in the apoptotic pathway.

Caspase-8 has been shown to be silenced by methylation of the promoter region of the caspase-8 gene (Teitz *et al.*, 2000). Inactivation of caspase-8 is a hallmark of defective apoptosis, and a mechanism by which tumour cells evade death by chemotherapeutics and develop MDR (Häcker *et al.*, 2010). Therefore, agents which can induce re-expression of caspase-8 may sensitise cells to apoptosis as activated caspase-8 may directly activate the extrinsic pathway (extrinsic pathway type I) or activate the intrinsic pathway through cleavage of Bid leading to release of cytochrome-c, activation of caspase-9 and caspase-3 (extrinsic pathway type II) (Tait *et al.*, 2010). Previously, caspase-8 has been shown to be undetectable or present at very low levels in SHSY5Y cells but expression has been induced though various means such as after treatment with interferon γ (Tong *et al.*, 2009) or a combination of interferon γ and valproic acid (Häcker *et al.*, 2010). Loss of caspase-8 expression was shown to result in chemoresistance, while induction of expression was demonstrated to restore sensitivity to TRAIL (Häcker *et al.*, 2009). Therefore, the role of caspase-8 in PBOX-6/carboplatin induced apoptosis was examined. The results presented herein would indicate that the PBOX-6/carboplatin-combination restores caspases-8 expression in SHSY5Y cells. Similar to caspase-9, inhibition of caspase-8 was found to significantly decrease apoptosis induced by the combination.

Activation of Bak, release of cytochrome c and activation of caspase-9 would support the hypothesis that apoptosis is being mediated by the intrinsic pathway but as crosstalk between the pathways may occur so involvement of the extrinsic pathway cannot be ruled out. Indeed, the caspase-8 activation demonstrated herein may indicate involvement of the extrinsic pathway. However, as caspase-8 can be activated by effector caspases such as caspase-3 (Ferreira *et al.*, 2012), and as DISC formation has not be demonstrated, it cannot be concluded that the extrinsic pathway type II is activated. It is possible that the PBOX-6/carboplatin combination occurs primarily through the intrinsic

pathway while caspase-8 activation may be present, not as a direct activator, but rather to augment the apoptotic process.

Mcl-1 overexpression has been shown to correlate with disease progression and degree of aggression suggesting a role in development of chemoresistance. RNA interference experiments showed that Mcl-1 knockdown sensitized SHSY5Y and CHLA-90 cells to carboplatin. Cell death or survival is mediated by a balance of pro and anti-apoptotic proteins, with some cells relying predominantly on Mcl-1 for survival. A reduction in apoptosis induced by the combination caused by overexpression of Mcl-1 would be necessary to definitively conclude the role of Mcl-1 is mediating apoptosis. Nevertheless we postulate that a decrease in Mcl-1 expression either through siRNA mediated knockdown or treatment with the combination, shifts the balance towards cell death, suggesting that Mcl-1 plays a key role in cell survival and response to chemotherapy. Inactivation of Mcl-1 by novel compounds such as PBOX-6 may present an innovative therapeutic strategy for future treatment of neuroblastoma.

Downregulation of Mcl-1 and reversion of suppression of caspase-8 expression in response to PBOX-6 has been demonstrated, therefore, it is possible that PBOX-6 may be modulating transcription in neuroblastoma cells. There have been previous reports in the literature of modulation of transcription by MTAs. Walker *et al.*, (2010) observed that microtubule based chemotherapeutics, such as paclitaxel or vinorelbine, inhibit STAT signalling. When treated with either of these drugs, MDA-MB-468 breast cancer cells, with constitutive activation of STAT3, displayed a loss of STAT3 phosphorylation. Additionally, paclitaxel disrupted interaction of STAT3 with tubulin. In contrast, other chemotherapeutics such as doxorubicin had no effect on STAT3. Loss of STAT3 phosphorylation resulted in a loss of transcription of STAT3 target genes. These findings, in addition to the effects on Mcl-1 and caspase-8 in neuroblastoma cells, would support the hypothesis that MTAs may modulate transcription in malignant cells, but further work is required to ascertain any direct effects of the PBOXs on transcription.

In chapter 3, PBOX-6 was found to induce apoptosis *in vitro* and reduce the viability of *ex vivo* patient samples, whilst in this chapter; PBOX-6 was shown to synergistically enhance the pro-apoptotic effects of carboplatin. It was next of interest to determine the effects

of the PBOX compounds in an *in vivo* neuroblastoma xenograft model. The BALB/C neuroblastoma model has previously been used to study the effects of chemotherapeutics such as cisplatin, on tumour burden, and this model has also been used to investigate combination therapy, such as the enhancement of cisplatin by YM155, a small molecule inhibitor of survivin (Liang *et al.,* 2013).

PBOX-6 has previously been shown to restrict tumour growth in an *in vivo* mouse mammary carcinoma (Greene *et al*, 2005) and an *in vivo* CML model (Bright *et al.*, 2010). Results from this study showed that PBOX-6 significantly inhibited neuroblastoma tumour growth when compared to mice receiving vehicle injections. Mice did not experience weight loss or exhibit any signs of distress during PBOX treatment suggesting PBOX-6 does not induce gross toxicity. In fact, all mice gained a small amount of weight during the study.

An investigation into the effects of carboplatin alone and in combination with PBOX-6 on tumour burden was also undertaken. However, the effects of carboplatin could not be determined due to adverse side effects observed following i.p. injections. Carboplatin treated mice were found to suffer excessive weight loss and had to be euthanised. This was unforeseen, as previous studies have indicated that the concentration of carboplatin employed in this study should not have had such deleterious effects on weight (Iwasa *et al.*, 2010). Higher concentrations of carboplatin have been associated with weight loss in *in vivo* models; Shalinsky *et al.*, (1999) reported that a concentration of 120 mg/kg carboplatin induced a 21.9% decrease in body while 60 mg/kg induced a 9% decrease in body weight, which is within the acceptable levels of toxicity.

Future studies examining a range of lower concentrations of carboplatin are planned, while the coadministration of squalene, an isoprenoid antioxidant, may also be worthwhile. Squalene has been reported to act as a potential cytoprotective agent against chemotherapy-induced toxicity (Das *et al.*, 2008). These authors reported that squalene significantly reduced the body weight loss of carboplatin-treated mice. The use of more advanced models such as an orthotopic neuroblastoma tumour model may also be employed in the future. In this model, luciferase stably-expressing neuroblastoma cell lines are induced through retroperitoneal injection in immunodeficient mice, allowing for

real time *in vivo* visualisation of luciferase expression, correlating to the degree of tumour burden in the animal. This would enable more accurate calculation of tumour growth and reduction.

In conclusion, it has been demonstrated that PBOX-6 has the ability to induce apoptosis in neuroblastoma cell lines alone and together with several chemotherapeutic agents; indicating that PBOX-6 represents a promising therapeutic alternative to currently available treatments. These findings provide novel insights into the signalling pathways which are activated in response to PBOX-6 in both drug sensitive and resistant neuroblastoma cell lines and in combination with carboplatin to achieve synergistic effects indicating the potential of the PBOXs, alone and in combination with standard chemotherapeutics, as an effective therapy against neuroblastoma.

Chapter 5

Investigation into the role of the AMPK/mTOR signalling pathways in PBOX-6 induced apoptosis in SHSY5Y neuroblastoma cells

Chapter 5

5.1 Introduction

The PBOXs are a series of microtubule targeting agents (Mulligan *et al.*, 2006) which have been shown to induce apoptosis in multiple tumour cells including drug sensitive and multiple drug resistant cancer cell lines (Greene *et al.*, 2005; Greene *et al.*, 2007; Bright *et al.*, 2010; Nathwani *et al.*, 2010; Lennon *et al.*, 2014), *ex vivo* patient samples (McElligott *et al.*, 2009; Bright *et al.*, 2010) and *in vivo* murine models (Greene *et al.*, 2005; Bright *et al.*, 2010). The molecular mechanisms through which these compounds induce apoptosis have been partially delineated; they have been shown to induce apoptosis though modulation of both the intrinsic and extrinsic pathways in both a caspase dependent and independent manner, which is dependent on cell type. Activation of the c-Jun N-terminal kinase (JNK) has been identified as a key mediator in PBOX-induced apoptosis (McGee *et al.*, 2002). The effect of these compounds on other cellular pathways such as angiogenesis, cell adhesion and migration has also been investigated (McElligott *et al.*, 2009; Nathwani *et al*, 2010; Lysaght *et al.*, 2013).

In chapters 3 and 4, PBOX-6-induced apoptosis in neuroblastoma cells mediated by a decrease and inactivation of anti-apoptotic Mcl-1 and Bcl-2, an increase in pro-apoptotic Bak and activation of caspases-3, -8 and -9 was demonstrated. Furthermore gene silencing of Mcl-1 was shown to sensitise both drug sensitive and multidrug resistant cells to carboplatin induced apoptosis, demonstrating the importance of Mcl-1 downregulation in the apoptotic pathway mediated by the PBOXs in neuroblastoma. The objective of this chapter was to identify the molecular events associated with Mcl-1 downregulation.

It has recently been reported in that glucose removal or the use of a nonmetabolizable form of glucose (2-deoxyglucose), leads to a decrease in Mcl-1 expression which has been attributed to a block in translation mediated by activation of 5' adenosine monophosphate-activated protein kinase (AMPK) in a number of cancer cell lines (Pradelli *et al.*, 2010). In a similar manner, TRAIL induced AMPK activation in ovarian cancer cell lines, lead to a block in Mcl-1 translation (Yang *et al.*, 2010). AMPK is a sensor of cellular homeostasis which is activated in response to a falling level of cellular ATP, to maintain energy balance within the cell. AMPK is phosphorylated when the ratio of AMP: ATP decreases leading to inhibition of ATP-consuming pathways and activation of ATP

producing pathways. Interestingly, recent reports have demonstrated that AMPK is involved in induction of apoptosis by a variety of chemotherapeutics (Chen *et al.*, 2011; Chen *et al.*, 2013; Wu *et al.*, 2014). For example, activation of AMPK by the activator AICAR was shown to inhibit the growth of EGFR-expressing glioblastomas. Additionally doxorubicin-induced apoptosis in breast (MCF-7), pancreatic (L3.6), ovarian (CaOV3) and melanoma (WM-115) cancer cell lines, was mediated by AMPK activation (Ji *et al.*, 2010). Furthermore, a recent study demonstrated that activation of AMPK is involved in apoptosis induced by the microtubule targeting agents, vincristine and taxol, in B16 melanoma cell (Chen *et al.*, 2011). Activation of the upstream kinase, LKB1, was shown to mediate activation of AMPK in response to vincristine. Knockdown of LKB1 by siRNA largely inhibited vincristine induced activation of AMPK. In addition to changes in ATP levels, Chen *et al.,* (2011) also found that LKB1 activation was dependent on the production of reactive oxygen species (ROS). Other studies have suggested anti-cancer agents may mediate their apoptotic effects through the production of oxidative stress such as the generation of ROS (Circu *et al.*, 2012). Chen *et al.,* (2010) observed a dramatic AMPK activation in response to hydrogen peroxide in primary murine neurons PC12 and SHSY5Y cells. Levels of phospho-AMPK and the downstream target acetyl-CoA carboxylase (ACC) were increased in a time- and dose-dependent manner in response to hydrogen peroxide. These reports lead us to postulate that the PBOXs could induce production of ROS in neuroblastoma cells which in turn results in activation of AMPK; therefore an investigation into the role of ROS production and AMPK activation in PBOX mediated apoptosis was undertaken.

Production of ROS may be inhibited by the antioxidant N-acetylcysteine (NAC). NAC, a precursor of glutathione, is a scavenger of free radicals and has been extensively used as a means to investigate the role of ROS production in various cellular pathways such as apoptosis, in addition to its role in various pathologies including cancer, inflammation, arthritis and cardiovascular disease (Kerksick *et al.*, 2005). There have been reports that pretreatment with NAC can impair or inhibit the apoptosis inducing ability of anti-cancer agents. Chen *et al.,* (2011) established the inhibitory effects of NAC on vincristine and taxol mediated apoptosis mediated by AMPK activation in B16 melanoma cells. Similarly Wu *et al.,* (2005) found that NAC blocked cisplatin-induced apoptosis in small cell lung

carcinoma cells by inhibiting the effects of cisplatin on multiple pro- and anti-apoptotic Bcl-2 proteins, and preventing activation of caspases. Consequently in this study, the effect of NAC on the apoptotic effects of PBOX-6 or-15 in SHSY5Y cell was determined.

AMPK phosphorylation triggers a phosphorylation cascade that regulates the activity of various downstream targets such as the mammalian target of rapamycin (mTOR) signalling pathway. Indeed AMPK activation has previously been shown to lead to inhibition of the mTOR signalling pathway resulting in a block in Mcl-1 translation (Pradelli *et al.*, 2010). mTOR is a highly conserved serine/threonine kinase which regulates a broad range of cellular events including transcription, translation, proliferation and division, therefore control of this pathway is of the upmost importance for maintaining normal cell division. Many studies point to mTOR playing a critical role in the progression of many cancers, including prostate (Bitting *et al.*, 2013), breast (Vinayak *et al.*, 2013), haematological malignancies (Barrett *et al.*, 2013) and hepatocellular carcinoma (Matter *et al.*, 2014). Oncogenic activation of this pathway induces several processes necessary for tumour growth and proliferation. Indeed, it is interesting to note that proteins in this signalling pathway have been shown to be constitutively activated in neuroblastoma cell lines and patient samples (Johnsen *et al.*, 2008). Inhibition of mTOR by rapamycin and other rapalogues have been shown to effectively induce cell death in neuroblastoma cells, indicating that inhibitors of this pathway may represent a promising new approach for the treatment of neuroblastoma. In this present study, the effect of PBOXs on the mTOR signalling pathway, namely mTOR and its downstream targets p70 S6 kinase, S6 ribosomal protein and eEF2K was undertaken.

Inhibition of mTOR is a strategy which is being extensively investigated for the treatment of many cancers. Currently there are 559 active clinical trials exploring the potential of mTOR inhibitors alone and in combination with other chemotherapeutics for the treatment of various cancers, six of which are specifically investigating the use of these inhibitors in neuroblastoma (ClinicalTrial.gov). Although inhibition of this pathway has been shown in multiple studies to have potent anti-cancer effects, there are reports of unwanted activation of survival pathways such as AKT and autophagy. Therefore, work was also undertaken to determine the ability of this MTA to induce autophagy in

neuroblastoma and consequently the effect of pharmacological inhibition of autophagy on PBOX-6 induced apoptosis was determined.

In this chapter, PBOX-6 is demonstrated for the first time to induce AMPK activation and downstream ACC phosphorylation in SHSY5Y neuroblastoma cells. ROS production appears to be involved in AMPK activation by PBOX-6. Furthermore, evidence is provided to support the suggestion that activation of AMPK mediates apoptosis in PBOX-6 treated SHSY5Y cells, through inhibition of the mTOR pathway. Finally, PBOX-6 is shown to induce autophagy in neuroblastoma cells which may function as a survival mechanism, and provides a rationale for the use of autophagy inhibitors to further promote PBOX-6-induced apoptosis in SHSY5Y neuroblastoma cells.

5.2 Results

5.2.1 PBOX-6 activates AMPK in SHSY5Y cells.

Numerous studies have demonstrated that AMPK plays a vital role in apoptosis induction in multiple cancers (Garcia-Gill *et al.*, 2003; Hadad *et al.*, 2009). Furthermore previous studies have indicated that MTAs such as vincristine, which induce apoptosis mediated by the production of reactive oxygen species, also activate AMPK (Chen *et al.*, 2011). It was hypothesised that PBOX-6 may induce the production of ROS in neuroblastoma cells which in turn activates AMPK. To test this hypothesis, SHSY5Y cells were treated with PBOX-6 and the activation of AMPK and phosphorylation of the downstream protein acetyl-CoA carboxylase (ACC) was monitored.

To assess activation of AMPK a phospho-specific antibody was utilised. When activated, AMPK is phosphorylated on Thr^{172} by an upstream MAPK kinase, LKB1. Activation of AMPK up to 6 hours post treatment with PBOX-6 was monitored and was shown to increase in a time dependent manner (Fig.5.1 A). A total AMPK antibody to confirm equal protein loading was utilised.

Upon observing activation of AMPK, the effect of PBOX-6 on the downstream target of AMPK, ACC was examined. ACC catalyses the carboxylation of acetyl CoA to malonyl CoA. Malonyl CoA is a key substrate for the synthesis of fatty acids, an anabolic process which consumes ATP. When AMPK is activated by phosphorylation it can phosphorylate ACC causing it to be inactivated thus switching off an ATP consuming pathway (Kim *et al.*, 2011). Following treatment of cells with PBOX-6, a time dependent phosphorylation of ACC in SHSY5Y cells (Fig. 5.1A) was observed, which correlated with the phosphorylation and activation of AMPK. No change in expression of total ACC was observed demonstrating equal protein loading.

Densitometric analysis of the bands followed by statistical analysis demonstrated a significant increase in phosphorylated AMPK and phosphorylated ACC within 2 hours of PBOX-6 treatment (Fig. 5.1 B).

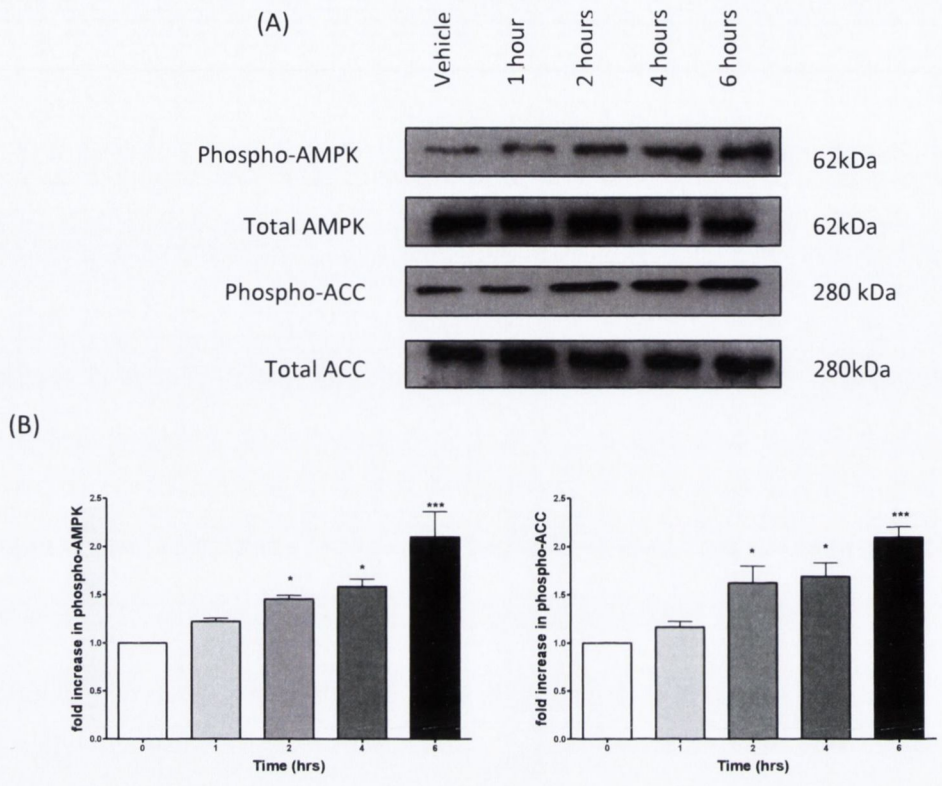

Figure 5.1 PBOX-6 activates AMPK and inactivates ACC in SHSY5Y cells in a time dependent manner

SHSY5Y cells were seeded at a density of 3.0 x 10^5 cells in T25cm^2 flasks and left to adhere overnight. The following day, cells were treated with 2.5 μM PBOX-6 for up to 6 hours. After the required incubation time, cells were harvested and lysates were prepared for Western blot analysis. 30 μg of protein was separated on a 6% or 10% resolving gel with 5% stacking gel, transferred to a PVDF membrane and probed with an anti-phospho-AMPK or anti-phospho-ACC antibody (A) Membranes were also probed for AMPK or ACC as a loading control. Results are representative of three separate experiments. (B) Western blots were normalised to total AMPK or ACC as a control and densitometric analysis of bands was carried out with the imageJ software. Statistical analysis was performed using one way ANOVA with Tukey's multiple comparison test. *** $p<0.001$, *$p<0.05$. The effect of 1, 2, 4 or 6 hours PBOX-6 treatment on phospho-AMPK expression was compared to the vehicle controlled cells.

5.2.2 PBOX-6 induces production of reactive oxygen species.

Having observed activation of AMPK and inactivation of ACC in response to PBOX-6 in SHSY5Y cells, examination of both the upstream and downstream events associated with AMPK activation in SHSY5Y cells was undertaken. Studies by Chen *et al.,* (2011) indicated that activation of the upstream kinase, LKB1, mediated the activation of AMPK in response to vincristine while knockdown of LKB1 by siRNA largely inhibited vincristine induced activation of AMPK. Furthermore, LKB1 activation was shown to be dependent on the production of ROS. Therefore, an investigation into the production of ROS by PBOX-6 using the ROS-Glo assay (Promega) was undertaken. Menadione, an analog of 1,4-naphthoquinone which produces ROS through redox cycling, was employed as a positive control for the production of ROS. A 15 minutes treatment with 50 μM menadione was found to induce ROS production when compared in control cells (Fig. 5.2A). Treatment with 2.5 μM PBOX-6 for up to 6 hours was shown to induce ROS production in SHSY5Y cells (Fig. 5.2A).

To further validate these findings, a second assay to monitor ROS production was employed. 2',7'-dichlorodihydrofluorescein diacetate (H_2DCFDA) is a cell permeable dye that measures hydroxyl, peroxyl and ROS activity within the cell. Upon entering the cell, H_2DCFDA is deacetylated by cellular esterases to a non-fluorescent compound. This compound is oxidised by ROS to 2', 7' –dichlorofluorescein (DCF). DCF is a highly fluorescent compound which can be detected by fluorescence spectroscopy with maximum excitation and emission spectra of 495 nm and 529 nm respectively. A second positive control, hydrogen peroxide, was utilised and found to induce ROS production as shown by the increase in fluorescence. Flow cytometric analysis of H_2DCFDA-stained cells indicated PBOX-6 induced ROS production as demonstrated by the increase in fluorescence (Fig. 5.2B). Taken together these results would suggest PBOX-6 induces ROS in SHSY5Y cells.

Cells possess an innate defence system in the form of detoxifying enzymes, such as glutathione which allows for a balance between the production and clearance of ROS. The antioxidant NAC is a precursor of cysteine which can enter the glutathione synthesis pathway. Glutathione (GSH) acts as a reducing agent and key antioxidant to maintain

control of a cells redox status. GSH levels have been shown to reduce after exposure to cytotoxic agents such as chemotherapeutics which induce oxidative stress such as ROS production. Depletion of GSH has been shown to correlate with induction of apoptosis whilst high GSH levels have been associated with resistance to apoptosis (Friesen *et al.*, 2004). Previous studies have shown that GSH supplementation with NAC may prevent apoptosis (Kirkland *et al.*, 2001; Franco *et al.*, 2006; 2007).

Having observed an increase in ROS production in response to PBOX-6, an experiment was next undertaken to assess the effect of pretreatment with NAC on PBOX-6 induced ROS production. ROS production was largely diminished by NAC pretreatment. Levels of ROS production were comparable to the vehicle control (Fig. 5.2A). These results indicate ROS production may be an early event (up to 6 hours post treatment) which precedes PBOX-6 induced G2/M arrest and apoptosis.

(A)

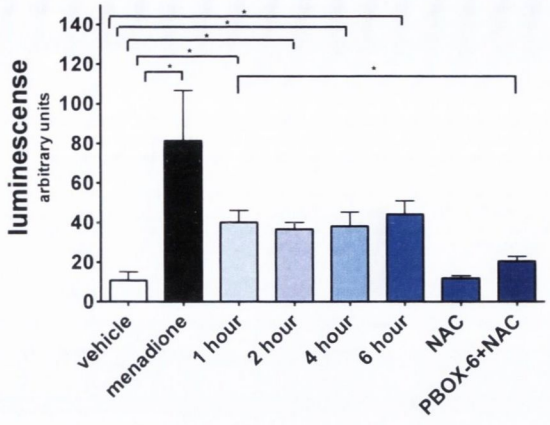

(B)

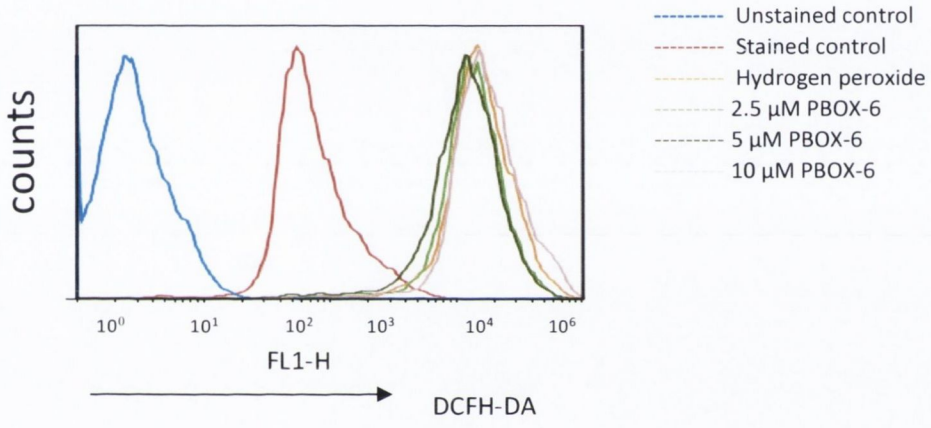

Figure 5.2 PBOX-6 induces production of reactive oxygen species.

ROS was detected using the ROS-Glo H_2O_2 assay. SHSY5Y cells were seeded in the log phase of growth at 2.5 X 10^4 cells/well and left to adhere overnight. The following day, the H_2O_2 substrate solution was added each will prior to treatment with 2.5 µM PBOX-6 for up to 6 hours. Cells were also pretreated with NAC for 1 hour and treated with 2.5 µM PBOX-6 for 1 hour. After the required incubation time, the ROS-Glo detection reagent was added to the cells and the plate was incubated for 20 mins at room temperature. Luminescence was read on the spectraMAX Gemini plate reader. Values represent the mean ± S.E.M of three independent experiments. Statistical analysis was performed using a paired student's t-test. (B) SHSY5Y cells were seeded at a density of 1.0 X 10^5 cells/ml in a six well plate and left to adhere overnight. The following day cells were treated with a range of concentrations of PBOX-6 (2.5, 5 and 10 µM) for 4 hours. After this time, cells were incubated in phenol free media containing 10 µM DCFH-DA for 30 mins at 37^0C. Cells were washed, trypsinised and resuspended in 400 µl ice cold PBS. Cells were analysed by flow cytometry; the 488 nm laser was used for excitation and DCFH-DA was detected in the FL-2 channel (535 nm). Results are representative of an experiment preformed twice.

5.2.3 Pretreatment with the antioxidant, N-acetylcysteine, inhibits the PBOX-6 mediated activation of AMPK and ACC.

Having identified ROS as a possible upstream activator of AMPK in response to PBOX-6 and having observing the inhibitory effects of NAC on ROS production, it was next decided to establish the effect of this antioxidant on phosphorylation of AMPK and the downstream target ACC in SHSY5Y cells. Cells were pretreated with 5 mM NAC for one hour followed by PBOX-6 for up to 6 hours. Pretreatment with NAC prevented PBOX-6 induced phosphorylation of AMPK while expression of total AMPK was unaffected (Fig. 5.3). Similar results were observed with ACC. These findings would support the role of ROS as an activator of AMPK in response to PBOX-6. It was next of interest to investigate the effects of this antioxidant on the anti-proliferative and pro-apoptotic effects of PBOX-6.

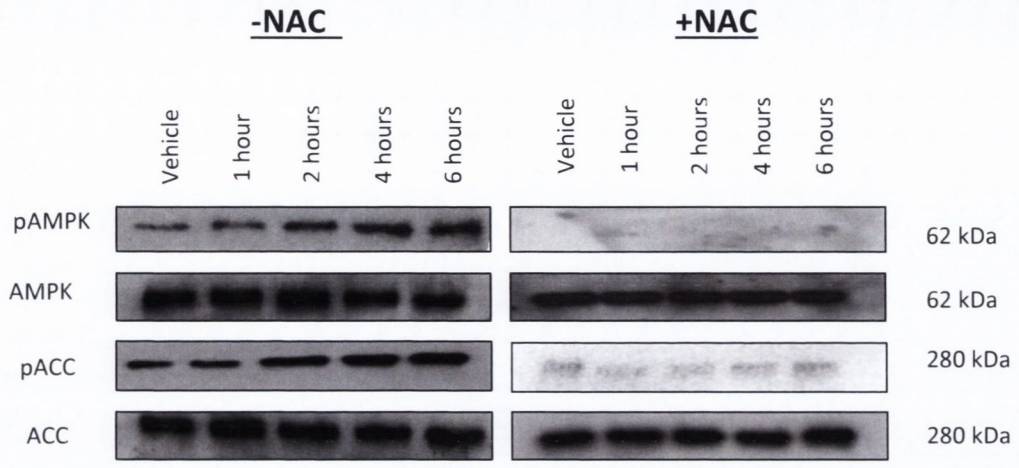

Figure 5.3 Pretreatment with NAC inhibits PBOX-6 mediated phosphorylation of AMPK and ACC in SHSY5Y cells.

SHSY5Y cells were seeded at a density of 3.0 x 10^5 cells in T25cm^2 flasks and left to adhere overnight. The following day, cells were treated with either 2.5 μM PBOX-6 or pretreated with 5 mM NAC followed by 2.5 μM PBOX-6 for the indicated times. After the required incubation time, cells were harvested and lysates were prepared for Western blot analysis. 30 μg of protein was separated on a 6% or 10% resolving gel with 5% stacking gel, transferred to a PVDF membrane and probed with an anti-phospho-AMPK or anti-phospho-ACC antibody. Membranes were also probed for AMPK or ACC as a loading control. Results are representative of three separate experiments.

5.2.4 The antioxidant N-acetylcysteine protects against the anti-proliferative effects of PBOX-6 and -15.

The AlamarBlue viability assay was used to assess the effect of PBOX-6 and -15 alone and in combination with NAC on the viability of SHSY5Y cells up to 48 hours post treatment. Prior to combination treatment with NAC, the IC_{50} value of each drug was determined after a 24 or 48 hour treatment period. After a 24 hour treatment period, the IC_{50} value of PBOX-6 was >10 μM and PBOX-15 >1 μM. The exact values could not be determined as the concentrations tested did not decrease cellular viability below 50%. The IC_{50} value 48 hours post treatment was determined as 2.03 μM for PBOX-6 and 0.10 μM for PBOX-15. Both MTAs were found to decrease the viability of SHSY5Y neuroblastoma cell in a time and dose dependent manner (Fig. 5.4).

Next, an investigation into the effects of NAC on the viability of SHSY5Y cells was undertaken. Pretreatment with NAC for one hour provided a protective effect against the anti-proliferative effects of the PBOXs in SHSY5Y cells. After 24 hours, pretreatment with NAC completely inhibited the effects of both PBOXs (Fig. 5.5, 5.6). 2.5 μM PBOX-6 on its own reduced the cellular viability by 21.66% ± 3.05 while the viability of cells pretreated with NAC and subsequently treated with PBOX-6 or -15 was maintained at 100% (Fig. 5.5A). Similar results were obtained for other concentrations of PBOX-6 (Fig 5.5A)

After 48 hours there was an even greater decrease in viability after treatment with PBOX-6 alone. A concentration of 2.5 μM PBOX-6 reduced viability by 67.05% ± 5.4 (Fig. 5.5B). Pretreatment with NAC reduced this decrease to 37%±2.7 (Fig. 5.5B). Comparable results were obtained at both time points using PBOX-15 (Fig. 5.6). These results indicate that the antioxidant NAC impairs the cytotoxic effects of PBOX-6 and -15 suggesting that ROS production by the PBOXs may play an important role in mediating their cytotoxic effects.

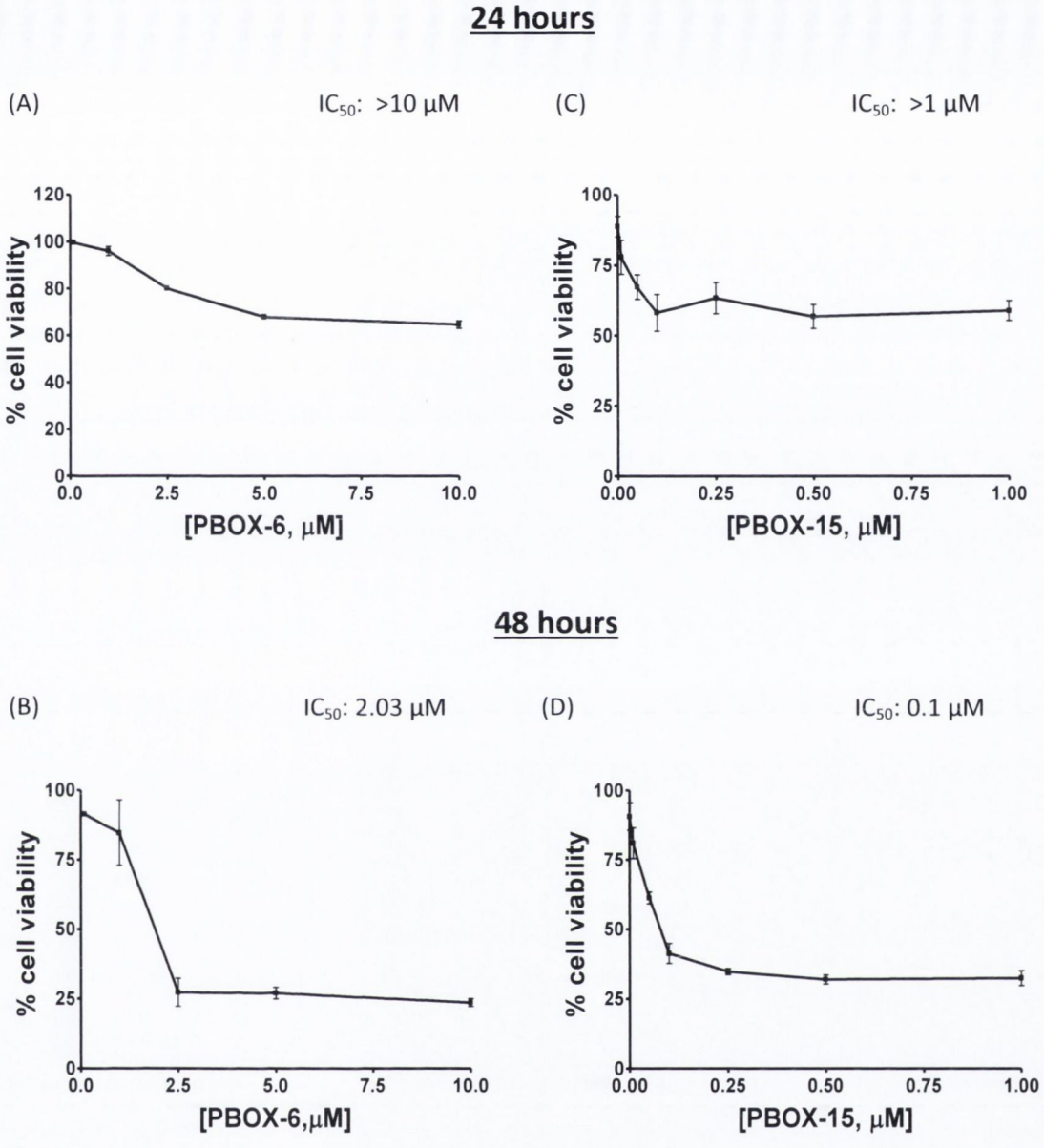

Figure 5.4 PBOX-6 and -15 reduce the viability of SHSY5Y neuroblastoma cells.

SHSY5Y cells were seeded at a density of 2.5 X 10^5 cells/ml in 96 well plates and left for overnight to attach. Cells were treated with a vehicle (1% (v/v) ethanol) or a range of concentrations of (A, B) PBOX-6 or (C, D) PBOX-15. After 24 (A, C) or 48 (B, D) hours, cells were harvested, and 20 μl alamarBlue was added to each well. Plates were incubated in the dark for up to 5 hours until a colour change was observed. Fluorescence was measured using a SpectraMax Gemini plate reader at excitation and emission wavelengths of 544nm and 590nm respectively. Values represent the mean ± S.E.M of three independent experiments.

(A)

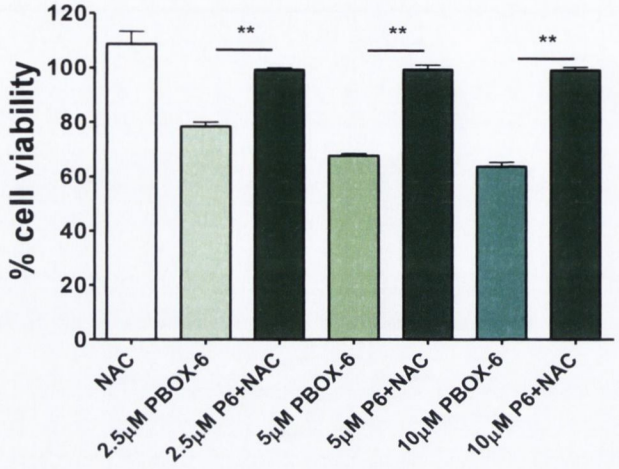

(B)

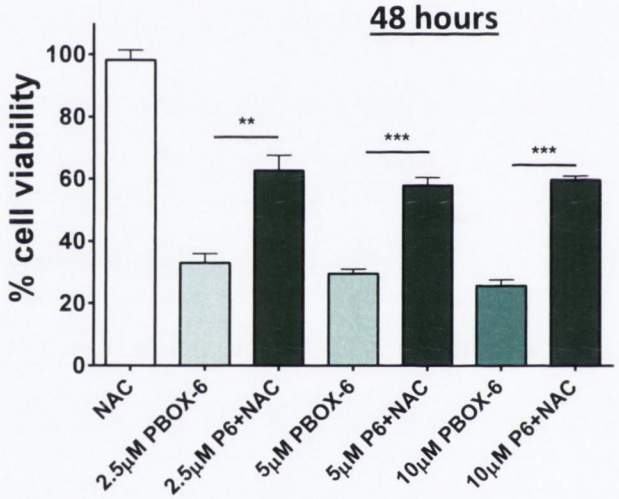

Figure 5.5 Pretreatment with the antioxidant NAC significantly inhibits the anti-proliferative effects of PBOX-6 in SHSY5Y cells.

SHSY5Y cells were seeded in the log phase of growth at 5 x 10^3 cells/well and left to adhere overnight. The following day cells were either treated with varying concentrations of PBOX-6 (2.5, 5, 10 μM), or pretreated with 5 mM NAC for 1 hour followed by varying concentrations of PBOX-6 (2.5, 5, 10 μM) for (A) 24 or (B) 48 hours. After the required incubation time, cells were harvested and 20 μl alamarBlue was added to each well. Plates were incubated in the dark for up to 5 hours until a colour change was observed. Fluorescence was measured using a SpectraMax Gemini plate reader at excitation and emission wavelengths of 544nm and 590nm respectively. Values represent the mean ± S.E.M of three independent experiments. Statistical analysis was performed using one way ANOVA with Tukey's multiple comparison test. *** $p<0.001$, ** $p<0.01$.

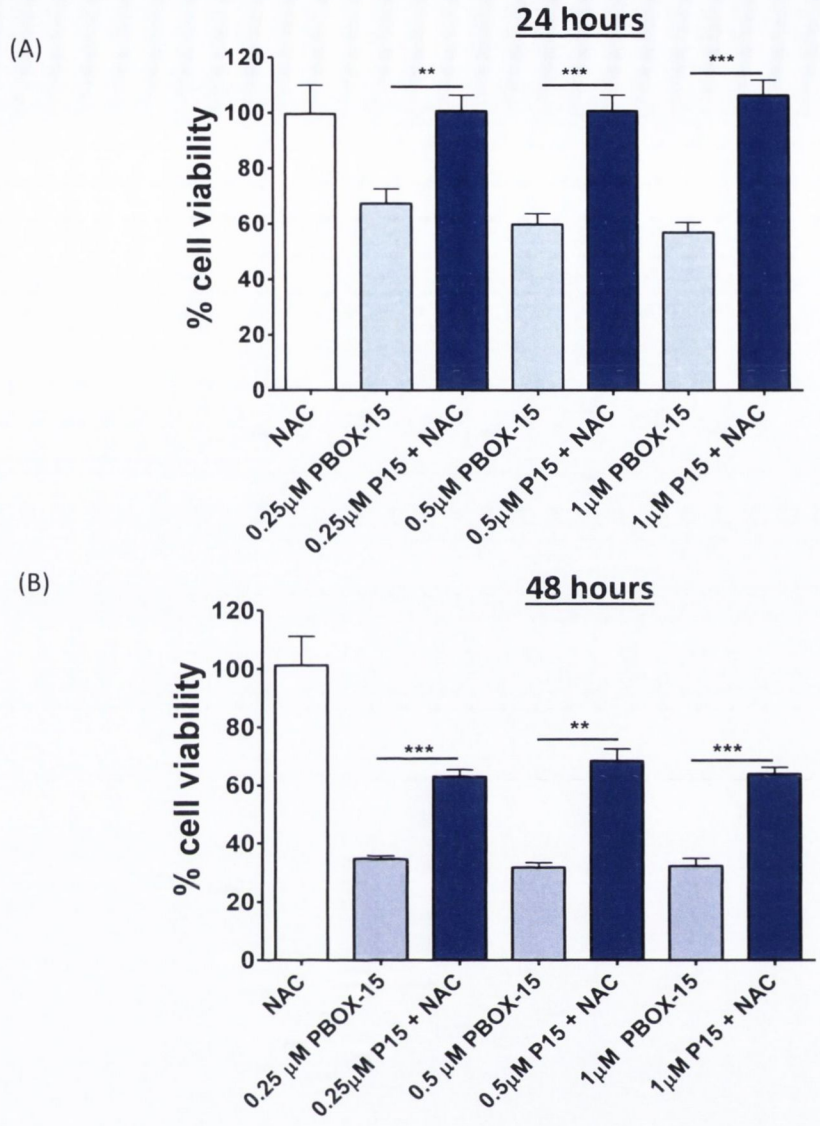

Figure 5.6 Pretreatment with the antioxidant NAC significantly inhibits the anti-proliferative effects of PBOX-15 in SHSY5Y cells.

SHSY5Y cells were seeded in the log phase of growth at 5 x 10^3 cells/well and left to adhere overnight. The following day cells were either treated with varying concentrations of PBOX-15 (0.25, 0.55, 1 μM), or pretreated with 5 mM NAC for 1 hour followed by varying concentrations of PBOX-15 (0.25, 0.55, 1 μM) for (A) 24 or (B) 48 hours. After the required incubation time, cells were harvested and 20μl alamar blue was added to each well. Plates were incubated in the dark for up to 5 hours until a colour change was observed. Fluorescence was measured using a SpectraMax Gemini plate reader at excitation and emission wavelengths of 544nm and 590nm respectively. Values represent the mean ± S.E.M of three independent experiments. Statistical analysis was performed using one way ANOVA with Tukey's multiple comparison test. *** $p<0.001$, ** $p<0.01$.

5.2.5 Pretreatment with N-acetylcysteine reduces PBOX induced apoptosis.

In chapter 3, the reduction in cell viability induced by the PBOXs was attributed to G2/M arrest and induction of apoptosis in SHSY5Y cells (Fig. 3.12, 3.14). Having observed the effects of NAC in combination with the PBOXs on the viability of SHSY5Y cells, an experiment was undertaken to establish the possible protective effects of NAC pretreatment on PBOX-induced apoptosis in these cells.

Pretreatment with NAC was found to significantly protect against induction of apoptosis by both PBOX-6 and -15 up to 48 hours post treatment. For example, after 24 hours 2.5 μM PBOX-6 induced between 21.16% ± 3.3 which decreased to 7.13% ± 3.3 after treatment with NAC (Fig. 5.7). After 48 hours the percentage of apoptosis induced by PBOX-6 alone increased to up to a maximum of 48.12% ± 3.32 which decreased to between 24.6% ± 4.4 and 6.06% ± 1.7 upon pretreatment with NAC (Fig. 5.7). Comparable results were found when cells were treated with PBOX-15 (Fig. 5.8).

These results indicated that NAC was protecting against PBOX-induced apoptosis possibly by inhibiting induction of reactive oxygen species. As apoptosis was only partially inhibited this could be one of a number of pathways through which the PBOXs mediate their anti-cancer effects.

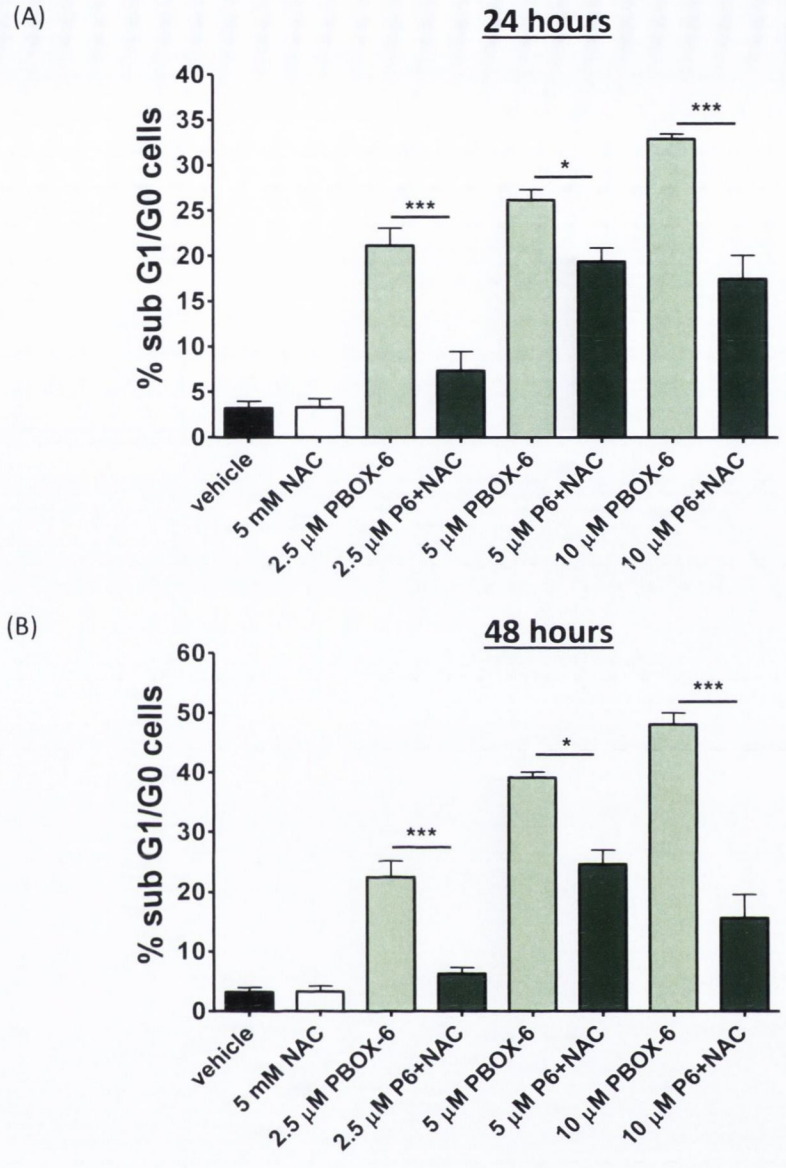

Figure 5.7 Pretreatment with the antioxidant NAC significantly inhibits induction of apoptosis by PBOX-6 in SHSY5Y cells.

SHSY5Y cells were treated with either varying concentrations of PBOX-6 (2.5, 5 or 10 μM) or pretreated with NAC for one hour followed by PBOX-6 (2.5, 5 or 10 μM) for (A) 24 hours or (B) 48 hours. After the required incubation time, cells were harvested, fixed in 2 mls ethanol and stained with propidium iodide. Cells were analyzed by flow cytometry for the percentage of cells undergoing apoptosis and determined by quantification of the sub G1/G0 peak. Values represent the mean ± S.E.M of three independent experiments. Statistical analysis was performed using one way ANOVA with Tukey's multiple comparison test. *** $p<0.001$, ** $p<0.01$, *$p<0.05$.

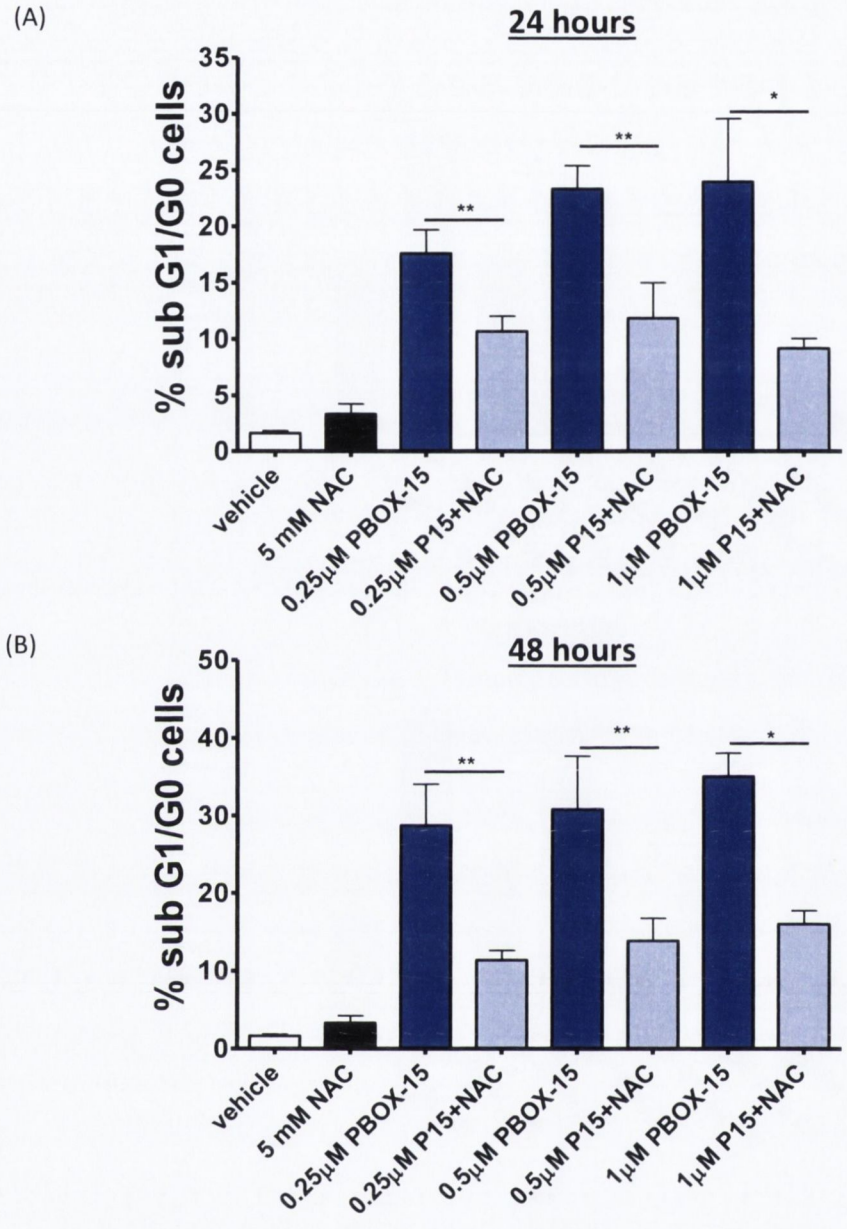

Figure 5.8 Pretreatment with the antioxidant NAC significantly inhibits induction of apoptosis by PBOX-15 in SHSY5Y cells.

SHSY5Y cells were treated with either varying concentrations of PBOX-15 (0.25, 0.55 or 1 μM) or pretreated with NAC for one hour followed by PBOX-15 (0.25, 0.5 or 1 μM) for (A) 24 hours or (B) 48 hours. After the required incubation time, cells were harvested, fixed in 2 mls ethanol and stained with propidium iodide. Cells were analyzed by flow cytometry for the percentage of cells undergoing apoptosis and determined by quantification of the sub G1/G0 peak. Values represent the mean ± S.E.M of three independent experiments. Statistical analysis was performed using one way ANOVA with Tukey's multiple comparison test. ** $p<0.01$, *$p<0.05$.

5.2.6 PBOX-6 inhibits the mTOR signalling pathway in SHSY5Y cells.

Many studies have identified mTOR as a downstream target of AMPK. Reports have indicated that activated AMPK phosphorylates TSC2 and RAPTOR to inhibit mTOR signalling (Gwinn *et al.*, 2008). As PBOX-6 was shown to increase phosphorylation of AMPK indicating activation, it was hypothesised that this MTA may inhibit the mTOR signalling pathway. Therefore assessment of the effects of PBOX-6 on mTOR and its downstream targets p70 S6 kinase, S6 ribosomal protein and eEF2K in SHSYSY cells was carried out.

Activation/inactivation of these proteins was assayed by Western blotting up to six hours post treatment with PBOX-6 was monitored. PBOX-6 was found to decrease phosphorylation of mTOR between 20 and 40 minutes after treatment with PBOX-6 (Fig. 5.9). This decrease was maintained up to six hours after drug exposure indicating inhibition of this pathway and potential inhibition of protein translation and synthesis (Fig. 5.10). Analysis of phosphorylation of p70 S6 kinase was next undertaken; a phospho-specific antibody which recognises phosphorylation at Thr^{389}, a site which has previously been shown to be essential for activation, was utilised. A time dependent decrease in phosphorylation of this site in response to PBOX-6 was observed. Comparable to phosphorylated mTOR this decrease in phosphorylation was first observed approximately 40 minutes post treatment with the maximum level of inhibition being observed 1 hour after exposure. This inhibition was seen to be transient with expression of phosphorylated p70 S6 kinase increasing between 1 and 2 hours, while it should be noted, phosphorylation did not return to the level of the vehicle (Fig. 5.9, 5.10). Previous studies have reported transient effects on p70 S6 kinase activation and inactivation (Choi *et al.*, 2011; Arsikin *et al.*, 2013).

To further examine the effects of the PBOXs in the mTOR signalling pathway, activation of the downstream target S6 ribosomal protein was investigated. When S6 ribosomal protein is phosphorylated, this facilitates the recruitment of the 40S ribosomal subunit onto actively translating polysomes and enhances the translation of 5' TOP mRNAs which code for ribosomal proteins and elongation factors to increase translation. When activated this protein is phosphorylated on multiple residues within the small carboxyl-

terminal region, therefore, the use of several phosphor specific antibodies which recognise multiple sites including Ser235, Ser 236, Ser240 and Ser244 were employed. The effect of PBOX-6 on phosphorylation of S6 ribosomal protein was comparable to those observed on p70 S6 kinase (Fig.5.9, 5.10). A time dependent decrease in phosphorylation of these sites in response to PBOX-6 was observed. A decrease in expression was first noted approximately 40 minutes post treatment with the maximum level of inhibition being observed 1 hour after exposure. This inhibition was seen to be transient with expression of phosphorylated S6 ribosomal protein increasing between 1 and 2 hours, while it should be noted, phosphorylation did not return to the level of the vehicle (Fig. 5.9, 5.10).

In addition to p70 S6 Kinase, the mTOR signalling pathway also regulates the translation elongation process through the phosphorylation of eukaryotic elongation factor 2 (eEF2). eEF2 is a GTP-binding protein that mediates the translocation step of elongation which is inactive when phosphorylated. eEF2 is phosphorylated by eEF2K at Thr^{56} in the GTP binding domain. This phosphorylation prevents eEF2 from binding the ribosome. As inhibition of upstream members of the mTOR signalling pathway had been observed, work was next undertaken to investigate the possible inhibitory effects of PBOX-6 on translation elongation process. Using a phosphor specific eEF2K antibody a decrease in phosphorylation was observed, beginning 40 minutes post treatment with significant inhibition evident from 2 hours post treatment. An almost complete inhibition in expression was observed after 6 hours (Fig 5.9, 5.10).

Taken together these results indicate that PBOX-6 inhibits multiple members of the mTOR signalling pathway in SHSY5Y which may potentially inhibit protein translation in this cell line.

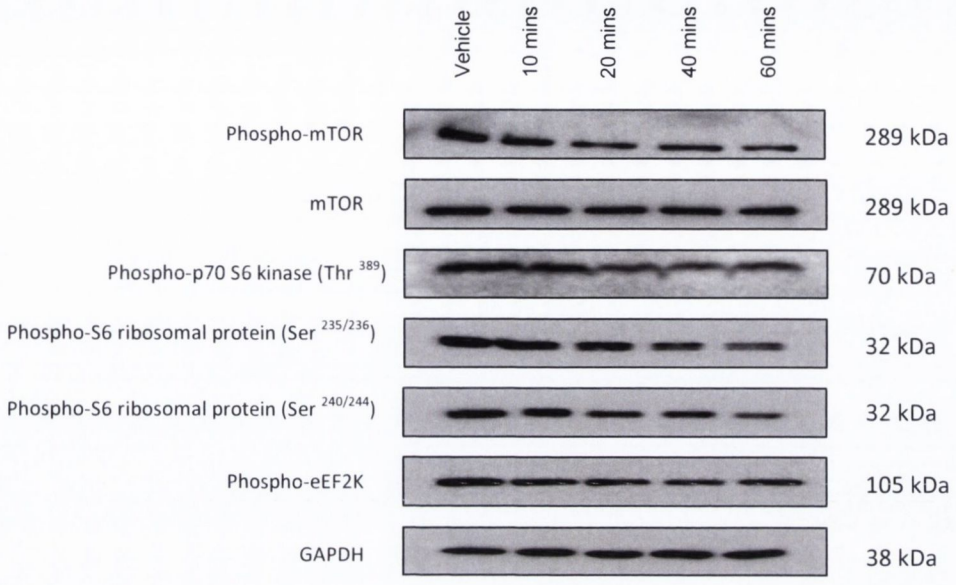

Figure 5.9 Inhibition of the mTOR signalling pathway in SHSY5Y cells in a time dependent manner within 40 minutes of PBOX-6 treatment.

SHSY5Y cells were seeded at a density of 3.0 x 10^5 cells in T25cm^2 flasks and left to adhere overnight. The following day, cells were treated with 2.5 μM PBOX-6 for up to 1 hour. After the required incubation time cells were harvested and lysates were prepared for Western blot analysis. 30 μg of protein was separated on a 6%, 10% or 12% resolving gel with 5% stacking gel, transferred to a PVDF membrane and probed with an anti-phospho-mTOR, anti-mTOR, anti-p70 S6 Kinase, anti-phospho-S6 ribosomal protein or anti-phospho-eEF2K antibody. Membranes were also probed for GAPDH as a loading control. Results are representative of three separate experiments.

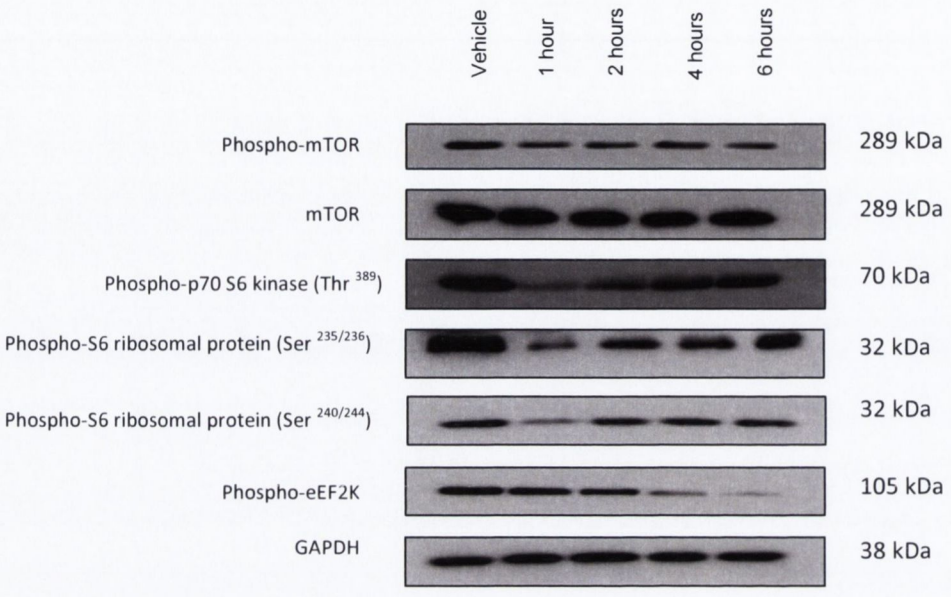

Figure 5.10 PBOX-6 inhibits the mTOR signalling pathway in SHSY5Y cells in a time dependent manner

SHSY5Y cells were seeded at a density of 3.0 x 10^5 cells in T25cm^2 flasks and left to adhere overnight. The following day, cells were treated with 2.5 μM PBOX-6 for up to 6 hours. After the required incubation time cells were harvested and lysates were prepared for Western blot analysis. 30 μg of protein was separated on a 12% resolving gel with 5% stacking gel, transferred to a PVDF membrane and probed with an anti-phospho-mTOR, anti-mTOR, anti-p70 S6 Kinase, anti-phospho-S6 ribosomal protein or anti-phospho-eEF2K antibody. Membranes were also probed for GAPDH as a loading control. Results are representative of three separate experiments.

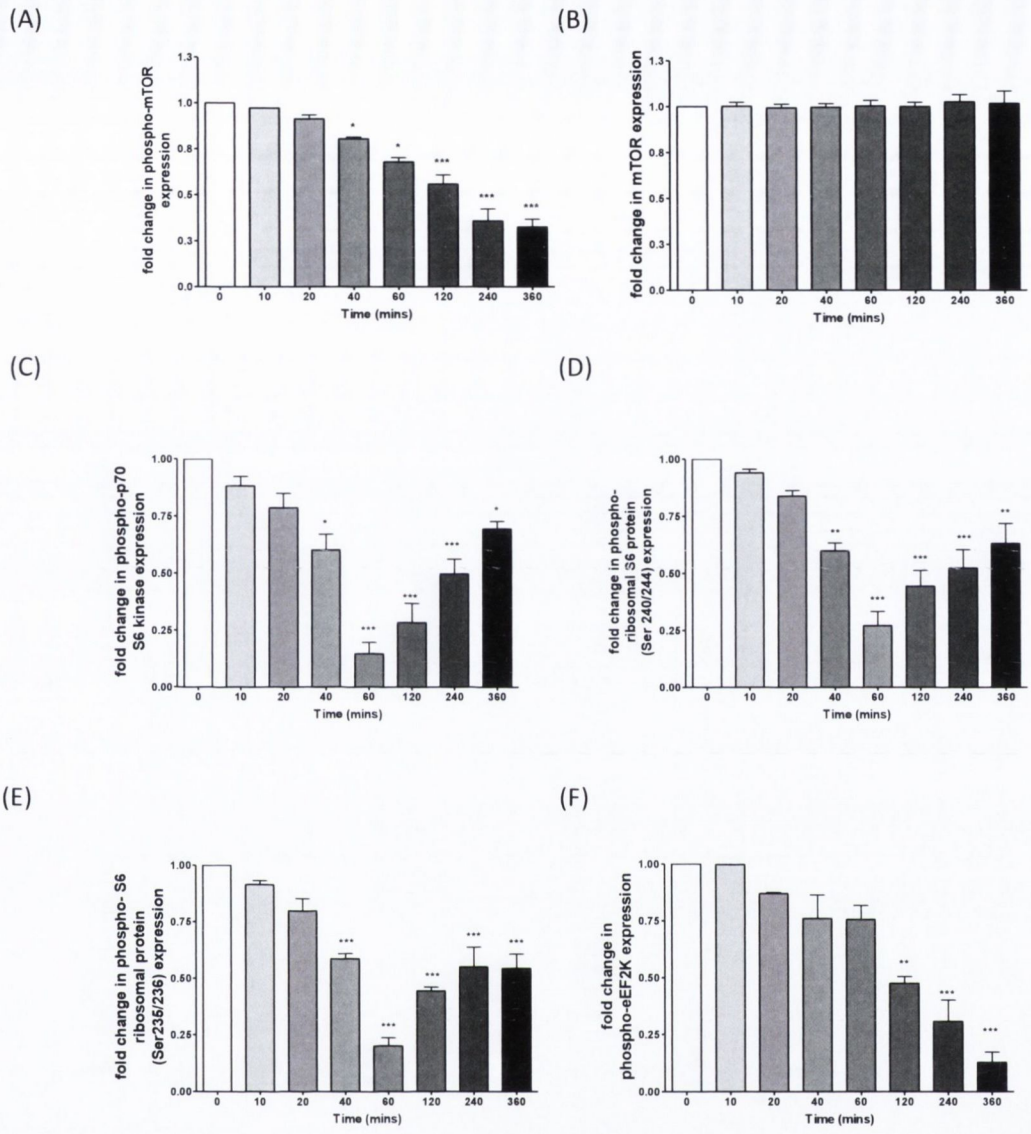

Figure 5.11 Densitometric analysis of phospho-mTOR, mTOR, phospho-p70 S6 kinase, phospho-S6kinase and phospho-eEF2K expression in SHSY5Y cells following PBOX-6 treatment.

Western blots from Fig. 5.9 and 5.10 were normalised to total GAPDH as a control and densitometric analysis of bands was carried out with the imageJ software programme. Statistical analysis was performed using one way ANOVA with Tukey's multiple comparison test. *** $p<0.001$, ** $p<0.01$, *$p<0.05$.

5.2.7 Pretreatment with the antioxidant N-acetylcysteine inhibits the PBOX-6-mediated decrease in Mcl-1 expression.

Primary neuroblastoma tumours have been shown to heterogeneously express Mcl-1, with high expression correlating to high-risk phenotype (Lestini *et al.*, 2009) while downregulation of Mcl-1 expression has been shown to sensitise neuroblastoma cells to chemotherapy (Lestini *et al.*, 2009). In chapter 3, PBOX-6 was shown to induce a time and dose dependent decrease in Mcl-1 expression in SHSY5Y cells (Fig 3.16), while in chapter 4, siRNA mediated knockdown of Mcl-1 sensitised neuroblastoma cells to carboplatin pointing to the importance of Mcl-1 in mediating apoptosis (Fig. 4.16).

Having observed AMPK activation and consequent inhibition of the mTOR signalling pathway, a regulator of protein synthesis controlling multiple components involved in the initiation and elongation stages of translation, it was hypothesised that PBOX-6 induced decrease in Mcl-1 expression may be mediated by activation of AMPK leading to mTOR inhibition, a decrease in phosphorylation of p70 S6 kinase, S6 ribosomal kinase and eEF2K. Altogether this may lead to an inhibition of translation of Mcl-1 and a decrease in expression. As NAC was found to inhibit both AMPK activation and the apoptotic effects of PBOX-6, the effect of this antioxidant on Mcl-1 expression was determined. SHSY5Y cells were pretreated with NAC for 1 hour followed by treatment with varying concentrations of PBOX-6. Pretreatment of cells with NAC prevented PBOX-6 mediated decrease in Mcl-1 expression (Fig. 5.12). These findings may suggest that PBOX-6 induced inhibition of Mcl-1 expression is mediated through the AMPK/mTOR signalling pathway in neuroblastoma cells.

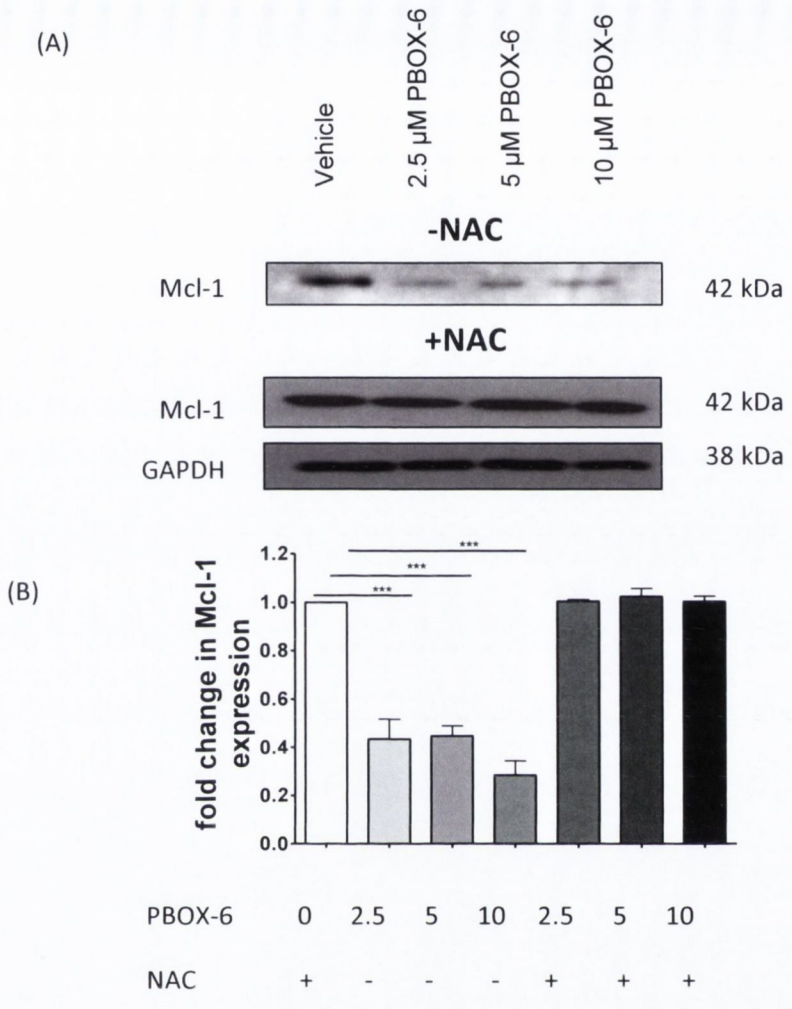

Figure 5.12 Pretreatment with the antioxidant NAC inhibits PBOX-6 mediated decrease in Mcl-1 expression.

(A) SHSY5Y cells were seeded at a density of 3.0 x 10^5 cells in T25cm^2 flasks and left to adhere overnight. The following day, cells were treated with varying concentrations of PBOX-6 (2.5 µM, 5 µM or 10 µM) or pretreated with 5 mM NAC for 1 hour followed by PBOX-6 2.5 µM, 5 µM or 10 µM). After 24 hours cells were harvested and lysates were prepared for Western blot analysis. 30 µg of protein was separated on a 12% resolving gel with 5% stacking gel, transferred to a PVDF membrane and probed with an anti-Mcl-1 antibody. Membranes were also probed for GAPDH as a loading control. Results are representative of three separate experiments. (B) Western blots were normalised to GAPDH and densitometric analysis of bands was carried out with the imageJ software. Statistical analysis was performed using one way ANOVA with Tukey's multiple comparison test. *** $p<0.001$. The effect of varying concentrations of PBOX-6 on Mcl-1 expression was compared to the effect of the vehicle on Mcl-1 expression.

5.2.8 PBOX-6 induces autophagy in SHSY5Y cells.

Autophagy, an evolutionary conserved pathway, is a cellular degradation system which allows for the delivery of cytoplasmic material to the lysosomes for degradation (Codogno *et al.*, 2014). Cytoplasmic components become enclosed in a double membrane structure which fuses with the lysosomes where the contents are hydrolysed. Amino acids and other biomolecules are transported back to the cytosol where they can be reused. In this way autophagy allows for the recycling of cellular material to maintain homeostasis. Rapamycin, a macrocyclic antibiotic produced by the bacterium *Streptomyces hygroscopicus*, was first discovered as an antifungal agent but has since been shown to possess potent immunosuppressive and anti-cancer effects (Seto *et al.*, 2012). Rapamycin binds simultaneously to the intracellular receptor FK506 binding protein 12 of mTORC1. A potential role for the use of rapamycin as an anti-cancer agent has emerged due to its ability to inhibit proliferation of cancer cells *in vitro*, as well as in several human and murine tumour models. Although the direct use of this drug is limited by its hydrophobicity and poor stability in solution, analogues (also referred to as rapalogues) with improved pharmacological feature have been developed and are currently in phase 1/2 clinical trials for various cancers (Albert *et al.*, 2010; De P *et al.*, 2013; Grunt *et al.*, 2013).

Studies of rapamycin have highlighted a possible consequence of mTOR inhibition; as mTOR is a negative regulator of autophagy (by inhibiting autophagasome formation), rapamycin has been shown to induce autophagy. Therefore, as PBOX-6 was demonstrated to inhibit the mTOR signalling pathway, the effects of PBOX-6 on induction of autophagy in neuroblastoma cell lines was next investigated. Autophagy was monitored by flow cytometric analysis of acridine orange stained cells. Acridine orange is a dye which crosses into lysosomes and other acidic compartments in the cell and becomes protonated, and can be detected in the red channel (Greene *et al.*, 2013). Acridine orange which is not protonated emits in the green channels. The red:green fluorescent ratio was calculated to determine the percentage of stained acidic vesicular organelles. PBOX-6 induced autophagy in a dose dependent manner in SHSY5Y cells (Fig 5.13A). Autophagy was first observed after treatment with 1 μM PBOX6 and increased in a dose dependent manner.

To confirm these findings, analysis of expression of LC3 by Western blot was next undertaken. LC3 is a soluble protein with a molecular mass of approximately 17 kDa which is distributed ubiquitously in eukaryotic cells. During autophagy, the autophagosomes engulf cytoplasmic components and a cytosolic form of LC3 (LC3-I) is conjugated to phosphatidylethanolamine to form LC3-phosphatidylethanolamine conjugate (LC3-II), which is recruited to autophagosomal membranes. As a result, the presence of autophagy in a cell can be observed by monitoring the conversion of LC3-I to LC3-II. A dose-dependent increase in the conversion of LC3-I to L3C-II in response to PBOX-6 was observed, indicating PBOX-6 does in fact induce autophagy in SHSY5Y cells. Western blots were also probed with GAPDH to ensure equal loading (Fig.5.13B). Densitometric analysis of Western blots confirmed that PBOX-6 significantly induced expression of LC3-II (Fig. 5.13C).

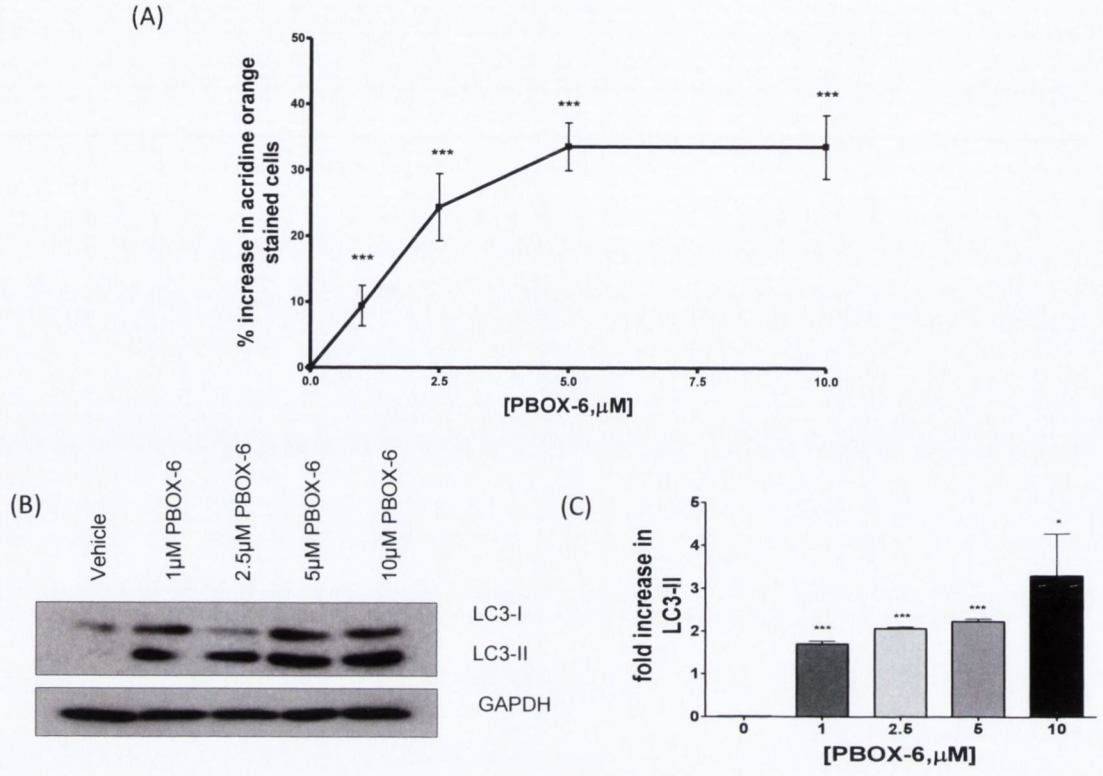

Figure 5.13 PBOX-6 induces autophagy in SHSY5Y cells as monitored by acridine orange staining of AVO and by the appearance of the LC3-II band by Western blotting.

(A) SHSY5Y cells were treated with varying concentrations of PBOX-6 (1 μM, 2.5 μM, 5 μM and 10 μM) for 48 hours. Quantification of PBOX-6-induced AVO formation was assessed by flow cytometric analysis of acridine orange stained cells using the FL3 mode to quantify the bright red fluorescence and the FL1 mode to quantify the green fluorescence. Results are expressed as mean values ± SEM of at least 3 independent experiments and analysed by the Student's *t*-test. *** P <0.001. The effect of varying concentrations of PBOX-6 on AVO expression was compared to vehicle treated cells. (B) SHSY5Y cells were seeded at a density of 3.0 x 10^5 cells in T25cm^2 flasks and left to adhere overnight. The following day, cells were treated with varying concentrations of PBOX-6 (1 μM, 2.5 μM, 5 μM and 10 μM). After 48 hours, cells were harvested and lysates were prepared for Western blot analysis. 30 μg of protein was separated on a 15% resolving gel with 5% stacking gel, transferred to a PVDF membrane and probed with an anti-LC3 antibody. Membranes were also probed for GAPDH as a loading control. Results are representative of thee separate experiments. (C) Western blots were normalised to total GAPDH as a control and densitometric analysis of bands was carried out with the imageJ software. The effect of varying concentrations of PBOX-6 on LC3-II expression was compared to the effect of the vehicle on LC3-II expression. Statistical analysis was performed using one way ANOVA with Tukey's multiple comparison test. *** p<0.001, *p<0.05.

5.2.9 Inhibition of autophagy enhances PBOX-6 induced apoptosis in SHSY5Y cells

Numerous chemotherapeutic drugs have been shown to induce autophagy in tumour cells although the tumour suppressor/survival role of autophagy is still very much debated. Many studies support a tumour survival role of autophagy (Qu *et al*, 2003; Liang *et al.*, 2006); however, some suggest autophagy works as a type of cell death in cancer cells (Clarke., 2012). As induction of autophagy by acridine orange staining of AVOs and an increase in LC3-II in response to PBOX-6 was observed in SHSY5Y cells, determination of whether autophagy was mediating pro-survival or pro-death effects was next undertaken in these cells. The use of two inhibitors of autophagy, bafilomycin-A1; an inhibitor of vascular type H+ ATPases, an enzyme which functions to pump protons across the plasma membrane and acidify intracellular compartments such as the lysosomes (Kanematsu *et al.*, 2010), and chloroquine; a weak base which inhibits lysosomal enzymes (Liang *et al.*, 2014) were employed. Both of these inhibitors disrupt the vesicular proton gradient and increase the pH of acidic vesicles preventing the fusion of autophagosomes with the lysosomes thereby inhibiting autophagy.

If PBOX-6 was inducing autophagic cell death (also referred to as type-II programmed cell death), it was postulated that inhibition of autophagy by bafilomycin-A1 or chloroquine, would decrease cell death, whereas, if autophagy was mediating cell survival, pretreatment with either inhibitor would be expected to increase cell death. SHSY5Y cells were pretreated with chloroquine (10 or 50 μM) or bafilomycin-A1 (10 or 20 nM) for 1 hour, followed by 2.5 μM PBOX-6 for 48 hours. Pretreatment with either inhibitor prevented the PBOX-6-induced increase in AVO formation as demonstrated by flow cytometry (Fig. 5.14, 5.15). Western blotting analysis of LC3 was also undertaken; as expected, both chloroquine and bafilomycin-A1 were shown to increase formation of the LC3- II band (Fig. 5.14, 5.15). As chloroquine is a weak base, it becomes protonated and accumulates inside the lysosome leading to a rise in pH. This increase in pH inactivates acidic lysosomal proteases causing an accumulation of autophagosomes, inhibiting the fusion of autophagosomes with lysosomes. Similarly bafilomycin-A1 inhibits vacuolar H+ ATPase preventing maturation of autophagic vacuoles by inhibiting fusion between autophagosomes and lysosomes. These inhibitors prevent completion of autophagy at the final step, resulting in an accumulation of LC3-II. Accumulation of LC3-II-positive

autophagosomes is evidence of efficient autophagic flux, while failure of LC3-II protein to increase in the presence of such inhibitors, would indicate a defect or delay earlier in the process, prior to degradation at the autolysosome (Barth *et al.*, 2010). Having confirmed both of these inhibitors were effectively inhibiting autophagy, investigation into their effects on PBOX-6 induced apoptotic cell death was next undertaken. Apoptosis was monitored by flow cytometric analysis of propidium iodide stained cells. Pretreatment with chloroquine or bafilomycin-A1 significantly increased PBOX-6 mediated apoptosis in SHSY5Y cells (Fig. 5.16, 5.17). This data, therefore, provides evidence that autophagy functions as a survival mechanism in neuroblastoma cells in response to PBOX-6, and a rationale for the use of autophagy inhibitors to further enhance PBOX-6 induced apoptosis.

Bafilomycin-A1 was chosen as the representative autophagy inhibitor for further investigation. To confirm apoptotic cell death, the cleavage of the DNA repair enzyme PARP was assessed by Western blotting. When a cell is undergoing apoptosis, the 116 kDa proform is cleaved by caspase-3 into an 89 kDa fragment. A decrease in the proform in response to both PBOX-6 and bafilomycin-A1 alone, with a complete disappearance of the proform band in the combination treated lane was observed (Fig. 5.18). These results correlated with the flow cytometry results presented in Fig. 5.17.

The effects of this combination on expression of anti-apoptotic Bcl-2 proteins Mcl-1 and Bcl-2 were next investigated by Western blotting. Both PBOX-6 and bafilomycin-A1 were shown to partially decrease Mcl-1 expression although almost complete inhibition of expression of Mcl-1 in SHSY5Y cells was found following treatment with the combination. The anti-apoptotic effects of Bcl-2 may be prevented through either a decrease in expression or cleavage of this protein. It has previously been reported that PBOX-6 induces cleavage of Bcl-2 in SHSH5Y cells resulting in formation of a pro-apoptotic cleavage fragment. Bafilomycin-A1 was found to induce a slight cleavage of Bcl-2. This cleavage band was more prominent in response to PBOX-6 alone and in combination with bafilomycin-A1 (Fig. 5.18). This study suggests that bafilomyin-A1 significantly enhances PBOX-6-mediated cell death though an apoptotic pathway mediated by a decrease in the anti-apoptotic proteins Mcl-1 and Bcl-2.

Finally, caspase-3 activation in response to either drug alone and in combination was determined. Casapse-3 activation was monitored by the disappearance of the pro-caspase-3 band by Western blotting. Both PBOX-6 and bafilomycin-A1 were shown to activate caspase-3; which correlated with flow cytometry results indicating that both compounds induce similar levels of apoptosis. In contrast, expression of the pro-caspase-3 band was completely diminished in response to a combination of PBOX-6 and bafilomcyin-A1 (Fig. 5.18). Densitometric analysis of Western blots confirmed that inhibition of autophagy by bafilomycin-A1 significantly enhanced PBOX-6 induced apoptosis (Fig. 5.19). Taken together these results indicate that inhibition of autophagy significantly enhances the pro-apoptotic effect of PBOX-6 in SHSY5Y neuroblastoma cells.

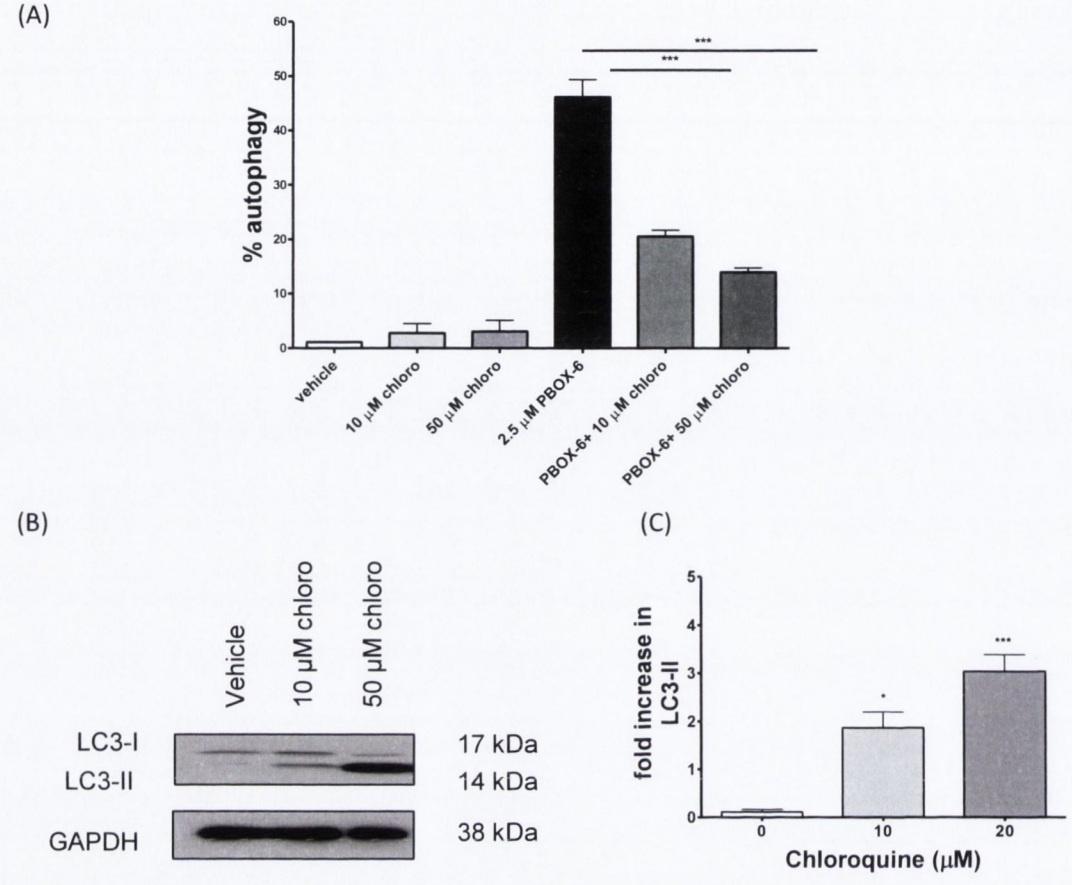

Figure 5.14 Chloroquine inhibits PBOX-6 induced autophagy in SHSY5Y cells.

(A) SHSY5Y cells were treated with either 2.5 μM PBOX-6, 10 or 50 μM chloroquine or a combination of PBOX-6 and chloroquine for 48 hours. Quantification of AVO formation was assessed by flow cytometric analysis of acridine orange stained cells as described in materials and methods. Chloroquine was added 45 min prior to acridine orange staining. Results are expressed as mean values ± SEM of at least 3 independent experiments and analysed by one-way Anova test followed by the Student's *t*-test. *** $P = 0.001$. (B) SHSY5Y cells were seeded at a density of 3.0 x 10^5 cells in T25cm^2 flasks and left to adhere overnight. The following day, cells were treated with varying concentrations of chloroquine (10 and 20μM). After 48 hours, cells were harvested and lysates were prepared for Western blot analysis. 30μg of protein was separated on a 15% resolving gel with 5% stacking gel, transferred to a PVDF membrane and probed with an anti-LC3 antibody. Membranes were also probed for GAPDH as a loading control. Results are representative of thee separate experiments. (C) Western blots were normalised to GAPDH as a control and densitometric analysis of bands was carried out with the imageJ software. The effect of chloroquine on LC3-II expression was compared to the effect of the vehicle on LC3-II expression. Statistical analysis was performed using one way ANOVA with Tukey's multiple comparison test. *** $p<0.001$, * $p<0.05$.

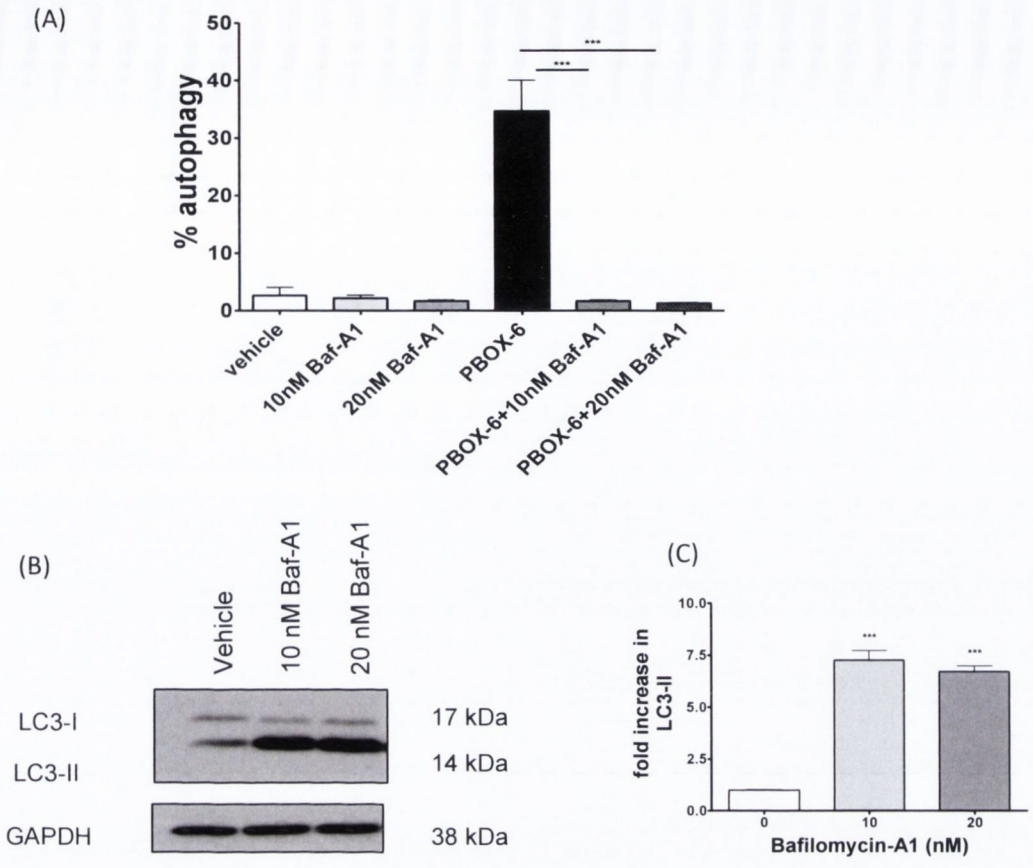

Figure 5.15 Bafilomycin-A1 inhibits PBOX-6 induced autophagy in SHSY5Y cells.

(A) SHSY5Y cells were treated with either 2.5 μM PBOX-6, 10 or 20 nM bafilomycin or a combination of PBOX-6 and bafilomycin-A1 for 48 hours. Quantification of AVO formation was assessed by flow cytometric analysis of acridine orange stained cells as described in materials and methods. Results are expressed as mean values ± SEM of at least 3 independent experiments and analysed using one way ANOVA with Tukey's multiple comparison test. *** $P = 0.001$. (B) SHSY5Y cells were seeded at a density of 3.0×10^5 cells in T25cm^2 flasks and left to adhere overnight. The following day, cells were treated with varying concentrations of bafilomycin-A1 (10 or 20 nM). After 48 hours, cells were harvested and lysates were prepared for Western blot analysis. 30μg of protein was separated on a 15% resolving gel with 5% stacking gel, transferred to a PVDF membrane and probed with an anti-LC3 antibody. Membranes were also probed for GAPDH as a loading control. Results are representative of thee separate experiments. (C) Western blots were normalised to GAPDH as a control and densitometric analysis of bands was carried out with the imageJ software. The effect of bafilomycin-A1 on LC3-II expression was compared to the effect of the vehicle on LC3-II expression. Statistical analysis was performed using one way ANOVA with Tukey's multiple comparison test. *** $p<0.001$.

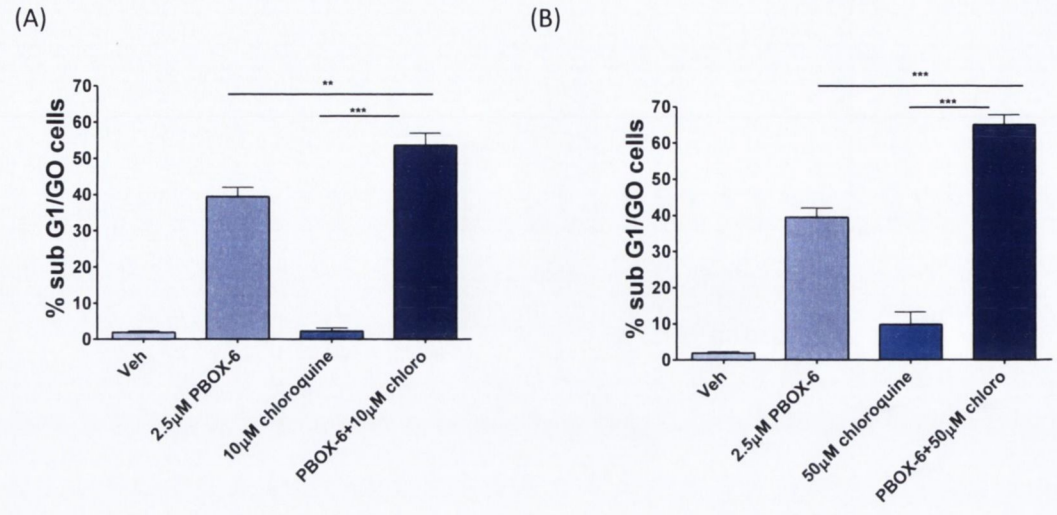

Figure 5.16 Inhibition of autophagy by chloroquine enhances PBOX-6-mediated apoptosis in SHSY5Y cells.

SHSY5Y cells were seeded at a density of 1.0 X 10^6 cells/ml in 6 well plates and left to adhere overnight. Cells were treated with vehicle (1% (v/v) ethanol), 2.5 μM PBOX-6, 10 μM or 50 μM chloroquine or a combination of both (A, B). After 72hrs cells were harvested, resuspended in 200 μL PBS, fixed in 2 mls ethanol and stained with propidium iodide. Cells were analysed by flow cytometry and the percentage of apoptotic cells was determined by quantification of the sub-G1/G0 peak. Values represent the mean ± S.E.M of at least three independent experiments. Statistical analysis was performed using one way ANOVA with Tukey's multiple comparison test. *** $p<0.001$, ** $p<0.01$.

(A)

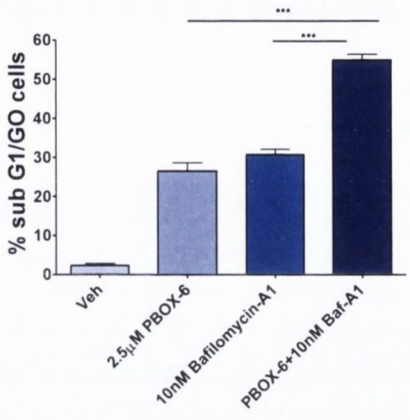

(B)

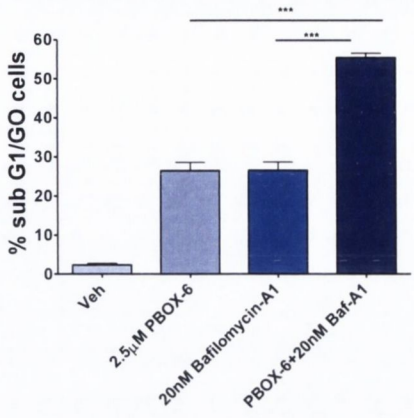

Figure 5.17 Inhibition of autophagy by bafilomycin-A1 enhances PBOX-6 mediated apoptosis in SHSY5Y cells.

SHSY5Y cells were seeded at a density of 1.0 X 10^6 cells/ml in 6 well plates and left to adhere overnight. Cells were treated with vehicle (1% (v/v) ethanol), 2.5μM PBOX-6, 10nM, 20nM or 50nM bafilomycin-A1 or a combination of both (A, B). After 72hrs cells were harvested, resuspended in 200 μL PBS, fixed in 2 mls ethanol and stained with propidium iodide. Cells were analysed by flow cytometry and the percentage of apoptotic cells was determined by quantification of the sub-G1/G0 peak. Values represent the mean ± S.E.M of at least three independent experiments. Statistical analysis was performed using one way ANOVA with Tukey's multiple comparison test. *** $p<0.001$.

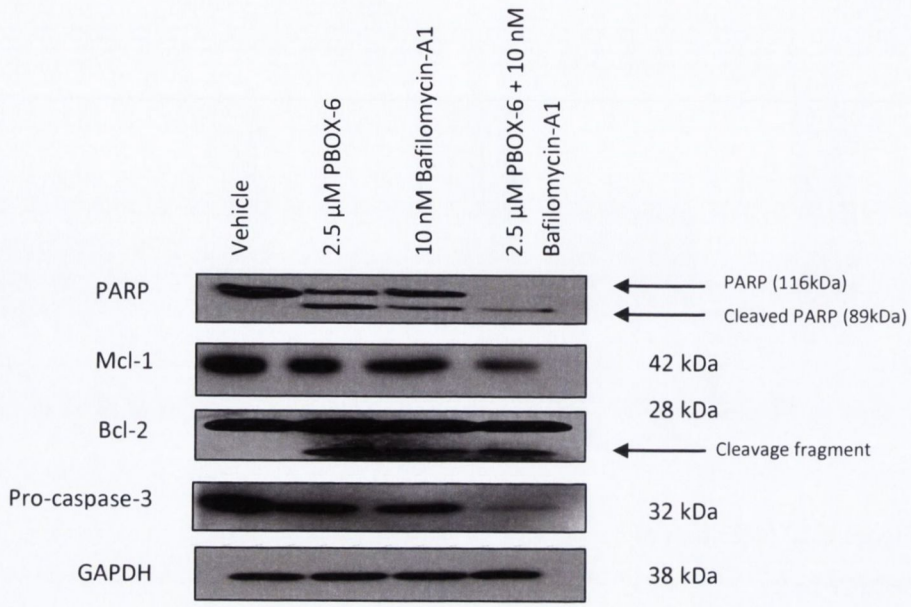

Figure 5.18 Autophagy inhibition enhances PBOX-6 mediated apoptosis though a decrease in anti-apoptotic Mcl-1, cleavage and inactivation of anti-apoptotic Bcl-2 and activation of executioner caspase-3.

SHSY5Y cells were seeded at a density of 3.0 x 10^5 cells in T25cm^2 flasks and left to adhere overnight. The following day, cells were treated with 2.5 µM PBOX-6, 10 nM bafilomycin-A1 or a combination of both. After 72 hours cells were harvested and lysates were prepared for Western blot analysis. 30 µg of protein was separated on a 10% or 12% resolving gel with 5% stacking gel, transferred to a PVDF membrane and probed with an anti-PARP, anti-Mcl-1, anti-Bcl-2 or anti-pro-caspase-3 antibody. Membranes were also probed for GAPDH as a loading control. Results are representative of three separate experiments.

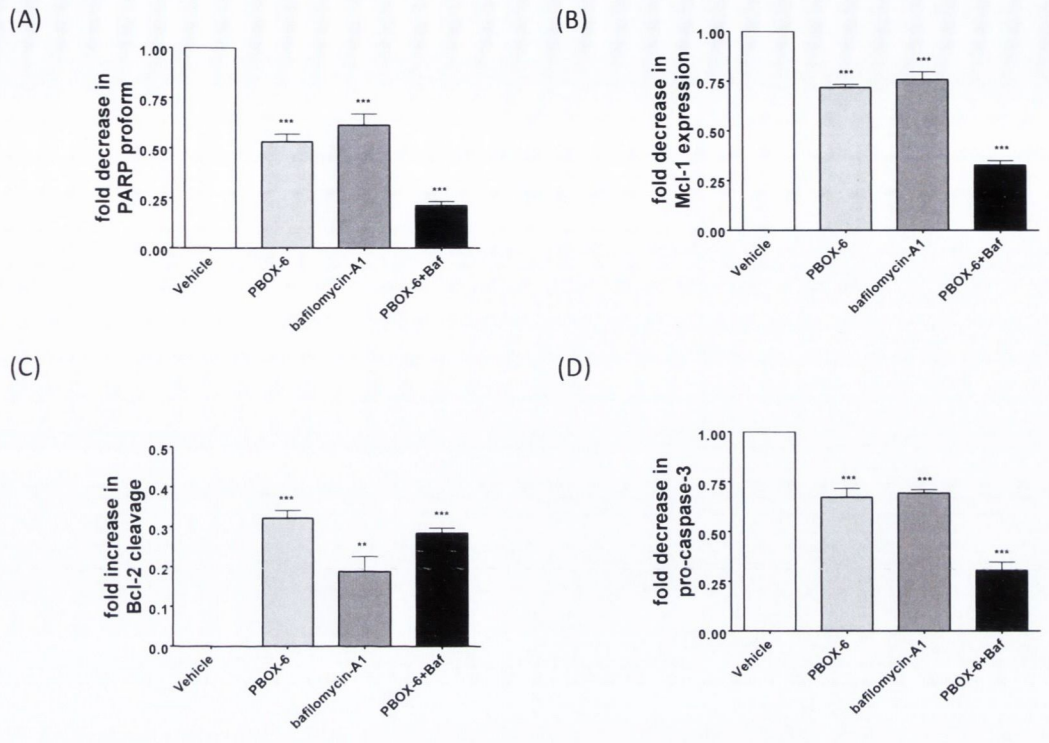

Figure 5.19 Densitometric analysis of PARP, Mcl-1, Bcl-2 and pro-caspase-3 expression in SHSY5Y cells

Results are representative of three separate experiments. Western blots from Fig. 5.18 were normalised to total GAPDH as a control and densitometric analysis of bands was carried out with the imageJ software. The fold change in protein expression was determined by comparison of PBOX-6, bafilomycin-A1 and combination treated cells to the vehicle. Statistical analysis was performed using one way ANOVA with Tukey's multiple comparison test. *** $p<0.001$, ** $p<0.01$, *$p<0.05$. The effect of PBOX-6, bafilomycin-A1 or a combination of the two on PARP cleavage, Mcl-1, Bcl-1 and caspase-3 expression was compared to vehicle treated cells.

5.3 Discussion

AMPK, a master regulator of homeostasis, is activated in response to stresses such as a decrease in glucose levels, ischaemia or hypoxia (Hardie *et al.*, 2012). AMPK functions to monitor the ratios of AMP/ATP and ADP/ATP; as ATP is consumed by the cells, levels of AMP and ADP increase. A decrease in ATP leads to AMPK activation; AMP directly binds to the γ subunit of AMPK to prevent dephosphorylation of the critical thr^{389} residue in the activation loop of the α subunit (Sanders *et al.*, 2007). Activation results in the inhibition of anabolic pathways which consume ATP such as protein synthesis and the switching on of catabolic pathways which produce ATP such as autophagy resulting in restoration of cellular energy homeostasis (Kim *et al.*, 2011). In order for a tumour to grow, a cell must redirect its bioenergetic resources towards the replication of components such as DNA, proteins and membranes etc., leading to an anabolic shift in cellular metabolism. As AMPK switches off anabolic pathways, activation of this kinase would appear to play a tumour suppressing role. Previous studies have demonstrated that activation of AMPK inhibits the synthesis of the majority of cellular macromolecules, proteins, ribosomal RNA, cholesterol and glycogen (Hardie *et al.*, 2007; 2011; 2012) while also causing cell cycle arrest associated with stabilization of p53 and the cyclin-dependent kinase inhibitors $p21^{WAF1}$ and $p27^{CIP1}$ (Jones *et al.*, 2005; Liang *et al.*, 2007). As multiple chemotherapeutics have been shown to induce AMPK activation, it was of interest to determine the effects of the PBOXs on AMPK activation in SHSY5Y cells.

Western blotting analysis was employed to elucidate the effects of PBOX-6 on AMPK activation and determined PBOX-6 induced activation in a time dependent manner. Additionally phosphorylation and inactivation of Acetyl-CoA carboxylase (ACC), a downstream target of AMPK was observed. These findings are in agreement with previous reports detailing AMPK activation in response to MTAs (Chen *et al.*, 2011). Both vincristine and taxol were found to induce AMPK activation in a time and dose dependent manner. siRNA-mediated knockdown of LKB1, the upstream activator of AMPK was shown to inhibit vincristine induced AMPK activation in B16 melanoma cells. Furthermore Chen *et al.,* (2009) highlighted the role of AMPK in mediating the pro-apoptotic effects of reactive oxygen species, H_2O_2. H_2O_2 induced a time and dose dependent phosphorylation and activation of AMPK in PC12 and primary neurons. Expression of a dominant negative

form of AMPK or downregulation of AMPK partially preventing induction of H_2O_2 induced cell death.

AMPK has been reported to promote apoptosis through regulation of downstream signalling pathways including JNK (Meisse *et al.*, 2002; Kang *et al.*, 2012), p53 (Okoshi *et al.*, 2008) and mTOR (Gwinn *et al.*, 2008). The role of JNK in PBOX-mediated apoptosis has previously been elucidated; pretreatment of K562 CML cells with dicoumarol, a JNK inhibitor prevented PBOX-6-induced phosphorylation of JNK substrates, c-Jun and ATF-2 and inhibited the induced apoptosis while transfection of K562 cells with the JNK scaffold protein, JIP-1, inhibited JNK activity and apoptosis induced by PBOX-6 (McGee *et al.*, 2002). Interestingly, AMPK activation has been shown to induce apoptosis through stimulation of JNK in MIN6 cells (Kefas *et al.*, 2003) while the organic anti-cancer agent plumbagin, was shown to activate AMPK and JNK preceding apoptosis in colon cancer cell lines (Chen *et al.*, 2013). Studies of the anti-diabetic, compound K, reported inhibition of palmitate induced apoptosis, while conversely the activator of AMPK, AICAR attenuated the inhibitory effects of compound K on AMPK and JNK activation (Guan *et al.,* 2014). Based on these studies and findings presented herein, it could be hypothesised that PBOX-6-mediated activation of AMPK may induce JNK activation preceding induction of G2/M arrest and apoptosis, although this would require further investigation in neuroblastoma cell lines.

Interestingly, AMPK has been implicated in the control of multidrug resistance (MDR). Kim *et al.,* (2011) reported that metformin inhibited P-gp expression in the MCF-7 breast cancer cell line by blocking MDR1 gene transcription. Metformin also significantly increased the intracellular accumulation of the fluorescent P-gp substrate rhodamine-123. It was found that suppression of MDR1 expression was mediated through metformin- induced activation of AMPK. siRNA mediated knockdown of AMPK attenuated the inhibition of P-gp while overexpression of a dominant-negative mutant of AMPK reversed the inhibitory effect of metformin on P-gp expression. Similar findings have been reported more recently by Wu *et al.,* (2014), cordycepin, the bioactive compound in genus Cordyceps, induced growth inhibition and apoptosis in a panel of gall bladder cell lines and inhibited P-gp expression though activation of AMPK signalling. Conversely AMPK shRNA depletion inhibited cordycepin-induced apoptosis. Two AMPK activators,

AICAR and A769662, were found to downregulate MDR expression which was largely inhibited by AMPK depletion. These reports further support the use of AMPK activating drugs as a novel treatment strategy for MDR cancers such as neuroblastoma.

Having observed PBOX-6-induced activation of AMPK, these findings prompted us to examine both the upstream and downstream events associated with AMPK activation in SHSY5Y cells. Determination of the role of ROS production in PBOX mediated apoptosis was next undertaken. PBOX-6 induced an early increase (from 1 hour) in ROS production. This is in agreement with reports detailing the effect of MTAs on ROS production where both vincristine and taxol were shown to induce apoptosis mediated by ROS production (Chen *et al.*, 2011).

Various mechanisms have been described to account for the generation of ROS in response to chemotherapeutics, including redox cycling, p53-mediated mitochondrial oxidase activation or electron transport chain disruption (Hwang *et al.*, 2001; Pelicano *et al.*, 2003, 2004). The electron transport chain, composed of four complexes, is located within the inner mitochondrial membrane. Electrons are transferred from NADPH dehydrogenase (complex 1) to succinate dehydrogenase (complex 2) to coenzyme Q10 and to cytochrome c (complex 3). The passing of electrons creates a proton gradient; finally these electrons pass to the ATP synthase (complex 4) which uses this protein gradient to drive the production of ATP. The electrons which pass from complex 3 to complex 4 result in the formation of 0_2 and H_20. About 2% of these electrons escape and react with molecular oxygen to form superoxide which is converted to hydrogen peroxide by SOD (Conklin *et al.*, 2004). Chemotherapeutic drugs may induce permeabilisation of the mitochondrial membrane leading to the release of cytochrome c (Pelicano *et al.*, 2003). When this occurs the flow of electrons along the electron transport chain is disrupted; electrons are diverted from the electron transport chain to oxygen by NADPH dehydrogenase and reduced coenzyme Q10 resulting in the formation of superoxide radicals. It is possible that the PBOXs are producing ROS through disruption of the electron transport chain but this would require further investigation.

The NADPH oxidase (NOX) family of proteins have also been implicated in the generation of ROS (Bedard *et al.*, 2007). The NOX family comprises seven members, NOX 1–5 and the

dual oxidases (DUOXs) DUOX 1 and DUOX 2. The NOX complexes were initially thought to be specific to phagocyte cells, but these enzymes are now recognized as being almost universally expressed in virtually every tissue in the body (Paletta-Silva *et al.*, 2013). They are composed of six subunits; a Rho GTPase and five 'phox' units (gp91phox, p21phox, p40phox, p47phox and p67phox) (Jiang *et al.*, 2011). These are transmembrane proteins which generate superoxide by transferring electrons from the inside of the cell across the membrane, coupling them to molecular oxygen to produce a superoxide anion which dismutases into hydrogen peroxide. NOX donates an electron from NADPH to molecular oxygen (O_2) to produce superoxide (O_2^-). MTAs have previously been reported to produce ROS mediated by NOX. Paclitaxel was found to increase expression of Rac1, a positive regulator of NOX and activate the membrane associated NOX, leading to extracellular release of superoxide, which is subsequently converted to hydrogen peroxide (Alexandre *et al.*, 2007). It is possible the PBOX-6 is producing ROS through an increase in NOX expression although this would require further investigation. To further support this theory, recent reports have suggested that the activity of NOX is regulated by the MAPK family, in particular JNK, a key mediator in PBOX-6-induced apoptosis (McGee *et al.*, 2002). Inhibition of JNK significantly attenuated NADPH oxidase activation and the upregulation of components, while also reducing production of H_2O_2 (Han *et al.*, 2012).

The antioxidant NAC, a scavenger of these free radicals, has been extensively used as a tool to elucidate the role of oxidative stress in numerous human pathologies including cancer, arthritis and cardiovascular disease among others. Pretreatment with the antioxidant NAC was found to inhibit the anti-proliferative effects of both PBOX-6 and -15 while an induction of apoptosis was diminished upon pretreatment with NAC. Taken together these results would point to a role of ROS in mediating PBOX-6-induced apoptosis in SHSY5Y cells. These findings are supported by previous reports in the literature detailing the effects of both ROS producing drugs and NAC on various cancer cell lines. Numerous ROS producing drugs have been shown to induce mitochondrial damage and cell death. Safingol, a sphingolipid currently in phase 1 clinical trials for the treatment of solid tumours, was found to produce a time and dose dependent increase in ROS in MDA-MB-23 and HT-29 cell lines (Ling *et al.*, 2011). Production of ROS was shown to damage cellular components and activate various pathways including autophagy while

pretreatment with NAC inhibited ROS production and consequently cell death. Similarly hydrogen peroxide was shown to induce apoptosis in PC12 and SHSY5Y cells which was associated with inhibition of proteins phosphatases and activation of the MAPK pathway. The expression of the prosurvival proteins, AKT and PDK1 were shown to be decreased after exposure to hydrogen peroxide. Furthermore hydrogen peroxide induced apoptosis in primary mouse neurons. In addition to these reports, cisplatin has been shown to induce ROS production in a panel of small cell lung carcinoma cell lines (Wu *et al.*, 2005). Cisplatin binds to DNA forming covalent platinum DNA adducts and triggers activation of multiple pathways including DNA repair, transcription inhibition, cell cycle arrest and apoptosis (Siddik *et al.*, 2003). Generation of ROS lead to activation of the intrinsic pathway as evidenced by the increase in pro-apoptotic Bax, activation of initiator caspase-9 and effector caspase-3 and an increase in PARP cleavage. The effects of cisplatin were prevented by pretreatment with NAC.

AMPK sits at the centre of a multitude of interconnecting signalling pathways which regulate a diverse range of cellular activities (Hardie *et al.*, 2012). Activation of AMPK triggers a phosphorylation cascade with targets ranging from transcription factors to enzymes and other regulatory proteins. Reports from several laboratories have identified one of the major growth regulatory pathways controlled in part by AMPK, the mTOR signalling pathway. mTOR is a serine/threonine kinase belonging to the PIKK family present in two distinct complexes mTORC1 and mTORC2. This kinase is highly conserved in eukaryotes as a regulator of cell growth. mTOR coordinates signals from multiple pathways and many observations have pointed to this pathway laying a critical role in oncogenesis and cancer progression in multiple cancers including neuroblastoma (Bitting *et al.*, 2013; Vinayak *et al.*, 2013; Barrett *et al.*, 2013; Matter *et al.*, 2014). Similar to AMPK, mTOR sits at a central point in a signalling pathway consisting of many components implicated in tumourigenesis including AKT, PI3K and eIF4E which may behave as oncoproteins, and PTEN, TSC1/TSC2 and LKB1 which may function as tumour suppressors. Therefore, regulation of this pathway is paramount to preventing development of cancer. Regulation of mTOR may play a critical anti-cancer role in neuroblastoma through either downregulation of tumour promoters or upregulation of tumour suppressors.

Numerous observations have drawn attention to the role of mTOR signalling in oncogenesis and cancer progression in certain cancers including neuroblastoma. Constitutive activation has been shown to correlate with deregulated metabolism, increased proliferation and resistance to apoptosis (Johnsen *et al.*, 2008). Johnsen *et al.*, (2008) investigated the phosphorylation status of key proteins in the mTOR pathway in a panel of neuroblastoma cell lines and tissue samples. They found all primary samples expressed phosphorylated mTOR indicating constitutive activation. A panel of neuroblastoma cell lines were treated with mTOR inhibitors (rapamycin and temsirolimus) and it was found that both inhibitors induced apoptosis which was accompanied by caspase-3 activation and PARP cleavage. It was noted that MYCN amplified cell lines were more sensitive to mTOR inhibitors (rapamycin and CCI-779); while cells with the lowest expression of MYCN exhibited the least sensitivity to rapamycin and temsirolimus. This is of particular interest as approximately 25% of patients are diagnosed with MCYN amplification, a diagnosis which correlates with advanced stage disease refractory to treatment. To further explore the differences in sensitivity, SH-EP neuroblastoma cells were stably transfected with an inducible MYCN construct. These MYCN-expressing cells were found to be significantly more sensitive to mTOR inhibitors than the mock transfected cells indicating that MYCN is a therapeutic target for mTOR inhibition. Furthermore, rapamycin and CCI-779-treated xenografts showed significant reduction of proliferation and increased apoptosis *in vivo* compared to untreated controls. Taken together these findings suggest that the mTOR signalling pathway is overactive in neuroblastoma and drugs which inhibit this pathway may represent a novel therapeutic strategy particularly for the treatment of advanced stage MYCN amplified tumours.

Therefore, having established the effect of PBOX-6 on ROS production and AMPK activation as well as the chemoprotective effects of NAC, we next sought to examine the effects on the mTOR pathway. A time dependent inhibition of mTOR in response to PBOX-6 was observed while a transient decrease in phosphorylation of the downstream target p70 S6 kinase and S6 ribosomal proteins was observed. Previous studies have reported transient effects on p70 S6 kinase activation and inactivation. AICAR was found to induce a decrease in phosphorylation (up to 1 hour post treatment) followed by a time-

dependent increase (up to 24 hours) which preceded a second decrease in phosphorylation (after 48 hours) in CAL62 thyroid carcinoma cell line, although the authors of this paper did not provide an explanation for these findings (Choi *et al.*, 2011). Similarly Arsikin *et al.,* (2012) observed a transient decrease in phospho-p70 S6kinase, despite continuous inhibition of phospho-mTOR in response to dopaminergic neurotoxin 6-hydroxydopamine (6-OHDA) in SHSY5Y cells. Similarly these authors did not provide an explanation for these findings.

Although mTOR phosphorylates p70 S6 kinase, other proteins have been implicated in its regulation. p70 S6 kinase has been reported to be phosphorylated by PDK1 (Alessi *et al.*, 1998). PDK1 is activated downstream of P13K. Over activation of the PI3K/Akt pathway in neuroblastoma has been reported to correlate with poor prognosis (Santo *et al.*, 2013). It is hypothesised that over activation of this pathway in SHSY5Y cells may lead to phosphorylation of p70 S6 kinase in spite of mTOR inhibition although this hypothesis would require further investigation.

Expression of eEF2K was also shown to decrease in a time dependent manner in response to PBOX-6. eEF2K activity is regulated by mTOR through p70 S6 Kinase and S6 ribosomal kinase and independently of mTOR by AMPK. Phosphorylation of eEF2K by p70 S6 kinase and S6 ribosomal kinase leads to inactivation of eEF2K, facilitating the dephosphorylation of eEF2 and thus promoting translation. A decrease in expression of both p70 S6 kinase and S6 ribosomal protein, a substrate of S6 ribosomal kinase, was noted in response to PBOX-6 approximately 40 minutes post treatment, potentially preventing phosphorylation and inactivation of eEF2K. It is possible that even transient inhibition of both p70 S6 kinase and S6 ribosomal protein may be sufficient to inhibit translation of elongation factors such as eEF2.

eEF2K expression may also be regulated by AMPK; it has previously been reported that activated AMPK phosphorylates and inactivates eEF2 via direct phosphorylation of eEF2K by AMPK, at a stimulatory eEF2K site that is different from the inhibitory site phosphorylated by S6 ribosomal kinase (Horman *et al.*, 2002; 2003). The results presented herein demonstrated that activation of this kinase is most evident after 6 hour treatment, during which time phosphorylation of p70 S6 Kinase and S6 ribosomal protein

has increased. In contrast, phosphorylation of AMPK was found to be maximal after 6 hours potentially indicating regulation of eEF2K by AMPK. Therefore, it is possible that both kinases are contributing to eEF2K activation in SHSY5Y cells. Taken together these results indicate that PBOX-6 inhibits multiple members of the mTOR signalling pathway in SHSY5Y which may potentially inhibit protein translation in this cell line.

mTOR inhibitors have been reported to execute their anti-cancer effects though two mechanisms; firstly by inhibiting proliferation by induction of cell cycle arrest. Secondly they act as cytotoxic agents which induce apoptosis. The ability of the PBOX compounds to induce both G2/M arrest and apoptosis in neuroblastoma had already been demonstrated in chapter 3. Furthermore in chapter 4, gene silencing of Mcl-1 had demonstrated the importance of Mcl-1 downregulation in the apoptotic pathway mediated by PBOX-6 in neuroblastoma cell lines. To further explore the role of mTOR inhibition in PBOX-6 induced cell death, the effects of NAC on Mcl-1 expression post PBOX-6 treatment was determined. As NAC was found to exhibit a protective effect against the action of PBOX-6, it was postulated this may occur by inhibiting the PBOX-6 mediated decrease in Mcl-1 expression. Pretreatment with NAC was found to abrogate the effects of PBOX-6 on Mcl-1 expression. This was in agreement with previous reports of the inhibition of the mTOR pathway by the diuretic, ethacrynic acid, leading to a block in translation of Mcl-1, which could be blocked by pretreatment with NAC in HL-60 cells (Liu *et al.*, 2013). It is likely that PBOX-6 induced mTOR inhibition is an early event (up to 6 hours) which precedes PBOX-6 induced cell cycle arrest and apoptosis in SHSY5Y cells.

In addition to the effects on proliferation and survival, inhibition of mTOR may have a potential role for the treatment of bone metastasis; a condition which reduces quality of life as they are associated with conditions such as nerve compression, bone pain and fractures. Destruction of bone is mediated by factors produced or induced by tumour cells such as receptor activator of NF-kappaB ligand (RANKL) (Lacey *et al.*, 1998). Osteoprotegerin (OPG) is a competitive inhibitor of RANKL, which has been proposed to be regulated by mTOR. Upregulation of OPG was found to decrease the incidence of bone lesions and metastasis in neuroblastoma, while in an *in vivo* neuroblastoma murine model, treatment with rapamycin significantly increased levels of serum OPG, which increased cortical bone density and delayed progression to fracture, indicating a

significant protective effect against metastatic disease (Hartwich *et al.*, 2013). Although the effect of the PBOXs on OPG production has not yet been investigated, these results would support the hypothesis that other mTOR inhibitors such as PBOX-6, may increase OPG production and prevent metastasis, further supporting the use of the PBOXs as a novel treatment strategy for neuroblastoma.

As a solid tumour, such as neuroblastoma, grows and metastasises, nutrient and oxygen availability decreases due to a poorly formed vasculature resulting in the development of hypoxia. Numerous studies have shown a correlation between hypoxia, the development of metastases and poor prognosis (Chang *et al.*, 2014; Gilkes *et al.*, 2014). Cells in this hypoxic environment adapt and the more aggressive, drug resistant cells are preferentially selected. Recent reports suggest that hypoxia activates autophagy to promote tumour cell survival; as a tumour develops, autophagic breakdown and recycling of damaged organelles provides the necessary components for continued tumour cell survival even in conditions of nutrient and growth factor deprivation (Mazure *et al.*, 2010; Hu *et al.*, 2012). To fully elucidate the role of autophagy in cancer, it will be necessary to develop models which enable monitoring of the activation/ inactivation of this pathway throughout the development of malignancy.

To date, despite detailed and systematic investigations, the role of autophagy in cancer remains highly controversial; with both a tumour suppressor and promoter function being proposed (Liang *et al.*, 2006; Yu *et al.*, 2008; Chen *et al.*, 2010; Yang *et al.*, 2011). Autophagy functioning as a form of cell death (termed type-II cell death) has been reported, although, in contrast, a vast number of studies have shown that inhibition of autophagy potentiates the anti-tumour effects of multiple chemotherapeutics, arguing in favour of autophagy functioning as a tumour promoter and survival mechanism (Kanzawa *et al.*, 2003; Longo *et al.*, 2008; Vazquez-Martin *et al.*, 2009; Liu *et al.*, 2009; Li *et al.*, 2012). SHSY5Y cells underwent autophagy in response to treatment with PBOX-6. These findings are in agreement with previous reports detailing PBOX-6-induced autophagy in colon cancer cells (Greene *et al.*, 2012). Having shown PBOX-6-induced autophagy in neuroblastoma cells, it was necessary to establish if activation of this pathway was mediating autophagic cell death or survival, potentially contributing to drug resistance. Greene *et al.*, (2012) found that PBOX-6 and -15 induced both apoptosis and protective

autophagy in human adenocarcinoma-derived colon cancer cells, while inhibition of late stage autophagy by bafilomycin-A1 enhanced the pro-apoptotic effects of PBOX-6. These findings indicate that manipulation of the autophagic pathway can lead to the development of a more effective anti-cancer response. In the present study pretreatment of neuroblastoma cells with chloroquine and bafilomycin-A1 significantly enhanced the apoptotic effects of PBOX-6 in SHSY5Y cells. The enhancement of PBOX-6 cell death by bafilomycin-A1 was characterised by an increase in PARP cleavage, a decrease in expression of Mcl-1, cleavage and inactivation of Bcl-2 and an increase in caspase-3 activation. These findings indicated that a combination of PBOX-6 and autophagy inhibitors represent a novel chemotherapeutic approach for the treatment of neuroblastoma.

Other MTAs have been shown to induce autophagy in cancer cells (Munafo *et al.*, 2001; Zhan *et al.*, 2012; Zhang *et al.*, 2013). Inhibition of paclitaxel-induced autophagy in non small cell lung carcinoma by pretreatment with 3-methyl adenine, a PI3K inhibitor which blocks formation of the autophagosomes, or siRNA against the autophagic gene *beclin 1* potentiated the paclitaxel-induced apoptotic response (Xi *et al.*, 2011), suggesting that comparable with the novel MTA, PBOX-6, paclitaxel-elicited autophagic response plays a protective role that impedes cell death.

CA-432, an analogue of combretastatin A4 (CA-4), a potent inhibitor of tubulin polymerisation, has been shown to induce autophagy in a time and dose dependent manner in adenocarcinoma derived colon cancer cells (Greene *et al.*, 2013). Pharmacological inhibition of autophagy did not inhibit CA-432-induced cell death ruling out type-II programmed cell death. In fact, pretreatment with bafilomycin-A1 significantly increased CA-432-mediated apoptosis, further supporting the hypothesis that the autophagic process may be manipulated to enhance the therapeutic effects of novel MTAs.

The enhancement of apoptosis though autophagic inhibition is not limited to MTAs; the anti-cancer activities of numerous other chemotherapeutics have been increased through modulation of this pathway. Sulfuraphane (SFN) is a potent dietary phytochemical which has been shown to induce cell death in multiple cancers in addition to reducing the

incidence of tumour in *in vivo* breast cancer models (Zhang *et al.*, 1994; Jackson *et al.*, 2004). SFN has also been found to induce protective autophagy in a panel of breast cancer cell lines (Kanematsu *et al.*, 2010). Bafilomycin-A1 mediated inhibition of late stage autophagy potentiated the apoptotic effects of SFN. Comparable with the effects of PBOX-6 and bafilomycin-A1, a combination of SFN and bafilomycin-A1 enhanced PARP cleavage and activation of caspase-3.

In addition to the studies discussed above, a vast number of laboratories have reported enhancement of cell death mediated by inhibition of autophagy. Autophagy inhibitors 3-MA and bafilomycin-A1, have been shown to enhance the cytotoxicity of anthocyanin to human hepatocellular carcinoma cells (Longo *et al.*, 2008), the cytotoxicity of arsenic trioxide to U373-MG human glioblastoma cells (Kanzawa *et al.*, 2003), the cytotoxicity of resveratrol to U251 human glioblastoma cells (Liu *et al.*, 2009) and the cytotoxicity of trastuzumab to trastuzumab-refractory SKBR human breast cancer cells (Vazquez-Martin *et al.*, 2009) further supporting the hypothesis that modulation of the autophagy process through the use of pharmacological inhibitors or knockdown using siRNA or shRNA, can enhance the pro-death effects of chemotherapeutics such as PBOX-6, to overcome resistance and move towards the development of more effective anti-cancer therapeutic strategies.

In conclusion, this study has shown for the first time that PBOX-6-induced production of ROS which preceded PBOX-mediated G2/M arrest and apoptosis. As a result AMPK became activated which inactivated the downstream target ACC leading to inhibition of the mTOR signalling pathway. Pretreatment with the antioxidant NAC partially inhibited the anti-proliferative and apoptotic effects of PBOX-6 and prevented PBOX-6-mediated decrease in Mcl-1 expression, which may suggest that PBOX-6-induced inhibition of Mcl-1 expression is mediated through the AMPK/mTOR signalling pathway in neuroblastoma cells. PBOX-6 was shown to induce autophagy in neuroblastoma cells which may function as a survival mechanism as pretreatment with autophagy inhibitors, chloroquine and bafilomycin-A1, resulted in a significant enhancement of PBOX-6-mediated apoptosis. These findings indicate that manipulation of the autophagic pathway can lead to the development of more effective anti-cancer response. This study provides new insights

into understanding the molecular and cellular mechanisms involved in PBOX-induced cell death in neuroblastoma.

Chapter 6
Concluding Remarks

Chapter 6

Neuroblastoma, a paediatric malignancy of the sympathetic nervous system is the most common extracranial tumour in childhood. Accounting for approximately 15% of all childhood cancer deaths, it is the third most common childhood cancer (Sharp *et al.*, 2013). Despite advances in the understanding of this cancer and the development of new therapeutic strategies, neuroblastoma continues to be one of the most difficult paediatric cancers to treat. Children diagnosed with high risk, advanced stage disease generally have a poor prognosis with less than 40% of these patients being long term survivors (Lunec *et al.*, 2012). High-risk metastatic disease is treated with multiple rounds of intensive chemotherapy leading to major organ toxicity. Up to 30% of patients do not achieve disease control and require further chemotherapy or undergo experimental treatment options. There is a direct correlation between achieving tumour response after induction chemotherapy and survival (Hallett *et al.*, 2012). Many of these who do not respond to treatment develop a progressive disease with failure to respond to chemotherapy.

Although successful for low and intermediate risk neuroblastoma, conventional treatment regimes have not achieved the desired survival rates for high risk patients; it is clear new approaches are necessary to improve survival rates of these patients. Therefore, an investigation into the effects of a series of novel microtubule targeting agents, the PBOXs, was undertaken. These compounds have been previously shown to induce apoptosis in several tumour models including drug resistant patient samples of CML and CLL an *in vivo* CML and breast cancer models. These results suggested the PBOXs present a promising therapeutic strategy for neuroblastoma. In the first part of this study, an investigation into the effects of pro-apoptotic members, PBOX-6 and -15 was undertaken. Both compounds were shown to reduce the viability of a panel of both drug sensitive and MDR neuroblastoma cell lines and to inhibit the clonogenicity of SHSY5Y cells in a dose-dependent manner.

The development of the MDR phenotype in neuroblastoma is characterised by amplification of the proto-oncogene MYCN, mutation/deletion of p53 and chromosomal aberrations such as deletion of loci at 1p or 11q (Maris *et al.*, 2010). This phenotype often includes overexpression of MDR proteins, such as P-gp, drug efflux pumps which use ATP hydrolysis to mediate the export of hydrophobic drugs from the cell. Interestingly, while numerous chemotherapeutics which are currently used to treat neuroblastoma are

substrates for these efflux pumps, the PBOX compounds are not (Nathwani *et al.*, 2010) indicating that they may possess advantages over standard chemotherapy currently in clinical use. In this study, the fold resistance of PBOX-6, -15 and four other chemotherapeutics (vincristine, doxorubicin, etoposide and carboplatin) currently used to treat high risk, advanced stage neuroblastoma, in MDR neuroblastoma cells was established. The PBOXs were both shown to exhibit a lower fold resistance when compared to standard therapeutics indicating a potential advantage other current treatment strategies.

In order to predict the potential clinical response, confirmation of the anti-cancer effects of these novel MTAs on primary neuroblastoma cells was vital. Primary cells more closely resemble the physiological state of cancer cells *in vivo* and provide a more realistic representation of the disease state. Metastasis is the main cause of death in patients with neuroblastoma, with the bone marrow being the major site of metastasis. In spite of aggressive therapy, children presenting with dissemination of malignant neuroblasts in the bone marrow have a poor prognosis; therefore in the first part of this study, cells were isolated from the bone marrow, representing the most advanced and drug resistant population. PBOX-6 was shown to decrease the viability of these primary neuroblastoma cells. Findings from this study though are limited by the low number of samples, and as a result further samples would be required to validate these initial findings. Despite the low sample number, this is a positive result and would support further investigation into the use of PBOX-6 for treatment of neuroblastoma.

Treatment of advanced neuroblastoma is characterised by multiple rounds of intensive courses of combination chemotherapy. This multimodal approach has numerous advantages by offering the benefit of targeting multiple cellular pathways that induce apoptosis. Frequently in advanced tumours, these pathways are defective leading to ineffective induction of cell death by chemotherapeutics (Maris *et al.*, 2010). Similarly amplification of the transcription factor MYCN, may lead to suppression of apoptosis and promotion of cell proliferation and survival (Gogolin *et al.*, 2010). Single agent chemotherapy may provide insufficient toxicity to overcome these pro-survival mechanisms and cells may develop multidrug resistance. Synergistic combinations of

chemotherapeutics may help to decrease the development of resistance while maximising the anti-tumour effects on the cell.

Currently vincristine is used in combination with other chemotherapeutics, such as, doxorubicin, cisplatin, etoposide, carboplatin or topotecan to treat advanced stage neuroblastoma (Kohler *et al.*, 2013). Having observed the pro-apoptotic effects of the PBOXs alone, an investigation into the potential additive or synergistic interactions between these novel MTAs and other chemotherapeutics was undertaken. The second part of this study explored the potential enhancement of chemotherapeutic induced cell death in drug-sensitive and MDR neuroblastoma cells. Combinations of PBOX-6 or -15 were found to synergistically enhance the apoptotic effects of carboplatin, doxorubicin and etoposide in neuroblastoma cell lines. A combination of low dose vincristine, carboplatin and etoposide has been shown to produce a successful outcome in infants with unresectable, non-metastatic neuroblastoma (Rubie *et al.*, 2011) however, immediate toxicity and possible long-term adverse effects of this regimens administered in young patients may limit their use.

Neuropathy is the dose-limiting side effect of all vinca alkaloids, with vincristine being the most severe (Park *et al.*, 2013). Vincristine produces motor and sensory neuropathy; thus, despite the success of vincristine and other MTAs, limitations in their use still exist. Therefore there is a definite need to develop novel MTAs. The PBOX-6 and -15 have previously been shown to elicit minimal toxicity to normal peripheral bone marrow cells (PMBC) (McGee *et al.*, 2004) and induce minimal inhibition of proliferation of normal B-cells and bone marrow progenitor cells (McElligott *et al.*, 2009). Furthermore, no effects on red blood cell, white blood cell or platelet counts have been observed in response to the PBOXs (unpublished data). A low level of vasorelaxing activity and a lack of inhibition of nitrendipine binding, both measures of calcium antagonism, suggest a general lack of cardiotoxicity (DMZ, unpublished data). It is interesting to note that previous *in vivo* studies (Greene *et al.*, 2005; Bright *et al.*, 2010), in addition, to the results presented in chapter 4 have shown no deleterious effects on animal weight following treatment with PBOX-6. This is in contrast to studies of vincristine and colchicine in which neurotoxicity strongly correlated to loss of body weight (Bacher *et al.*, 2001), suggesting that PBOX-6 does not elicit neurotoxicity, although further studies would be required to substantiate

this. Numerous assays for neurotoxicity have been described in the literature which could be employed to investigate any potential induction of neuropathy by the PBOX-6 (Moser *et al.*, 2011).

In the second part of this study, the molecular events underlying PBOX-6 enhancement of carboplatin-induced apoptosis was determined. The PBOX-6/carboplatin combination decreased Mcl-1 expression, induced cleavage and inactivation of Bcl-2 and activated pro-apoptotic Bak leading to the formation of pores in the mitochondrial membrane and release of cytochrome c. This resulted in activation of initiator caspases-8 and -9 and executioner caspase-3. In particular, this study sought to determine the role of Mcl-1 in PBOX-6-induced apoptosis induction in these cells, as Mcl-1 overexpression has been shown to correlate with disease progression and degree of aggression, suggesting a role in development of chemoresistance. Cell death or survival is mediated by a balance of pro- and anti-apoptotic Bcl-2 proteins, with some cells relying predominantly on Mcl-1 for survival. Results presented herein indicate that a decrease in Mcl-1 expression either through siRNA mediated knockdown or treatment with the PBOX-6/carboplatin combination, shifts the balance towards cell death, suggesting that Mcl-1 plays a key role in cell survival and response to chemotherapy. Inactivation of Mcl-1 by novel compounds such as PBOX-6 may present a promising therapeutic strategy for future treatment of neuroblastoma.

In the final part of this study, the molecular events associated with PBOX-6-induced Mcl-1 downregulation were further examined. Recent reports have indicated that a decrease in Mcl-1 expression may be attributed to a block in translation mediated by activation of AMPK. As PBOX-6 was shown to decrease expression of Mcl-1 and induce apoptosis in SHSY5Y and CHLA-90 neuroblastoma cell lines, this study sought to investigate the effects of PBOX-6 on the AMPK signalling pathway in neuroblastoma cells. PBOX-6 was shown to induce activation of AMPK and inactivation of the downstream target ACC. This was in agreement with previous findings indicating MTAs may induce apoptosis through activation of AMPK. Previous studies have shown that AICAR can enhance the anti-cancer effects of vincristine in melanoma cell lines through an increase in activation of AMPK, an enhanced decrease in viability and a synergistic enhancement of apoptosis (Chen *et al.*, 2011). PBOX-6 was found to induce the early production of ROS, while the antioxidant N-

acetylcysteine impaired both ROS production and the anti-cancer effects of this novel MTA. PBOX-6 mediated activation of AMPK was found to result in inhibition of mTOR, a highly conserved serine/threonine kinase which regulates a broad range of cellular events including transcription, translation, proliferation and division. Inhibition of mTOR and its downstream targets, p70 S6 Kinase, S6 ribosomal protein and eEF2K, indicated that PBOX-6 may potentially inhibit translation. This study proposes that the PBOX-6 mediated decrease in Mcl-1 may be attributable to inhibition of the mTOR pathway resulting in a block in Mcl-1 translation.

As mTOR is a negative regulator of autophagy, many studies have reported induction of autophagy following inhibition of the mTOR pathway. PBOX-6 induced autophagy in SHSY5Y cells, while pretreatment with bafilomycin-A1 or chloroquine, was found to block autophagy and enhance the apoptotic effects of PBOX-6. This suggests that autophagy was functioning as a survival mechanism and provides a rationale for the use of autophagy inhibitors to further promote PBOX-6-induced apoptosis in neuroblastoma. These findings are supported by numerous other studies which have demonstrated enhancement of chemotherapy induced cell death through modulation of the autophagic pathway (Longo *et al.*, 2008; Liu *et al.*, 2009; Vazquez-Martin *et al.*, 2009; Kanematsu *et al.*, 2010).

In conclusion, the results presented herein have demonstrated the ability of the novel MTA, PBOX-6 to induce apoptosis in drug sensitive and resistant neuroblastoma cells, in *ex vivo* patient samples and to reduce tumour burden in an *in vivo* neuroblastoma model. Furthermore these compounds have been shown to synergise with current treatments for neuroblastoma, providing substantial rationale for the continued development of these novel MTAs for the treatment of neuroblastoma. This study provides novel insights into understanding the molecular and cellular mechanism involved in PBOX-induced apoptosis.

Summary

- PBOX-6 and -15 were shown to reduce the viability of drug sensitive and multidrug resistant neuroblastoma cell lines with similar potency.
- PBOX-6 and-15 inhibited the clonogenicity of SHSY5Y cells.
- PBOX-6 and -15 exhibited a lower fold resistance in multidrug resistant cell lines when compared to vincristine, doxorubicin, carboplatin and etoposide, all of which are currently used in the clinic to treat neuroblastoma.
- PBOX-6 induced apoptosis in drug sensitive and multidrug resistant cell lines.
- Apoptosis was shown to be mediated by a decrease in anti-apoptotic Mcl-1 expression, cleavage and inactivation of anti-apoptotic Bcl-2 and an increase in pro-apoptotic Bak in SHSY5Y and CHLA-90 cell lines.
- Downregulation of Mcl-1 expression was found to sensitise drug sensitive and multidrug resistant cell lines to carboplatin, indicating the importance of Mcl-1 in apoptosis induction in neuroblastoma cell lines.
- PBOX-6 was found to reduce the viability of primary neuroblastoma cells isolated from bone marrow samples and reduce tumour volume in an *in vivo* xenograft model of neuroblastoma.
- PBOX-6 was found to induce production of ROS, activation of AMPK and inhibition of the mTOR signalling pathway in the SHSY5Y cell line.
- Pretreatment of SHSY5Y cells with NAC partially inhibited the anti-proliferative effects and anti-apoptotic effects of PBOX-6 and -15, while pretreatment with NAC inhibited the PBOX-6 mediated decrease in Mcl-1 expression in SHSY5Y cells.

In conclusion, this work has demonstrated the immense potential of the novel microtubule targeting agents, the PBOXs, as a future treatment strategy for neuroblastoma. In particular this work has shown the anti-tumour effects of PBOX-6 is not limited to *in vitro* cell lines, showing anti-cancer activity in both primary neuroblastoma cells and in an *in vivo* xenograft model of neuroblastoma, thus providing considerable justification for further investigation into these compounds as a promising therapeutic strategy for neuroblastoma.

Chapter 7

Future works

For the PBOXs to progress to the clinical phase of development, further pre-clinical investigation would be necessary. In particular a large scale study of primary neuroblastoma samples would be required. Isolation of primary cells from primary tumours and other sites of metastases would be of interest to determine the degree of drug resistance from cells from each of these sites. Isolation of cancer stem cells (CSC) would also be of interest. Studies of solid tumours support the existence of a subpopulation within the total tumour cell mass, CSCs (Winquist *et al.*, 2009). These CSCs may undergo differentiation, self renewal and retain the ability to reconstitute the primary tumour phenotype when transplanted into recipient animals (Magee *et al.*, 2012); therefore, they may play a role as master regulators in both the development of tumours and MDR. CSCs express specific markers such as CD133 which correlate with clinical stage; high expression of CD133 has been shown in tumours with unfavourable histology and decreased survival rates (Alisi *et al.*, 2013). Differentiation of neuroblastoma cell lines and primary neuroblastoma cells has been reported to be inhibited by knockdown of CD133 (Takenobu *et al.*, 2011; Kamijo *et al.*, 2012), while CD133-positive cells isolated from neuroblastoma cell lines have been shown to have gains on 16p13.3, 19p13.3, and 19q13.33, in contrast to CD133-negative cells. A correlation between the presence of a gain of 16p13 and expression of CD133 has recently been reported (Courneyer *et al.*, 2012). Studies have demonstrated that CD133-positive cells from MDR neuroblastoma patient samples are enriched *in vivo* after treatment with chemotherapeutics such as cisplatin, etoposide, doxorubicin, and paclitaxel, while these chemotherapeutics have been shown to be less effective in inducing cell death in these cells when compared to non-stem cell cancerous cells (Winquist *et al.*, 2009). Techniques to isolate these cells are currently being developed in a number of cancers (Wang *et al.*, 2013; Vidal *et al.*, 2014). Therefore, it would be of particular interest to determine the effects of the PBOXs on this sub population of cells.

The therapeutic potential of chemotherapeutics may be limited by expression of inhibitor of apoptosis proteins (IAP) expressed by multiple cancer cells (Hassan *et al.*, 2014). IAPs are a family of evolutionarily conserved suppressors of apoptosis, which mediate their effects though interaction with caspases via one or more BIR (baculovirus iap repeat) domains. Members of this family include survivin, livin, XIAP, cIAP1, and cIAP2 (Smolewski

et al., 2008). IAPs may be antagonised by proteins such as SMAC (Diablo) and HtrA2 (Omi), which are sequestered inside mitochondria in healthy cells but are released into the cytosol during apoptosis; once released they bind to IAP via their BIR domains (Obexer *et al.*, 2014)

While IAPs are overexpressed in many cancers contributing to cell survival and resistance to chemotherapy (Obexer *et al.*, 2014), targeting of these proteins has been shown to induce apoptosis in tumour cell lines or sensitise cells to anticancer drugs, while SMAC and HrtA2 mimetics have been reported to induce apoptosis in cancer cell lines and xenograft models (Bai *et al.*, 2014), indicating targeting of these proteins is a worthwhile therapeutic strategy. Previous reports have indicated that the PBOX-6 may target IAP expression in cancer. Bright *et al.*, (2010) reported a decrease in expression of survivin in response to a combination of PBOX-6 and flavopiridol, while siRNA mediated knockdown of survivin expression enhanced the apoptotic effects of PBOX-6. This is of particular interest as overexpression of these IAPs correlates with development of MDR in neuroblastoma. Lamers *et al.*, (2011) showed a correlation between high expression of survivin in neuroblastoma patient samples and poor prognosis. Overexpression of the apoptotic regulator, X-linked inhibitor of apoptosis protein (XIAP), one of the best characterised members of the IAP family, has been associated with chemotherapy resistance in neuroblastoma (Eschenburg *et al.*, 2012). Smac peptides have also been shown to prime neuroblastoma cells for TRAIL induced apoptosis (Fulda *et al.*, 2002) while more recently Abhari *et al.*, (2013) have reported that small-molecule IAP inhibitors at subtoxic concentrations cooperate with monoclonal antibodies against TRAIL R1 (Mapatumumab) or TRAIL-R2 (Lexatumumab) to induce apoptosis in neuroblastoma cells in a highly synergistic manner.

A thorough investigation into the role of IAP in neuroblastoma in response to the PBOX-6 and -15 should be undertaken. It would now be of interest to firstly determine the expression of each member of the IAP family of proteins in a panel of drug sensitive and MDR neuroblastoma cell lines, to ascertain if expression is contributing to MDR. Secondly, to establish any potential effects of the PBOX and standard chemotherapeutics on their expression, and finally determine any potential correlation between response to a given chemotherapeutic and IAP expression. Previously a high level of livin expression was

found to correlate with MYCN amplification and decreased survivin in a study of *ex vivo* neuroblastoma patient samples (Kim *et al.*, 2005). Should IAP expression be found to be high in neuroblastoma cells lines, investigation into a combination of the PBOXs and a Smac mimetic may potentially enhance PBOX induced apoptosis particularly in MDR cells. Recently targeted therapy with LBW242, a Smac mimetic resulted in sensitisation of neuroblastoma cells to the MTA vincristine, while this mimetic was also found to enhance the effects of doxorubicin and etoposide, all currently used in neuroblastoma treatment regimens (Eschenberg *et al.*, 2012). Although the numbers of clinical trials employing the Smac mimetics are currently limited, this is a field undergoing thorough investigation and will most likely expand in the coming years.

Work presented herein has demonstrated the importance of some Bcl-2 family members, in particular Mcl-1, in mediating the apoptotic response to the PBOX-6. Further work on the role played by pro-apoptotic members such as Bim, are required. A mechanism by which certain cancer cells are 'primed for death' may account for the differences in response to chemotherapy in various cancers (Sarosiek *et al.*, 2012). It is suggested that certain cells live in a state in which they depend on the expression of anti-apoptotic proteins, which sequester activator BH3-only proteins such as Bim, for their survival. Inhibition of the anti-apoptotic proteins in these 'primed' cells results in Bak/Bax oligomerisation and MOMP in contrast to 'unprimed' cells. These cells which depend on Bcl-2 and Mcl-1 for survival are 'primed for death' and generally responded better to chemotherapy. Goldsmith *et al.,* (2012) performed mitochondrial profiling on a panel of neuroblastoma cell lines and found that neuroblastoma cells and primary tumours are primed for death with tonic sequestration of Bim by either Bcl-2 or Mcl-1, with Bim being identified as the principle mediator of response to chemotherapy. In the first part of this study, a PBOX-6 mediated decrease in Mcl-1 was noted indicating Bim may be activated in response to PBOX-6, therefore, a time- and dose-dependent study of Bim expression in response to PBOX-6 could be undertaken to determine if this protein plays a role in mediating the apoptotic response to the PBOX-6.

In healthy cells, Bim may be localised to the dynein light chain or the mitochondrial membrane where it interacts with anti-apoptotic Bcl-2 proteins (Luo *et al.*, 2012). Upon exposure to apoptotic stimuli, Bim may be phosphorylated by JNK causing dissociation

from the dynein light chain or Mcl-1 or Bcl-2. Previous studies have reported PBOX-6-mediated activation of JNK preceding G2/M arrest and apoptosis (McGee *et al.*, 2004). It is plausible that PBOX-6 mediates activation of JNK, allowing for phosphorylation of Bim by JNK and dissociation from Mcl-1 leading to its activation. Western blot analysis of both JNK and Bim activation in response to PBOXs in neuroblastoma cell lines could be carried out. Should Bim be found to be activated, siRNA mediated knockdown may establish the possible importance of Bim in PBOX-mediated apoptosis.

In this study, investigations into the apoptotic signalling pathways initiated by PBOX-6 in neuroblastoma cells primarily focused on the intrinsic pathway and the involvement of caspase-9. However, having observed caspase-8 activation, further investigation into the involvement of the extrinsic pathway would be of interest. Previously Maginn *et al.*, (2011) have reported upregulation of death receptors and potentiation of TRAIL-mediated apoptosis in multiple myeloma cells indicating that the mechanism of action of PBOX-6 may involve the extrinsic pathway. This is of particular interest as a recent study has highlighted a link between TRAIL signalling and natural killer (NK) cell activation in neuroblastoma cells (Sheard *et al.*, 2013). As previously discussed, neuroblastoma cells do not express HLA so they can evade detection by T lymphocytes, but unlike T lymphocytes, NK cells are activated by cells lacking HLA so can recognise and destroy neuroblastoma cells. TRAIL may be expressed as a soluble or membrane bound protein, while ligation of TRAIL to the TRAIL receptor results in formation of the DISC complex, activation of caspase-8 and caspase-3 leading to apoptosis. Membrane-bound TRAIL was shown to supplement NK cell cytotoxicity in neuroblastoma cells (Sheard *et al.*, 2013). Chemotherapeutics such as etoposide have been reported to synergistically enhance the effects of TRAIL by increasing expression of TRAIL R2 in caspase-8 expressing neuroblastoma cell lines (Kim *et al.*, 2012). These reports, in addition to previous PBOX studies, would support the use of a PBOX/TRAIL combination as a novel therapeutic intervention for neuroblastoma and would warrant further investigation. Indeed the monoclonal antibody, HG strategyS-ETR2, a TRAIL R2 ligand, is currently undergoing a phase I clinical trial for the treatment of refractory, metastatic neuroblastoma (clinicaltrials.gov; NCT00428272).

In the final part of this study, PBOX-6 was shown to induce activation of AMPK and inactivation of the downstream target ACC. It would now be interesting to determine if apoptosis could be enhanced by combinations of PBOX-6 and activators of AMPK. 5-amino-1-β-D-ribofuranosyl-imidazole-4-carboxamide (AICAR), an analog of AMP, is an activator of AMPK. Previous studies have shown that AICAR can enhance the anti-cancer effects of vincristine in melanoma cell lines through an increase in activation of AMPK, an enhanced decrease in viability and a synergistic enhancement of apoptosis (Chen *et al.*, 2011). Conversely, it would also be interesting to determine the effects of compound c, an inhibitor of AMPK, or the effects of siRNA mediated knockdown of AMPK on PBOX-6 induced apoptosis.

As ROS has been shown to play a role in PBOX-6-induced apoptosis, further investigation into the molecular mechanism of ROS generation in response to PBOX-6 and -15 would be of interest. As discussed in chapter 5, various mechanisms have been described to account for the production of ROS in response to chemotherapeutics, including redox cycling, NADPH oxidase (NOX) activation or electron transport chain disruption (Hwang *et al.*, 2001; Pelicano *et al.*, 2003, 2004). PBOX-6 induced ROS production may be mediated by an increase in NOX in SHSY5Y cells. To further investigate this, western blotting analysis of NOX subunits could be undertaken to determine any possible increase in expression of specific NOX components in response to the PBOX-6 and -15. Employing the use of NOX inhibitors may help to further elucidate the involvement of this pathway. Diphenylene iodonium (DPI) is the most commonly used NOX inhibitor (Bedard *et al.*, 2007). If pretreatment with DPI inhibited PBOX-6 induced ROS production, this may point to a role for NOX in the generation of ROS. Similarly this inhibitor could be utilised to further explore the possible involvement of JNK in NOX activation, in response to the PBOXs. Previous studies have reported a decrease in expression of p22phox, p47phox, gp91phox, JNK and p38 following treatment with NOX inhibitors (Tsai *et al.*, 2012).

The role of the mitochondria in PBOX-6-mediated ROS production should also be investigated. NOX may not be the only source of PBOX-6-induced ROS production. Previous reports in cell free systems have indicated that early mitochondrial superoxide production in response the paclitaxel occurs upstream of caspase activation (Alexandre *et al.*, 2006). In this study it was hypothesised that interaction of paclitaxel with

mitochondrial tubulin may account for the effects on the mitochondria. The use of specific inhibitors of the electron transport chain may help to further elucidate the involvement of this pathway, for example antimycin A (complex III inhibitor) and rotenone (complex I inhibitor). It is possible PBOX-6 may activate NOX but also disrupt the electron transport chain through interactions with mitochondrial tubulin.

In the final part of this study, PBOX-6 mediated inhibition of members of the mTOR signalling pathway. Further elucidation of the effects of the PBOX-6 and -15 on the mTOR pathway would now be of interest. As mTOR is at a critical node in a complex signalling cascade involving multiple components which have been implicated to play roles in the development of tumourigenesis, in particular the PI3Kinase/AKT survival pathway it would now be of interest to determine the effects of PBOX-6 on this pathway. Particular interest could be paid to investigating the effects of the PBOX-6 on the transcription factor and potential tumour suppressor, FOXO3a. This is a forkhead domain-containing transcription factor which is an important downstream effector of the PI3K/AKT pathway (Santo *et al.*, 2013). FOXO3a has been found to be inactivated by constitutively active PI3K/AKT (Yang *et al.*, 2008). Santo *et al.*, (2013) recently reported elevation of FOXO3a expression in early-stage neuroblastoma tumours and normal embryonal neuroblasts, but a reduction in expression in advanced stage neuroblastoma. Inactivation of FOXO3a by AKT was shown to be essential for neuroblastoma cell survival, while treatment of neuroblastoma cells with PI-103, a dual PI3K/mTOR inhibitor, activated FOXO3a and triggered apoptosis.

In order for anti-cancer agents to produce minimal side effects on surrounding non-malignant cells, targeted delivery to the tumour site is crucial. In the last few decades huge advances have been made in improving drug delivery, particularly the advent of nanoparticles. Targeted delivery of nanoparticles allows for a prolonged, localised interaction of a given drug with a tumour (Sultana *et al.*, 2013). Identification of cancer specific antigens such as GD_2 has aided in the development of targeted drug delivery (Ritter *et al.*, 1991). To date no attempt has been made to encapsulate the PBOXs in nanoparticles or other such vehicles such as liposomes, therefore, this would be of interest in the future, in particular encapsulation in nanoparticles conjugated to tumour

specific antibodies. Successful encapsulation of the PBOX may increase their anti-cancer potential and reduce toxicity, particularly *in vivo.* In addition to the results presented in chapter 4, it has previously been reported that PBOX-6 inhibited tumour growth in breast carcinoma and CML animal models. However, PBOX-6 did not completely retard tumour growth, possibly due to metabolism of the compound; thus nanoparticle encapsulation may enhance PBOX uptake directly into neuroblastoma tumour cells and lead to an enhanced therapeutic effect.

The use of nanoparticles for the treatment of neuroblastoma is currently under investigation. Tivnan *et al.,* (2012) found that encapsulation of microRNA-34a, a pro-apoptotic miRNA, in nanoparticles conjugated to an anti-GD_2 antibody, resulted in a significant decrease in tumour growth, increased apoptosis and a reduction in vascularisation in a murine neuroblastoma orthotopic model.

Another potential benefit of nanoparticle technology is the potential to deliver multiple chemotherapeutics to a tumour site simultaneously. This has recently been achieved *in vitro* by Liao *et al.,* (2014); these authors reported on the release of cisplatin, doxorubicin and camptothecin from a single nanoparticle in ovarian cancer cell lines. In chapter 4, a PBOX-6-mediated synergistic enhancement of carboplatin induced cell death was observed. Should the encapsulation of the PBOXs in nanoparticles be successful, it would be pertinent to explore combinations with carboplatin and other chemotherapeutics. In principle, the maximum therapeutic index could be achieved by simultaneous dosing of each drug at or near its maximum tolerated dose.

As with all novel therapeutics, the eventual goal for the PBOXs is to enter a clinical testing phase. It would be necessary to study the ADMET (absorption, distribution, metabolism, elimination and toxicity) properties of the PBOXs as these factors will have a great impact on the likelihood of success *in vivo.* Additionally prior to clinical testing, further investigation into the structure activity relationship (SAR) of the PBOXs would be required. Both apoptotic and non-apoptotic members of this family of compounds have been identified, suggesting that the ability of these compounds to induce apoptosis may be based on structure. In particular, the pro-apoptotic members' possess a naphthyl side chain which may be required for induction of apoptosis. It would now be of interest to

synthesise more PBOX derivatives, to determine the importance of the naphthyl side chain with the eventual aim of producing more potent anti-cancer agents. In conclusion, the results presented herein provide substantial rationale for the continued development of these novel MTAs for the potential future treatment of neuroblastoma.

References

Abhari BA., Cristofanon S., Kappler R., von Schweinitz D., Humphreys R., Fulda S. RIP1 is required for IAP inhibitor-mediated sensitization for TRAIL-induced apoptosis via a RIP1/FADD/caspase-8 cell death complex. Oncogene. 2013; 32(27): 3263-73.

Abulwerdi F., Liao C., Liu M., Azmi AS., Aboukameel A., Mady AS et al. A novel small-molecule inhibitor of mcl-1 blocks pancreatic cancer growth in vitro and in vivo. Mol Cancer Ther. 2014; 13(3): 565-75.

Ackler S., Mitten MJ, Foster K, Oleksijew A, Refici M, Tahir SK, The Bcl-2 inhibitor ABT-263 enhances the response of multiple chemotherapeutic regimens in hematologic tumors in vivo. Cancer Chemother Pharmacol. 2010; 66(5): 869-80.

Adair SJ & Hogan KT. Treatment of ovarian cancer cell lines with 5-aza-2'-deoxycytidine upregulates the expression of cancer-testis antigens and class I major histocompatibility complex-encoded molecules. Cancer Immunol Immunother. 2009; 58(4): 589-601.

Albert S., Serova M., Dreyer C., Sablin MP., Faivre S., Raymond E. New inhibitors of the mammalian target of rapamycin signalling pathway for cancer. Expert Opin Investig Drugs. 2010; 19(8):919-30.

Alexandre J., Batteux F., Nicco C., Chereau C., Laurent A., Guillevin L et al. Accumulation of hydrogen peroxide is an early and crucial step for paclitaxel-induced cancer cell death both in vitro and in vivo. Int J Cancer. 2006; 119: 41–48.

Alessi DR., Kozlowski MT., Weng QP., Morrice N., Avruch J. 3-Phosphoinositide-dependent protein kinase 1 (PDK1) phosphorylates and activates the p70 S6 kinase in vivo and in vitro. Curr Biol. 1998 Jan 15; 8(2):69-81.

Alisi A., Cho WC., Locatelli F., Fruci D. Multidrug resistance and cancer stem cells in neuroblastoma and hepatoblastoma. Int J Mol Sci. 2013; 14(12): 24706-25.

Althoff K., Beckers A., Bell E., Nortmeyer M., Thor T., Sprüssel A et al. A Cre-conditional MYCN-driven neuroblastoma mouse model as an improved tool for preclinical studies. Oncogene. 2014 Sep 1. (ahead of print).

Alnemri ES., Livingston DJ., Nicholson DW., Salvesen G., Thornberry NA., Wong WW et al. Human ICE/CED-3 protease nomenclature. Cell. 1996; 87(2): 171.

Amman JU., Haag C., Kasperczyk H., Debatin KM and Fulda, S. Sensitization of neuroblastoma cells for TRAIL-induced apoptosis by NFkB inhibition. Int. J. Cancer. 2009; 124: 1301-11.

Ando K., Ohira M., Ozaki T., Nakagawa A., Akazawa K., Suenaga Y et al. Expression of TSLC1, a candidate tumor suppressor gene mapped to chromosome 11q23, is downregulated in unfavorable neuroblastoma without promoter hypermethylation. Int J Cancer. 2008; 123(9):2087–2094.

Arsikin K., Kravic-Stevovic T., Jovanovic M., Ristic B., Tovilovic G., Zogovic N et al. . Autophagy-dependent and -independent involvement of AMP-activated protein kinase in 6-hydroxydopamine toxicity to SH-SY5Y neuroblastoma cells. Biochim Biophys Acta. 2012; 1822(11): 1826-36.

Attiyeh EF., London WB., Mossé YP., Wang Q., Winter C., Khazi D et al. Chromosome 1p and 11q deletions and outcome in neuroblastoma. N Engl J Med. 2005; 353(21):2243–2253.

Bacher G., Nickel B., Emig P., Vanhoefer U., Seeber S., Shandra A. D-24851, a novel synthetic microtubule inhibitor, exerts curative antitumoral activity in vivo, shows efficacy toward multidrug-resistant tumour cells, and lacks neurotoxicity. Cancer Res. 2001; 61:392-399.

Bai L., Smith DC., Wang S. Small-molecule SMAC mimetics as new cancer therapeutics. Pharmacol Ther. 2014; 144(1): 82-95.

Bakhshi A., Jensen JP., Goldman P., Wright JJ., McBride OW., Epstein AL et al. Cloning the chromosomal breakpoint of t(14;18) human lymphomas: clustering around JH on chromosome 14 and near a transcriptional unit on 18. Cell. 1985; 41(3): 899-906.

Balayssac D., Authier N., Cayre A., Coudore F. Does inhibition of P-glycoprotein lead to drug-drug interactions? Toxicol Lett. 2005; 156: 319–329.

Bao L., Dunham K., Lucas K. MAGE-A1, MAGE-A3, and NY-ESO-1 can be upregulated on neuroblastoma cells to facilitate cytotoxic T lymphocyte-mediated tumor cell killing. Cancer Immunol Immunother. 2011; 60(9): 1299-307.

Barth S., Glick D., Macleod KF. Autophagy: assays and artifacts. J Pathol. 2010 Jun;221(2):117-24.

Barrett D., Brown VI., Grupp SA., Teachey DT. Targeting the PI3K/AKT/mTOR signaling axis in children with hematologic malignancies. Paediatr Drugs. 2012; 14(5): 299-316.

Baur JA., Sinclair DA. Therapeutic potential of resveratrol: the in vivo evidence. Nat Rev Drug Discov. 2006; 5(6): 493-506.

Beck MT., Chen NY., Franek KJ., Chen WY. Experimental therapeutics prolactin antagonist-endostatin fusion protein as a targeted dual-functional therapeutic agent for breast cancer. Cancer Res. 2003; 63: 3598–3604.

Bedard K & Krause KH. The NOX family of ROS-generating NADPH oxidases: physiology and pathophysiology. Physiol Rev. 2007; 87(1): 245-313.

Beltinger C., Fulda S., Walczak H., Debatin KM. TRAIL enhances thymidine kinase/ganciclovir gene therapy of neuroblastoma cells. Cancer Gene Ther. 2002; 9(4): 372-81.

Bender A., Opel D., Naumann I., Kappler R., Friedman L., Von Schweinitz D., Debatin K. M., Fulda S. (2011). PI3K inhibitors prime neuroblastoma cells for chemotherapy by shifting the balance towards pro-apoptotic Bcl-2 proteins and enhanced mitochondrial apoptosis. Oncogene. 2011; 30: 494–503.

Bénard J., Raguénez G., Kauffmann A., Valent A., Ripoche H., Joulin V et al. MYCN-non-amplified metastatic neuroblastoma with good prognosis and spontaneous regression: a molecular portrait of stage 4S. Mol Oncol. 2008; 2(3): 261-71.

References

Beroukhim R., Mermel C., Porter D., Wei G., Raychaudhuri S., Donovan J. The landscape of somatic copy-number alteration across human cancers. Nature 2010; 46 (7283): 899-905.

Bettayeb K., Baunbæk D., Delehouze C., Loaëc N., Hole AJ., Baumli S. CDK Inhibitors Roscovitine and CR8 Trigger Mcl-1 Down-Regulation and Apoptotic Cell Death in Neuroblastoma Cells. Genes Cancer. 2010; 1(4): 369–80.

Bhandari S., Cheung NK., Kushner BH., Kramer K., Modak S., Larson SM et al. Hypothyroidism after 131I-monoclonal antibody treatment of neuroblastoma. Pediatr Blood Cancer. 2010; 55(1): 76-80.

Bitting RL & Armstrong AJ. Targeting the PI3K/Akt/mTOR pathway in castration-resistant prostate cancer. Endocr Relat Cancer. 2013; 20(3): R83-99.

Boiani M., Daniel C., Liu X., Hogarty MD., Marnett LJ. The stress protein BAG3 stabilizes Mcl-1 protein and promotes survival of cancer cells and resistance to antagonist ABT-737. J Biol Chem. 2013; 288(10): 6980-90.

Bordow SB, Haber M, Madafiglio J, Cheung B, Marshall GM, Norris MD. Expression of the multidrug resistance-associated protein (MRP) gene correlates with amplification and overexpression of the N-myc oncogene in childhood neuroblastoma. Cancer Res. 1994; 54(19): 5036-40.

Bottino C., Dondero A., Bellora F., Moretta L., Locatelli F., Pistoia V et al. Natural killer cells and neuroblastoma: tumor recognition, escape mechanisms, and possible novel immunotherapeutic approaches. Front Immunol. 2014; 5: 56.

Bourhis J., Bénard J., Hartmann O., Boccon-Gibod L., Lemerle J., Riou G. Correlation of MDR1 gene expression with chemotherapy in neuroblastoma. J Natl Cancer Inst. 1989; 81(18):1401-5.

Bresler SC. Wood AC., Haglund EA., Courtright J., Belcastro LT., Plegaria JS, et al. Differential inhibitor sensitivity of anaplastic lymphoma kinase variants found in neuroblastoma. Sci trans med. 2011; 3:108.

Bright SA., Greene LM., Greene TF, Campiani G, Butini S, et al. The novel pyrrolo-1,5-benzoxazepine, PBOX-21, potentiates the apoptotic efficacy of STI571 (imatinib mesylate) in human chronic myeloid leukaemia cells. Biochem Pharmacol. 2008; 77 (3): 310-21.

Bright SA., Campiani G., Deininger MW., Lawler M., Williams DC and Zisterer DM. Sequential treatment with flavopiridol synergistically enhances pyrrolo-1,5-benzoxazepine-induced apoptosis in human chronic myeloid leukaemia cells including those resistant to imatinib treatment. Biochem Pharmacol. 2010; 80(1): 31-8.

Bright SA., Greene LM., Greene TF, Campiani G, Butini S, et al. The novel pyrrolo-1,5-benzoxazepine, PBOX-21, potentiates the apoptotic efficacy of STI571 (imatinib mesylate) in human chronic myeloid leukaemia cells. Biochem Pharmacol. 2007; 77 (3): 310-21.

Bristow RG & Hill RP. Hypoxia and metabolism. Hypoxia, DNA repair and genetic instability. Nat Rev Cancer. 2008; 8(3): 180-92.

Brodeur GM., Pritchard J., Berthold F., Carlsen NL., Castel V., Castelberry RP et al. Revisions of the international criteria for neuroblastoma diagnosis, staging, and response to treatment. J Clin Oncol, 1993; 11 (8): 1466-77.

Brodeur GM., Seeger RC., Barrett A., Berthold F., Castleberry RP., D'Angio G et al. International criteria for diagnosis, staging and response to treatment in patients with neuroblastoma. J Clin Oncol 1988; 6:1874-1881.

Burkhart CA., Watt F., Murray J., Pajic M., Prokvolit A., Xue et al. Small-molecule multidrug resistance-associated protein 1 inhibitor reversan increases the therapeutic index of chemotherapy in mouse models of neuroblastoma. Cancer Res. 2009; 69(16): 6573-80.

Byrne GI., Ojcius DM. Chlamydia and apoptosis: life and death decisions of an intracellular pathogen. Nat Rev Microbiol. 2004; 2(10): 802-8.

Cairns RA., Harris IS., Mak TW. Regulation of cancer cell metabolism. Nat Rev Cancer. 2011; 11(2): 85-95.

Caren H., Kryh H., Nethander M., Sjoberg RM., Trager C., Nilsson S et al. High-risk neuroblastoma tumours with 11q deletion display a poor prognostic, chromosome instability phenotype with later onset. Proc Natl Acad Sci USA. 2010; 107 (9): 4324-8.

Carr-Wilkinson J., O'Toole K., Wood KM., Challen CC., Baker AG., Board JRet al. High Frequency of p53/MDM2/p14ARF Pathway Abnormalities in Relapsed Neuroblastoma. Clin Cancer Res. 2010; 16(4): 1108-18.

Casellas P., Galiegue S., Basile AS. Peripheral benzodiazepine receptors and mitochondrial function. Neurochem Int. 2002; 40(6): 475-86.

Castle VP., Heidelberger KP., Bromberg J., Ou X., Dole M., Nuñez G. Expression of the apoptosis-suppressing protein bcl-2, in neuroblastoma is associated with unfavorable histology and N-myc amplification. Am J Pathol. 1993; 143(6): 1543-50.

Chai J &Shi. Apoptosome and inflammasome: conserved machineries for caspase activation. Nat Sci Rev. 2014; 1 (1): 101-118.

Chaitanya GV., Steven AJ., Babu PP. PARP-1 cleavage fragments: signatures of cell-death proteases in neurodegeneration. Cell Commun Signal. 2010; 8:31-41.

Chalhoub N & Baker SJ. PTEN and the PI3-kinase pathway in cancer. Nature. 2013; 497(7448): 217-23.

Chan HS., Haddad G., Thorner PS., DeBoer G., Lin YP., Ondrusek N et al. P-glycoprotein expression as a predictor of the outcome of therapy for neuroblastoma. N Engl J Med. 1991; 325 (23): 1608–14.

Chan WH, Wu HJ, and Hsuuw YD. Curcumin inhibits ROS formation and apoptosis in methylglyoxal-treated human hepatoma G2 cells. Ann NY Acad Sci. 2005; 1042: 372–378.

Chen MB., Shen WX., Yang Y., Wu XY., Gu JH., Lu PH. Activation of AMP-activated protein kinase is involved in vincristine-induced cell apoptosis in B16 melanoma cell. J Cell Physiol. 2011; 226(7): 1915-25.

Chen MB., Zhang Y., Wei MX., Shen W., Wu XY., Yao C et al. Activation of AMP-activated protein kinase (AMPK) mediates plumbagin-induced apoptosis and growth inhibition in cultured human colon cancer cells. Cell Signal. 2013; 25(10): 1993-2002.

Chen L., Zhao Y., Halliday GC., Berry P., Rousseau RF., Middleton SA et al. Structurally diverse MDM2-p53 antagonists act as modulators of MDR-1 function in neuroblastoma. Br J Cancer. 2014; 111(4):716-25

Chen S, Rehman SK, Zhang W, Wen A, Yao L, Zhang J. Autophagy is a therapeutic target in anticancer drug resistance. Biochim Biophys Acta. 2010; 1806: 220-229.

Chen SH., Chan NL., Hsieh TS. New mechanistic and functional insights into DNA topoisomerases. Annu Rev Biochem. 2013; 82: 139-70.

Chen Y., Takita J., Choi YL., Kato M., Ohira M., Sanada M et al. Oncogenic mutations of ALK kinase in neuroblastoma. Nature. 2008; 455(7215): 971–974.

Chen Z., Lin Y., Barbieri E., Burlingame S., Hicks J., Ludwig A et al. Mdm2 deficiency suppresses MYCN-Driven neuroblastoma tumorigenesis in vivo. Neoplasia. 2009; 11(8): 753-62.

Cheng EH., Kirsch DG., Clem RJ., Ravi R., Kastan MB., Bedi A et al. Conversion of Bcl-2 to a Bax-like death effector by caspases. Science. 1997; 278(5345): 1966-8.

Cheok CF., Verma CS., Baselga J., Lane, D. P. Translating p53 into the clinic. Nat. Rev. Clin. Oncol. 2011; 8: 25–37.

Cheung NK & Dyer MA. Neuroblastoma: developmental biology, cancer genomic and immunotherapy. Nat Rev Cancer. 2013; 13 (6):397-411.

Choi HJ., Kim TY., Chung N., Yim JH., Kim WG., Kim JA et al. The influence of the BRAF V600E mutation in thyroid cancer cell lines on the anticancer effects of 5-aminoimidazole-4-carboxamide-ribonucleoside. J Endocrinol. 2011; 211(1): 79-85.

Chou TC, Talalay P. Quantitative analysis of dose-effect relationships: the combined effects of multiple drugs or enzyme inhibitors. Adv Enzyme Regul. 1984; 22:27–55.

Chou TC. Drug combination studies and their synergy quantification using the Chou-Talalay method. Cancer Res. 2010; 70(2): 440-6.

Cobleigh MA. Other options in the treatment of advanced breast cancer. Semin Oncol. 2011; 38 Suppl 2: S11-6.

Combaret V., Boyault S., Iacono I., Brejon S., Rousseau R., Puisieux A. Effect of bortezomib on human neuroblastoma: analysis of molecular mechanisms involved in cytotoxicity. Mol Can. 2008; 7: 50-61.

Conklin KA. Free radicals: the pros and cons of antioxidants. Cancer chemotherapy and antioxidants J. Nutr. 2004; 134: 3201-3204.

Circu ML., Aw TY. Reactive oxygen species, cellular redox systems, and apoptosis. Free Radic Biol Med. 2010; 48(6):749-62.

Clarke PG, Puyal J. Autophagic cell death exists. Autophagy 2012; 8(6): 867-9.

Clohessy JG., Zhuang J., Brady HJ. Characterisation of Mcl-1 cleavage during apoptosis of haematopoietic cells. Br. J. Haematol. 2004; 125:655-665.

Codogno P. Shining light on autophagy. Mol Cancer Ther. 2011; 10(9): 1533-41.

Cohen GM. Caspases: the executioners of apoptosis. Biochem J. 1997; 326 (Pt 1):1-16.

Cohen NA. A competitive stapled peptide screen identifies a selective small molecule that overcomes MCL-1-dependent leukemia cell survival. Chem. Biol. 2012; 19: 1175–1186.

Cohen SL., Pearson AD., London WB., Monclair T., Ambros PF., Brodeur GM et al. INRG Task Force.The International Neuroblastoma Risk Group (INRG) classification system: an INRG Task Force report. J Clin Oncol. 2009; 27(2): 289-97.

Coley HM. Overcoming multidrug resistance in cancer: clinical studies of p-glycoprotein inhibitors. Methods Mol Biol. 2010; 596: 341-58.

Conde de la Rosa L., Schoemaker MH., Vrenken TE., Buist-Homan M., Havinga R., Jansen PL et al. Superoxide anions and hydrogen peroxide induce hepatocyte death by different mechanisms: involvement of JNK and ERK MAP kinases. J Hepatol. 2005; 44: 918–929.

Cotterill SJ., Pearson AD., Pritchard J., Kohler. Foot AB; European Neuroblastoma Study Group and United Kingdom Children's Cancer Study Group. Late relapse and prognosis for neuroblastoma patients surviving 5 years or more: a report from the European Neuroblastoma Study Group "Survey". Med Pediatr Oncol. 2001; 36 (1): 235-8.

Cournoyer S., Nyalendo C., Addioui A., Belounis A., Beaunoyer M., Aumont A et al. Genotype analysis of tumor initiating cells expressing CD133 in neuroblastoma. Genes Chromosomes Cancer. 2012; 51:792–804.

Cozzi DA., Mele E., Ceccanti S., Natale F., Clerico A., Schiavetti A et al. Long-term follow-up of the "wait and see" approach to localized perinatal adrenal neuroblastoma. World J Surg. 2013; 37(2): 459-65.

Czabator PE., Lessene G., Strasser A., Adams JM. Control of apoptosis by the BCL-2 protein family: implications for physiology and therapy. Nat Rev Mol Cell Biol. 2014; 15(1): 49-63.

Dalvai M., Schubart K., Besson A., Matthias P. Oct1 is required for mTOR-induced G1 cell cycle arrest via the control of p27(Kip1) expression. Cell Cycle. 2010; 9(19):3933-44.

Danial NN., Korsmeyer SJ. Cell death: critical control points. Cell. 2004; 116(2): 205-19.

Das B., Antoon R., Tsuchida R., Lotfi S., Morozova O., Farhat W et al. Squalene selectively protects mouse bone marrow progenitors against cisplatin and carboplatin-induced cytotoxicity in vivo without protecting tumor growth. Neoplasia. 2008; 10(10): 1105-19.

Decensi A., Puntoni M., Goodwin P., Cazzaniga M., Gennari A., Bonanni B et al. Metformin and cancer risk in diabetic patients: a systematic review and meta-analysis. Cancer Prev Res (Phila). 2010; 3(11): 1451-61.

Deininger MW., Goldman JM., Melo JV. The molecular biology of chronic myeloid leukemia. Blood. 2000; 96(10): 3343-56.

Dewson G & Kluck RM. Mechanisms by which Bak and Bax permeabilise the mitochondira during apoptosis. J Cell Sci. 2009; 122(Pt 16): 2801-8.

Dhup S., Dadhich RK., Porporato PE., Sonveaux P. Multiple biological activities of lactic acid in cancer: influences on tumor growth, angiogenesis and metastasis. Curr Pharm Des. 2012; 18(10): 1319-30.

Dijkhuis AJ., Douwes J., Kamps W., Sietsma H., Kok JW. Differential expression of sphingolipids in P-glycoprotein or multidrug resistance-related protein 1 expressing human neuroblastoma cell lines. FEBS Lett. 2003; 548: 28–32.

Ding Q., He X., Hsu JM., Xia W., Chen CT et al. Degradation of Mcl-1 by beta-TrCP mediates glycogen synthase kinase 3-induced tumor suppression and chemosensitization. Mol Cell Biol. 2007; 27(11): 4006-17.

Dole M., Nuñez G., Merchant AK., Maybaum J., Rode CK., Bloch CA and Castle VP. Bcl-2 inhibits chemotherapy-induced apoptosis in neuroblastoma. Cancer Res. 1994; 54 (12): 3253-9.

De P., Miskimins K., Dey N., Leyland-Jones B. Promise of rapalogues versus mTOR kinase inhibitors in subset specific breast cancer: old targets new hope. Cancer Treat Rev. 2013; 39(5):403-12.

Dufner A & Thomas G. Ribosomal S6 kinase signaling and the control of translation. Exp Cell Res. 1999; 253:100-109.

Duong HQ., Hwang JS., Kim HJ., Seong YS., Bae I. BML-275, an AMPK inhibitor, induces DNA damage, G2/M arrest and apoptosis in human pancreatic cancer cells. Int J Oncol. 2012; 41(6): 2227-36.

Egan CM., Nyman U., Skotte J., Streubel G., Turner S., O'Connell DJ et al. CHD5 is required for neurogenesis and has a dual role in facilitating gene expression and polycomb gene repression. Dev Cell. 2013; 26(3): 223-36.

Egan D, Kim J, Shaw RJ, Guan KL. The autophagy initiating kinase ULK1 is regulated via opposing phosphorylation by AMPK and mTOR. Autophagy. 2011; 7(6): 643-4.

Eglan R & Reisine T. Primary cells and stem cells in drug discovery: emerging tools for high-throughput screening. Assay Drug Dev Technol. 2011; 9(2): 108-24.

Eschenburg G., Eggert A., Schramm A., Lode HN., Hundsdoerfer P. Smac mimetic LBW242 sensitizes XIAP-overexpressing neuroblastoma cells for TNF-α-independent apoptosis. Cancer Res. 2012; 72(10): 2645-56.

Esser R., Muller T., Stefes D., Kloess S., Seidel D., Gillies SD et al. NK cells engineered to express a GD2 -specific antigen receptor display built-in ADCC-like activity against tumour cells of neuroectodermal origin. J Cell Mol Med. 2012; 16(3): 569–581.

Evangelisti C., Tazzari PL., Riccio M., Fiume R., Hozumi Y., Falà F et al. Nuclear diacylgylcerol kinase-zeta is a negative regulator of cell cycle progression in C2C12 mouse myoblasts. FASEB J. 2007; 21(12):3297-307.

Ezoe S. Secondary Leukaemia associated with the anti-cancer agent, etoposide, a topoisomerase II inhibitor. Int J Environ Res Public Health. 2012; 9(7): 2444-53.

Fang H., Harned TM., Kalous O., Maldonado V., DeClerck YA., Reynolds CP. Synergistic activity of fenretinide and the Bcl-2 family protein inhibitor ABT-737 against human neuroblastoma. Clin Cancer Res. 2011; 17(22): 7093-104.

Faubert B., Boily G., Izreig S., Griss T., Samborska B., Dong Z et al. MPK is a negative regulator of the Warburg effect and suppresses tumor growth in vivo. Cell Metab. 2013; 17(1): 113-24.

Fay JR., Steele V., Crowell JA. Energy homeostasis and cancer prevention: the AMP-activated protein kinase. Cancer Prev Res (Phila). 2009; 2(4): 301-9.

Ferreira KS., Kreutz C., Macnelly S., Neubert K., Haber A., Bogyo M. Caspase-3 feeds back on caspase-8, Bid and XIAP in type I Fas signaling in primary mouse hepatocytes. Apoptosis. 2012; 17(5): 503-15.

Flahaut M., Meier R., Coulon A., Nardou KA., Niggli FK., Martinet D et al. The Wnt receptor FZD1 mediates chemoresistance in neuroblastoma through activation of the Wnt/beta-catenin pathway. Oncogene. 2009; 28(23): 2245-56.

Fletcher DA1, Mullins RD. Cell mechanics and the cytoskeleton. Nature. 2010; 463(7280): 485-92.

Fong CT., Dracopoli NC., White PS., Merrill PT., Griffith RC., Housman DE et al. Loss of heterozygosity for the short arm of chromosome 1 in human neuroblastomas: correlation with N-myc amplification. Proc Natl Acad Sci U S A. 1989; 86(10): 3753-7.

Forde JC., Maginn EN., McNamara G., Martin LM., Campiani G., Williams DC., Zisterer D., McElligott AM., Lawler M., Lynch TH., Hollywood D., Marignol L. Microtubule-targeting-compound PBOX-15 radiosensitizes cancer cells in vitro. Cancer Biol Ther. 2011; 11(4): 421-8.

Franco R., Panayiotidis MI., Cidlowski JA. Glutathione depletion is necessary for apoptosis in lymphoid cells independent of reactive oxygen species formation. J Biol Chem 2007; 282: 30452–30465.

Fujita T, et al. CHD5, a tumour suppressor gene deleted from 1p36.31 in neuroblastomas. J Natl Cancer Inst. 2008; 100(13): 940–949.

Fulda S, Wick W, Weller M, Debatin KM. Smac agonists sensitize for Apo2L/TRAIL- or anticancer drug-induced apoptosis and induce regression of malignant glioma in vivo. Nat Med 2002; 8: 808–815.

Furfaro AL., Piras S., Passalacqua M., Domenicotti C., Parodi A., Fenoglio D et al. HO-1 up-regulation: a key point in high-risk neuroblastoma resistance to bortezomib. Biochim Biophys Acta. 2014; 1842(4): 613-22.

Gamble LD., Kees UR., Tweddle DA., Lunec J. MYCN sensitizes neuroblastoma to the MDM2-p53 antagonists Nutlin-3 and MI-63. Oncogene. 2012; 31(6): 752-63.

Garcia-Gil M., Pesi R., Perna S. 5'-aminoimidazole-4-carboxamide riboside induces apoptosis in human neuroblastoma cells. Neuroscience. 2003; 117:811–820.

García-Sáez AJ., Fuertes G., Suckale J., Salgado J. Permeabilization of the outer mitochondrial membrane by Bcl-2 proteins. Adv Exp Med Biol. 2010; 677: 91-105.

Germain M, Duronio V. The N terminus of the anti-apoptotic BCL-2 homologue MCL-1 regulates its localization and function. J Biol Chem. 2007 Nov 2; 282(44): 32233-42.

Gilkes DM., Semenza GL., Wirtz D. Hypoxia and the extracellular matrix: drivers of tumour metastasis. Nat Rev Cancer. 2014; 14(6): 430-9.

Gogolin S., Dreidax D., Becker G., Ehemann V., Schwab M., Westermann F. MYCN/MYC-mediated drug resistance mechanisms in neuroblastoma. Int J Clin Pharmacol Ther. 2010; 48(7): 489-91.

Goldsmith KC., Gross M., Peirce S., Luyindula D., Liu X., Vu A et al. Mitochondrial Bcl-2 family dynamics define therapy response and resistance in neuroblastoma. Cancer Res. 2012; 72(10): 2565-77.

Goldstein LJ., Fojo AT., Ueda K. Expression of the multidrug resistance, MDR1, gene in neuroblastomas. J. Clin. Oncol. 1999; 8: 128-36.

Gormand A., Henriksson E., Ström K., Jensen TE., Sakamoto K., Göransson O. Regulation of AMP-activated protein kinase by LKB1 and CaMKK in adipocytes. J Cell Biochem. 2011; 112(5): 1364-75.

Green DR., Reed JC. Mitochondria and apoptosis. Science. 1998; 281(5381): 1309-12.

Greene LM., Campiani G., Lawler M., Williams DC., Zisterer DM. BubR1 is required for a sustained mitotic spindle checkpoint arrest in human cancer cells treated with tubulin-targeting pyrrolo-1,5-benzoxazepines. Mol Pharmacol. 2008; 73(2): 419-30.

Greene LM., Fleeton M., Mulligan J., Gowda C., Sheahan BJ., Atkins GJ et al. The pyrrolo-1, 5-benzoxazepine, PBOX-6, inhibits the growth of breast cancer cells in vitro independent of estrogen receptor status, and inhibits breast tumour growth in vivo. Oncol Rep. 2005; 14 (5): 1357–63.

Greene LM., Kelly L., Onnis V., Campiani G., Lawler M., Williams DC et al. STI-571 enhances the apoptotic efficacy of PBOX-6, a novel microtubule targeting agent, in both STI-571-sensitive and –resistant Bcr-Abl positive human chronic myeloid leukemia cells. J. Pharmacol. Exp. Ther. 2007; 321(1): 288-97.

Greene LM., Wang S., O'Boyle NM., Bright SA., Reid JE., Kelly P et al. Combretazet-3 a novel synthetic cis-stable combretastatin A-4-azetidinone hybrid with enhanced stability and therapeutic efficacy in colon cancer. Oncol Rep. 2013; 29 (6): 2451-8.

Grotzer MA., Castelletti D., Fiaschetti G., Shalaby T., Arcaro A. Targeting Myc in pediatric malignancies of the central and peripheral nervous system. Curr Cancer Drug Targets. 2009; 9(2): 176-88.

Grunt TW & Mariani GL. Novel approaches for molecular targeted therapy of breast cancer: interfering with PI3K/AKT/mTOR signalling. Curr Cancer Drug Targets. 2013; 13(2): 188-204.

Grzmil M & Hemmings BA. Translation regulation as a therapeutic target in cancer. Cancer Res. 2012; 72(16): 3891-900.

Guan FY., Gu J., Li W., Zhang M., Ji Y., Li J et al. Compound K protects pancreatic islet cells against apoptosis through inhibition of the AMPK/JNK pathway in type 2 diabetic mice and in MIN6 β-cells. Life Sci. 2014; 107(1-2): 42-9.

Guo C., White PS., Weiss MJ., Hogarty MD., Thompson PM., Stram DO et al. Allelic deletion at 11q23 is common in MYCN single copy neuroblastomas. Oncogene. 1999; 18(35): 4948–4957.

Gwinn DM., Shackelford DB., Egan DF., Mihaylova MM., Mery A., Vasquez DS et al. AMPK phosphorylation of raptor mediates a metabolic checkpoint. Mol Cell. 2008; 30(2): 214-26.

Häcker S., Dittrich A., Mohr A., Schweitzer T., Rutkowski S., Krauss J et al. Histone deacetylase inhibitors cooperate with IFN-gamma to restore caspase-8 expression and overcome TRAIL resistance in cancers with silencing of caspase-8. Oncogene. 2009; 28 (35): 3097-110.

Han JE & Choi JW. Control of JNK for an activation of NADPH oxidase in LPS-stimulated BV2 microglia. Arch Pharm Res. 2012; 35(4): 709-15.

Haber M., Smith J., Bordow S. B., Flemming C., Cohn S. L., London W. B., et al. Association of high-level MRP1 expression with poor clinical outcome in a large prospective study of primary neuroblastoma. J. Clin. Oncol. 2006; 24:1546–1553

Hadad SM., Appleyard V., Thompson AM. Therapeutic metformin/AMPK activation promotes the angiogenic phenotype in the ERalpha negative MDA-MB-435 breast cancer model. Breast Cancer Res Treat 2009; 114: 391.

Hallberg B & Palmer RH. Mechanistic insight into ALK receptor tyrosine kinase in human cancer biology. Nat Rev Cancer. 2013; 13(10): 685-700.

Hallett A & Traunecker H. A review and update on neuroblastoma. Paediatrics and Child Health. 2012; 22 (3):103-107.

Hara J. Development of treatment strategies for advanced neuroblastoma.Int J Clin Oncol. 2012; 17(3): 196-203.

Hara T., Nakamura K., Matsui M., Yamamoto A., Nakahara, Y., Suzuki-Migishima et al. Suppression of basal autophagy in neural cells causes neurodegenerative disease in mice. Nature. 2006; 441: 885-889.

Hardie DG. AMP-activated protein kinase: an energy sensor that regulates all aspects of cell function. Genes Dev. 2011; 25(18): 1895-908.

Hardie DG. AMP-activated/SNF1 protein kinases: conserved guardians of cellular energy. Nat Rev Mol Cell Biol 2007; 8: 774–785.

Hardie DG. Minireview: the AMP-activated protein kinase cascade: the key sensor of cellular energy status. Endocrinology. 2003; 144(12): 5179-83.

Hardie DG., Ross FA., Hawley SA. AMPK: a nutrient and energy sensor that maintains energy homeostasis. Nat Rev Mol Cell Biol. 2012; 13: 251–262.

Hartwich JE., Orr WS., Ng CY., Spence Y., McLaughlin JM., Furman WL et al. Rapamycin increases neuroblastoma xenograft and host stromal derived osteoprotegerin inhibiting osteolytic bone disease in a bone metastasis model. J Pediatr Surg. 2013; 48(1): 47-55.

Hassan M., Watari H., AbuAlmaaty A., Ohba Y., Sakuragi N. Apoptosis and molecular targeting therapy in cancer. Biomed Res Int. 2014; 2014:150845.

Heller G., Geradts J., Ziegler B., Newsham I., Filipits M., Markis-Ritzinger EM et al. Downregulation of TSLC1 and DAL-1 expression occurs frequently in breast cancer. Breast Cancer Res Treat. 2007; 103: 283–291.

Henderson MJ., Haber M., Porro A., Munoz M.A., Iraci N., Xue C et al. ABCC multidrug transporters in childhood neuroblastoma: Clinical and biological effects independent of cytotoxic drug efflux. J. Natl. Cancer Inst. 2011; 103: 1236–1251.

Heinrich KO, et al. CAMTA1, a 1p36 tumor suppressor candidate, inhibits growth and activates differentiation programs in neuroblastoma cells. Cancer Res. 2011; 71(8): 3142–3151.

High LM., Szymanska B., Wilczynska-Kalak U., Barber N., O'Brien R., Khaw SL et al. The Bcl-2 homology domain 3 mimetic ABT-737 targets the apoptotic machinery in acute lymphoblastic leukemia resulting in synergistic in vitro and in vivo interactions with established drugs. Mol Pharmacol. 2010; 77(3): 483-94.

Hiyama E, Hiyama K, Nishiyama M, Reynolds CP, Shay JW, Yokoyama T. Differential gene expression profiles between neuroblastomas with high telomerase activity and low telomerase activity. J Pediatr Surg. 2003; 38(12): 1730-4.

Hoffman B., Liebermann DA. Apoptotic signaling by c-MYC. Oncogene. 2008; 27(50): 6462-72.

Holliday DL & Speirs V. Choosing the right cell line for breast cancer research. Breast Cancer Res. 2011; 13(4): 215.

Houshmandi SS., Surace EI., Zhang HB., Fuller GN., Gutmann DH. Tumor suppressor in lung cancer-1 (TSLC1) functions as a glioma tumor suppressor. Neurology. 2006; 67: 1863–1866.

Horman S., Beauloye C., Vertommen D., Vanoverschelde JL., Hue L., Rider MH. Myocardial ischemia and increased heart work modulate the phosphorylation state of eukaryotic elongation factor-2. J Biol Chem. 2003; 278:41970–41976.

Horman S., Browne G., Krause U., Patel J., Vertommen D., Bertrand L et al. Activation of AMP-activated protein kinase leads to the phosphorylation of elongation factor 2 and an inhibition of protein synthesis. Curr Biol 2002; 12: 1419–1423.

Hu YL., DeLay M., Rose SD., Carbonell WS., Aghi MK. Hypoxia-induced autophagy promotes tumor cell survival and adaptation to anti-angiogenic treatment in glioblastoma. Cancer Res. 2012; 72: 1-11.

Huang JM., Sheard MA., Ji L., Sposto R., Keshelava N. Combination of vorinostat and flavopiridol is selectively cytotoxic to multidrug-resistant neuroblastoma cell lines with mutant TP53. Mol Cancer Ther. 2010; 9(12): 3289-301.

Huang M & Weiss WA. Neuroblastoma and MYCN. Cold Spring Harb Perspect Med. 2013; 3(10): a014415.

Hwang PM, Bunz F, Yu J, Rago C, et al. Ferredoxin reductase affects p53-dependent, 5-fluorouracil-induced apoptosis in colorectal cancer cells. Nat Med 2001; 7: 1111–7.

Ichikawa Y., Ghanefar M., Bayeva M., Wu R., Khechaduri A., Naga Prasad SV et al. Cardiotoxicity of doxorubicin is mediated through mitochondrial iron accumulation. J Clin Invest. 2014; 124(2): 617-30.

Inoki K., Ouyang H., Zhu T., Lindvall C., Wang Y., Zhang X et al. TSC2 integrates Wnt and energy signals via a coordinated phosphorylation by AMPK and GSK3 to regulate cell growth. Cell. 2006; 126(5): 955-68.

Inuzuka H., Shaik S., Onoyama I., Gao D., Tseng A et al. SCFFBW7 regulates cellular apoptosis by targeting MCL1 for ubiquitylation and destruction. Nature. 2011; 471: 104–109.

Iwasa T., Okamoto I., Takezawa K., Yamanaka K., Nakahara T., Kita A et al. Marked anti-tumour activity of the combination of YM155, a novel survivin suppressant, and platinum-based drugs. Br J Cancer. 2010; 103(1): 36-42.

Izycka-Swieszewska E., Drozynska E., Rzepko R., Kobierska-Gulida G., Grajkowska W., Perek D, et al. Analysis of PI3K/AKT/mTOR signalling pathway in high risk neuroblastic tumours. Pol J Pathol. 2010; 61:192–8.

Jackson SJ & Singletary KW. Sulforaphane: a naturally occurring mammary carcinoma mitotic inhibitor, which disrupts tubulin polymerization. Carcinogenesis 2004; 25: 219-227.

Jakacki RI., Bouffet E., Adamson PC., Pollack IF., Ingle AM., Voss SD et al. A phase 1 study of vinblastine in combination with carboplatin for children with low-grade gliomas: a Children's Oncology Group phase 1 consortium study. Neuro Oncol. 2011; 13(8): 910-5.

Janoueix-Lerosey I., Schleiermacher G., Michels E, et al. Overall genomic pattern is a predictor of outcome in neuroblastoma. J Clin Oncol. 2009; 27: 1026-1033.

Ji C., Yang B., Yang YL., He SH., Miao DS., He L et al. Exogenous cell-permeable C6 ceramide sensitizes multiple cancer cell lines to Doxorubicin-induced apoptosis by promoting AMPK activation and mTORC1 inhibition. Oncogene. 2010; 29(50): 6557-68.

Jiang F., Zhang Y., Dusting GJ. NADPH oxidase-mediated redox signaling: roles in cellular stress response, stress tolerance, and tissue repair. Pharmacol Rev. 2011; 63(1): 218-42.

Johnsen JI., Segerström L., Orrego A., Elfman L., Henriksson M., Kågedal B et al. Inhibitors of mammalian target of rapamycin downregulate MYCN protein expression and inhibit neuroblastoma growth in vitro and in vivo. Oncogene. 2008; 27(20): 2910-22.

Jones RG., Plas DR., Kubek S., et al. AMP-activated protein kinase induces a p53-dependent metabolic checkpoint. Mol Cell. 2005; 18: 283–293.

Jordan MA & Wilson L. Microtubules as a target for anticancer drugs. Nat Rev Cancer. 2004; 4(4): 253-65.

Jordan MA., Thrower D., Wilson L. Effects of vinblastine, podophyllotoxin and nocodazole on mitotic spindles. Implications for the role of microtubule dynamics in mitosis. J Cell Sci. 1992; 102: 401–416.

Jordan MA., Wendell KL., Gardiner S., Derry WB., Copp H., Wilson L. Mitotic block induced in HeLa cells by low concentrations of paclitaxel (Taxol) results in abnormal mitotic exit and apoptotic cell death. Cancer Res. 1996; 56: 816–825.

Joseph TL., Lane DP., Verma CS. Stapled BH3 peptides against MCL-1: mechanism and design using atomistic simulations. PLoS One. 2012; 7(8): e43985

Juin P., Geneste O., Gautier F., Depil S., Campone M. Decoding and unlocking the BCL-2 dependency of cancer cells. Nat Rev Cancer. 2013; 13(7): 455-65.

Jung CH., Jun CB., Ro SH., Kim YM., Otto NM., Cao J et al. ULK-Atg13-FIP200 complexes mediate mTOR signaling to the autophagy machinery. Mol Biol Cell. 2009; 20: 1992–2003.

Kaliki S., Shields CL., Shah SU., Eagle RC Jr., Shields JA., Leahey A. Postenucleation adjuvant chemotherapy with vincristine, etoposide, and carboplatin for the treatment of high-risk retinoblastoma. Arch Ophthalmol. 2011; 129(11): 1422-7.

Kanzawa T., Kondo Y., Ito H., Kondo S., Germano I. Induction of autophagic cell death in malignant glioma cells by arsenic trioxide. Cancer Res 2003; 63: 2103-2108.

Kapse-Mistry S., Govender T., Srivastava R., Yergeri M. Nanodrug delivery in reversing multidrug resistance in cancer cells. Front Pharmacol. 2014; 10; 5

Kamijo T., Nakagawara A. Molecular and genetic bases of neuroblastoma. Int. J. Clin. Oncol. 2012; 17:190–195.

Kanematsu S., Uehara N., Miki H., Yoshizawa K., Kawanaka A., Yuri T., Tsubura A. Autophagy inhibition enhances sulforaphane-induced apoptosis in human breast cancer cells. Anticancer Res. 2010; 30(9):3381-90.

Kang MR., Park SK, Lee CW, Cho IJ, Jo YN, Yang JW, Kim JA, Yun J, Lee KH, Kwon HJ, Kim BW, Lee K, Kang JS, Kim HM. Widdrol induces apoptosis via activation of AMP-activated protein kinase in colon cancer cells. Oncol Rep. 2012; 27(5): 1407-12.

Karami H., Baradaran B., Esfehani A., Sakhinia M., Sakhinia E. Down-regulation of Mcl-1 by small interference RNA induces apoptosis and sensitizes HL-60 leukemia cells to etoposide. Asian Pac J Cancer Prev. 2014; 15(2): 629-35.

Kasai T., Nakamura K, Vaidyanath A, Chen L, Sekhar S, El-Ghlban S, Okada M, Mizutani A, Kudoh T, Murakami H, Seno M. Chlorotoxin Fused to IgG-Fc Inhibits Glioblastoma Cell Motility via Receptor-Mediated Endocytosis. J Drug Deliv. 2012; 2012: 975763.

Kato K., Ogura T., Kishimoto A., Minegishi Y., Nakajima N., Miyazaki M et al. Critical roles of AMP-activated protein kinase in constitutive tolerance of cancer cells to nutrient deprivation and tumor formation. Oncogene. 2002; 21: 6082–6090.

Kefas BA., Cai Y., Ling Z., Heimberg H., Hue L., Pipeleers D et al. AMP-activated protein kinase can induce apoptosis of insulin-producing MIN6 cells through stimulation of c-Jun-N-terminal kinase. J Mol Endocrinol. 2003; 30(2): 151-61.

Kerksick C & Willoughby D. The antioxidant role of glutathione and N-acetyl-cysteine supplements and exercise-induced oxidative stress. J Int Soc Sports Nutr. 2005; 9(2): 38-44

Keshelava N., Groshen S and Reynolds CP. Cross-resistance of topoisomerase I and II inhibitors in neuroblastoma cell lines. Can Chem Pharmacol. 2000; 45 (1): pp.1-8.

Keshelava N., Seeger RC., Groshen S and Reynolds CP. Drug resistance patterns of human neuroblastoma cell lines derived from patients at different phases of therapy. Cancer Res. 1998; 58 (23): 5396-405.

Keshelava N., Zuo JJ., Waidyaratne NS., Triche TJ and Reynolds CP. p53 mutations and loss of p53 function confer multidrug resistance in neuroblastoma. Med Pediatr Oncol. 2000; 35 (6): 563-8.

Khoo KH., Verma CS., Lane DP. Drugging the p53 pathwya: understanding the route to clinical efficiency. Nat Rev Drug Disc. 2014; 13(3): 217-36.

Kim DK., Alvarado CS., Abramowsky CR., Gu L., Zhou M., Soe MM, , Findley HW. Expression of inhibitor-of-apoptosis protein (IAP) livin by neuroblastoma cells: correlation with prognostic factors and outcome. Pediatr Dev Pathol. 2005; 8(6): 621-9.

Kim HR., Lee MW., Kim DS., Jo HY., Lee SH., Chueh HW et al. Etoposide sensitizes neuroblastoma cells expressing caspase 8 to TRAIL. Cell Biol Int Rep. 2012; 19(1): e00017.

Kim J., Kundu M., Viollet B., Guan KL. AMPK and mTOR regulate autophagy through direct phosphorylation of Ulk1. Nat Cell Biol. 2011; 13(2): 132-41.

Kirkland RA & Franklin JL. Evidence for redox regulation of cytochrome C release during programmed neuronal death: antioxidant effects of protein synthesis and caspase inhibition. J Neurosci. 2001; 21: 1949–1963.

Kirsch DG., Doseff A., Chau BN., Lim DS., de Souza-Pinto NC., Hansford R et al. Caspase-3-dependent cleavage of Bcl-2 promotes release of cytochrome c. J Biol Chem. 1999; 274(30): 21155-61.

Klco JM., Spencer DH., Lamprecht TL., Sarkaria SM., Wylie T., Magrini V et al. Genomic impact of transient low-dose decitabine treatment on primary AML cells. Blood. 2013; 121(9): 1633-43.

Kohler JA., Rubie H., Castel V., Beiske K., Holmes K., Gambini C et al. Treatment of children over the age of one year with unresectable localised neuroblastoma without MYCN amplification: results of the SIOPEN study. Eur J Cancer. 2013; 49(17):3671-9.

Komatsu M., Waguri S., Chiba T., Murata S., Iwata J., Tanida I et al. Loss of autophagy in the central nervous system causes neurodegeneration in mice. Nature. 2006; 441: 880-884.

Kowalczyk A., Gil M., Horwacik I., Odrowaz Z., Kozbor D., Rokita H. The GD2-specific 14G2a monoclonal antibody induces apoptosis and enhances cytotoxicity of chemotherapeutic drugs in IMR-32 human neuroblastoma cells. Cancer Lett. 2009; 281(2): 171-82.

Kozopas KM., Yang T., Buchan HL., Zhou P., Craig RW. MCL1, a gene expressed in programmed myeloid cell differentiation, has sequence similarity to BCL2. Proc Natl Acad Sci USA. 1993; 90(8): 3516-20.

Kramer K., Humm JL., Souweidane MM., Zanzonico PB., Dunkel IJ., Gerald WL et al. Phase I study of targeted radioimmunotherapy for leptomeningeal cancers using intra-Ommaya 131-I-3F8. J Clin Oncol. 2007; 25: 5465–5470.

Krishnadas DK., Shapiro T., Lucas K. Complete remission following decitabine/dendritic cell vaccine for relapsed neuroblastoma. Pediatrics. 2013; 131(1): 336-41.

Kuss S., Cornut R., Beaulieu I., Mezour MA., Annabi B., Mauzeroll J. Assessing multidrug resistance protein 1-mediated function in cancer cell multidrug resistance by scanning electrochemical microscopy and flow cytometry. Bioelectrochemistry. 2011; 82(1): 29-37.

Lacey DL., Timms E., Tan HL. Osteoprotegerin ligand is a cytokine that regulates osteoclast differentiation and activation. Cell. 1998; 93: 165-176.

Lamers F., Schild L., den Hartog IJ., Ebus ME., Westerhout EM., Ora I et al. Targeted BCL2 inhibition effectively inhibits neuroblastoma tumour growth. Eur J Cancer. 2012; 48(16): 3093-103.

Lamers F., van der Ploeg I., Schild L., Ebus ME., Koster J., Hansen BR. Knockdown of survivin (BIRC5) causes apoptosis in neuroblastoma via mitotic catastrophe. Endocr Relat Cancer. 2011; 18(6): 657-68.

Lamkanfi M & Dixit VM. Manipulation of host cell death pathways during microbial infections. Cell Host Microbe. 2010; 8(1): 44-54.

Lane DP. Cancer. p53, guardian of the genome. Nature. 1992; 358(6381): 15-6.

Le XF., Hittelman WN., Liu J., McWatters A., Li C., Mills GB et al. Paclitaxel induces inactivation of p70 S6 kinase and phosphorylation of Thr421 and Ser424 via multiple signalling pathways in mitosis. Prog Mol Biol Transl Sci. 2009; 90: 109-53.

Lestini BJ., Goldsmith KC., Fluchel MN., Liu X., Chen N.L, Goyal B et al. Mcl-1 downregulation sensitizes neuroblastoma to cytotoxic chemotherapy and small molecule Bcl2-family antagonists. Cancer Biol Ther. 2009; 8 (16):1587-95.

Levine B & Yuan J. Autophagy in cell death: an innocent convict? J. Clin. Invest. 2005; 115: 2679-2688.

Li AP. The use of the Integrated Discrete Multiple Organ Co-culture (IdMOC) system for the evaluation of multiple organ toxicity. Altern Lab Anim. 2009; 37(4): 377-85.

Li P., Nijhawan D., Budihardjo I., Srinivasula SM., Ahmad M., Alnemri ES et al. Cytochrome c and dATP-dependent formation of Apaf-1/caspase-9 complex initiates an apoptotic protease cascade. Cell. 1997; 91(4): 479-89.

Li Y., Yuan H., Yang K., Xu W., Tang W., Li X. The structure and functions of P-glycoprotein. Curr Med Chem. 2010; 17(8): 786-800.

Liang C., Feng P., Ku B., Dotan I., Canaani D., Oh BH et al. Autophagic and tumour suppressor activity of a novel Beclin1-binding protein UVRAG. Nat Cell Biol. 2006; 8(7): 688-99.

Liang H., Zhang L., Xu R., Ju XL. Silencing of survivin using YM155 induces apoptosis and chemosensitization in neuroblastomas cells. Eur Rev Med Pharmacol Sci. 2013; 17(21): 2909-15.

Liang J, Shao SH, Xu ZX, et al. The energy sensing LKB1-AMPK pathway regulates p27(kip1) phosphorylation mediating the decision to enter autophagy or apoptosis. Nat Cell Biol. 2007; 9: 218–224.

Liang X., Tang J., Liang Y., Jin R., Cai X. Suppression of autophagy by chloroquine sensitizes 5-fluorouracil-mediated cell death in gallbladder carcinoma cells. Cell Biosci. 2014; 4(1):10.

Liao L., Liu J., Dreaden EC., Morton SW., Shopsowitz KE., Hammond PT et al. A convergent synthetic platform for singlenanoparticle combination cancer therapy: ratiometric loading andcontrolled release of cisplatin, doxorubicin, and camptothecin. J Am Chem Soc. 2014; 136(16): 5896-9.

Ling LU., Tan KB., Lin H., Chiu GN. The role of reactive oxygen species and autophagy in safingol-induced cell death. Cell Death Dis. 2011; 2: e129.

Liu G., Wang R., Wang Y., Li P., Zhao G., Zhao L et al. Ethacrynic acid oxadiazole analogs induce apoptosis in malignant hematologic cells through downregulation of Mcl-1 and c-FLIP, which was attenuated by GSTP1-1. Mol Cancer Ther. 2013; 12(9): 1837-47.

Liu Y., Wu HW., Sheard MA., Sposto R., Somanchi SS., Cooper LJ et al. Growth and activation of natural killer cells ex vivo from children with neuroblastoma for adoptive cell therapy. Clin Cancer Res. 2013; 19(8): 2132-43.

Liu Z, et al. CASZ1, a candidate tumor-suppressor gene, suppresses neuroblastoma tumour growth through reprogramming gene expression. Cell Death Differ. 2011; 18(7): 1174–1183.

Loayza-Puch F., Drost J., Rooijers K., Lopes R., Elkon R., Agami R. p53 induces transcriptional and translational programs to suppress cell proliferation and growth. Genome Biol. 2013; 14(4): R32.

London WB., Castel V., Monclair T., Ambros PF., Pearson AD., Cohn SL et al. Clinical and biologic features predictive of survival after relapse of neuroblastoma: a report from the International Neuroblastoma Risk Group project. J Clin Oncol. 2011; 29(24): 3286-92.

Long YC., Zierath JR. AMP-activated protein kinase signaling in metabolic regulation. J Clin Invest. 2006; 116(7): 1776-83.

Longo L., Platini F., Scardino A., Alabiso O., Vasapollo G., Tessitore L. Autophagy inhibition enhances anthocyanin-induced apoptosis in hepatocellular carcinoma. Mol Cancer Ther. 2008; 7: 2476-2485.

Löschmann N., Michaelis M., Rothweiler F., Zehner R., Cinatl J., Voges Y et al. Testing of SNS-032 in a Panel of Human Neuroblastoma Cell Lines with Acquired Resistance to a Broad Range of Drugs. Transl Oncol. 2013; 6(6): 685-96.

Loriot Y., Massard C., Gross-Goupil M., Di Palma M., Escudier B., Bossi A et al. Combining carboplatin and etoposide in docetaxel-pretreated patients with castration-resistant prostate cancer: a prospective study evaluating also neuroendocrine features. Ann Oncol. 2009; 20(4): 703-8.

Lu Z., Luo RZ., Lu Y., Zhang X., Yu Q., Khare S et al. The tumor suppressor gene ARHI regulates autophagy and tumor dormancy in human ovarian cancer cells. J Clin Invest. 2008; 118: 3917–29.

Luo JH., Hua WF., Rao HL., Liao YJ., Kung HF., Zeng YX et al. Overexpression of EIF-5A2 predicts tumour recurrence and progression in pTa/pT1 urothelial carcinoma of the bladder. Cancer Sci. 2009; 100: 896–902.

Luo S., Garcia-Arencibia M., Zhao R., Puri C., Toh PP., Sadiq O et al. Bim inhibits autophagy by recruiting Beclin 1 to microtubules. Mol Cell. 2012; 47(3): 359-70.

Lysaght J., Verma NK., Maginn EN., Ryan JM., Campiani G., Zisterer DM et al. The microtubule targeting agent PBOX-15 inhibits integrin-mediated cell adhesion and induces apoptosis in acute lymphoblastic leukaemia cells. Int J Oncol. 2013; 42(1): 239-46.

Magee JA., Piskounova E., Morrison SJ. Cancer stem cells: impact, heterogeneity, and uncertainty. Cancer Cell. 2012; 21(3):283-96.

Maginn EN., Browne PV., Hayden P., Vandenberghe E., MacDonagh B., Evans P et al. PBOX-15, a novel microtubule targeting agent, induces apoptosis, upregulates death receptors, and potentiates TRAIL-mediated apoptosis in multiple myeloma cells. Br J Cancer. 2011; 104 (2): 281-9.

Manohar CF., Bray JA., Salwen HR., Madafiglio J., Cheng A., Flemming C et al. MYCN-mediated regulation of the MRP1 promoter in human neuroblastoma. Oncogene. 2004; 23(3): 753-62.

Marchi S., Giorgi C., Suski JM., Agnoletto C., Bononi A., Bonora M et al. Mitochondria-ros crosstalk in the control of cell death and aging. J Signal Transduct. 2012; 2012: 329635.

Maris JM. Recent advances in neuroblastoma. N Engl J Med 2010; 362 (23): 2202-11.

Maris JM., White PS., Beltinger CP., Sulman EP., Castleberry RP., Shuster JJ et al. Significance of chromosome 1p loss of heterozygosity in neuroblastoma. Cancer Res. 1995; 55(20): 4664-9.

Marleau AM., Chen CS., Joyce JA., Tullis RH. Exosome removal as a therapeutic adjuvant in cancer. J Transl Med. 2012; 10: 134.

Martinez-Ruiz G., Maldonado V., Ceballos-Cancino G., Grajeda JP., Melendez-Zajgla J. Role of Smac/DIABLO in cancer progression. J Exp Clin Cancer Res. 2008; 27: 48.

Matthay KK., Reynolds CP., Seeger RC., Shimada H., Adkins ES., Haas-Kogan et al. Long-term results for children with high-risk neuroblastoma treated on a randomized trial of myeloablative therapy followed by 13-cis-retinoic acid: a Children's Oncology Group study. J. Clin. Oncol. 2009; 2 (7):1007–13.

Matter MS., Decaens T., Andersen JB., Thorgeirsson SS. Targeting the mTOR pathway in hepatocellular carcinoma: current state and future trends. J Hepatol. 2014; 60(4): 855-65.

Mazure NM & Pouysségur J. Hypoxia-induced autophagy: cell death or cell survival? Curr Opin Cell Biol. 2010; 22(2): 177-80.

Mavromoustakos T., Durdagi S., Koukoulitsa C., Simcic M., Papadopoulos MG., Hodoscek M et al. Strategies in the rational drug design. Curr Med Chem. 2011;18(17): 2517-30.

Mayer LD., Janoff AS. Optimizing combination chemotherapy by controlling drug ratios. Mol Interv. 2007; 7(4): 216-23.

McGee MM., Campiani G., Ramunno A., Fattorusso C., Nacci V., Lawler M et al. Pyrrolo-1,5-benzoxazepines induce apoptosis in chronic myelogenous leukemia (CML) cells by bypassing the apoptotic suppressor bcr-abl. J Pharmacol Exp Ther. 2001; 296 (1):31-40.

McGee MM., Greene, L.M., Ledwidge S., Campiani G., Nacci V., Lawler M et al. Selective Induction of Apoptosis by Pyrrolo-1,5-benzoxazepine (PBOX-6) in Leukaemia cells Occurs via the c-Jun NH2-Terminal Kinase-Dependent Phosphorylation and Inactivation of Bcl-2 and Bcl-xl. J Pharmacol Exp Ther. 2004; 310 (3): 1084-95

McGee MM., Greene, L.M., Ledwidge S., Campiani G., Nacci V., Lawler M et al. Selective Induction of Apoptosis by Pyrrolo-1,5-benzoxazepine (PBOX-6) in Leukaemia cells Occurs via the c-Jun NH2-Terminal Kinase-Dependent Phosphorylation and Inactivation of Bcl-2 and Bcl-xl. J Pharmacol Exp Ther. 2004; 310 (3):1084-95.

McElligott AM., Maginn EN., Greene LM., McGuckin S., Hayat A., Browne PV et al. The novel tubulin-targeting agent pyrrolo-1,5-benzoxazepine-15 induces apoptosis in poor prognostic subgroups of chronic lymphocytic leukemia. Cancer Res. 2009; 69 (21):8366-75.

McFadden JW, Corl BA. Activation of AMP-activated protein kinase (AMPK) inhibits fatty acid synthesis in bovine mammary epithelial cells.Biochem Biophys Res Commun. 2009; 390: 388–93.

McIlwain DR., Berger T., Mak TW. Caspase functions in cell death and disease. Cold Spring Harb Perspect Biol. 2013; 5(4): a008656.

Mehra R., Camidge DR., Sharma S., Felip E., Tan DS., Vansteenkiste JF, et al. First-in-human phase 1 study of the ALK inhibitor LDK378 in ALK+ solid tumors. Journal of Clinical Oncology (Meeting Abstracts) 2012; 30 Abstract nr 3007.

Meisse D., Van de Casteele M, Beauloye C, Hainault I, Kefas BA, Rider MH et al. Sustained activation of AMP-activated protein kinase induces c-Jun N-terminal kinase activation and apoptosis in liver cells. FEBS Lett. 2002; 526(1-3): 38-42.

Meyuhas O & Dreazen A. Ribosomal protein S6 kinase from TOP mRNAs to cell size. Crit Rev Food Sci Nutr. 2012; 52(5): 373-81.

Michaelis M., Rothweiler F., Klassert D., von Deimling A., Weber K., Fehse B et al. Reversal of P-glycoprotein-mediated multidrug resistance by the murine double minute 2 antagonist nutlin-3. Cancer Res. 2009; 69(2): 416-21.

Michels E., Hoebeeck J., De Preter K., Schramm A., Brichard B., De Paepe A et al. CADM1 is a strong neuroblastoma candidate gene that maps within a 3.72 Mb critical region of loss on 11q23. BMC Cancer. 2008; 8: 173.

Mohan N., Banik NL., Ray SK. Combination of N-(4-hydroxyphenyl) retinamide and apigenin suppressed starvation-induced autophagy and promoted apoptosis in malignant neuroblastoma cells. Neurosci Lett. 2011; 502(1): 24-9.

Modak S & Cheung NK. Antibody-based targeted radiation to pediatric tumors. J Nucl Med. 2005; 46 Suppl 1:157S–163S.

Modak S., Guo HF., Humm JL., Smith-Jones PM., Larson SM., Cheung NK. Radioimmunotargeting of human rhabdomyosarcoma using monoclonal antibody 8H9. Cancer Biother Radiopharm. 2005; 20: 534–546.

Modak S., Kramer K., Gultekin SH., Guo HF., Cheung NK. Monoclonal antibody 8H9 targets a novel cell surface antigen expressed by a wide spectrum of human solid tumours. Cancer Res. 2001; 61: 4048–4054.

Mojsa B., Lassot I., Desagher S. Mcl-1 ubiquitination: unique regulation of an essential survival protein. Cells. 2014; 3(2): 418-37.

Molenaar JJ., Ebus ME., Geerts D., Koster J., Lamers F., Valentijn LJ et al. Inactivation of CDK2 is synthetically lethal to MYCN over-expressing cancer cells. Proc Natl Acad Sci USA. 2009; 106(31): 12968-73.

Moretta L., Locatelli F., Pende D., Sivori S., Falco M., Bottino C et al. Human NK receptors: from the molecules to the therapy of high risk leukemias. FEBS Lett. 2011; 585: 1563–710.

Moser VC. Functional assays for neurotoxicity testing. Toxicol Pathol. 2011; 39 (1): 36-45.

Mosse YP., Laudenslager M., Khazi D., Carlisle AJ., Winter CL., Rappaport E et al. Germline PHOX2B mutation in hereditary neuroblastoma. Am J Hum Genet. 2004; 75(4): 727–730.

Mossé YP., Laudenslager M., Longo L., Cole KA., Wood A., Attiyeh EF et al. Identification of ALK as a major familial neuroblastoma predisposition gene. Nature. 2008; 455(7215): 930–935.

Mossé YP., Lim MS., Voss SD., Wilner K., Ruffner K., Laliberte J et al. Safety and activity of crizotinib for paediatric patients with refractory solid tumours or anaplastic large-cell lymphoma: a Children's Oncology Group phase 1 consortium study. Lancet Oncol. 2013; 14(6):472-80.

Moudi M., Go R., Nazare N., Yien CY. Vinca Alkaloids. Int J Prev Med. 2013; 4(11): 1231–1235.

Mueller S., Matthay KK. Neuroblastoma: biology and staging. Curr Oncol Rep. 2009; 11(6): 431-8.

Muller PA & Vousden KH. p53 mutations in cancer. Nat Cell Biol. 2013; 15(1): 2-8.

Mulligan JM., Greene LM., Cloonan S., Mc Gee MM., Onnis V., Campiani G et al. Identification of tubulin as the molecular target of proapoptotic pyrrolo-1,5-benzoxazepines. Mol Pharmacol. 2006; 70 (1): 60-70.

Munafó DB & Colombo MI. A novel assay to study autophagy: regulation of autophagosome vacuole size by amino acid deprivation. J Cell Sci. 2001; 114(Pt 20): 3619-29.

Murphy KM., Ranganathan V., Farnsworth ML., Kavallaris M., Lock RB. Bcl-2 inhibits Bax translocation from cytosol to mitochondria during drug-induced apoptosis of human tumor cells. Cell Death Differ. 2000; 7(1): 102-11.

Musacchio A & Salmon ED. The spindle-assembly checkpoint in space and time. Nat Rev Mol Cell Biol. 2007; 8(5): 379-93.

Nasmyth K., Peters JM., Uhlmann F. Splitting the chromosome: cutting the ties that bind sister chromatids. Science. 2000; 288(5470): 1379-85.

Nathwani SM., Butler S., Fayne D., McGovern N., Sarkadi B., Meegan MJ et al. Novel microtubule targeting agents, pyrrolo-1,5-benzoxazepines, induce apoptosis in multi-drug resistant (MDR) cancer cells. Cancer Chemother Pharmacol. 2010; 66 (3): 585-96.

Nathwani SM., Cloonan SM., Stronach M., Campiani G., Lawler M., Williams DC et al. Novel microtubule-targeting agents, pyrrolo-1,5-benzoxazepines, induce cell cycle arrest and apoptosis in prostate cancer cells. Oncol Rep. 2010; 24(6): 1499-507.

Neefjes J., Jongsma ML., Paul P., Bakke O. Towards a systems understanding of MHC class I and MHC class II antigen presentation. Nat Rev Immunol. 2011; 11(12): 823-36.

Nelson NJ. Targeting the right treatments for neuroblastoma. J Natl Cancer Inst. 2011; 103(16): 1218-21.

Nguyen M., Marcellus RC., Roulston A., Watson M., Serfass L., Murthy Madiraju SR et al. Small molecule obatoclax (GX15-070) antagonizes MCL-1 and overcomes MCL-1-mediated resistance to apoptosis. Proc Natl Acad Sci USA. 2007; 104(49): 19512-7.

Noble RL, Beer CT, Cutts JH. Role of chance observations in chemotherapy: Vinca rosea. Ann N Y Acad Sci. 1958; 76(3): 882-94.

Nogales E., Wolf SG., Downing KH. Structure of the alpha beta tubulin dimer by electron crystallography. Nature. 1998; 391(6663): 199-203.

Nogueira V & Hay N. Molecular pathways: reactive oxygen species homeostasis in cancer cells and implications for cancer therapy. Clin Cancer Res. 2013; 19(16): 4309-14

Nowacki S., Skowron M., Oberthuer A., Fagin A., Voth H., Brors B, et al. Expression of the tumour suppressor gene CADM1 is associated with favourable outcome and inhibits cell survival in neuroblastoma. Oncogene. 2008; 27(23): 3329–3338.

Nuchtern JG., London WB., Barnewolt CE., Naranjo A., McGrady PW., Geiger JD et al. A prospective study of expectant observation as primary therapy for neuroblastoma in young infants: a Children's Oncology Group study. Ann Surg. 2012; 256 (4): 573-80.

Obexer P & Ausserlechner MJ. X-linked inhibitor of apoptosis protein - a critical death resistance regulator and therapeutic target for personalized cancer therapy. Front Oncol. 2014; 4: 197.

Opel D, Poremba C, Simon T, Debatin KM, Fulda S. Activation of Akt predicts poor outcome in neuroblastoma. Cancer Res 2007; 67: 735–45.

Ow YP., Green DR., Hao Z., Mak TW. Cytochrome c: functions beyond respiration. Nat Rev Mol Cell Biol. 2008; 9(7): 532-42.

Pajic M., Norris MD., Cohn SL., Haber M. The role of the multidrug resistance-associated protein 1 gene in neuroblastoma biology and clinical outcome. Cancer Lett. 2005; 228(1-2): 241-6.

Paletta-Silva R., Rocco-Machado N., Meyer-Fernandes JR. NADPH oxidase biology and the regulation of tyrosine kinase receptor signaling and cancer drug cytotoxicity. Int J Mol Sci. 2013; 14(2): 3683-704.

Pan C., Kumar C., Bohl S., Klingmueller U., Mann M. Comparative proteomic phenotyping of cell lines and primary cells to assess preservation of cell type-specific functions. Mol Cell Proteomics. 2009; 8(3): 443-50.

Papadopoulos V., Amri H., Boujrad N., Cascio C., Culty M., Garnier M et al. Peripheral benzodiazepine receptor in cholesterol transport and steroidogenesis. Steroids. 1997; 62(1): 21-8.

Park JG., Kramer BS., Lai SL., Goldstein LJ., Gazdar AF. Chemosensitivity patterns and expression of human multidrug resistance-associated MDR1 gene by human gastric and colorectal carcinoma cell lines. J Natl Cancer Inst. 1990; 82(3): 193-8.

Park SB., Goldstein D., Krishnan AV., Lin CS., Friedlander ML., Cassidy et al. Chemotherapy-induced peripheral neurotoxicity: a critical analysis. CA Cancer J Clin. 2013; 63(6): 419-37.

Peaston AE., Gardaneh M., Franco AV., Hocker JE., Murphy KM., Farnsworth ML et al. MRP1 gene expression level regulates the death and differentiation response of neuroblastoma cells. Br J Cancer. 2001; 85(10): 1564-71.

Pelicano H, Carney D, Huang P. ROS stress in cancer cells and therapeutic implications. Drug Resist Updat. 2004; 7: 97–110.

Pelicano H., Feng L., Zhou Y., Carew JS., Hileman EO., Plunkett W et al. Inhibition of mitochondrial respiration: a novel strategy to enhance drug-induced apoptosis in human leukemia cells by a reactive oxygen species-mediated mechanism. J Biol Chem 2003; 278: 37832–9.

Petroni M., Veschi V., Gulino A. & Giannini G. Molecular mechanisms of MYCN-dependent apoptosis and the MDM2-p53 pathway: an Achille's heel to be exploited for the therapy of MYCN-amplified neuroblastoma. Front. Oncol. 2012; 2: 141.

Piacentini M., Piredda L., Starace DT., Annicchiarico-Petruzzelli M., Mattei M., Oliverio S et al. Differential growth of N- and S-type human neuroblastoma cells xenografted into scid mice. correlation with apoptosis. J Pathol. 1996; 180(4):415-22.

Pignata S., Scambia G., Katsaros D., Gallo C., Pujade-Lauraine E et al. Carboplatin plus paclitaxel once a week versus every 3 weeks in patients with advanced ovarian cancer(MITO-7): a randomised, multicentre, open-label, phase 3 trial. Lancet Oncol. 2014; 15(4): 396-405.

Pirlich M, Kiok K, Sandig G, Lochs H, and Grune T. Alpha-lipoic acid prevents ethanol-induced protein oxidation in mouse hippocampal HT22 cells. Neurosci Lett. 2002; 328: 93–96.

Plantaz D., Vandesompele J., Van Roy N., Lastowska M., Bown N., Combaret V et al. Comparative genomic hybridization (CGH) analysis of stage 4 neuroblastoma reveals high frequency of 11qdeletion in tumors lacking MYCN amplification. Int J Cancer. 2001; 91(5): 680-6.

Porro A., Haber M., Diolaiti D., Iraci N., Henderson M., Gherardi S., et al. Direct and coordinate regulation of ATP-binding cassette transporter genes by Myc factors generates specific transcription signatures that significantly affect the chemoresistance phenotype of cancer cells. J. Biol. Chem. 2010; 285: 19532–19543

Pradelli LA., Bénéteau M., Chauvin C., Jacquin MA., Marchetti S., Muñoz-Pinedo C et al. Glycolysis inhibition sensitizes tumor cells to death receptors-induced apoptosis by AMP kinase activation leading to Mcl-1 block in translation. Oncogene. 2010; 29(11): 1641-52.

Qu, X. et al. Promotion of tumorigenesis by heterozygous disruption of the beclin 1 autophagy gene. J. Clin. Invest. 2003; 112: 1809–1820.

Raina V., Sharma A., Mohanti BK., Kumar R., Dawar R., Rath GK. Etoposide, vinblastine, adriamycin and prednisolone (EVAP) combination chemotherapy as first-line treatment for Hodgkin's disease. Natl Med J India. 2003; 16(4): 199-203.

Ramani P & Lu QL. Expression of bcl-2 gene product in neuroblastoma. J Pathol. 1994; 172(3): 273-8.

Rapino F., Naumann I., Fulda S. Bortezomib antagonizes microtubule-interfering drug-induced apoptosis by inhibiting G2/M transition and MCL-1 degradation. Cell Death Dis. 2013; 4: e925.

Ritter G & Livingston PO. Ganglioside antigens expressed by human cancer cells. Semin Cancer Biol. 1991; 2(6): 401-9.

Ronghe M., Hargrave D., Bartels U., Tabori U., Vaidya S., Chandler C et al. Vincristine and carboplatin chemotherapy for unresectable and/or recurrent low-grade astrocytoma of the brainstem. Pediatr Blood Cancer. 2010; 55(3): 471-7.

Rosenwald IB., Wang S., Savas L., Woda B. & Pullman J. Expression of translation initiation factor eIF-2α is increased in benign and malignant melanocytic and colonic epithelial neoplasms. Cancer. 2003; 98: 1080–1088.

Ross RA, Biedler JL, Spengler BA. A role for distinct cell types in determining malignancy in human neuroblastoma cell lines and tumors. Cancer Lett. 2003; 197(1-2): 35-9.

Rubie H., De Bernardi B., Gerrard M., Canete A., Ladenstein R., Couturier J. Excellent outcome with reduced treatment in infants with nonmetastatic and unresectable neuroblastoma without MYCN amplification: results of the prospective INES 99.1. J Clin Oncol. 2011; 29(4): 449-55.

Rusan NM, Fagerstrom CJ, Yvon AM, Wadsworth P. Cell cycle-dependent changes in microtubule dynamics in living cells expressing green fluorescent protein-alpha tubulin. Mol Biol Cell. 2001; 12(4): 971-80.

Saelens X., Festjens N., Vande Walle L., van Gurp M., van Loo G., Vandenabeele P. Toxic proteins released from mitochondria in cell death. Oncogene. 2004; 23(16): 2861-74.

Sampath J., Sun D., Kidd VJ., Grenet J., Gandhi A., Shapiro LH et al. Mutant p53 cooperates with ETS and selectively up-regulates human MDR1 not MRP1. J Biol Chem. 2001; 276(42): 39359-67.

Santo EE., Stroeken P., Sluis PV., Koster J., Versteeg R., Westerhout EM. FOXO3a is a major target of inactivation by PI3K/AKT signaling in aggressive neuroblastoma. Cancer Res. 2013; 73(7): 2189-98.

Saraswathy M & Gong S. Different strategies to overcome multidrug resistance in cancer. Biotechnol Adv. 2013; 31(8): 1397-407.

Sarkadi B., Homolya L., Szakacs G and Varadi A. Human multidrug resistance ABCB and ABCG transporters: participation in a chemoimmunity defence system. Physiol Rev. 2006; 86: 1179–236.

Sarosiek KA., Ni Chonghaile T., Letai A. Mitochondria: gatekeepers of response to chemotherapy. Trends Cell Biol. 2013; 23(12): 612-9.

Scaruffi P., Morandi F., Gallo F., Stigliani S., Parodi S., et al. Bone marrow of neuroblastoma patients shows downregulation of CXCL12 expression and presence of IFN signature. Pediatr Blood Cancer. 2012; 59(1): 44-51.

Schaich M., Soucek S., Thiede C., Ehninger G., Illmer T; SHG AML96 Study Group. MDR1 and MRP1 gene expression are independent predictors for treatment outcome in adult acute myeloid leukaemia. Br J Haematol. 2005; 128(3): 324-32.

Schleiermacher G., Mosseri V, London WB, Maris JM, Brodeur GM, Attiyeh E et al. Segmental chromosomal alterations have prognostic impact in neuroblastoma: a report from the INRG project. Br J Cancer. 2012; 107(8): 1418-22.

Schmidt ML., Lukens JN., Seeger RC., Brodeur GM., Shimada H., Gerbing RB et al. Biologic factors determine prognosis in infants with stage IV neuroblastoma: A prospective Children's Cancer Group study. J Clin Oncol. 2000; 18(6): 1260-8.

Schwickart M., Huang X., Lill JR., Liu J., Ferrando R., French DM et al. Deubiquitinase USP9X stabilizes MCL1 and promotes tumour cell survival. Nature. 2010; 463(7277): 103-7.

Sengupta S., Peterson TR., Sabatini DM. Regulation of the mTOR complex 1 pathway by nutrients, growth factors, and stress. Nat Rev Mol Cell Biol. 2014; 15(3): 153.

Seto B. Rapamycin and mTOR: a serendipitous discovery and implications for breast cancer. Clin Transl Med. 2012; 1(1): 29.

Seto T., Kiura K., Nishio M., Nakagawa K., Maemondo M., Inoue A, et al. CH5424802 (RO5424802) for patients with ALK-rearranged advanced non-small-cell lung cancer (AF-001JP study): a single-arm, open-label, phase 1-2 study. Lancet Oncol. 2013; 14(7): 590-8.

Shah NP., Nicoll JM., Nagar B., Gorre ME., Paquette RL., Kuriyan J et al. Multiple BCR-ABL kinase domain mutations confer polyclonal resistance to the tyrosine kinase inhibitor imatinib (STI571) in chronic phase and blast crisis chronic myeloid leukemia. Cancer Cell. 2002; 2: 99–102.

Shalinsky DR., Brekken J., Zou H., Bloom LA., McDermott CD., Zook S et al. Marked antiangiogenic and antitumor efficacy of AG3340 in chemoresistant human non-small cell lung cancer tumors: single agent and combination chemotherapy studies. Clin Cancer Res. 1999; 5(7): 1905-17.

Sharp SE., Parisi MT., Gelfand MJ., Yanik GA., Shulkin BL. Functional-metabolic imaging of neuroblastoma. Q J Nucl Med Mol Imaging. 2013; 57(1): 6-20.

She QB., Halilovic E., Ye Q., Zhen W., Shirasawa S, et al. 4E-BP1 is a key effector of the oncogenic activation of the AKT and ERK signalling pathways that integrates their function in tumours. Cancer Cell. 2010; 18: 39–51.

Sheard MA., Asgharzadeh S., Liu Y., Lin TY., Wu HW., Ji L et al. Membrane-bound TRAIL supplements natural killer cell cytotoxicity against neuroblastoma cells. J Immunother. 2013; 36(5): 319-29.

Shveygert M., Kaiser C., Bradrick SS., Gromeier M. Regulation of eukaryotic initiation factor 4E (eIF4E) phosphorylation by mitogen-activated protein kinase occurs through modulation of Mnk1-eIF4G interaction. Mol Cell Biol. 2010; 30(21): 5160-7.

Siddik ZH. Cisplatin: mode of cytotoxic action and molecular basis of resistance. Oncogene. 2003; 22: 7265-7279.

Sieczkowski E., Lehner C., Ambros PF., Hohenegger M. Double impact on p-glycoprotein by statins enhances doxorubicin cytotoxicity in human neuroblastoma cells. Int J Cancer. 2010; 126(9): 2025-35.

Silvera D & Schneider RJ. Inflammatory breast cancer cells are constitutively adapted to hypoxia. Cell Cycle. 2009; 8: 3091–3096.

Silvera D., Formenti SC., Schneider RJ. Translational control in cancer. Nat Rev Cancer. 2010; 10(4): 254-66.

Simon HU., Haj-Yehia A. and Levi-Schaffer F. Role of reactive oxygen species (ROS) in apoptosis induction. Apoptosis. 2000; 5: 415-418.

Slack A., Chen Z., Tonelli R., Pule M., Hunt L., Pession A et al. The p53 regulatory gene MDM2 is a direct transcriptional target of MYCN in neuroblastoma. Proc Natl Acad Sci USA. 2005; 102(3): 731-6.

Smolewski P & Robak T. Inhibitors of apoptosis proteins (IAPs) as potential molecular targets for therapy of hematological malignancies. Curr Mol Med. 2011; 11(8): 633-49.

Sondel PM & Hank JA. Antibody-directed, effector cell-mediated tumour destruction. Hematol Oncol Clin North Am. 2001; 15(4): 703–721.

Sonenberg N & Hinnebusch AG. Regulation of translation initiation in eukaryotes: Mechanisms and biological targets. Cell. 2009; 136: 731–745.

Srinivasula SM., Ahmad M., Fernandes-Alnemri T., Alnemri ES. Autoactivation of procaspase-9 by Apaf-1-mediated oligomerization. Mol Cell. 1998; 1(7): 949-57.

Srivastava RK., Srivastava AR., Korsmeyer SJ., Nesterova M., Cho-Chung YS., Longo DL. Involvement of microtubules in the regulation of Bcl2 phosphorylation and apoptosis through cyclic AMP-dependent protein kinase. Mol Cell Biol. 1998; 18(6): 3509-17.

Stewart DJ. Mechanisms of resistance to cisplatin and carboplatin. Crit Rev Oncol Hematol. 2007; 63(1): 12-31.

Strenger V., Kerbl R., Dornbusch HJ., Ladenstein R., Ambros PF., Ambros IM et al. Diagnostic and prognostic impact of urinary catecholamines in neuroblastoma patients. Pediatr Blood Cancer. 2007; 48(5): 504-9.

Strother DR., London WB., Schmidt ML., Brodeur GM., Shimada H., Thorner P. Outcome after surgery alone or with restricted use of chemotherapy for patients with low-riskneuroblastoma: results of Children's Oncology Group study P9641. J Clin Oncol. 2010; 30(15): 1842-8.

Stupack DG. Teitz T., Potter MD., Mikolon D., Houghton PJ., Kidd VJ et al. Potentiation of neuroblastoma metastasis by loss of caspase-8. Nature. 2006; 439(7072):95-9.

Sugioka R., Shimizu S., Funatsu T., Tamagawa H., Sawa Y., Kawakami T. BH4-domain peptide from Bcl-xL exerts anti-apoptotic activity in vivo. Oncogene. 2003; 22(52):8 432-40.

Sui X., Chen R., Wang Z., Huang Z., Kong N., Zhang M et al. Autophagy and chemotherapy resistance: a promising therapeutic target for cancer treatment. Cell Death Dis. 2013; 10(4):e838.

Sultana S., Khan MR., Kumar M., Kumar S., Ali M. Nanoparticles-mediated drug delivery approaches for cancer targeting: a review. J Drug Target. 2013; 21(2): 107-25.

Suzuki M., Youle RJ., Tjandra N. Structure of Bax: coregulation of dimer formation and intracellular localization. Cell. 2000; 103: 645–654.

Svennerholm L., Boström K., Fredman P., Jungbjer B., Lekman A., Månsson JE et al. Gangliosides and allied glycosphingolipids in human peripheral nerve and spinal cord. Biochim Biophys Acta. 1994; 1214(2): 115–123.

Tacar O., Sriamornsak P., Dass CR. Doxorubicin: an update on anticancer molecular action, toxicity and novel drug delivery systems. Jour Pharm Pharmacol. 2013; 65 (2): 157–70.

Tait SW, Green DR. Mitochondria and cell death: outer membrane permeabilization and beyond. Nat Rev Mol Cell Biol. 2010; 11(9):621-32.

Takenobu H., Shimozato O., Nakamura T., Ochiai H., Yamaguchi Y., Ohira M., Nakagawara A., Kamijo T. CD133 suppresses neuroblastoma cell differentiation via signal pathway modification. Oncogene. 2011; 30:97–105.

Tanaka TU., Stark MJ., Tanaka K. Kinetochore capture and bi-orientation on the mitotic spindle. Nat Rev Mol Cell Biol. 2005; 6(12): 929-42.

Teitz T., Inoue M., Valentine MB., Zhu K., Rehg JE., Zhao W et al. Th-MYCN mice with caspase-8 deficiency develop advanced neuroblastoma with bone marrow metastasis. Cancer Res. 2013; 73(13): 4086-97.

Teitz T., Wei T., Valentine MB., Vanin EF., Grenet J., Valentine VA. Caspase 8 is deleted or silenced preferentially in childhood neuroblastomas with amplification of MYCN. Nat Med. 2000; 6(5): 529-35.

Temirak A., Abdulla M., Elhefnawi M. Rational drug design for identifying novel multi-target inhibitors for hepatocellular carcinoma. Anticancer Agents Med Chem. 2012; 12(9):1088-97.

Thiebaut F, Tsuruo T, Hamada H, Gottesman MM, Pastan I, Willingham MC. Cellular localization of the multidrug-resistance gene product P-glycoprotein in normal human tissues. Proc Natl Acad Sci USA. 1987; 84(21):7735-8.

Thomas LW., Lam C., Edwards SW. Mcl-1; the molecular regulation of protein function. FEBS Lett. 2010; 584(14): 2981-9.

Thompson PM., Gotoh T., Kok M., White PS., Brodeur GM et al. CHD5, a new member of the chromodomain gene family, is preferentially expressed in the nervous system. Oncogene. 2003; 22(7): 1002–1011.

Thornberry NA. The caspase family of cysteine proteases. Br Med Bull. 1997; 53(3):478-90

Tivnan A., Orr WS., Gubala V., Nooney R., Williams DE., McDonagh C et al. Inhibition of neuroblastoma tumor growth by targeted delivery of microRNA-34a using anti-disialoganglioside GD2 coated nanoparticles. PLoS One. 2012; 7(5): e38129.

Tong H., Lu C., Yang Y., Zhang J and Zhang J. Role of caspase 8 as a determinant in trail sensitivity of neuroblastoma cell lines. Pediatr Hematol Oncol. 2009; 26 (8): 549-59.

Tsai KH., Wang WJ., Lin CW., Pai P., Lai TY., Tsai CY et al. NADPH oxidase-derived superoxide anion-induced apoptosis is mediated via the JNK-dependent activation of NF-κB in cardiomyocytes exposed to high glucose. J Cell Physiol. 2012; 227(4): 1347-57.

Tsujimoto Y, Cossman J, Jaffe E, Croce CM. Involvement of the bcl-2 gene in human follicular lymphoma. Science. 1985; 228(4706): 1440-3.

van der Vaart B., Akhmanova A., Straube A. Regulation of microtubule dynamic instability. Biochem Soc Trans. 2009; 37(Pt 5): 1007-13.

Van Maerken T., Rihani A., Van Goethem A., De Paepe A., Speleman F., Vandesompele J. Pharmacologic activation of wild-type p53 by nutlin therapy in childhood cancer. Cancer Lett. 2014; 344(2): 157-65.

van Noesel MM & Versteeg R. Pediatric neuroblastomas: genetic and epigenetic 'danse macabre'. Gene. 2004; 325:1-15.

van Noesel MM. Neuroblastoma stage 4S: a multifocal stem-cell disease of the developing neural crest. Lancet Oncol. 2012; 13(3): 229-30.

Vassilev LT., Vu BT., Graves B., Carvajal D., Podlaski F.,Filipovic et al.,In vivo activation of the p53 pathway by small-molecule antagonists of MDM2. Science. 2004; 303: 844–848.

Vaux DL, Cory S, Adams JM. Bcl-2 gene promotes haemopoietic cell survival and cooperates with c-myc to immortalize pre-B cells. Nature. 1988; 335(6189): 440-2.

Vazquez-Martin A., Oliveras-Ferraros C., Menendez JA. Autophagy facilitates the development of breast cancer resistance to the anti-HER2 monoclonal antibody trastuzumab. PLoS One. 2009; 4: e6251.

Veenman L &Gavish M. The role of 18 kDa mitochondrial translocator protein (TSPO) in programmed cell death, and effects of steroids on TSPO expression. Curr Mol Med. 2012; 12(4): 398-412.

Vermeulen J., De Preter K, Mestdagh P, Laureys G, Speleman F, Vandesompele J. Predicting outcomes for children with neuroblastoma. Discov Med. 2010; 10(50): 29-36.

Vidal SJ., Quinn SA., de la Iglesia-Vicente J., Bonal DM., Rodriguez-Bravo V., Firpo-Betancourt A et al. Isolation of cancer stem cells from human prostate cancer samples. J Vis Exp. 2014; (85).

Vinayak S & Carlson RW. mTOR inhibitors in the treatment of breast cancer. Oncology (Williston Park). 2013; 27(1): 38-44.

Vogler M., Dinsdale D., Dyer MJ., Cohen GM. Bcl-2 inhibitors: small molecules with a big impact on cancer therapy. Cell Death Differ. 2009; 16(3): 360-7.

W.F. Ooi., A. Re., V. Sidarovich., V. Canella., N. Arseni., V. Adami et al. Segmental chromosome aberrations converge on overexpression of mitotic spindle regulatory genes in high-risk neuroblastoma. Genes, Chromosomes & Cancer. 2012; 51(6): 545-56

Walczak H, Krammer PH. The CD95 (APO-1/Fas) and the TRAIL (APO-2L) apoptosis systems. Exp Cell Res. 2000; 256(1): 58-66.

Walker SR., Chaudhury M., Nelson EA., Frank DA. Microtubule-targeted chemotherapeutic agents inhibit signal transducer and activator of transcription 3 (STAT3) signaling. Mol Pharmacol. 2010; 78(5): 903-8.

Wall ME & Wani MC. Recent progress in plant anti-tumour agents. Paper M-006, 153rd National Meeting (1967), American Chemical Society, Miami Beach, Florida.

Wander SA., Hennessy BT., Slingerland JM. Next-generation mTOR inhibitors in clinical oncology: how pathway complexity informs therapeutic strategy. J Clin Invest. 2011; 121(4): 1231-41.

Wang P., Gao Q., Suo Z., Munthe E., Solberg S., Ma L., Wang M et al. Identification and characterization of cells with cancer stem cell properties in human primary lung cancer cell lines. PLoS One. 2013; 8(3): e57020.

Wang X., Gu Z2., Li G., Zhang S., Cao Z., Yang Z., Liu G. Norcantharidin enhances ABT-263-mediated anticancer activity in neuroblastoma cells by upregulation of Noxa. Oncol Rep. 2014; 32(2): 716-22.

Wang XA., Xiang SS., Li HF., Wu XS., Li ML., Shu YJ et al, Cordycepin induces S phase arrest and apoptosis in human gallbladder cancer cells. Molecules. 2014; 19(8): 11350-65.

Weiss WA., Aldape K., Mohapatra G., Feuerstein BG., Bishop JM. Targeted expression of MYCN causes neuroblastoma in transgenic mice. EMBO J. 1997; 16: 2985–2995.

Westermann F., Henrich KO., Wei JS., Lutz W., Fischer M., Konig R et al. High Skp2 expression characterizes high-risk neuroblastomas independent of MYCN status, Clin Can Res 13. 2007; 4695–4703.

Wertz IE., Kusam S., Lam C., Okamoto T., Sandoval W., Anderson DJ et al. Sensitivity to antitubulin chemotherapeutics is regulated by MCL1 and FBW7. Nature. 2011; 471 (7336): 110–14.

Wickström M., Johnsen JI., Ponthan F., Segerström L., Sveinbjörnsson B., Lindskog M et al. The novel melphalan prodrug J1 inhibits neuroblastoma growth in vitro and in vivo. Mol Cancer Ther. 2007; 6 (9): 2409-17.

Williams CR., Tabiosa R., Linehana WM., Neckersa L. Intratumor injection of the Hsp90 inhibitor 17AAG decreases tumor growth and induces apoptosis in a prostate cancer xenograft model. J Urol. 2007; 178: 1528–1532.

Willis SN., Chen L., Dewson G., Wei A., Naik E., Fletcher JI et al. Proapoptotic Bak is sequestered by Mcl-1 and Bcl-xL, but not Bcl-2, until displaced by BH3-only proteins. Genes Dev. 2005; 19 (11): 1294-305.

Winquist RJ., Boucher DM., Wood M., Furey BF. Targeting cancer stem cells for more effective therapies: Taking out cancer's locomotive engine. Biochem Pharmacol. 2009; 78(4): 326-34.

Wolff SN., Hainsworth JD., Greco FA. High dose etoposide: from phase I to component of curative therapy. J Clin Oncol. 2008; 26(33):5310-2.

Wong RP., Khosravi S., Martinka M., Li G. Myeloid leukemia-1 expression in benign and malignant melanocytic lesions. Oncol Rep. 2008; 19(4):933-7.

Wood LD, et al. The genomic landscapes of human breast and colorectal cancers. Science. 2007; 318: 1108–1113.

Wu WD., Hu ZM., Shang MJ., Zhao DJ., Zhang CW., Hong D et al. Cordycepin down-regulates multiple drug resistant (MDR)/HIF-1α through regulating AMPK/mTORC1 signaling in GBC-SD gallbladder cancer cells. Int J Mol Sci. 2014; 15(7): 12778-90.

Wu YJ., Muldoon LL., Neuwelt EA. The chemoprotective agent N-acetylcysteine blocks cisplatin-induced apoptosis through caspase signaling pathway. J Pharmacol Exp Ther. 2005; 312(2): 424-31.

Wyllie AH, Kerr JF, Currie AR. Cell death: the significance of apoptosis. Int Rev Cytol. 1980; 68:251-306.

Xi G., Hu X., Wu B., Jiang H., Young CY., Pang Y., Yuan H. Autophagy inhibition promotes paclitaxel-induced apoptosis in cancer cells. Cancer Lett. 2011; 307(2):141-8.

Xie D., Ma NF., Pan ZZ., Wu HX., Liu YD., Wu GQ et al. Overexpression of EIF-5A2 is associated with metastasis of human colorectal carcinoma. Hum Pathol. 2008; 39(1): 80–86.

Xiong X., Sui M., Fan W., Kraft AS. Cell cycle dependent antagonistic interactions between paclitaxel and carboplatin in combination therapy. Cancer Biol Ther. 2007; 6(7): 1067-73.

Yang JM., Hung CM., Fu CN., Lee JC., Huang CH., Yang MH et al. Hispidulin sensitizes human ovarian cancer cells to TRAIL-induced apoptosis by AMPK activation leading to Mcl-1 block in translation. J Agric Food Chem. 2010; 58(18): 10020-6.

Yang JY., Zong CS., Xia W., Yamaguchi H., Ding Q., Xie X et al. ERK promotes tumorigenesis by inhibiting FOXO3a via MDM2-mediated degradation. Nat Cell Biol. 2008; 10: 138–48.

Yang RK & Sondel PM. Anti-GD2 Strategy in the Treatment of Neuroblastoma. Drugs Future. 2010; 35(8): 665.

Yang S., Wang X., Contino G., Liesa M., Sahin E., Ying H et al. Pancreatic cancers require autophagy for tumour growth. Genes Dev. 2011; 25: 717–29

Yang X., Merchant MS., Romero ME et al. Induction of caspase 8 by interferon gamma renders some neuroblastoma (NB) cells sensitive to tumour necrosis factor-related apoptosis-inducing ligand (TRAIL) but reveals that a lack of membrane TR1/TR2 also contributes to TRAIL resistance in NB. Cancer Res. 2003; 63: 1122–1129.

Yang ZJ., Chee CE., Huang S., Sinicrope FA. The role of autophagy in cancer: therapeutic implications. Mol Cancer Ther. 2011; 10(9): 1533-41.

Youle RJ and Strasser A. The BCL-2 protein family: opposing activities that mediate cell death. Nat Rev Mol Cell Biol. 2008; 9 (1): 47-59.

Yu AL., Gilman AL., Ozkaynak MF., London WB., Kreissman SG., Chen HX et al. Anti-GD2 antibody with GM-CSF, interleukin-2, and isotretinoin for neuroblastoma. N Engl J Med. 2010; 363(14): 1324-34.

Yu K., Toral-Barza L., Shi C., Zhang WG., Lucas J., Shor B et al. Biochemical, cellular, and in vivo activity of novel ATP-competitive and selective inhibitors of the mammalian target of rapamycin. Cancer Res. 2009; 69(15): 6232–6240.

Yu SW., Baek SH., Brennan RT., Bradley CJ., Park SK., Lee YS et al. Autophagic death of adult hippocampal neural stem cells following insulin withdrawal. Stem Cells. 2008; 26: 2602-2610.

Yuste VJ., Sánchez-López I., Solé C., Encinas M., Bayascas JR., Boix J et al. The prevention of the staurosporine-induced apoptosis by Bcl-X(L), but not by Bcl-2 or caspase inhibitors, allows the extensive differentiation of human neuroblastoma cells. J Neurochem. 2002; 80(1): 126-39.

Zage PE & Ater JL. Neuroblastoma. In: Kliegman RM, Behrman RE, Jenson HB, Stanton BF, eds. Nelson Textbook of Pediatrics. 19th ed. Philadelphia, Pa: Saunders Elsevier; 2011: chap 492.

Zhan Z., Li Q., Wu P., Ye Y., Tseng HY., Zhang L., Zhang XD. Autophagy-mediated HMGB1 release antagonizes apoptosis of gastric cancer cells induced by vincristine via transcriptional regulation of Mcl-1. Autophagy. 2012; 8(1):109-21.

Zhang B., Gojo I., Fenton RG. Myeloid cell factor-1 is a critical survival factor for multiple myeloma. Blood. 2002; 99(6):1885-93.

Zhang Q., Si S., Schoen S., Chen J., Jin XB., Wu G. Suppression of autophagy enhances preferential toxicity of paclitaxel to folliculin-deficient renal cancer cells. J Exp Clin Cancer Res. 2013; 32:99.

Zhang Y., Kensler TW., Cho CG., Posner GH., Talalay P. Anticarcinogenic activities of sulforaphane and structurally related synthetic norbornyl isothiocyanates. Proc Natl Acad Sci USA. 1994; 91: 3147-3150.

Zheng B, Jeong JH, Asara JM, Yuan YY, Granter SR, Chin L, Cantley LC. Oncogenic B-RAF negatively regulates the tumor suppressor LKB1 to promote melanoma cell proliferation. Mol Cell. 2009; 33(2): 237-47.

Zhong DT., Shi CM., Chen Q., Hunag JZ., Liang JG., Lin D. Etoposide, vincristine, doxorubicin and dexamethasone (EVAD) combination chemotherapy as second-line treatment for advanced AIDS-related Kaposi's sarcoma. J Cancer Res Clin Oncol. 2012; 138(3): 425-30.

Zhu S., Lee JS., Guo F., Shin J., Perez-Atayde AR., Kutok JL et al. Overexpression of EIF-5A2 is associated with metastasis of human colorectal carcinoma. Hum. Pathol. 2008; 39: 80–86.

Zisterer DM., Campiani., Nacci V and Williams DC. Pyrrolobenzoxazepines induce apoptosis in HL-60, Jurkat and Hut-78 cells: A new class of apoptotic agents. J. Pharmacol. Exp. Ther. 2000; 293 (1): 48-59.

Zou H, Henzel WJ, Liu X, Lutschg A, Wang X. Apaf-1, a human protein homologous to C. elegans CED-4, participates in cytochrome c-dependent activation of caspase-3. Cell. 1997; 90(3): 405-13.

Zou H, Li Y, Liu X, Wang X. An APAF-1.cytochrome c multimeric complex is a functional apoptosome that activates procaspase-9. J Biol Chem. 1999; 274(17): 11549-56.

Appendix

(A)

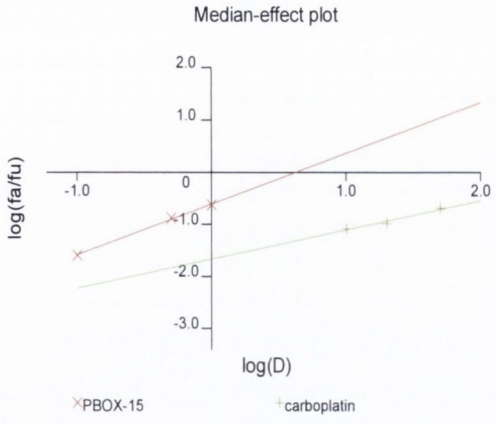

(B)

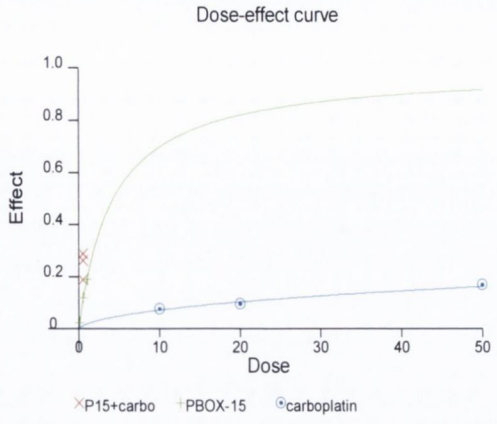

(C)

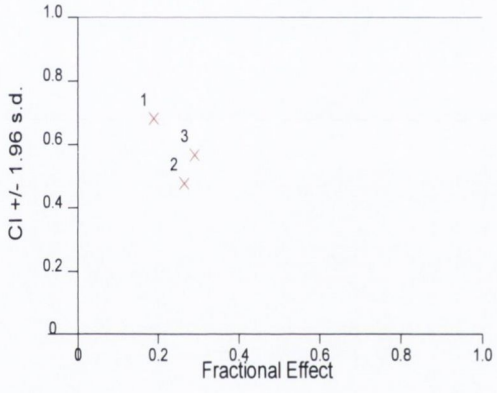

Antagonism

Synergism

1. 0.5 μM P15+10 μM carbo
2. 0.5 μM P15+20 μM carbo
3. 0.5 μM P15+50 μM carbo

Appendix figure 1 PBOX-15 synergistically enhances the apoptotic effects of carboplatin in SHSY5Y cells.

Median dose effect analysis was carried out on SHSY5Y cells using Calcusyn. Cells were treated with 0.5 μM PBOX-15, 10 μM, 20 μM or 50 μM carboplatin or a combination of both for 48hrs. (**A**) Median dose plot, (**B**) dose-effect curve and **(C)** CI value versus fraction affected.

(A)

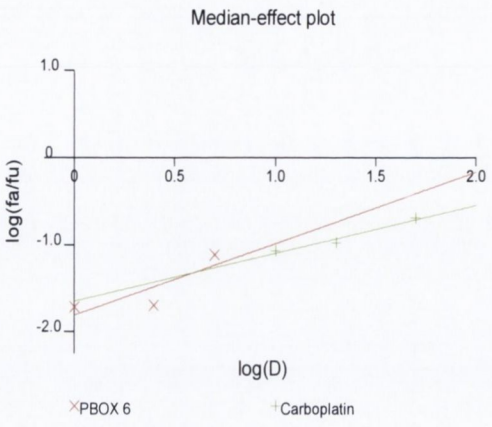

(B)

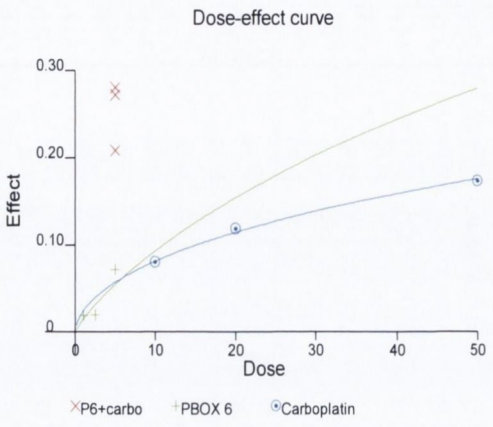

(C)

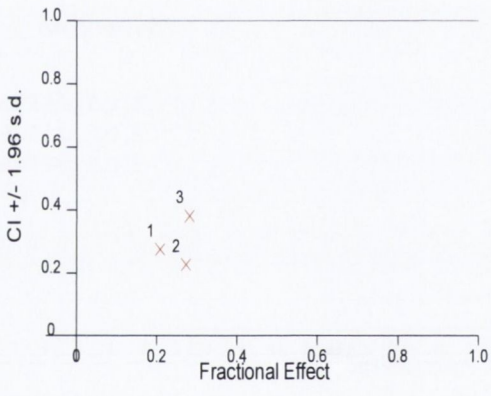

Antagonism

Synergism

1. 5 μM P6 + 10 μM carbo
2. 5 μM P6 + 20 μM carbo
3. 5 μM P6 + 50 μM carbo

Appendix figure 2 PBOX-6 synergistically enhances the apoptotic effects of carboplatin in SHSY5Y cells.

Median dose effect analysis was carried out on SHSY5Y cells using Calcusyn. Cells were treated with 5 μM PBOX-15, 10 μM, 20 μM or 50 μM carboplatin or a combination of both for 48hrs. **(A)** Median dose plot, **(B)** dose-effect curve and **(C)** CI value versus fraction affected.

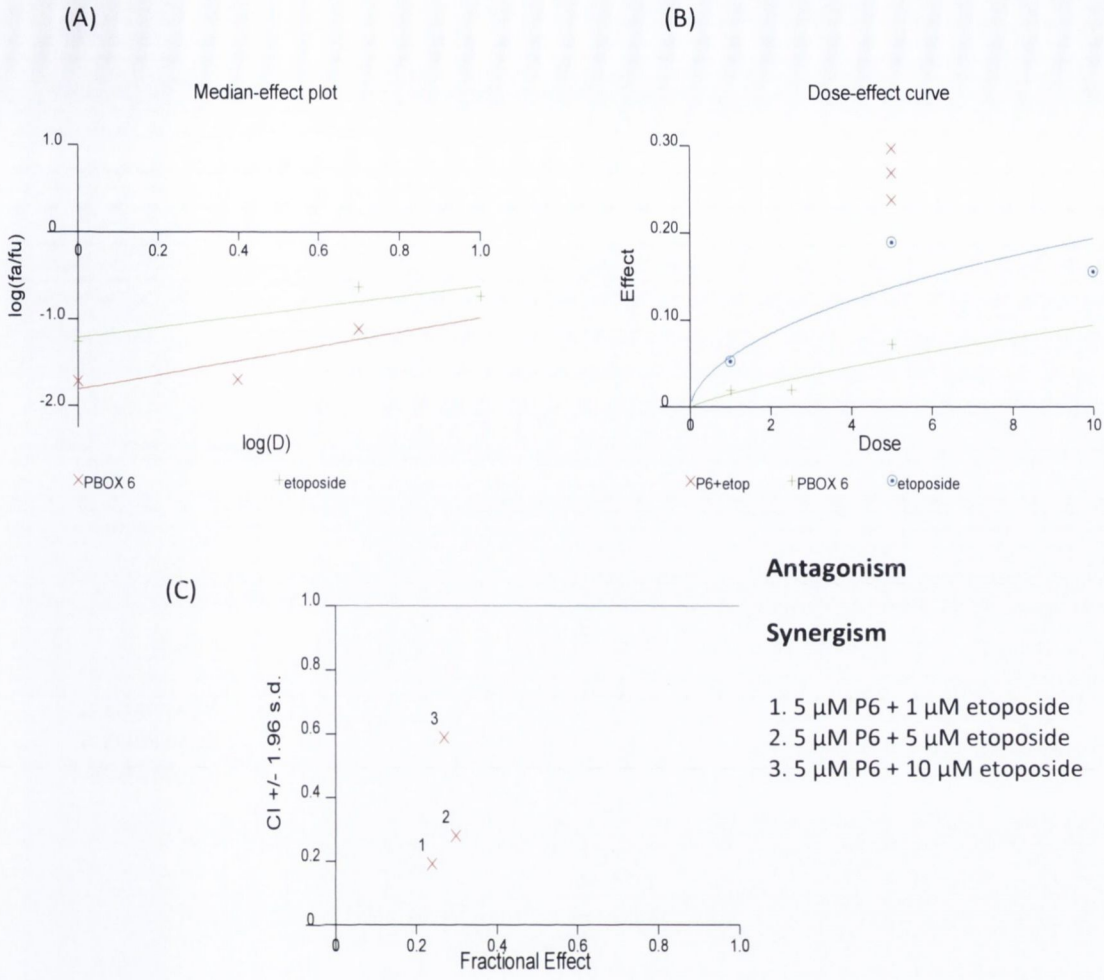

Appendix figure 3 PBOX-6 synergistically enhances the apoptotic effects of etoposide in SHSY5Y cells.

Median dose effect analysis was carried out on SHSY5Y cells using Calcusyn. Cells were treated with 5 μM PBOX-15, 1 μM, 5 μM or 10 μM etoposie or a combination of both for 48hrs. (**A**) Median dose plot, (**B**) dose-effect curve and **(C)** CI value versus fraction affected.

(A)

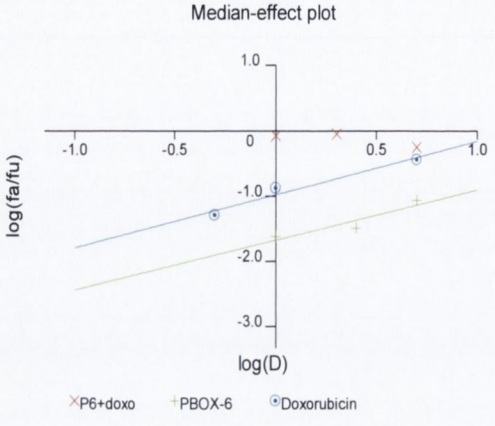

(B)

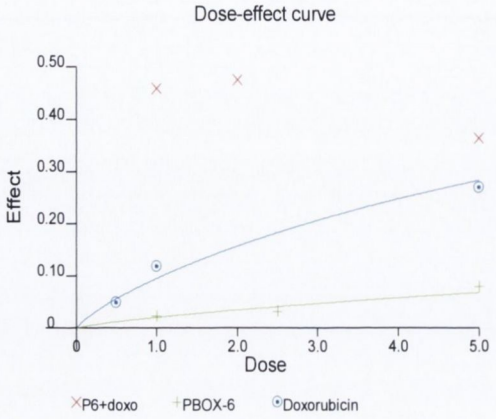

(C)

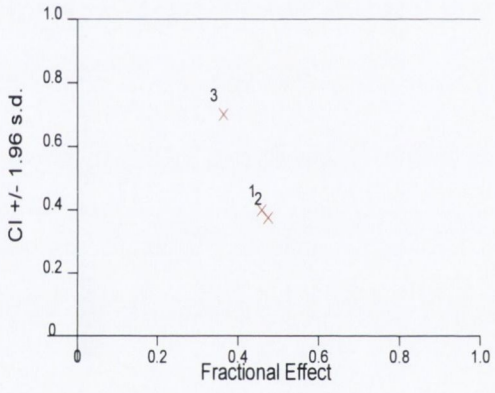

Antagonism

Synergism

1. 5 μM doxo + 1 μM PBOX-6
2. 5 μM doxo + 5 μM PBOX-6
3. 5 μM doxo + 10 μM PBOX-6

Appendix figure 4 PBOX-6 synergistically enhances the apoptotic effects of doxorubicin in SHSY5Y cells.

Median dose effect analysis was carried out on SHSY5Y cells using Calcusyn. Cells were treated with 5 μM doxorubicin or 1 μM, 5 μM or 10 μM PBOX-6 or a combination of both for 48hrs. **(A)** Median dose plot, **(B)** dose-effect curve and **(C)** CI value versus fraction affected.

(A)

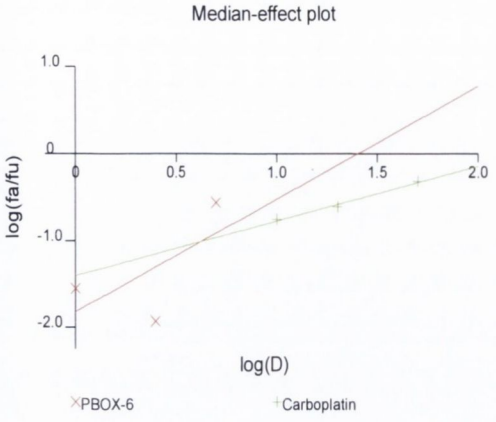

(B)

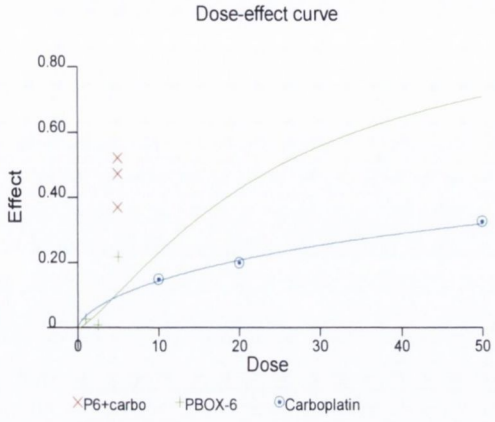

(C)

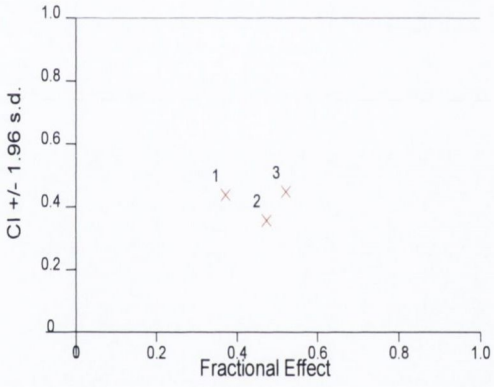

Antagonism

Synergism

1. 5 μM P6 + 10 μM carbo
2. 5 μM P6 + 20 μM carbo
3. 5 μM P6 + 50 μM carbo

Appendix figure 5 PBOX-6 synergistically enhances the apoptotic effects of carboplatin in SHSY5Y cells.

Median dose effect analysis was carried out on SHSY5Y cells using Calcusyn. Cells were treated with 5 μM PBOX-15, 10 μM, 20 μM or 50 μM carboplatin or a combination of both for 72 hrs. **(A)** Median dose plot, **(B)** dose-effect curve and **(C)** CI value versus fraction affected.

.

(A)

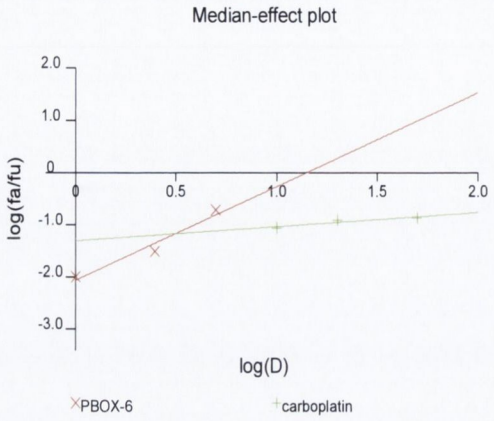

(B)

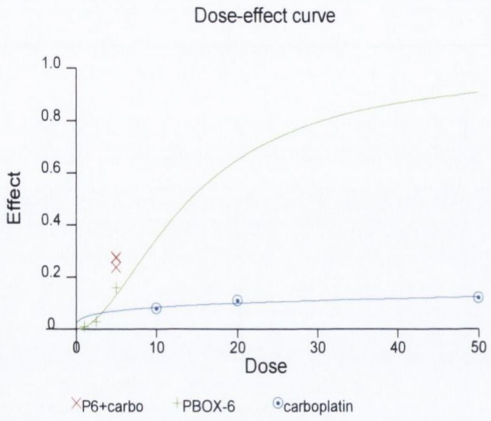

(C)

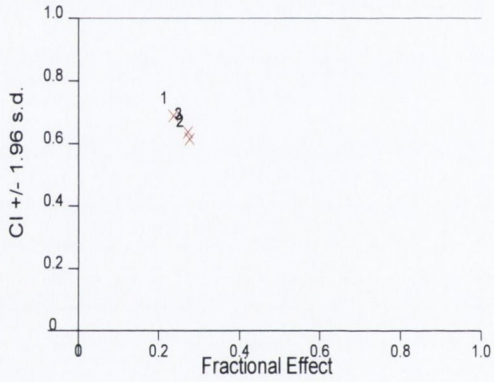

Antagonism

Synergism

1. 5 μM P6 + 10 μM carbo
2. 5 μM P6 + 20 μM carbo
3. 5 μM P6 + 50 μM carbo

Appendix figure 6 PBOX-6 synergistically enhances the apoptotic effects of carboplatin in CHLA-90 cells.

Median dose effect analysis was carried out on SHSY5Y cells using Calcusyn. Cells were treated with 5 μM PBOX-15, 10 μM, 20 μM or 50 μM carboplatin or a combination of both for 48 hrs. **(A)** Median dose plot, **(B)** dose-effect curve and **(C)** CI value versus fraction affected.

.

(A)

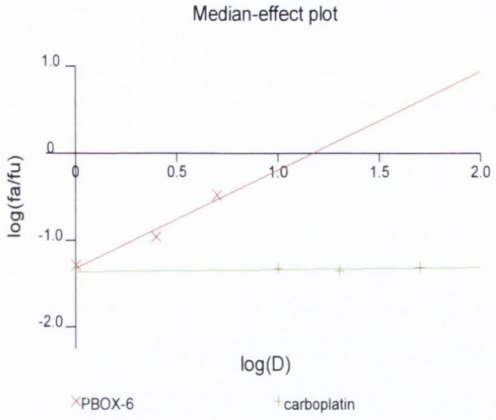

(B)

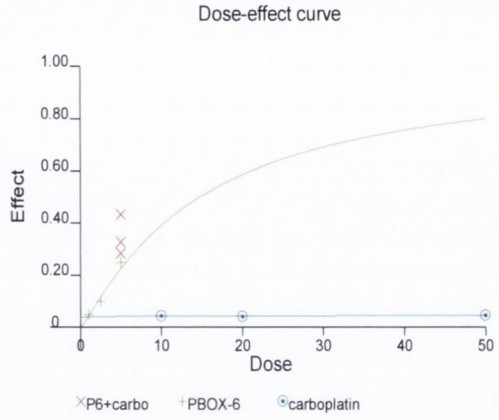

(C)

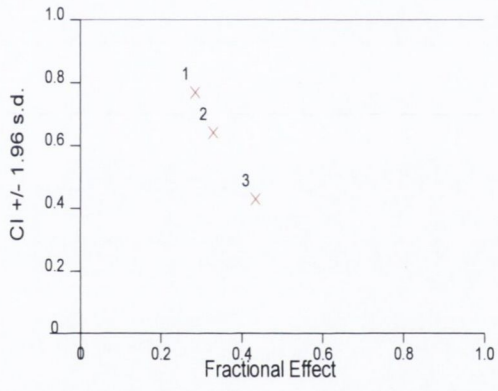

Antagonism

Synergism

1. 5 μM P6 + 10 μM carbo
2. 5 μM P6 + 20 μM carbo
3. 5 μM P6 + 50 μM carbo

Appendix figure 6 PBOX-6 synergistically enhances the apoptotic effects of carboplatin in CHLA-90 cells.

Median dose effect analysis was carried out on SHSY5Y cells using Calcusyn. Cells were treated with 5 μM PBOX-15, 10 μM, 20 μM or 50 μM carboplatin or a combination of both for 72 hrs. (**A**) Median dose plot, (**B**) dose-effect curve and **(C)** CI value versus fraction affected.

Publications

Biochemical Pharmacology 87 (2014) 611–624

Contents lists available at ScienceDirect

Biochemical Pharmacology

journal homepage: www.elsevier.com/locate/biochempharm

The novel pyrrolo-1,5-benzoxazepine, PBOX-6, synergistically enhances the apoptotic effects of carboplatin in drug sensitive and multidrug resistant neuroblastoma cells

Jennifer C. Lennon [a,b,*], Sandra A. Bright [a], Eilis Carroll [a], Stefania Butini [c], Giuseppe Campiani [c], Anne O'Meara [d], D. Clive Williams [a], Daniela M. Zisterer [a]

[a] School of Biochemistry and Immunology, Trinity Biomedical Sciences Institute, Trinity College Dublin, 152-160 Pearse Street, Dublin 2, Ireland
[b] The National Children's Research Centre, Crumlin, Dublin, Ireland
[c] European Research Centre for Drug Discovery & Development, University of Siena, Siena, Italy
[d] Our Lady's Childrens Hospital, Crumlin, Dublin, Ireland

ARTICLE INFO

Article history:
Received 2 September 2013
Received in revised form 19 December 2013
Accepted 20 December 2013
Available online 6 January 2014

Keywords:
PBOX-6
Carboplatin
Neuroblastoma
Apoptosis
Synergy

ABSTRACT

Neuroblastoma, a malignancy of neuroectoderrmal origin, accounts for 15% of childhood cancer deaths. Despite advances in understanding the biology, it remains one of the most difficult paediatric cancers to treat. A major obstacle in the effective treatment of neuroblastoma is the development of multidrug resistance (MDR). There is thus a compelling demand for new treatment strategies for this cancer that can bypass such resistance mechanisms. The pyrrolo-1,5-benzoxazepine (PBOX) compounds are a series of novel microtubule-targeting agents that potently induce apoptosis in various cancer cell lines, *ex vivo* patient samples and *in vivo* cancer models. In this study we examined the ability of two members, PBOX-6 and -15, to exhibit anti-cancer effects in a panel of drug sensitive and MDR neuroblastoma cell lines. The PBOX compounds potently reduced the viability of all neuroblastoma cells examined and exhibited a lower fold resistance in MDR cells when compared to standard chemotherapeutics. In addition, the PBOX compounds synergistically enhanced apoptosis induced by etoposide, carboplatin and doxorubicin. Exposure of drug sensitive and resistant cell lines to PBOX-6/carboplatin induced cleavage of Bcl-2, a downregulation of Mcl-1 and a concomitant increase in Bak. Furthermore, activation of caspase-3, -8 and -9 was demonstrated. Finally, gene silencing of Mcl-1 by siRNA was shown to sensitise both drug sensitive and multidrug resistant cells to carboplatin-induced apoptosis demonstrating the importance of Mcl-1 downregulation in the apoptotic pathway mediated by the PBOX compounds in neuroblastoma. In conclusion, our findings indicate the potential of the PBOX compounds in enhancing chemosensitivity in neuroblastoma.

© 2014 Elsevier Inc. All rights reserved.

1. Introduction

The paediatric malignancy neuroblastoma arises in cells of the neural crest [1]. It is both the most commonly diagnosed tumour in the first year of life and the most common extra cranial solid tumour in early childhood accounting for 15% of cancer deaths in young children [2]. Despite both advances in understanding the biology of the cancer and aggressive treatment strategies, including surgery, chemotherapy, radiation therapy, immunotherapy and differentiation therapy, it continues to be one of the most difficult paediatric cancers to successfully treat with more than 60% of patients presenting at diagnosis with adverse features with less than 40% of these whom achieve disease free long term survival [3]. A major obstacle in the effective treatment of neuroblastoma is the development of multidrug resistance (MDR) to a broad range of cytotoxic drugs [4–6] including vinca alkaloids, alkylating agents, platinum compounds and anthracyclines. This MDR phenotype often includes amplification of the proto oncogene MYCN, mutation/deletion of p53, deletion of loci at 1p or 11q and over expression of MDR proteins leading to altered drug transport and an increase in drug efflux [1]. There is therefore an urgent need for alternative approaches to treatment.

Abbreviations: Bcl-2, B cell lymphoma-2; BCRP, breast cancer resistance protein; CML, chronic myeloid leukaemia; DTT, Dithiothreitol; FAC, fluorescence associated cell sorter; FBS, foetal bovine serum; Mcl-1, Myeloid cell leukaemia 1; MDR, multidrug resistance; MRP1, multidrug resistance associated protein; MTA, microtubule targeting agent; PARP, Poly (ADP-ribose) polymerase; PBOX, pyrrolo-1,5-benzoxazepine.

* Corresponding author.
E-mail addresses: lennonje@tcd.ie (J.C. Lennon), brightsandi@gmail.com (S.A. Bright), e.carroll@dundee.ac.uk (E. Carroll), butini3@unisi.it (S. Butini), campiani@unisi.it (G. Campiani), amwom@eircom.net (A. O'Meara), clive.williams@tcd.ie (D.C. Williams), dzistrer@tcd.ie (D.M. Zisterer).

0006-2952/$ – see front matter © 2014 Elsevier Inc. All rights reserved.
http://dx.doi.org/10.1016/j.bcp.2013.12.017

MDR proteins are members of a family of transmembrane ABC (ATP binding cassette) transporters that use ATP hydrolysis to mediate the export of hydrophobic drugs from the cell. Some of the best studied multidrug resistant proteins of the ABC family are ABCB1 (also called multidrug resistant protein (MDR-1) or *P*-glycoprotein (*p*-gp)), ABCC1 (also called multidrug resistance associated protein (MRP-1)) and breast cancer resistance protein (BCRP) [7]. The 170 kDa -gp is a transmembrane efflux pump with low substrate specificity and this MDR protein has been shown to be overexpressed in neuroblastoma patients where it predicts poor outcome [8] indicating that there is a need for alternative chemotherapeutic agents which are not substrates for these transporters.

Some PBOX compounds have been identified as novel microtubule-targeting agents (MTAs) [9] that possess the ability to potently induce cell cycle arrest and apoptosis in a number of cancer cell lines derived from both solid tumours and haematological malignancies [10–16]. Additionally these compounds have been shown to be efficacious in *in vivo* chronic myeloid leukaemia (CML) [14] and breast cancer animal models [17] and in *ex vivo* studies [11,14]. We previously demonstrated that PBOX-15 induces apoptosis both in *ex vivo* B-cell lymphocytic leukaemia (CLL) cells harbouring poor prognostic indicators and fludarabine resistance-associated p53 deletions [11] and in primary CML patient samples including those resistant to STI-571, the current frontline treatment for CML [13]. Unlike many chemotherapeutic agents, the PBOX compounds are not substrates for many MDR drug efflux pumps [12]. PBOX-6 and 15 were shown to induce comparable levels of apoptosis in both drug sensitive and MDR human promyelocytic leukaemia and ovarian carcinoma cell lines expressing either *p*-gp or BCRP, two of the main ABC transporters associated with MDR, indicating that they may possess advantages over standard chemotherapy which is currently in clinical use.

In this article, we extend our study of the PBOX compounds to neuroblastoma cells including those displaying resistance to chemotherapeutics currently used in the clinic. We show that two representative PBOX compounds reduce the viability of a panel of drug sensitive and MDR neuroblastoma cell lines with similar potency. We also delineate part of the mechanism of PBOX anti-cancer activity in these cells.

We demonstrate caspase-dependent apoptosis. Additionally we demonstrate an early downregulation of anti-apoptotic Mcl-1 and a concomitant upregulation in pro-apoptotic Bak. Importantly, we show that the PBOX compounds synergise with standard chemotherapy in both drug sensitive and MDR neuroblastoma cells and we elucidate part of the mechanism of PBOX potentiation of carboplatin-induced apoptosis in neuroblastoma cells. This study suggests that the PBOX compounds, either alone or in combination with standard chemotherapeutics, have potential as an effective therapy against neuroblastoma.

2. Materials and methods

2.1. Cell culture

SHSY5Y and SK-N-BE(1) cells were cultured in DMEM/F12 + GlutaMAX medium supplemented with 10% (v/v) foetal bovine serum (FBS) and 1% (v/v) penicillin/streptomycin. Kelly and SK-N-BE(2)c cells were grown in RPMI 1640 + GlutaMAX medium supplemented with 10% (v/v) (FBS) and 1% (v/v) penicillin/streptomycin. SK-N-FI cells were grown in DMEM + Glutamax medium supplemented with 10% FBS and 1% penicillin/streptomycin. CHLA-90 cells were grown in IMDM medium supplemented with 1% (v/v) insulin/transferrin/selenium, 10% (v/v) (FBS) and 1% (v/v) penicillin/streptomycin. Cells were incubated in a humidified environment at 95% O_2 and 5% CO_2 and passaged twice a week.

2.2. Reagents

The pyrrolo-1,5-benzoxazepine compounds, 7-[(*N,N*-dimethylcarbamoyl)oxy]-6-(naphth-1-yl)pyrrolo[2,1-][1,5]benzoxazepine (PBOX-6) and 4-acetoxy-5-(1-(naphthyl)naphtho[2,3]pyrrolo[2,1-D][1,4]oxazepine (PBOX-15) were synthesised as described previously [18] and dissolved in ethanol. Vincristine (Tocris, Bristol, U.K), doxorubicin (Sigma Aldrich, St Louis, MO, USA) and carboplatin (Sigma Aldrich, St Louis, MO, USA) were dissolved in dH_20 and sterile filtered. Etoposide (Sigma Aldrich, St Louis, MO, USA) was reconstituted in DMSO (Sigma Aldrich, St Louis, MO, USA. All antibodies with the exception of cytochrome which was sourced from BD Bioscience (Oxford, UK) and Bax which was sourced from Santa Cruz (Santa Cruz Biotechnology, Santa Cruz, CA) were obtained from Millipore (Cork, Ireland). Caspase inhibitors were purchased from Millipore (Cork, Ireland). All media and FBS were obtained from Invitrogen (Paisley, U.K.). The enhanced chemiluminescence reagents were supplied by Amersham Biosciences (Buckinghamshire, U.K.), The BCA reagents were from Pierce (Illinois, U.S.), the polyvinylidene difluoride membranes from Millipore (Cork, Ireland), while the protease inhibitors were obtained from Roche (Clare, Ireland). Unless otherwise stated all chemicals were obtained from Sigma-Aldrich (Sigma Aldrich, St Louis, MO, USA), cell culture materials were sourced from Greiner Bio-One GmbH (Stonehouse, U.K.).

2.3. AlamarBlue viability assay

Cells were seeded at densities varying from 25 000–80 000 cells/mL in a 96 well plate in a volume of 200 μL medium, left overnight to attach and treated with a range of concentrations of PBOX-6, vincristine, doxorubicin, etoposide and carboplatin for 72 h AlamarBlue (final concentration 10% (v/v)) was added to each well and left to incubate in the dark at 37 °C for 5 h. Fluorescence was measured using a SpectraMax Gemini plate reader (Molecular Devices, Sunnyvale, CA) at excitation and emission wavelengths of 544 nm and 590 nm, respectively. The mean of each triplicate was calculated. Vehicle treated wells were set at 100% viability and treated wells were calculated as a percentage of the vehicle control. Dose response curves were plotted and IC_{50} values obtained using Prism GraphPad 4.

2.4. Flow cytometry

Following the required treatment, floating and adherent cells were harvested and fixed in 70% ethanol/PBS. Fixed samples were stored at −20 °C until required. Ethanol was removed by centrifugation and pellets were incubated in 400 μL FACS flow sheath fluid supplemented with 10 μg/mL RNase A (Sigma Aldrich, St Louis, MO, USA) and 100 μg/mL propidium iodide (Sigma Aldrich, St Louis, MO, USA). Cells were incubated in the dark at 37 °C for 30 min. Analysis was performed on a FACScalibur Fluorescence Associated Cell Sorter (FACS) (Becton–Dickinson, San Jose, CA, USA) using Cell Quest and Quanti-Quest software. Samples were first gated using a vehicle control to eliminate debris and cell aggregates from analysis. 10 000 cells from each sample were counted and results were visualised on histrograms.

Mitochondrial membrane potential was analysed using 5,5,6,6-tetrachloro-1,1,3,3-tetraethylbenzimidazolcarbocyanineiodide (JC-1) (Invitrogen, Paisley, U.K.) an aggregate forming lipophilic dye. JC-1 was stored as a 200 μM solution in DMSO and added to cells at a final concentration of 5 μM for 20 min at 37 °C. Cells were collected by centrifugation at 300 × *g* for 5 min and the pellets were re-suspended in 400 μL PBS. Cells were treated with 50 mM Carbonylcyanide *m*-chlorophenylhydrazone (CCCP), a mitochondrial membrane depolariser, for 5 min as a positive control for

depolarisation. Flow cytometry analysis was then performed within 10 min by using a FACScalibur Fluorescence Associated Cell Sorter (FACS) (Becton–Dickinson, San Jose, CA, USA) using Cell Quest and Quanti-Quest software. Cells were gated to exclude debris and standard compensation was performed using the positive control. The green:red fluorescence ratio was measured using the FITC and PE channels. Complete depolarisation was defined by a gate setting the CCCP control as 98–100% depolarised. Response to each treatment was listed as the percentage of cells within the depolarised gate.

2.5. Analysis of drug interactions

Using the software programme Calcusyn, median dose analysis was undertaken to study interactions between different drugs. This method is based on the drug effect equation of Chao and Talalay [19] providing quantitative determination for synergism (CI < 1), additive effect (CI = 1) and antagonism (CI > 1). The lower the combination index value (CI), the greater the degree of synergism. A CI value of 0.1–0.3 indicates strong synergism (++++), 0.3–0.7 indicates synergism (+++), 0.7–0.85 indicates moderate synergism (++) and 0.85–0.9 indicates slight synergism (+).

2.6. Statistics

The statistical analysis of experimental data was performed using the computer program Prism GraphPad 4. Results were presented as mean ± S.E.M. For comparison of two groups, values were determined using a Student's paired *t* test. For comparison of more than two groups, one way ANOVA followed by Tukey's multiple comparison test was employed. A value of $P < 0.05$ was deemed to be significant.

2.7. Western blot

Cells were harvested in Laemmli buffer (1× =30mM Tris-base pH 6.2, 2% (v/v) SDS, 10% (v/v) glycerol in dH_2O) and sonicated for 5 s to degrade DNA. DTT (to a final concentration of 50 mM) and bromophenol blue were added to each sample followed by boiling for 3 min at 100 °C. Equal quantities of protein (as determined by a BCA assay) were separated on polyacrylamide gels followed by transfer to PVDF membranes. Membranes were blocked in 5% marvel in PBS-tween for 1 h. Membranes were incubated in the relevant primary antibodies overnight, washed and incubated in horseradish peroxidase conjugated secondary antibody for 1 h and washed again. Enhanced chemiluminescence was used for detection of protein expression. Western blot analysis was performed using antibodies directed against PARP (Millipore, Cork, Ireland), Mcl-1 (Millipore, Cork, Ireland), Bcl-2 (Millipore, Cork, Ireland), Bax (Santa Cruz Biotechnology, Santa Cruz, CA), Bak (Millipore, Cork, Ireland), activated Bak (Millipore, Cork, Ireland), caspase-9 (Millipore, Cork, Ireland), caspase-8 (Millipore, Cork, Ireland), cytochrome *c* (BD) and GAPDH (Millipore, Cork, Ireland) followed by incubation with a horseradish peroxidase-conjugated anti-mouse or anti-rabbit antibody (Promega, Madison, WI, USA). All blots were probed with anti-GAPDH to confirm equal loading. The 72 h GAPDH is shown and is representative of equal loading of all blots. Western blots were normalised to GAPDH as a control and densitometric analysis of bands was carried out using imageJ software. The densitometric measures of Mcl-1, Bcl-2 cleavage, Bak, Bax, caspase-9 cleavage, caspase-8 cleavage and pro-caspase-3 levels were expressed as a fold increase/decrease in comparison to the control. PARP cleavage was expressed as the fold increase when compared to the pro-form. Activated Bak was calculated as the fold increase when compared to the GAPDH control.

For preparation of cytosolic fractions, following the required treatment time cells were trypsinised, pelleted at 600 × *g* and washed in 1 mL ice cold PBS. The pellet was incubated in 100 μL isotonic buffer (200 mM mannitol, 70 mM sucrose, 1 mM EGTA, 10 mM HEPES pH 6.9, 1 mM DTT in dH_2O and one EDTA-free COMPLETE protease inhibitor tablet (Roche, Clare Ireland)) for 10 min on ice then drawn though a 21G needle approximately 30 times and incubated on ice for a further 15 min. Cells were pelleted at 500 × *g* for 10 min and the supernatant was removed. The supernatant was pelleted at 10,000 × *g* for 20 min at 4 °C to produce the cytosolic fractions which were stored at −80 °C until required.

2.8. siRNA knockdown of Mcl-1

SHSY5Y and CHLA-90 cells were seeded in the log phase of growth. The following day cells were trypsinised, pelleted and transfected using the neon transfection system (Invitrogen, Paisley, U.K.) with 200 nM siRNA validated to target Mcl-1 (Invitrogen, Paisley, U.K.) Transfection conditions were previously optimised to ensure maximum knockdown of protein expression. Cells were examined by SDS-PAGE up to 72 h post transfection to ensure knockdown was successful. Transfected cells were treated with varying concentrations of carboplatin and the levels of apoptosis were analysed by flow cytometric analysis of propidium iodide stained cells.

3. Results

3.1. PBOX-6 and -15 reduce the viability of a panel of drug sensitive and resistant neuroblastoma cell lines in a dose-dependent manner

Six neuroblastoma cell lines, three drug sensitive and three drug resistant were treated with a range of concentrations of PBOX-6 and 15 or with a series of standard chemotherapeutic agents currently used to treat neuroblastoma namely vincristine, etoposide, doxorubicin and carboplatin. Cell were treated for 72 h after which time cell viability was measured using the AlamarBlue viability assay and the IC_{50} value for each drug was determined (Table 1A). IC_{50} values of PBOX-6 ranged from 1.47 μM to 2.10 μM in the three sensitive and 1.08 μM to 3.73 μM in the resistant cell lines (Table 1A). Similarly the IC_{50} values for PBOX-15 were comparable between the sensitive and resistant cell lines. The IC_{50} values of the standard chemotherapeutics were also determined (Table 1A) and values are similar to previous reports [20].

3.2. PBOX-6 and -15 exhibit lower fold resistance in MDR cell lines when compared to standard chemotherapy

Development of drug resistance is a major obstacle for the successful treatment of neuroblastoma. Many mechanisms of resistance have been proposed including amplification of MYCN, mutated or deleted p53 and overexpression of drug efflux pumps [1]. SK-N-FI, CHLA-90 and SK-N-BE(2)c are three representative MDR neuroblastoma cell lines. All three cell lines have mutated p53, the SK-N-BE(2)c is MYCN amplified, while the SK-N-FI and CHLA-90 cell lines over express the MDR protein *p*-gp [21,22]. The degree of resistance of each drug in the three MDR cell lines in comparison to each of the three sensitive cell lines was established (Table 1B). The fold resistance for a given drug was determined as the ratio of the IC_{50} of a given cell line to the IC_{50} of a sensitive cell line. In comparison to all sensitive cell lines, SK-N-BE(2)c cells displayed no resistance to PBOX-6 and -15 (Table 1B) which was in contrast to etoposide, doxorubicin and carboplatin, all of which exhibited increased IC_{50} values. The CHLA-90 cell line, also displayed no resistance to PBOX-6 and -15. This was in contrast

Table 1
IC_{50} values of PBOX compounds and standard chemotherapeutic drugs in a range of neuroblastoma cell lines.

(A)

Cell lines	IC_{50} (μM)					
	PBOX-6	PBOX-15	Vincristine	Doxorubicin	Etoposide	Carboplatin
SHSY5Y	1.73 ± 0.08	0.06 ± 0.06	0.07 ± 0.01	0.21 ± 0.03	0.51 ± 0.06	24.35 ± 0.04
Kelly	1.47 ± 0.09	0.06 ± 0.06	0.02 ± 0.05	0.18 ± 0.07	0.34 ± 0.05	15.75 ± 0.04
SK-N-BE(1)	2.10 ± 0.03	0.11 ± 0.09	0.03 ± 0.06	0.10 ± 0.05	0.60 ± 0.07	40.5 ± 0.05
SK-N-BE(2)c	1.08 ± 0.05	0.04 ± 0.09	0.06 ± 0.05	0.65 ± 0.05	1.70 ± 0.05	62.42 ± 0.04
CHLA-90	1.58 ± 0.01	0.06 ± 0.07	0.92 ± 0.01	1.83 ± 0.07	>20	>100
SK-N-FI	3.73 ± 0.05	0.11 ± 0.1	0.15 ± 0.09	0.91 ± 0.06	9.76 ± 0.10	>100

(B)

Drug sensitive cell line		MDR cell line		
		SK-N-BE(2)c	CHLA-90	SK-N-FI
	IC_{50} PBOX-6 (μM)	Fold resistance	Fold resistance	Fold resistance
SHSY5Y	1.73	None	None	2.10
Kelly	1.47	None	None	2.50
SK-N-BE(1)	2.10	None	None	1.77
	IC_{50} PBOX-15(μM)			
SHSY5Y	0.06	None	None	1.70
Kelly	0.06	None	None	1.70
SK-N-BE(1)	0.11	None	None	None
	IC_{50} vincristine (μM)			
SHSY5Y	0.07	None	12.4	2.13
Kelly	0.02	2.85	13.78	7.52
SK-N-BE(1)	0.03	1.53	23.66	4.05
	IC_{50} etoposide (μM)			
SHSY5Y	0.51	3.20	>20 μM	18.80
Kelly	0.34	4.90	>20 μM	28.2
SK-N-BE(1)	0.60	2.82	>20 μM	16.1
	IC_{50} doxorubicin (μM)			
SHSY5Y	0.21	3.04	8.55	4.35
Kelly	0.18	3.51	9.85	5.08
SK-N-BE(1)	0.10	6.20	17.4	8.71
	IC_{50} carboplatin (μM)			
SHSY5Y	24.35	2.56	>100 μM	>100 μM
Kelly	15.75	3.96	>100 μM	>100 μM
SK-N-BE(1)	40.50	1.54	>100 μM	>100 μM

Neuroblastoma cells were treated with a vehicle (1% v/v) ethanol or a range of concentrations of PBOX-6, vincristine, doxorubicin, etoposide or carboplatin. After the incubation period, we assessed cells for cell viability by the AlamarBlue viability assay. Values represent the mean ± S.E.M. of three independent experiments performed in triplicate. IC_{50} values were obtained using Prism Graphpad 4.Values are shown as averages ± standard deviation for three independent determinations (A). Fold resistance of PBOX-6 and -15 in multidrug resistant SK-N-BE(2)c, CHLA-90 and SK-N-FI cells in comparison to the fold resistance of vincristine, doxorubicin, etoposide and carboplatin was determined (B).

to another MTA, vincristine which demonstrated elevated levels of resistance, with an IC_{50} value 23 times higher evident in CHLA-90 cells in comparison to the drug sensitive Kelly cell line. Following treatment with etoposide, the IC_{50} value was greater than 20 μM. The exact value could not be determined as it exceeded the limits of solubility, although it is clear this cell line is extremely resistant to etoposide. Similarly the IC_{50} value of carboplatin was greater than 100 μM again indicating marked resistance to this drug.

One mechanism of resistance in the SK-N-FI cell line is the expression of the drug efflux pump *p*-gp. It has been previously demonstrated that PBOX-6 and 15 are not substrates for this protein [12]. Similarly in this cell line both PBOX-6 and 15 showed a lower fold resistance than all other cytotoxic agents tested (Table 1B). These results demonstrate the potential of the PBOX compounds for the treatment of resistant neuroblastoma.

3.3. PBOX-6 and 15 induce a G_2/M arrest and apoptosis in SHSY5Y neuroblastoma cells

Flow cytometric analysis of propidium iodide stained cells was next employed to assess the effects of the drugs on cell cycle progression and induction of apoptosis. The apoptotic population was quantified as the percentage of cells in the sub G1/G0 fraction. PBOX-6 induced apoptosis in SHSY5Y cells in a time-dependent manner. An apoptotic population was first observed between 6 h and 16 h after which time 10 μM PBOX-6 induced 12.7% ± 1.2% apoptosis which continued to rise to a maximum of 47.7 ± 1.0% at 72 h (Fig. 1B). Similar results were obtained with the other analogue PBOX-15 (FigB and E–J). Additionally SHSY5Y cells were treated with varying concentrations of PBOX-6 or -15 for 72 h and found to induce apoptosis in a dose-dependent manner (Fig. 2C and D).

The effect of the PBOX compounds on cell cycle progression was also established. PBOX-6 (10 μM) induced a transient G_2/M arrest which peaked at 16 h (36.56 ± 4.9%) and decreased to 10.8 ± 1.9% after 48 h and 6.14 ± 3.9% after 72 h (Fig. 1A). Thus as percentage of cells in the G2/M phase of the cell cycle decreased, the percentage of cells undergoing apoptosis increased. PBOX-15 also induced a transient G_2/M arrest prior to induction of apoptosis (Fig. 2A). The observed G_2/M arrest induced by both these drugs was in agreement with previous reports demonstrating that the PBOX's target the microtubules [9].

Western blot analysis of Poly (ADP) ribose polymerase (PARP) cleavage was undertaken to confirm that the pre-G1 peaks observed by flow cytometric analysis were representative of an apoptotic cell population. We found that, consistent with results from flow cytometric analysis, PARP was cleaved in a time and dose-dependent manner in SHSY5Y neuroblastoma cells (Fig. 1C).

3.4. PBOX-6 cleaves Bcl-2, downregulates Mcl-1 and upregulates Bak

We examined the molecular mechanisms through which PBOX-6 induces apoptosis in neuroblastoma cells. As the Bcl-2 family of

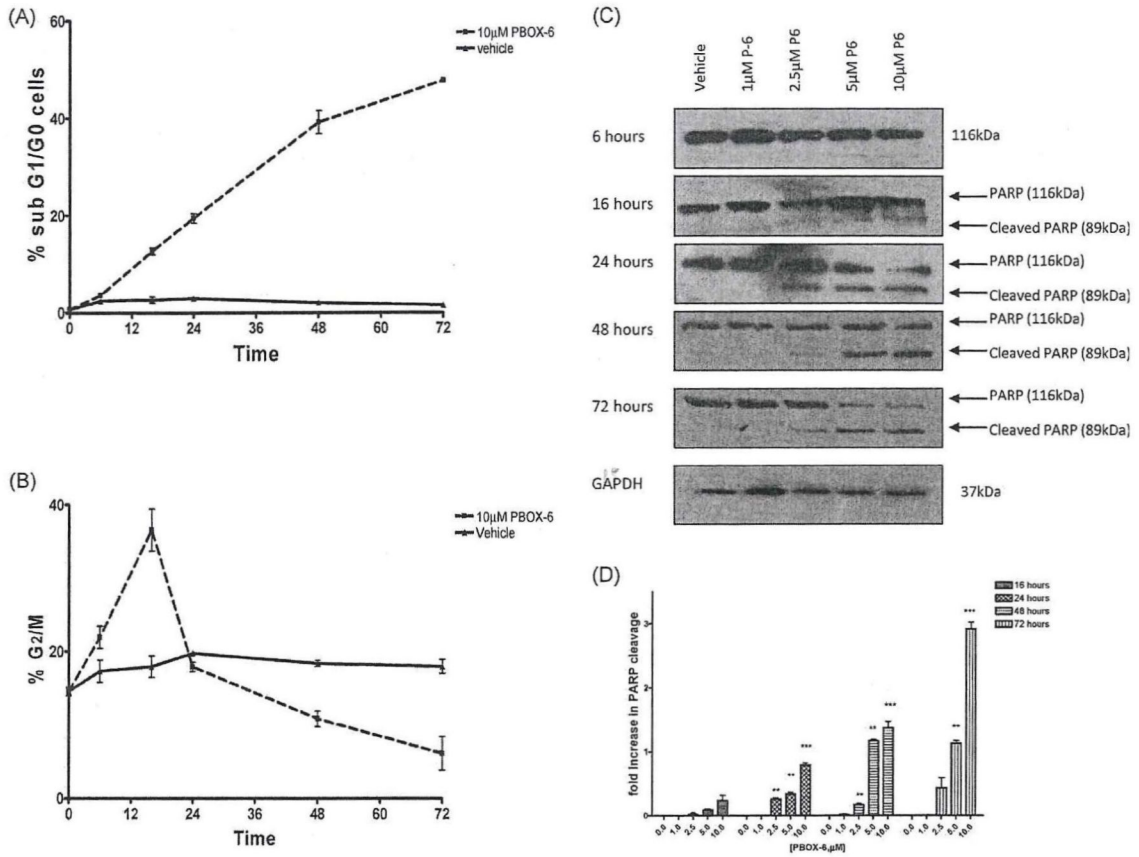

Fig. 1. PBOX-6 induced G2/M arrest precedes apoptosis in SHSY5Y cells.
SHSY5Y cells were treated with a vehicle (1% v/v) ethanol or a range of concentrations of PBOX-6. After the 72 h incubation period, cells were analysed by flow cytometry for the percentage of cells in the G2/M phase of the cell cycle (A) and sub G1/GO (B). Values represent the mean ± S.E.M. of three independent experiments.
Apoptosis was confirmed by western blot analysis of PARP (C). SHSY5Y cells were treated with varying concentrations of PBOX-6 (1 μM, 2.5 M, 5 μM and 10 μM). After the required time cells were harvested and lysates were prepared for western blot analysis. The membrane was probed with an anti-PARP antibody and GAPDH as a loading control. The 72 h GAPDH loading control shown is representative of all time points. Results are representative of three separate experiments. Western blots were normalised to GAPDH as a control and densitometric analysis of bands was carried out with the imageJ software. PARP cleavage was expressed as a fold-change in comparison to the proform (D). Statistical analysis was performed using one way ANOVA with Tukey's multiple comparison test. $^{***}p < 0.001$, $^{**}p < 0.01$, $^{*}p < 0.05$.

proteins control the induction or inhibition of apoptosis by exerting either pro- or anti-apoptotic effects on the cell, we sought to analyse the expression levels of different members of this family and determine their role in inhibition or induction of apoptosis. PBOX-6 was found to induce cleavage of Bcl-2 (Fig. 3A). This cleaved fragment represents a form of the Bcl-2 protein which has lost its anti-apoptotic activity [23,24]. Cleavage occurred in a dose-dependent manner (Fig. 3A).

We next examined the effect of PBOX-6 on anti-apoptotic Mcl-1 expression. PBOX-6 reduced Mcl-1 expression in a time and dose-dependent manner (Fig 3B). A decrease was first noted 16 h post treatment, with almost complete abolition of expression after 72 h.

We also sought to examine the effect of PBOX-6 on expression of pro-apoptotic Bak and Bax. Upon PBOX-6 treatment, an increase in Bak expression was noted after 24 h and continued to increase with time (Fig. 3C) but no change in Bax expression was observed (Fig. 3D). Pro-apoptotic cytochrome *c* is released though pores which form in the outer mitochondrial membrane in an apoptotic cell. These pores have been postulated to form when Bak and Bax oligomerise and insert into the membrane [25]. This oligomerisation requires a conformational change that involves exposure of N-terminal epitopes. Therefore we sought to determine whether the increase in Bak expression observed after treatment with PBOX-6 represented an activated form of Bak which was capable of forming pores and consequently the release of cytochrome *c*. We utilised an anti-Bak antibody specific for the conformationally active form of Bak (anti-Bak-NT; activated Bak) and demonstrated that Bak was indeed activated at 72 h in a dose-dependent manner by PBOX-6 (Fig. 3C).

3.5. PBOX-6 synergistically enhances the apoptotic effects of a panel of chemotherapeutic drugs

Regardless of stage, all neuroblastoma patients that receive chemotherapy are treated by combination therapy. This indicated there was potential for the PBOX compounds to be used in combination with other chemotherapeutic drugs, in particular those which are currently used in the clinic. It was proposed that the PBOXs may work in combination with doxorubicin, etoposide and carboplatin and may synergistically enhance the apoptotic effects of these drugs on neuroblastoma cells. The percentage of apoptosis induced by these drugs alone and in combination was assessed by flow cytometric analysis of the pre-G1 peak of propidium iodide stained cells.

SHSY5Y cells were treated for 48 h with either PBOX-6 or PBOX-15 and varying concentrations of carboplatin (Table 2). All combinations were shown to be synergistic. Overall the results showed that PBOX-6 induced a higher degree of synergism than PBOX-15, therefore it was decided to continue to investigate this drug in combination with doxorubicin and etoposide, two other chemotherapeutics which are currently used to treat neuroblastoma. Analysis by Calcusyn confirmed that PBOX-6

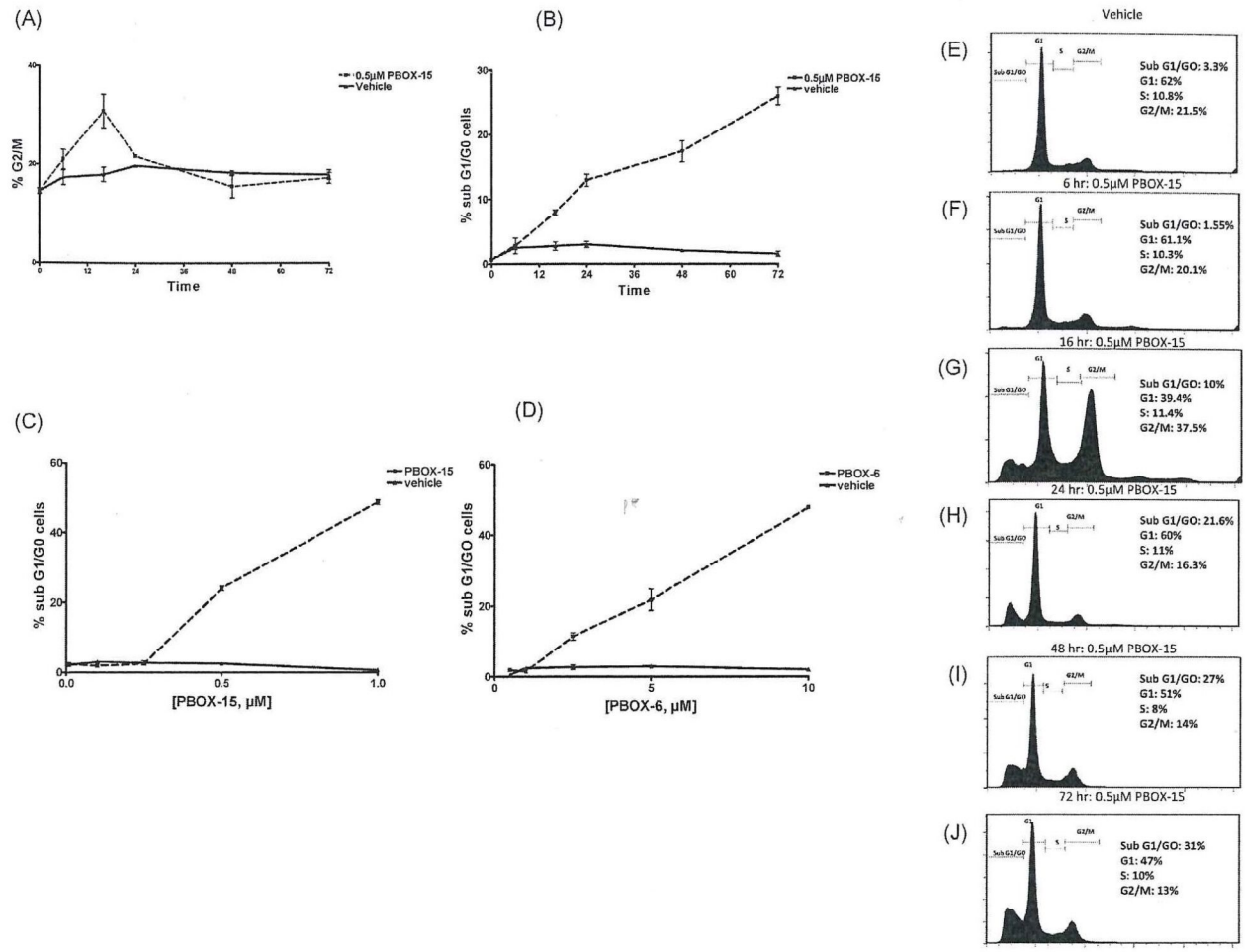

Fig. 2. PBOX-6 and -15 induced G2/M arrest precedes apoptosis in SHSY5Y cells.
SHSY5Y cells were treated with a vehicle (1% v/v) ethanol or a range of concentrations of PBOX-6 or -15. After the 72 h incubation period, cells were analysed by flow cytometry (E–J) for the percentage of cells in G2/M (A) or sub-G1/G0 (B–D). Values represent the mean ± S.E.M. of three independent experiments.

Table 2
PBOX-6 and -15 synergistically enhance the apoptotic effects of standard chemotherapeutics.

PBOX-15 (μM)	Carboplatin	% Sub G1/G0 cells	CI value	Rating
0.5	10	18.91	0.618	++
0.5	20	26.44	0.477	+++
0.5	50	28.97	0.569	+++
PBOX-6 (μM)	Etoposide	% Sub G1/G0 cells	CI value	Rating
5	1	23.8	0.181	+++++
5	5	29.7	0.240	++++
5	10	26.9	0.490	+++
PBOX-6 (μM)	Doxorubicin	% Sub G1/G0 cells	CI value	Rating
1	5	45.99	0.398	+++
2.5	5	47.54	0.380	+++
5	5	36.49	0.700	++

SHSY5Y cells were treated with a vehicle (1% (v/v) ethanol), 0.5 μM PBOX-15, a range of concentrations of carboplatin or a combination of both, 5 μM PBOX-6, a range of concentrations of etoposide or a combination of both or a range of concentrations of PBOX-6, 5 μM doxorubicin or a combination of both. After 48 h cells were harvested, fixed in ethanol and stained with propidium iodide. Cells were analysed by flow cytometry and the percentage of apoptotic cells was determined by quantification of the sub-G1/G0 peak. Statistical analysis was performed using one way ANOVA with Tukey's multiple comparison test. *** $p < 0.001$, ** $p < 0.01$, * $p < 0.05$. CI values of for each combination were determined. Statistical analysis was also carried out using the software Calcusyn (Biosoft, U.K). Data from flow cytometry experiments was used to analyse the interactions between PBOX-15 and carboplatin using the isobologram method described by Chou and Talalay. A CI value of >1, =1 and <1 indicated antagonism (−), and additive effect (+) and synergism (+), respectively. Fa—Fraction of cells affected by apoptosis.

also synergistically augmented the apoptotic effects of etoposide and doxorubicin (Table 2).

The PBOX-6/carboplatin combination was chosen as the representative combination treatment and their effects on SHSY5Y cells 72 h post treatment was further investigated. Statistical analysis was performed using a one way ANOVA with Tukey's multiple comparison test. All p values obtained were less than 0.05 indicating that results were significant (Fig. 4B). Analysis by Calcusyn also confirmed that PBOX-6 synergistically increased the apoptotic effects of carboplatin in SHSY5Y cells after 72 h treatment. CI values for each combination were less than 0.45 indicating strong to very strong synergism (Fig. 4C).

Having found that this combination is synergistic in drug sensitive cell lines we next wished to test it in an MDR cell line. The CHLA-90 cell line derived from an 8 1/2 year old child with stage 4 neuroblastoma, post bone marrow transplantation, is p53 mutated, overexpresses the MDR protein p-gp and has been shown to be resistant to multiple chemotherapeutics which are currently used in the treatment of neuroblastoma such as carboplatin, doxorubicin and etoposide [2]. We therefore chose this as a representative MDR cell line. CHLA90 cells were treated with 5 μM PBOX-6 and varying concentrations of carboplatin alone and in combination for 48 and 72 h (Fig. 4D and E). Statistical analysis was performed using a one way ANOVA with Tukey's multiple comparison test. All p values obtained were less than 0.05 indicating that results were

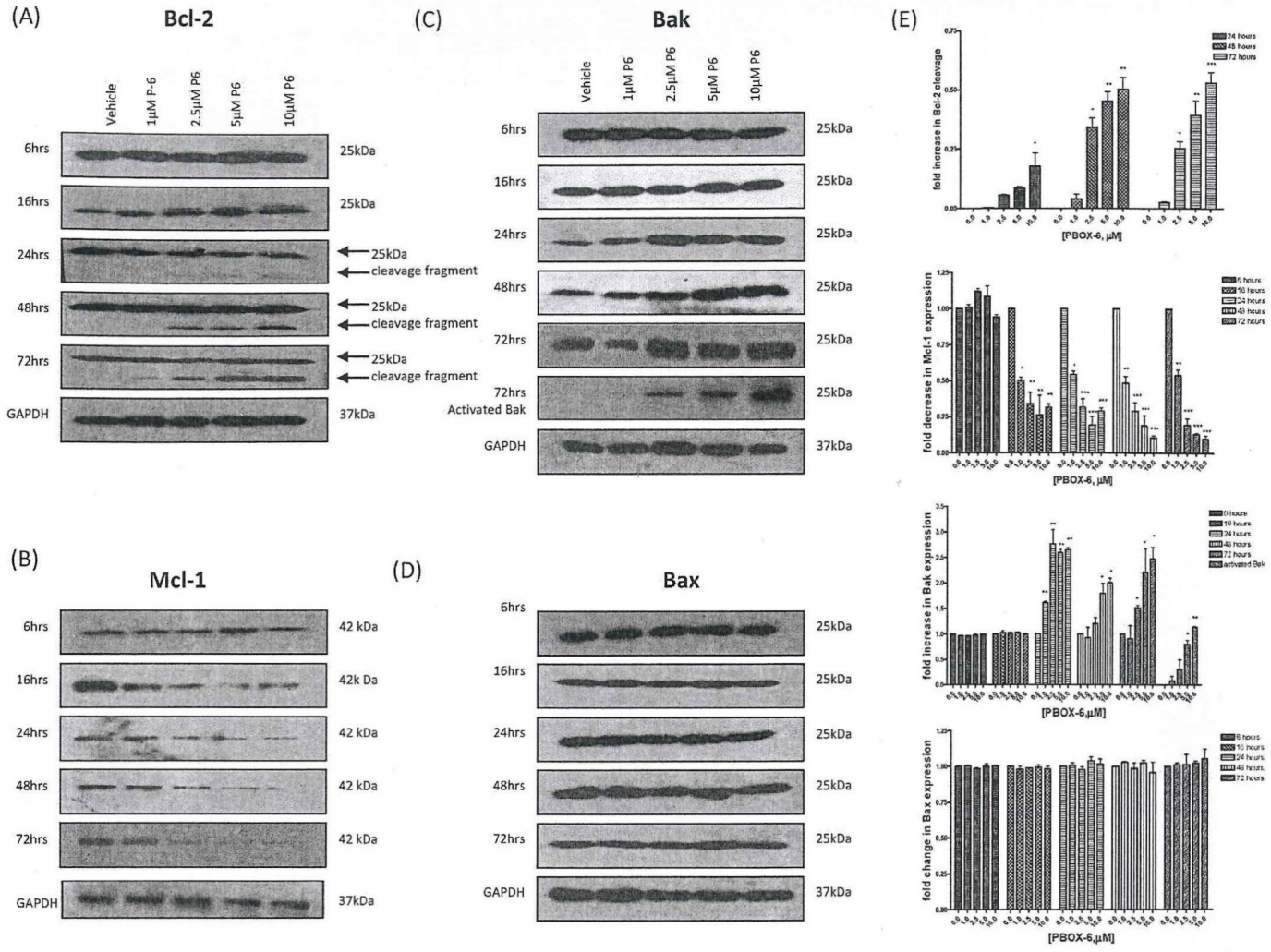

Fig. 3. PBOX-6 cleaves Bcl-2, downregulates Mcl-1 and upregulates Bak.
SHSY5Y cells were treated with varying concentrations of PBOX-6. After the required time cells were harvested and separated by SDS PAGE. The membrane was probed with an anti-Bcl-2 (A), anti-Mcl-1 (B), anti-Bak (C), anti-Bak-NT (activated Bak) (C) or anti-Bax antibodies (D). Membranes were also probed for GAPDH as a loading control. The 72 h GAPDH loading control shown is representative of all time points. Results are representative of three separate experiments. Western blots were normalised to GAPDH as a control and densitometric analysis of bands was carried out with the imageJ software (E). Statistical analysis was performed using one way ANOVA with Tukey's multiple comparison test. $^{***}p < 0.001$, $^{**}p < 0.01$, $^{*}p < 0.05$.

significant. Analysis by Calcusyn confirmed that PBOX-6 synergistically increased the apoptotic effects of carboplatin at both time points. CI values for each combination was less than 0.8 indicating synergy (Fig. 4F).

3.6. PBOX-6/carboplatin treatment is accompanied by an enhanced downregulation of Mcl-1, upregulation of Bak and release of cytochrome c

We next sought to determine the molecular events that underlie this enhancement of apoptosis. Western blotting showed an increase in PARP cleavage in the combination treatment in comparison to either agent alone (Fig. 5A), confirming the flow cytometric results demonstrating potentiation of apoptosis. The PBOX-6/carboplatin combination induced a cumulative decrease in expression of Mcl-1, induced cleavage of Bcl-2 and upregulated expression of conformationally active Bak (Fig. 5A) in both the drug sensitive SHSY5Y and MDR CHLA-90 cell lines. PBOX-6 alone upregulated Bak but this upregulation was further enhanced in the combination treatment. This was in contrast to carboplatin treatment alone which had no effect on the expression of any of these Bcl-2 family members (Fig. 5A).

These findings indicated that this combination may work through the intrinsic pathway; we therefore performed a series of experiments to test this hypothesis. The observed increase in conformationally active Bak would indicate that Bak is homodimerising and forming pores in the mitochondrial membrane. When this occurs the electrochemical gradient across the mitochondrial membrane collapses and the membrane is depolarised. This can be visualised by JC-1, a cationic dye which detects loss of mitochondrial membrane potential. As can be seen in Fig. 5B, we observed depolarisation of the mitochondrial membrane 24 h post treatment.

Formation of pores and depolarisation enables the release of pro-apoptotic proteins such as cytochrome *c*. Previous studies have demonstrated that in response to some apoptotic stimuli, cytochrome *c* is released from the mitochondria and accumulates in the cytosol. Therefore cytosolic fractions were prepared and cytochrome *c* expression was analysed by western blotting in both SHSY5Y and CHLA-90 cells. PBOX-6 alone and the PBOX-6/carboplatin combination triggered the release of cytochrome *c* into the cytosol which correlated with induction of apoptosis (Fig. 5C). In contrast, in cells treated with carboplatin alone, cytochrome *c* release was not observed in either cell line. The

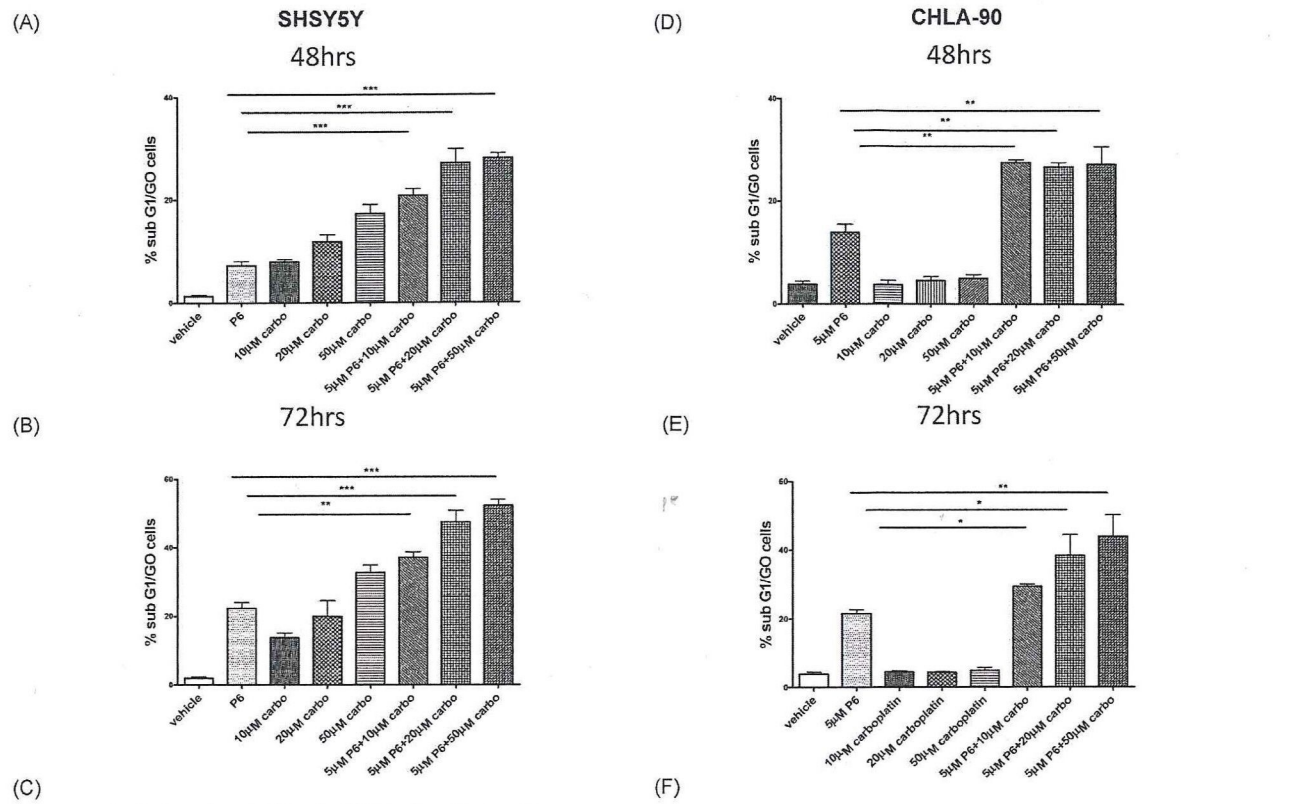

(C)

Time (hrs)	PBOX-6 (μM)	Carboplatin (μM)	% sub G1/GO cells	CI value	Rating
48	5	10	0.20	0.299	++++
	5	20	0.27	0.249	++++
	5	50	0.28	0.430	+++
72	5	10	0.37	0.440	+++
	5	20	0.47	0.359	+++
	5	50	0.53	0.450	+++

(F)

Time (hrs)	PBOX-6 (μM)	Carboplatin (μM)	% sub G1/G0 cells	CI value	Rating
48	5	10	0.23	0.727	++
	5	20	0.27	0.644	+++
	5	50	0.27	0.657	+++
72	5	10	0.28	0.771	++
	5	20	0.32	0.642	+++
	5	50	0.43	0.431	+++

Fig. 4. PBOX-6 synergistically enhances the apoptotic effects of carboplatin in SHSY5Y and CHLA-90 cells.
SHSY5Y and CHLA-90 cells were treated with a vehicle (1% (v/v) ethanol), 5 μM PBOX-6, 10 μM, 20 μM or 50 μM carboplatin or a combination of both. After 48 (A and D) or 72 h (B and E) cells were harvested, fixed in ethanol and stained with propidium iodide. Cells were analysed by flow cytometry and the percentage of apoptotic cells was determined by quantification of the sub-G1/G0 peak. Statistical analysis was performed using one way ANOVA with Tukey's multiple comparison test. $^{***}p < 0.001$, $^{**}p < 0.01$, $^{*}p < 0.05$. CI values of PBOX-6 in combination with carboplatin in SHSY5Y cells were determined. Statistical analysis was carried out using the software Calcusyn (Biosoft, U.K). Data from flow cytometry experiments was used to analyse the interactions between PBOX-6 and carboplatin using the isobologram method described by Chou and Talalay. A CI value of >1, =1 and <1 indicated antagonism (−), and additive effect (+) and synergism (+), respectively. Fa—Fraction of cells affected by apoptosis (C and F). A CI value of 0.1–0.3 indicates strong synergism (++++), 0.3–0.7 indicates synergism (+++), 0.7–0.85 indicates moderate synergism (++) and 0.85–0.9 indicates slight synergism (+).

antibody utilised recognises both monomeric and polymeric cytochrome *c*. In the combination treated SHSY5Y cells, cytochrome *c* was observed in both the monomeric and polymeric form.

3.7. Involvement of caspase-3, 8 and -9 in the apoptotic pathway induced by the PBOX-6/carboplatin combination

The release of cytochrome *c* triggers formation of the apoptosome leading to the processing and activation of procaspase-9 and in turn cleavage and activation of executioner caspases-3 and -7. We have previously reported that PBOX-6 induced apoptosis may involve both caspase-dependent and -independent pathways [26,27]. We therefore sought to determine the involvement of caspases in the pathway initiated in neuroblastoma cells.

We utilised a series of pharmacologic inhibitors of caspase activity. Pre-treatment of SHSY5Y and CHLA-90 cells with zVAD-fmk, a pan-caspase inhibitor significantly inhibited PBOX-6/carboplatin-induced apoptosis indicating caspases play a role in the apoptotic pathway induced by the combination in both SHSY5Y and CHLA-90 cells (Fig. 6A). We next investigated the role of various caspases through the use of caspase inhibitors (Z-LEHD-fmk which inhibits caspase-9 and Z-IETD-fmk which inhibits caspase-8). We found apoptosis was significantly inhibited by pre-treatment with a caspase-9 inhibitor (Fig 6B). Activation of caspase-9 was investigated by western blot analysis. In the pro-form, caspase-9 is present as a 47 kDa band which when activated through cleavage appears as a 37 kDa band. As shown in Fig. 6D, treatment of cells with a combination of PBOX-6 and carboplatin resulted in a decrease of the pro-form and appearance of a lower molecular weight band at 37 kDa indicating cleavage and activation of caspase-9. Comparable results were observed in cells treated with PBOX-6 alone.

Similarly we found pre-treatment with a caspase-8 inhibitor significantly decreased apoptosis after treatment with the PBOX-6/carboplatin combination suggesting possible involvement of the extrinsic pathway in mediating apoptosis (Fig. 6C). To confirm the involvement of caspase-8 in the apoptotic pathway, cleavage and activation was visualised by western blot (Fig. 6D). The pro-form was expressed at very low levels in the vehicle treated cells while expression of the proform was increased in cells treated with carboplatin alone with a slight cleavage band visible. Cleaved caspase-8 was present in lanes treated with PBOX-6 alone and in

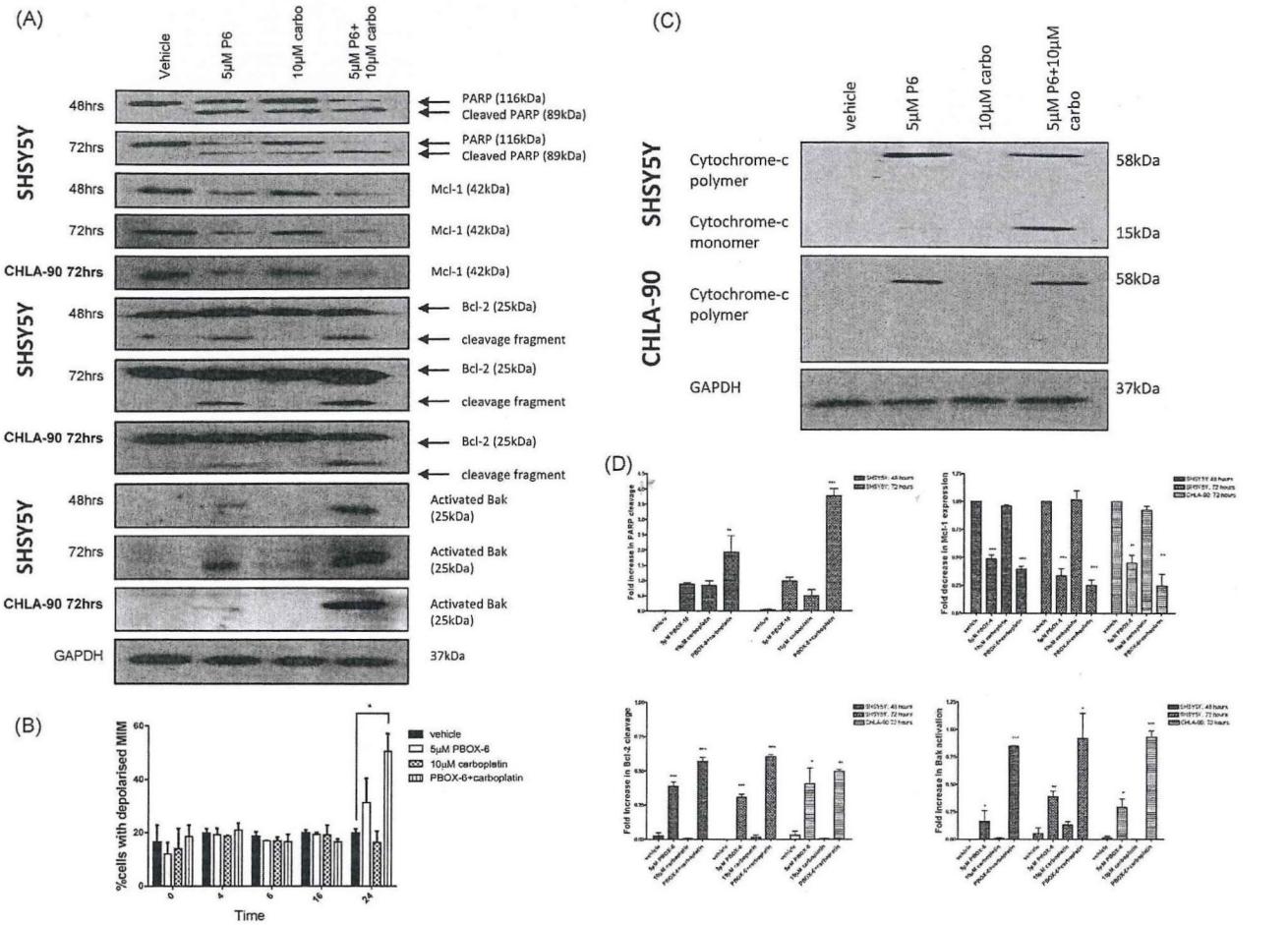

Fig 5. The PBOX-6/carboplatin combination cleaves Bcl-2, downregulates Mcl-1, upregulates expression of conformationally active Bak, induces depolarisation of the mitochondrial membrane and release of cytochrome *c*.

SHSY5Y and CHLA-90 cells were treated with 5 μM PBOX-6, 10 μM carboplatin or a combination of PBOX-6 and carboplatin. After the required time cells were harvested and protein was separated by SDS-PAGE. The membrane was probed with an anti PARP, anti-Bcl-2, anti-Mcl-1 or anti-Bak-NT antibodies. Membranes were also probed for GAPDH as a loading control. The 72 h GAPDH loading control is representative of both 48 and 72 h time points demonstrating even loading. Results are representative of three separate experiments (A). SHSY5Y cells were treated as indicated above and stained with JC-1 for 15 min. Depolarisation of the mitochondrial membrane was assessed by flow cytometry as described in materials and methods. (B). Results are representative of two separate experiments. Cytochrome *c* release was monitored by western blotting. Cytosolic extracts were prepared as described in the experimental procedures. Protein was separated on a 12% resolving gel transferred to a PVDF membrane and probed with an anti-cytochrome *c* antibody (C). Membranes were also probed for GAPDH as a loading control. Western blots were normalised to GAPDH as a control and densitometric analysis of bands was carried out with the imageJ software (D). Statistical analysis was performed using one way ANOVA with Tukey's multiple comparison test. $^{***}p < 0.001$, $^{**}p < 0.01$, $^{*}p < 0.05$.

combination with carboplatin indicating activation (Fig 6D). Previously, caspase-8 has been shown to be undetectable or present at very low levels in SHSY5Y cells but expression has been induced though various means such as after treatment with interferon γ [28] or a combination of interferon γ and valproic acid [29]. Our results would indicate that the PBOX-6/carboplatin combination restores caspases-8 expression in SHSY5Y cells as previously reported in the literature. Consequently we also examined activation of executioner caspase-3 and found similar to caspase-8 and -9, caspase-3 was activated in cells treated with PBOX-6 alone and in combination with carboplatin in both drug sensitive and resistant neuroblastoma cell lines.

3.8. Knockdown of Mcl-1 sensitises SHSY5Y and CHLA-90cells to carboplatin

Finally we sought to determine the importance of Mcl-1 in the apoptotic pathway through the use of siRNA to knockdown Mcl-1 and to assess whether this could sensitise neuroblastoma cells to carboplatin. SHSY5Y and CHLA-90 cells were transfected with siRNA targeted against Mcl-1 using the Neon transfection system. Effective downregulation of the expression levels of the Mcl-1 protein was confirmed by western blot analysis (Fig. 7A). Following knockdown, cells were treated with varying concentrations 10, 20 and 50 μM) of carboplatin and assessed by flow cytometry for induction of apoptosis after 48 h (Fig. 7B). We found that a knockdown of Mcl-1 expression sensitised both cell lines to carboplatin. There was a significant increase in the percentage of cells undergoing apoptosis following knockdown of Mcl-1 at all carboplatin concentrations examined pointing to the importance of Mcl-1 in mediating apoptosis. As Mcl-1 overexpression has been shown to contribute to treatment failure in patients with neuroblastoma, drug combinations including PBOX-6/carboplatin which target this protein would appear to be a promising therapeutic strategy.

4. Discussion

Despite improvement in outcome for most childhood cancers, disease free survival in neuroblastoma remains at approximately

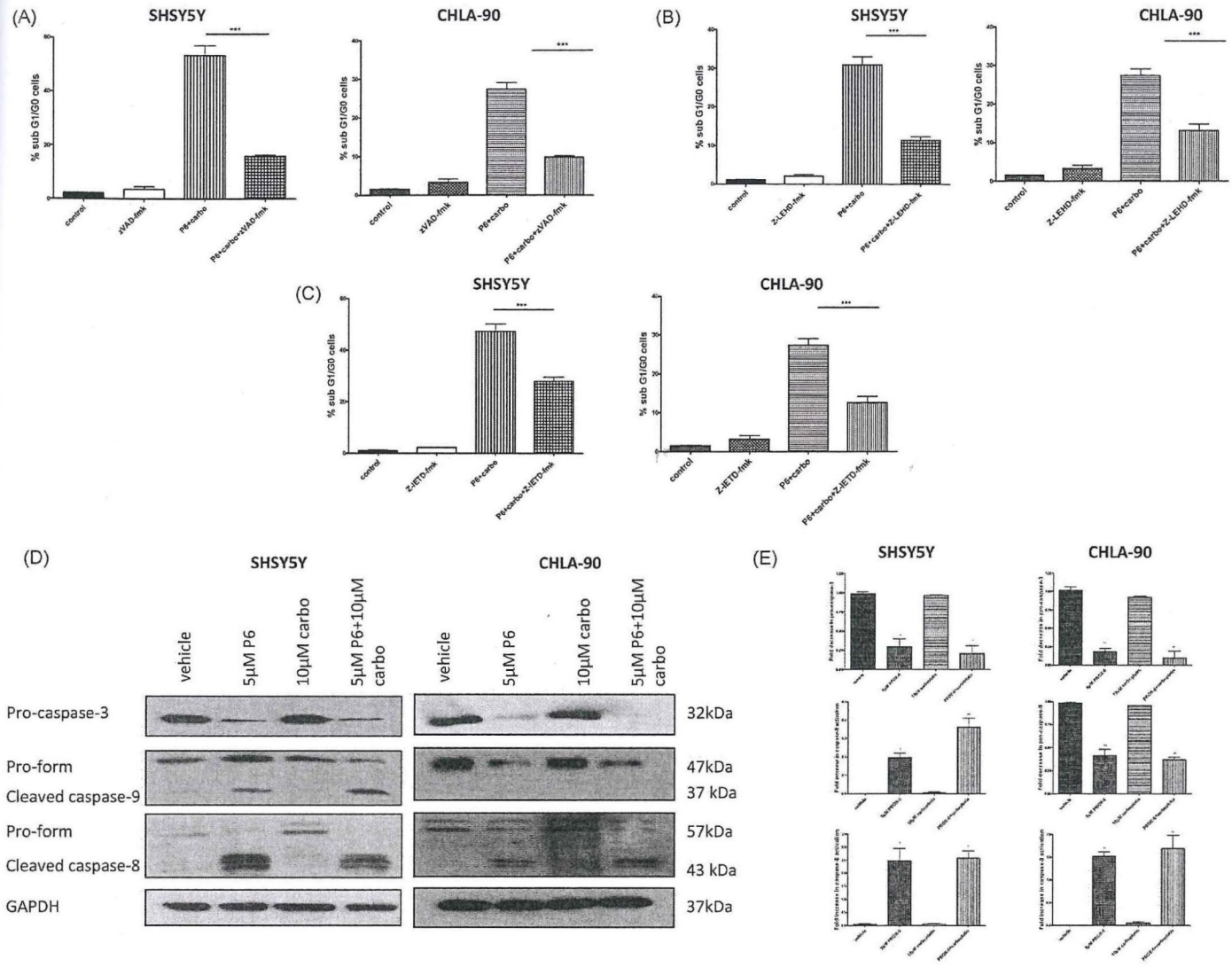

Fig. 6. PBOX-6/carboplatin induced activation of caspase-3, -8 and -9.
SHSY5Y and CHLA-90 cells were pre-treated with (A) zVAD-fmk, a general caspase inhibitor, (B) a caspase-9 inhibitor or (C) a caspase-8 inhibitor before being treated with the PBOX-6/carboplatin combination. Apoptosis was measured by flow cytometric analysis of PI stained cells. Values represent the mean ± S.E.M. of three independent experiments. Statistical analysis was performed using one way ANOVA with Tukey's multiple comparison test. $^{***}p < 0.001$. Caspase-9, -8 and -3 activation was monitored by estern blot (D). The 72 h GAPDH loading control shown is representative of all time points. Results are representative of three separate experiments. Western blots were normalised to GAPDH as a control and densitometric analysis of bands was carried out with the imageJ software (E). Statistical analysis was performed using one way ANOVA with Tukey's multiple comparison test. $^{***}p < 0.001$, $^{**}p < 0.01$, $^{*}p < 0.05$.

40% for those patients presenting with advanced stage. This is mostly due to the development of resistance to a broad range of chemotherapeutic drugs [4–6]. Several mechanisms such as amplification of MYCN, p53 loss of function or overexpression of drug efflux pumps have been reported to contribute to the development of MDR. As many chemotherapeutic drugs used in the treatment of neuroblastoma, such as etoposide, vincristine and doxorubicin have been shown to be substrates for these pumps [30] it is clear that there is a need to investigate alternative compounds which are not effluxed by these drug transporters.

It has been previously shown that the novel microtubule targeting drugs, the PBOX compounds are not substrates for these MDR proteins [12]. Although the PBOX compounds had not previously been tested in neuroblastoma cells, they have been shown to potently induce apoptosis in a number of cell lines, *ex vivo* leukaemia patient samples and in several murine cancer models [10–12,14,15]. The aim of this study was to determine the effects of novel PBOX compounds on the viability of neuroblastoma cell lines, to identify any potential additive or synergistic effects with other chemotherapeutics and to establish the molecular mechanisms underlying any enhanced apoptotic effects observed in combination treatments.

The effects of the PBOX compounds on the viability of a panel of drug sensitive and resistant neuroblastoma cell lines was investigated The IC_{50} values of PBOX-6 and 15 were determined in each of these cell lines and were found to be in a similar range in all six, both drug sensitive and resistant. This was in contrast to all four other cytotoxic agents tested which displayed increased fold resistance in the MDR cell lines [11,17]. The IC_{50} values obtained for both PBOX-6 and 15 were consistent with previous published results. Nathwani et al. [12] established the IC_{50} value of PBOX-6 in two MDR leukaemia cells lines, HL60-*p*-gp (overexpresses *p*-gp) and HL60-ABCG2 (overexpresses BCRP) and found no increase in this value between the parental and resistant cell lines in contrast to two other microtubule targeting agents, vincristine and paclitaxel which exhibited substantially increased IC_{50} values.

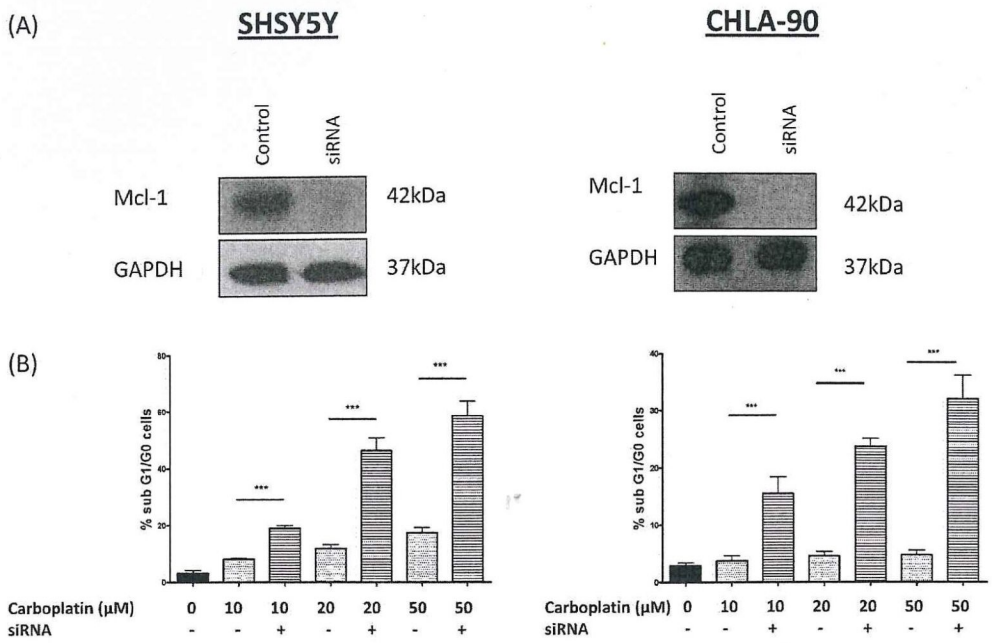

Fig. 7. Knockdown of Mcl-1 sensitises SHSY5Y and CHLA-90 cells to carboplatin.
SHSY5Y and CHLA-90 cells were transfected with siRNA targeting Mcl-1. The degree of knockdown was assessed by western blotting (A). Membranes were also probed with GAPDH to ensure even loading. Cells were subsequently treated with varying concentrations of carboplatin for 48 h after which they were harvested, fixed in ethanol and stained with propidium iodide. Apoptosis was measured by quantification of the subG1/G0 peak (B). Values represent the mean ± S.E.M. of three independent experiments. Statistical analysis was performed using one way ANOVA with Tukey's multiple comparison test. *** $p < 0.001$.

Comparable results were found in the present study; in the *p*-gp expressing SK-N-FI cell line, the fold resistance of the PBOXs was significantly lower in comparison to each of the other drugs tested.

MTAs have been reported to disrupt formation of the mitotic spindle blocking cells in the G_2/M phase of the cell cycle, consequently resulting in apoptosis. Results presented herein demonstrated that a G_2/M arrest preceded apoptosis, with arrest peaking at 16 h indicating that tubulin is the molecular target of the PBOX compounds, as previously reported in the literature [9,15].

One hallmark of neuroblastoma is heterogeneity at both a cellular and clinical level. Neuroblasts are present in tumours at different stages of differentiation therefore both neuroblastoma tumours and cell lines have a number of distinct cell types, the 'N' or neural type of a neuronal lineage, 'S' or schwannian of a glial lineage and the 'I' type which is an intermediate with the ability to progress towards a neuronal or glial lineage upon differentiation [31]. The difference in malignant properties between S- and N-type cell subtypes may have clinical relevance. It has been previously demonstrated that N and S type cells exhibit differences in response to treatment with MTAs. S type cells undergo mitotic arrest in contrast to N type cells which undergo apoptosis [32]. This would support our finding that N type cells (SHSY5Y, Kelly and SK-N-BE(1)) undergo apoptosis in response to our novel MTA.

Treatment of advanced neuroblastoma entails the incorporation of intensive courses of combination chemotherapy. Conventional chemotherapy can often target DNA triggering events in the cell such as activation of p53, cell cycle arrest and apoptosis. Frequently in advanced tumours, these pathways are defective, for example p53 may be mutated or deleted leading to ineffective induction of cell death by chemotherapeutics. Single agent chemotherapy may provide insufficient toxicity and cells may develop MDR. Combination therapy offers the benefit of targeting multiple cellular pathways that induce apoptosis, and has proven in other paediatric cancers to be efficacious leading to higher rates of long term survival. Members of the PBOX family have previously been shown to work in combination with other drugs to synergistically increase apoptosis. These include flavopiridol, a pan Cdk inhibitor and STI-571, a receptor tyrosine kinase inhibitor [13]. There have also been previous reports in the literature of other novel compounds potentiating the effects of standard chemotherapeutics *via* modulation of the Bcl-2 family of proteins. Mohan et al. [33] demonstrated that 2,3-DCPE (a small molecule inhibitor of the anti-apoptotic protein Bcl-xL) in combination with 4-HPR (a synthetic retinoid) works synergistically to significantly increase apoptosis in SK-N-DZ and SH-SY5Y neuroblastoma cells *via* downregulation of the anti-apoptotic proteins Bcl-xL, Bcl-2 and Mcl-1 and upregulation of the pro-apoptotic proteins Bax, p53, Puma and Noxa, ultimately causing activation of caspase-3. Similarly Fang et al. [34] found that 4-HPR synergises with ABT-737, a small-molecule BH3-mimetic in neuroblastoma cell lines. They propose that inhibition of anti-apoptotic Bcl-2 proteins induced by ABT-737 enhances 4-HPR activity in neuroblastoma cell lines though an increase in pro-apoptotic Bcl-2 proteins such as Bax, Bak and tBid.

Prompted by these findings an investigation was undertaken to assess the effects of PBOX-6 in combination with doxorubicin, etoposide and carboplatin on SHSY5Y cells. PBOX-6 was shown to synergistically enhance the apoptotic effects of all three drugs tested. While PBOX-6 has been shown to target the microtubule network, doxorubicin, etoposide and carboplatin each mediate apoptosis though a number of different means. We propose that this enhancement in apoptosis is likely caused by multiple pathways being targeted simultaneously.

The PBOX-6/carboplatin combination was chosen as a representative combination for further investigation as this combination demonstrated the strongest synergism. Entry into the mitochondrial pathway is controlled by binding of pro-death Bcl-2 proteins to pro-survival Bcl-2 proteins which can inhibit the pro-apoptotic activity of these proteins [35]. Activation of anti-apoptotic members may tip the balance towards survival and contribute to chemoresistance. Bcl-2 has previously been shown to

be expressed in a significant percentage of untreated neuroblastoma tumours with expression correlating with poor prognosis [36]. It was found that PBOX-6 induced a dose-dependent cleavage of Bcl-2 in neuroblastoma cells which results in the formation of a Bcl-2 cleavage fragment and the loss of its anti-apoptotic activity consistent with previous reports [12,37]. Although Bcl-2 is an anti-apoptotic protein it has been reported that the cleavage results in the formation of a pro-apoptotic fragment lacking the N-terminal 34 amino acids of Bcl-2 [24] which has been shown to promote the release of cytochrome *c* [38]. In this study, results indicate that PBOX-6 induced cleavage of Bcl-2 may promote apoptosis by preventing inhibition of pro-apoptotic Bcl-2 proteins such as Bak and by formation of a pro-apoptotic fragment which induces cytochrome *c* release.

Mcl-1 is a pro-survival Bcl-2 protein which has been implicated to have a role in chemoresistance in a range of cancers. Increased expression of Mcl-1 has been shown to be associated with poor prognosis and the development of MDR in multiple cancers including multiple myeloma, melanoma, acute myeloid leukaemia, chronic lymphoid leukaemia and acute lymphatic leukaemia [39–44]. A recent screen of over 3000 human tumours found that Mcl-1 was amplified in 11% of cases [45]. It has been postulated to function as an oncogene in neuroblastoma contributing to pathogenesis through prevention of apoptosis. Antagonism of Mcl-1 has been shown to have anti-cancer activity in a number of different malignancies including sarcoma, myeloma, lymphoma and small and non-small cell lung cancer while phase 1 and 2 clinical trials of small molecule Mcl-1 antagonists are currently being undertaken. A recent study demonstrated that down regulation of Mcl-1 by RNA interference lead to induction of apoptosis in high risk neuroblastoma cell lines [46]. Silencing of Mcl-1 reduced resistance to cytotoxic chemotherapy or Bcl-2 antagonists.

Mcl-1 has recently been postulated to be a critical regulator of apoptosis induced by MTAs [47]. Therefore as PBOX-6 is a MTA; we hypothesised that it may affect expression of Mcl-1 in neuroblastoma cells. PBOX-6 induced a dose-dependent reduction in Mcl-1 with almost complete abolition of expression following 72 h treatment. This is the first report of PBOX-6 alone decreasing the expression of Mcl-1 but is consistent with our previous findings which demonstrated that PBOX-15 completely abolished Mcl-1 expression in multiple myeloma cell lines [15]. This result is of particular interest as several studies had found downregulation of Mcl-1 to be an effective strategy to enhance neuroblastoma cells to Fas- or chemotherapy-induced apoptosis [48]. Similarly Betteyab et al. [49] found that CDK inhibitors roscovitine and CR8 induce apoptosis in neuroblastoma by downregulating Mcl-1. Taken together these results would indicate that down-regulation of Mcl-1 expression would be favourable for the treatment of neuroblastoma.

It has been proposed that some Bcl-2 proteins exert their anti-apoptotic function by inhibiting translocation of Bax to the mitochondria where it heterodimerises with Bak to form pores in the mitochondrial membrane. When Bcl-2, Bcl-xL and Mcl-1 levels are decreased or inactivated though cleavage or phosphorylation, Bax and Bak are free to dimerise allowing for the potential release of cytochrome *c* and consequent activation of caspases, therefore we investigated the effects of drug treatment on these proteins. We found Bak expression increased up to 72 h post treatment with PBOX-6 while no increase in Bax was observed. This is the first report in the literature describing the effect of PBOX-6 treatment on expression of Bak. It has previously been shown that in healthy cells Bak is sequestered by Mcl-1 and not Bcl-2 [50]. In this study we hypothesise that a PBOX-6-induced reduction of Mcl-1 correlates with an increase in Bak expression in SHSY5Y cells due to release of Bak from the Mcl-1 complex. The shift in the ratio of these proteins initiates a conformational change in Bak, as demonstrated by western blot analysis of the conformationally active form of Bak, allowing for formation of pores in the mitochondrial membrane, causing depolarisation and release of pro-apoptotic proteins such as cytochrome *c*.

Having investigated the molecular events leading to PBOX-6 induced apoptosis, we sought to identify the possible mechanism by which PBOX-6 enhances carboplatin induced apoptosis. Carboplatin treatment alone had no effect on the anti-apoptotic Bcl-2 and Mcl-1 proteins or the pro-apoptotic Bak, whereas the PBOX-6/carboplatin combination resulted in cleavage of Bcl-2, a downregulation of Mcl-1 and upregulation of Bak in both drug sensitive and MDR neuroblastoma cell lines. The disturbance of the microtubule network induce signals that initiate cell death *via* the mitochondrial pathway indicating that microtubules, the mitochondria and cell death are very much linked. We found that PBOX-6 in combination with carboplatin provoked depolarisation of the mitochondria, release of cytochrome *c* and activation of caspase-9 and -3. Pre-treatment with caspase-9 inhibitors demonstrated the importance of caspase-9 activation in the apoptotic pathway.

Caspase-8 has been shown to be silenced by methylation of the promoter region of the caspase-8 gene [51]. Inactivation of caspase-8 is a hallmark of defective apoptosis and a mechanism by which tumour cells evade death by chemotherapeutics and develop MDR [29]. Therefore, agents which can induce re-expression of caspase-8 may sensitise cells to apoptosis as activated caspase-8 may directly activate the extrinsic pathway (extrinsic pathway type I) or activate the intrinsic pathway through cleavage of Bid leading to release of cytochrome *c*, activation of caspase-9 and caspase-3 (extrinsic pathway type II) [52]. Therefore we were wished to identify the role of caspase-8 in PBOX-6/carboplatin induced apoptosis. Previously caspase-8 has been shown to be undetectable or present at very low levels in SHSY5Y cells but expression has been induced though various means such as after treatment with interferon γ [28] or a combination of interferon γ and valproic acid [29]. Loss of caspase-8 expression was shown to result in chemoresistance while induction of expression was demonstrated to restore sensitivity to TRAIL [29]. Our results would indicate that the PBOX-6/carboplatin combination restores caspases-8 expression in SHSY5Y cells as previously reported in the literature. Similar to caspase-9, inhibition of caspase-8 was found to significantly decrease apoptosis induced by the combination.

Activation of Bak, release of cytochrome *c* and activation of caspase-9 would support the hypothesis that apoptosis is being mediated by the intrinsic pathway but as crosstalk between the pathways may occur we cannot rule out involvement of the extrinsic pathway. Indeed the caspase-8 activation demonstrated herein may indicate involvement of the extrinsic pathway. However, as caspase-8 can be activated by effector caspases such as caspase-3 [53], and as we have not demonstrated DISC formation, we cannot say with certainty that the extrinsic pathway type II is activated. We hypothesise that the PBOX-6/carboplatin combination occurs primarily through the intrinsic pathway while caspase-8 activation may be present, not as a direct activator, but rather to augment the apoptotic process.

Mcl-1 overexpression has been shown to correlate with disease progression and degree of aggression suggesting a role in development of chemoresistance. RNA interference experiments showed that Mcl-1 knockdown sensitised SHSY5Y and CHLA-90 cells to carboplatin. Cell death or survival is mediated by a balance of pro and anti-apoptotic proteins, with some cells relying predominantly on Mcl-1 for survival. A reduction in apoptosis induced by the combination caused by overexpression of Mcl-1 would be necessary to definitively conclude the role of Mcl-1 is mediating apoptosis. Nevertheless we postulate that a decrease in

Mcl-1 expression either through siRNA mediated knockdown or treatment with the combination, shifts the balance towards cell death, suggesting that Mcl-1 plays a key role in cell survival and response to chemotherapy. Inactivation of Mcl-1 by novel compounds such as PBOX-6 may present an innovative therapeutic strategy for future treatment of neuroblastoma.

We have demonstrated downregulation of Mcl-1 and reversion of suppression of caspase-8 expression in response to PBOX-6 therefore it is possible PBOX-6 may be modulating transcription in neuroblastoma cells. There have been previous reports in the literature of modulation of transcription by MTAs. Walker et al. [54] observed that microtubule based chemotherapeutics such as paclitaxel or vinorelbine inhibit STAT signalling. When treated with either of these drugs, MDA-MB-468 breast cancer cells with constitutive activation of STAT3, display a loss of STAT3 phosphorylation. Additionally paclitaxel disrupted interaction of STAT3 with tubulin. In contrast other chemotherapeutics such as doxorubicin had no effect on STAT3. Loss of STAT3 phosphorylation resulted in a loss of transcription of STAT3 target genes. These findings, in addition to the effects on Mcl-1 and caspase-8 in neuroblastoma cells, would support the hypothesis that MTAs may modulate transcription in malignant cells, but further work is required to ascertain any direct effects of the PBOXs on transcription.

Further studies are warranted to establish the effects of PBOX-6 on primary neuroblastoma cells while additional preclinical studies including the use of an *in vivo* neuroblastoma animal model is necessary to establish the potential of this novel MTA for the treatment of neuroblastoma.

In conclusion, we have demonstrated that PBOX-6 has the ability to induce apoptosis in neuroblastoma cell lines alone and together with several chemotherapeutic agents; indicating that PBOX-6 represents a promising therapeutic alternative to currently available treatments. Our findings provide novel insights into the signalling pathways which are activated in response to PBOX-6 in both drug sensitive and resistant neuroblastoma cell lines and in combination with carboplatin to achieve synergistic effects indicating the potential of the PBOXs, alone and in combination with standard chemotherapeutics, as an effective therapy against neuroblastoma.

Acknowledgements

We are grateful to Prof. Raymond Stallings of the Department of Cancer Genetics, Royal College of Surgeons in Ireland for useful discussions on this work. This study was funded by the National Children's Research Centre, Our Lady's Children's Hospital, Crumlin, Dublin, Ireland.

References

[1] Maris JM. Recent advances in neuroblastoma. N Engl J Med 2010;362:2202–11.
[2] Brodeur GM, Pritchard J, Berthold F, Carlsen NL, Castel V, Castelberry RP, et al. Revisions of the international criteria for neuroblastoma diagnosis, staging, and response to treatment. J Clin Oncol 1993;11(8):1466–77.
[3] Matthay KK, Reynolds CP, Seeger RC, Shimada H, Adkins ES, Haas-Kogan. et al. Long-term results for children with high-risk neuroblastoma treated on a randomized trial of myeloablative therapy followed by 13-cis-retinoic acid: a Children's Oncology Group study. J Clin Oncol 2009;2(7):1007–13.
[4] Keshelava N, Seeger RC, Groshen S, Reynolds CP. Drug resistance patterns of human neuroblastoma cell lines derived from patients at different phases of therapy. Cancer Res 1998;58(23):5396–405.
[5] Keshelava N, Zuo JJ, Waidyaratne NS, Triche TJ, Reynolds CP. p53 mutations and loss of p53 function confer multidrug resistance in neuroblastoma. Med Pediatr Oncol 2000;35(6):563–8.
[6] Keshelava N, Groshen S, Reynolds CP. Cross-resistance of topoisomerase I and II inhibitors in neuroblastoma cell lines. Cancer Chemother Pharmacol 2000;45(1):1–8.
[7] Sarkadi B, Homolya L, Szakacs G, Varadi A. Human multidrug resistance ABCB and ABCG transporters: participation in a chemoimmunity defence system. Physiol Rev 2006;86:1179–236.
[8] Chan HS, Haddad G, Thorner PS, DeBoer G, Lin YP, Ondrusek N, et al. *P*-glycoprotein expression as a predictor of the outcome of therapy for neuroblastoma. N Engl J Med 1991;325(23):1608–14.
[9] Mulligan JM, Greene LM, Cloonan S, Mc Gee MM, Onnis V, Campiani G, et al. Identification of tubulin as the molecular target of proapoptotic pyrrolo-1,5-benzoxazepines. Mol Pharmacol 2006;70(1):60–70.
[10] Greene LM, Kelly L, Onnis V, Campiani G, Lawler M, Williams DC, et al. STI-571 enhances the apoptotic efficacy of PBOX-6, a novel microtubule targeting agent, in both STI-571-sensitive and-resistant Bcr-Abl positive human chronic myeloid leukemia cells. J Pharmacol Exp Ther 2007;321(1):288–97.
[11] McElligott AM, Maginn EN, Greene LM, McGuckin S, Hayat A, Browne PV, et al. The novel tubulin-targeting agent pyrrolo-1,5-benzoxazepine-15 induces apoptosis in poor prognostic subgroups of chronic lymphocytic leukemia. Cancer Res 2009;69(21):8366–75.
[12] Nathwani SM, Butler S, Fayne D, McGovern N, Sarkadi B, Meegan MJ, et al. Novel microtubule targeting agents, pyrrolo-1,5-benzoxazepines, induce apoptosis in multi-drug resistant (MDR) cancer cells. Cancer Chemother Pharmacol 2010;66(3):585–96.
[13] Bright SA, Greene LM, Greene TF, Campiani G, Butini S, et al. The novel pyrrolo-1,5-benzoxazepine, PBOX-21, potentiates the apoptotic efficacy of STI571 (imatinib mesylate) in human chronic myeloid leukaemia cells. Biochem Pharmacol 2007;77(3):310–21.
[14] Bright SA, Campiani G, Deininger MW, Lawler M, Williams DC, Zisterer DM. Sequential treatment with flavopiridol synergistically enhances pyrrolo-1,5-benzoxazepine-induced apoptosis in human chronic myeloid leukaemia cells including those resistant to imatinib treatment. Biochem Pharmacol 2010;80(1):31–8.
[15] Maginn EN, Browne PV, Hayden P, Vandenberghe E, MacDonagh B, Evans P, et al. PBOX-15, a novel microtubule targeting agent, induces apoptosis, upregulates death receptors, and potentiates TRAIL-mediated apoptosis in multiple myeloma cells. Br J Cancer 2011;104(2):281–9.
[16] Greene LM, Wang S, O'Boyle NM, Bright SA, Reid JE, Kelly P, et al. Combretazet-3 a novel synthetic cis-stable combretastatin A-4-azetidinone hybrid with enhanced stability and therapeutic efficacy in colon cancer. Oncol Rep 2013;29(6):2451–8.
[17] Greene LM, Fleeton M, Mulligan J, Gowda C, Sheahan BJ, Atkins GJ, et al. The pyrrolo-1, 5-benzoxazepine, PBOX-6, inhibits the growth of breast cancer cells in vitro independent of estrogen receptor status, and inhibits breast tumour growth in vivo. Oncol Rep 2005;14(5):1357–63.
[18] Campiani G, Nacci V, Fiorini I, De Filippis MP, Garofalo A, Ciani SM. Synthesis, biological activity, and SARs of pyrrolobenzoxazepine derivatives, a new class of specific 'peripheral-type' benzodiazepine receptor ligands. J Med Chem 1996;39(18):3435–50.
[19] Chou TC, Talalay P. Quantitative analysis of dose–effect relationships: the combined effects of multiple drugs or enzyme inhibitors. Adv Enzyme Regul 1984;22:27–55.
[20] Wickström M, Johnsen JI, Ponthan F, Segerström L, Sveinbjörnsson B, Lindskog M, et al. The novel melphalan prodrug J1 inhibits neuroblastoma growth in vitro and in vivo. Mol Cancer Ther 2007;6(9):2409–17.
[21] Dijkhuis AJ, Douwes J, Kamps W, Sietsma H, Kok JW. Differential expression of sphingolipids in *P*-glycoprotein or multidrug resistance-related protein 1 expressing human neuroblastoma cell lines. FEBS Lett 2003;548(1):28–32.
[22] Maurer BJ, Kalous O, Yesair DW, Wu X, Janeba J, Maldonado V. Improved oral delivery of *N*-(4-hydroxyphenyl)retinamide with a novel LYM-X-SORB organized lipid complex. Clin Cancer Res 2007 May 15;13(10):3079–86.
[23] Kamei T, Inui M, Nakamura S, Okumura K, Goto A, Tagawa T. Interferon-gamma and anti-Fas antibody-induced apoptosis in human melanoma cell lines and its relationship to bcl-2 cleavage and bak expression. Melanoma Res 2004;13(2):153–9.
[24] Cheng EH-Y, Kirsch DG, Clem RJ, Ravi R, Kastan MB, Bedi A, et al. Conversion of bcl-2 to a bax death effector by caspases. Science 1997;278(5345):1966–8.
[25] Dewson G, Kluck RM. Mechanisms by which Bak and Bax permeabilise mitochondria during apoptosis. J Cell Sci 2009;122(Pt 16):2801–8.
[26] Zisterer DM, Campiani Nacci V, Williams DC. Pyrrolobenzoxazepines induce apoptosis in HL-60, Jurkat and Hut-78 cells: a new class of apoptotic agents. J Pharmacol Exp Ther 2000;293(1):48–59.
[27] Mc Gee MM, Campiani G, Ramunno A, Fattorusso C, Nacci V, Lawler M, et al. Pyrrolo-1,5-benzoxazepines induce apoptosis in chronic myelogenous leukemia (CML) cells by bypassing the apoptotic suppressor bcr-abl. J Pharmacol Exp Ther 2001;296(1):31–40.
[28] Tong H, Lu C, Yang Y, Zhang J, Zhang J. Role of caspase 8 as a determinant in trail sensitivity of neuroblastoma cell lines. Pediatr Hematol Oncol 2009;26(8):549–59.
[29] Häcker S, Dittrich A, Mohr A, Schweitzer T, Rutkowski S, Krauss J, et al. Histone deacetylase inhibitors cooperate with IFN-gamma to restore caspase-8 expression and overcome TRAIL resistance in cancers with silencing of caspase-8. Oncogene 2009;28(35):3097–110.
[30] Balayssac D, Cayre A, Authier N, Bourdu S, Penault-Llorca F, Gillet JP, et al. Patterns of *P*-glycoprotein activity in the nervous system during vincristine-induced neuropathy in rats. J Peripher Nerv Syst 2005;10(3):301–10.
[31] Ross RA, Biedler JL, Spengler BA. A role for distinct cell types in determining malignancy in human neuroblastoma cell lines and tumors. Cancer Lett 2003;197(1–2):9–35.
[32] Piacentini M, Piredda L, Starace DT, Annicchiarico-Petruzzelli M, Mattei M, Oliverio S, et al. Differential growth of N- and S-type human neuroblastoma

cells xenografted into scid mice. correlation with apoptosis. J Pathol 1996;180(4):415–22.
[33] Mohan N, Banik NL, Ray SK. Combination of *N*-(4-hydroxyphenyl) retinamide and apigenin suppressed starvation-induced autophagy and promoted apoptosis in malignant neuroblastoma cells. Neurosci Lett 2011;502(1):24–9.
[34] Fang H, Harned TM, Kalous O, Maldonado V, DeClerck YA, Reynolds CP. Synergistic activity of fenretinide and the Bcl-2 family protein inhibitor ABT-737 against human neuroblastoma. Clin Cancer Res 2011;17(22):7093–104.
[35] Youle RJ, Strasser A. The BCL-2 protein family: opposing activities that mediate cell death. Nat Rev Mol Cell Biol 2008;9(1):47–59.
[36] Dole M, Nuñez G, Merchant AK, Maybaum J, Rode CK, Bloch CA, Castle VP. Bcl-2 inhibits chemotherapy-induced apoptosis in neuroblastoma. Cancer Res 1994;54(12):3253–9.
[37] Mc Gee MM, Greene LM, Ledwidge S, Campiani G, Nacci V, Lawler M, et al. Selective induction of apoptosis by pyrrolo-1,5-benzoxazepine (PBOX-6) in leukaemia cells occurs via the c-Jun NH2-terminal kinase-dependent phosphorylation and inactivation of Bcl-2 and Bcl-xl. J Pharmacol Exp Ther 2004;310(3):1084–95.
[38] Kirsch DG, Doseff A, Chau BN, Lim DS, de Souza-Pinto NC, Hansford R, et al. Caspase-3-dependent cleavage of Bcl-2 promotes release of cytochrome c. J Biol Chem 2009;274(30):21155–61.
[39] Zhang B, Gojo I, Fenton RG. Myeloid cell factor-1 is a critical survival factor for multiple myeloma. Blood 2002;99(6):1885–93.
[40] Kaufmann SH, Karp JE, Svingen PA. Elevated expression of the apoptotic regulator Mcl-1 at the time of leukemic relapse. Blood 1998;91(3):991–1000.
[41] Stam RW, Den Boer ML, Schneider P. Association of high-level MCL-1 expression with in vitro and in vivo prednisone resistance in MLL-rearranged infant acute lymphoblastic leukemia. Blood 2010;115(5):1018–25.
[42] Pepper C, Lin TT, Pratt G. Mcl-1 expression has in vitro and in vivo significance in chronic lymphocytic leukemia and is associated with other poor prognostic markers. Blood 2008;112(9):3807–17.
[43] Kitada S, Andersen J, Akar S. Expression of apoptosis-regulating proteins in chronic lymphocytic leukemia: correlations with in vitro and in vivo chemoresponses. Blood 1998;91(9):3379–89.
[44] Wong RP, Khosravi S, Martinka M, Li G. Myeloid leukemia-1 expression in benign and malignant melanocytic lesions. Oncol Rep 2008;19(4):933–7.
[45] Beroukhim R, Mermel C, Porter D, Wei G, Raychaudhuri S, Donovan J. The landscape of somatic copy-number alteration across human cancers. Nature 2010;46(7283):899–905.
[46] Lestini BJ, Goldsmith KC, Fluchel MN, Liu X, Chen NL, Goyal B, et al. Mcl-1 downregulation sensitizes neuroblastoma to cytotoxic chemotherapy and small molecule Bcl2-family antagonists. Cancer Biol Ther 2009;8(16):1587–95.
[47] Wertz IE, Kusam S, Lam C, Okamoto T, Sandoval W, Anderson DJ, et al. Sensitivity to antitubulin chemotherapeutics is regulated by MCL1 and FBW7. Nature 2011;471(7336):110–4.
[48] Amman JU, Haag C, Kasperczyk H, Debatin KM, Fulda S. Sensitization of neuroblastoma cells for TRAIL-induced apoptosis by NFkB inhibition. Int J Cancer 2009;124:1301–11.
[49] Bettayeb K, Baunbæk D, Delehouze C, Loaëc N, Hole AJ, Baumli S. CDK inhibitors roscovitine and CR8 trigger Mcl-1 down-regulation and apoptotic cell death in neuroblastoma cells. Genes Cancer 2010;1(4):369–80.
[50] Willis SN, Chen L, Dewson G, Wei A, Naik E, Fletcher JI, et al. Proapoptotic Bak is sequestered by Mcl-1 and Bcl-xL, but not Bcl-2, until displaced by BH3-only proteins. Genes Dev 2005;19(11):1294–305.
[51] Teitz T, Wei T, Valentine MB, Vanin EF, Grenet J, Valentine VA. Caspase 8 is deleted or silenced preferentially in childhood neuroblastomas with amplification of MYCN. Nat Med 2000;6(5):529–35.
[52] Tait SW, Green DR. Mitochondria and cell death: outer membrane permeabilization and beyond. Nat Rev Mol Cell Biol 2010;11(9):621–32.
[53] Ferreira KS, Kreutz C, Macnelly S, Neubert K, Haber A, Bogyo M. Caspase-3 feeds back on caspase-8, Bid and XIAP in type I Fas signaling in primary mouse hepatocytes. Apoptosis 2012;17(5):503–15.
[54] Walker SR, Chaudhury M, Nelson EA, Frank DA. Microtubule-targeted chemotherapeutic agents inhibit signal transducer and activator of transcription 3 (STAT3) signaling. Mol Pharmacol 2010;78(5):903–8.